AMBRA1 and Loricrin as prognostic biomarkers to identify high risk melanoma patient subgroups and as companion biomarkers for novel stratified treatment to prevent TGF-β2 mediated tumour metastasis

Diana Yao Li Tang

Thesis submitted in partial fulfilment of the requirements of the regulations for the degree of

Doctor of Medicine

Newcastle University
Faculty of Medical Sciences
Institute of Cellular Medicine
July 2017

Abstract

AMBRA1 and Loricrin as prognostic biomarkers to identify high risk melanoma patient subgroups and as companion biomarkers for novel stratified treatment to prevent TGF-β2 mediated tumour metastasis

Cutaneous melanoma remains an increasing world health problem, emphasised by the lack of credible biomarkers able to identify the risk of disease progression of seemingly low risk tumours, or stratify such patients for early novel adjuvant precision-based therapies to prevent metastasis. Data leading to the present study identified the loss of epidermal differentiation proteins, AMBRA1 and Loricrin as putative prognostic biomarkers for AJCC stage I melanomas and their associated loss of expression with increased tumoural secretion of isoform specific TGF-β2. The aim of the present study was to validate the combined loss of AMBRA1 and Loricrin (AMLo) overlying AJCC stage I melanomas as a prognostic and companion biomarker marker to stratify high risk tumour subsets for novel adjuvant treatment strategies targeting TGF-β2 signalling.

Semi-quantitative immunohistochemical analysis of AMLo expression in 236 AJCC stage I melanomas identified a high risk subset (defined as tumours with complete loss of AMBRA1 and any break in epidermal Loricrin expression), for which univariate analysis demonstrated a significant decrease in disease free survival in tumours stratified as high risk. Addtionally, semi-quantitative immunohistochemical analysis of TGF-β2 in high risk AJCC stage I melanomas revealed the significant correlation between increased tumoural TGF-β2 expression and loss of epidermal AMLo. Furthermore, high risk AJCC stage I melanomas were associated with a concurrent loss of peri-tumoural endothelial AMBRA1 where treatment of endothelial cells with exogenous TGF-β2 induced the significant downregulation of AMBRA1 and junctional proteins VE-Cadherin or Claudin-5, the effect of which was partially rescued by the stable knockdown of TGF-β2 in melanoma cells.

Combined bioinformatics of the AMBRA1 promoter, the analysis of TGF-β2 receptor expression and Smad signalling in endothelial cells revealed the contribution of non-canonical TGF-β2 signalling to enhanced proliferation and loss of endothelial integrity. Finally, combined studies of ALK1 and ALK5 inhibition suggest, targeting ALK1 in high risk AJCC stage I melanomas may provide a novel adjuvant therapeutic strategy to prevent metastasis, for which the loss of AMLo is a companion biomarker.

This work is dedicated to my parents

Frank KH Tang & Bernadine SH Chieng

Thank you for being my greatest supporters and always believing in me

Acknowledgements

This work was funded by a British Skin Foundation Fellowship award, Melanoma Focus, the North Eastern Skin Research Fund and the South Tees Hospitals NHS Foundation Trust.

My biggest thanks goes my main supervisor Professor Penny Lovat who has always been there for me as both a teacher and a friend. From the get-go, she took me under her wing and nurtured my transition from a clinician with no prior research experience into a now clinician-scientist. Her constant patience, enthusiasm and dedication towards her work and her research group is greatly admirable and I will always appreciate all she has done for me.

To my other supervisor Rob Ellis, thank you for being such a great mentor and friend. Your cheerful disposition and ongoing optimism is always a breath of fresh air, which had helped me get through many a time when things have not gone as planned. I will always be grateful for your constant support and look forward to many more years of working together as a team!

A massive thank you to my collaborators including Dr Gareth Inman and Lindsay Spender at the University of Dundee for their continued support of my work. A special thanks to Dr Marco Corazzari and the rest of the lab at the University of Rome 'Tor Vergata', for all their help and for making me feel so welcomed during my time there. They are reason I now have a soft spot for espressos and cornettis. Mr Stuart Horswell at Cancer Research UK has been a patient teacher and invaluable in helping me with statistics as well as prompt advice despite his ever busy schedule.

I have grown to admire and respect Dr Paola Giglio, who has helped me tremendously in my work and played a massive role in aiding my development as scientist. Her attention to detail, dedication to her work and patience in teaching has inspired me and I can only hope to be as good a scientist as she is one day! In her, I have also made a friend for life. *Grazie per tutto quello che hai fatto per me.*

A special thanks to Miss Alison Greenwood at JCUH pathology for all her help with coordinating the retrieval and staining of patient tissue sections and for her dedicating so many of her precious weekends to help me meet my deadlines. Also to all members of Penny's group and dermatology, thanks for all the advice and help you have given me over the past 2 years and for putting up with my endless questions.

Finally, I could not have done this without the love and support of my family, especially my parents whom this work is dedicated to and my sisters Jasmine and Lilian who have always been there for me. Also to Jae who has been my constant rock-thanks for always believing in me especially at times when I doubted myself. As always, you have been amazing and I could not have made it this far without you!

Declarations

This thesis is submitted for the degree of Doctor of Medicine at Newcastle University. The research was performed in the Department of Dermatological Sciences at the Institute of Cellular Medicine under the supervision of Professor Penny Lovat, as well as Dr Rob Ellis (Department of Dermatology, South Tees NHS Foundation Trust). This thesis is my own work unless otherwise stated within the text. I certify that none of the material offered in this thesis has been previously submitted by me for a degree or any other qualification at this, or any other university.

Contents

Abstract.....i

Dedication.....iii

Acknowledgements.....iv

Declarations.....vi

Contents.....vii

Tables and Figures.....xvi

Abbreviations.....xxiv

1 Introduction

1.1 Melanocyte development and role in melanin synthesis 3
1.2 Cutaneous melanoma: a malignant transformation of melanocytes 5
1.2.1 Melanoma genesis: From melanocytes to metastases 5
1.2.2 Incidence and mortality 10
1.2.3 Genetic and environmental risk factors 12
1.2.4 Oncogenic mutations in BRAF and NRAS 14
1.3 Melanoma Disease Staging, Biomarkers and Targeted therapies 17
1.3.1 The American Joint Committee on Cancer (AJCC) 7th edition melanoma staging criteria 17
1.3.2 The American Joint Committee on Cancer (AJCC) 8th edition staging criteria 21
1.3.3 Epidermal differentiation and tumour ulceration 22
1.3.4 Biomarkers in melanoma 25
1.3.5 Current Pathway Targeted therapies 29
1.4 Pilot data leading to present study: Down regulation of epidermal AMBRA1 and relationship with TGF-β signalling 32
1.4.1 Role of AMBRA1 in cellular differentiation and proliferation 32
1.4.2 TGF-β signalling cascade and implications in melanoma 36
1.4.3 Current strategies to target TGF-β2 signalling in tumourigenesis 44
1.5 Hypothesis, Aims and Objectives 47

2 Materials and Methods

2.1 Growth and maintenance of primary human keratinocytes, endothelial cells, human endothelial and melanoma cell line 53

2.1.1 Human Umbilical Vein Endothelial Cells (HUVEC) 53

2.1.2 Primary Human Dermal Lymphatic Endothelial Cells (HDLEC) 53

2.1.3 CCD1106 Keratinocytes 54

2.1.4 Human A375 melanoma cells pre subjected to stable knockdown of TGF-β2 54

2.2 Isolation, growth and calcium induced differentiation of primary human keratinocytes 55

2.3 Isolation of primary human dermal endothelial (HDEC) cells 56

2.3.1 Isolation of HDEC using endothelial cell-specific antibody EN4 coated wells.....56

2.3.2 Isolation of HDEC using PE anti human CD31 antibody and Miltenyi Biotech Magnetic Columns 57

2.4 Treatment of HUVEC, HDLEC cells and CCD1106 keratinocytes with human recombinant TGF-β2 in the presence or absence of an ALK5 inhibitor 58

2.5 Treatment of HUVECs and HDLECs with TGF-β2 rich melanoma supernatants or supernatants derived from melanoma cells in which TGF-β2 has been stably knocked down.....59

2.6 CellTiter 96® Aqueous Non-Radioactive Cell Proliferation Assay (MTS) 60

2.7 siRNA-mediated knockdown of ALK1 in HUVEC cells 61

2.8 Real Time Reverse Transcriptase Polymerase Chain Reaction (qPCR).....63

2.9 Western blotting 67

2.10 Immunohistochemistry for formalin fixed paraffin embedded (FFPE) tissue 70

2.10.1 Immunohistochemistry for AMBRA1, Loricrin, CD31 and TGF-β2 using DAB counterstaining 70

2.10.2 Bleaching of FFPE melanoma tissue prior to analysis of TGF-β2 using DAB counterstaining 72

2.10.3 Immunohistochemistry for AMBRA1 and TGF-β2 using VIP counterstaining 72

2.11 Immunofluorescence for AMBRA1 and CD31 expression in FFPE HUVEC cell pellets and melanoma tissue 74

2.12 Patient Cohort Selection and Database development 76

2.13 Analysis of Immunohistochemistry by Slide Scanner 80

2.13.1 Analysis and scoring of epidermal and endothelial AMBRA1 expression 80

2.13.2 Analysis and scoring of epidermal Loricrin expression 84

2.13.3 Analysis of tumoural TGF-β2 expression 85

2.14 Statistics and Bioinformatics Analysis 86

3 Combined loss of epidermal AMBRA1 and Loricrin (AMLo): A novel prognostic biomarker for AJCC stage I melanomas

3.1 Introduction 92

3.2 Results 95

3.2.1 Loss of AMBRA1 in the overlying AJCC stage I melanomas is a putative prognostic biomarker 95

3.2.2 Loss of Loricrin in the epidermis overlying AJCC stage I melanomas is a putative prognostic biomarker.....99

3.2.3 Validation of visual analysis of epidermal AMBRA1 expression as a robust mean of identifying 'loss of AMBRA1 expression' in AJCC stage I melanomas .....
.....105

3.2.4 Combined loss of epidermal AMBRA1 and Loricrin (AmLo) identifies a high risk AJCC stage I melanoma subgroup.....110

3.2.5 Combined loss of epidermal AMBRA1 and Loricrin (AmLo) identifies a high risk AJCC stage IB (AJCC 8th edition) melanoma subgroup. 116

3.3 Discussion.....120

4 Melanoma secretion of TGF-β2 mediates the down regulation of epidermal and endothelial integrity

4.1 Introduction 127

4.2 Results 129

4.2.1 Increased TGF-β2 by AJCC stage I melanomas correlates with the decreased expression of epidermal AMBRA1 129

4.2.2 High Risk AJCC stage I melanomas are associated with increased tumoural TGF-β2 135

4.2.3 TGF-β2 induces the down regulation of calcium-induced differentiation of primary keratinocytes 139

4.2.4 TGF-β2 induces the down regulation of AMBRA1 and junctional proteins in endothelial cells 141

4.2.5 Knockdown of TGF-β2 in metastatic melanoma cell lines prevents TGF-β2-induced down regulation of AMBRA1 and Claudin-5 in endothelial cells 148

4.2.6 Loss of endothelial AMBRA1 is associated with high risk AJCC stage I melanomas 153

4.3 Discussion 160

5 Contribution of canonical and non-canonical TGF-β2 signalling to melanoma metastasis

5.1 Introduction 168

5.2 Results 171

5.2.1 Bioinformatics analysis of the AMBRA1 promoter identifies TGF-β2 responsive elements 171

5.2.2 ALK1 and ALK5 are differentially expressed in keratinocytes and endothelial cells 173

5.2.3 TGF-β2-induced deregulation of keratinocyte (CCD1106) differentiation and AMBRA1 down regulation is mediated by canonical TGF-β signalling 175

5.2.4 TGF-β2 induces both canonical and non-canonical signalling in HUVEC endothelial cells 178

5.2.5 Non-canonical TGF-β2 signalling is increased in the endothelium of metastatic AJCC stage I melanomas 180

5.2.6 Inhibition of ALK5 prevents canonical TGF-β2 signalling-mediated down regulation of AMBRA1 in calcium-induced keratinocytes 182

5.2.7 Inhibition of ALK5 in HUVEC endothelial cells exacerbates non-canonical TGF-β2 signalling and does not prevent TGF-β2-induced endothelial AMBRA1 down regulation. 184

5.2.8 SiRNA-mediated knockdown of ALK1 prevents non-canonical TGF-β2 mediated endothelial AMBRA1 downregulation. 186

5.2.9 Inhibition of canonical TGF-β2 signaling by ALK5 inhibition promotes endothelial cell proliferation 190

5.3 Discussion 194

6 Final discussion and future perspectives

6.1 AMLo as a follow-up stratification tool for AJCC stage I melanoma following primary melanoma excision 203

6.2 AMLo as a companion biomarker for adjuvant therapy targeting TGF-β2 signalling 206

6.3 The role of Vitamin D in TGF-β2 mediated AMBRA1 down regulation and melanoma metastasis 208

References 214

Appendices 234

Appendix 1: The REMARK guidelines 235

Published manuscripts, abstracts & submissions arising from this work 239

Tables and Figures

Tables

Table 1.1: Risk factors for melanoma. **13**

Table 1.2: Tumour thickness (T) classification in TNM staging with associated 10-year survival. **18**

Table 1.3: AJCC 2009 Melanoma Staging and 5-year overall survival for stage I-II disease. **19**

Table 1.4: AJCC 2009 Melanoma Staging and 5-year overall survival for stage III-IV disease. **20**

Table 2.1: Duplex siRNA oligoribonucleotides targeting human ALK1. ..... **61**

Table 2.2: Constituents of a single Reverse Transcription Reaction. **64**

Table 2.3: Primer sets for amplification of L34, ALK1, ALK5 and AMBRA1 gene sequences. **65**

Table 2.4: Constituents of a single qPCR reaction using the Maxima SYBR Green Assay. **66**

Table 2.5: Optimal primary and secondary antibody conditions for respective western blot analysis. **69**

Table 2.6: Optimal conditions for AMBRA1, Loricrin, CD31 and TGF-β2 detection using the Ventana Benchmark XT automated IHC system. **71**

Table 2.7: Optimal primary and secondary antibody conditions for immunofluorescence detection of AMBRA1 and CD31 expression. **75**

Table 2.8: Study cohort patient demographics **79**

Table 2.9: Visual scores of epidermal AMBRA1 expression/staining intensity overlying primary melanomas. **81**

Table 4.1: Stratification of 15 AJCC stage I melanomas with known epidermal AMBRA1 status according to peri-tumoural endothelial AMBRA1 status, associated AMLo score and eventual outcome. **157**

Table 6.1: Potential effect of Vitamin D and Vitamin A status on prognosis of AJCC stage I melanomas in association with melanoma TGF-β2 secretion..... **213**

Figures

Figure 1.1: Schematic of an epidermal melanin unit. **4**

Figure 1.2: Model of melanocyte transformation and melanoma invasion. **6**

Figure 1.3: Mechanism of melanoma cell entry into the vasculature for dissemination to secondary sites of metastasis. **8**

Figure 1.4: Age specific incidence of malignant melanoma in the UK 2012 – 2014. 11

Figure 1.5: Schematic representation of the MAPK signalling cascade. **14**

Figure 1.6: Mutations in BRAF or NRAS lead to constitutive activation of the MAPK signalling pathway. **16**

Figure 1.7: Epidermal differentiation markers expression at different layers of the epidermis. **23**

Figure 1.8: Epidermal differentiation is associated with increased expression of AMBRA1 ..... **33**

Figure 1.9: Epidermal AMBRA1 loss is not associated with the degree of tumour invasion. **34**

Figure 1.10: The canonical TGF-β/Smad signalling pathway. **37**

Figure 1.11: Schematic model for activation of TGF-β mediated ALK 1 and 5 signalling in endothelial cells. **38**

Figure 1.12: Effects of TGF-β on melanoma cells and the tumour microenvironment. **40**

Figure 1.13: Loss of Epidermal AMBRA1 overlying primary cutaneous melanomas correlates with increased tumoural secretion of TGF-β2. ..... **43**

Figure 1.14: Hypothesis for TGF-β2 mediated AMBRA1 down regulation, loss of epidermal and endothelial integrity, tumour ulceration and metastasis. **48**

Figure 2.1: Graphical illustration of exclusion of samples from initial identification of potential samples using the JCUH Department of Plastic and Reconstructive surgery melanoma database, to inclusion in the final biomarker validation study cohort. **77**

Figure 2.2: AMBRA1 expression in normal epidermis and the epidermis overlying primary AJCC stage I melanomas.....**81**

Figure 2.3: Peri-tumoural AMBRA1 and CD31 expression in primary AJCC stage I melanomas.....**83**

Figure 2.4: Loricrin expression in normal epidermis and the epidermis overlying primary melanomas.....**84**

Figure 2.5: AMBRA1 upstream promoter sequence.....**89**

Figure 3.1: Loss of epidermal AMBRA1 expression overlying tumours correlates with decreased disease free survival in all AJCC stage melanomas. **96**

Figure 3.2: Loss of AMBRA1 expression in the epidermis overlying AJCC stage I melanomas correlates with decreased disease free survival.....**98**

Figure 3.3: Loss of Loricrin expression overlying primary melanomas of differing AJCC stage correlates with decreased disease free survival. **100**

Figure 3.4: Loss of Loricrin expression in the epidermis overlying primary AJCC stage I melanomas correlates with decreased disease free survival.....**101**

Figure 3.5: Combined loss of AMBRA1 and Loricrin expression overlying primary melanomas is a highly sensitive and specific prognostic biomarker for the prediction of disease free survival in AJCC stage I melanomas. **103**

Figure 3.6: Correlation of qualitative visual scoring of epidermal AMBRA1 expression with semi-quantitative scoring. **107**

Figure 3.7: Comparison of ‘complete loss’ with a combination of ‘no or some loss’ of AMBRA1 expression in the epidermis overlying AJCC stage I melanomas with semi-quantitative analysis. **109**

Figure 3.8: Loss of AMBRA1 expression in the epidermis overlying AJCC stage I melanomas is associated with decreased disease free survival..... **111**

Figure 3.9: Loss of Loricrin expression in the overlying AJCC stage I melanomas is associated with decreased disease free survival..... **113**

Figure 3.10: Combined loss of epidermal AMBRA1 and Loricrin (AMLo) expression in the epidermis overlying AJCC stage I melanomas identifies a high risk sub group. **115**

Figure 3.11: Combined loss of epidermal AMLo expression is a prognostic biomarker in AJCC 8th edition criteria stage IA melanomas. **118**

Figure 3.12: Combined loss of epidermal AMBRA1 and Loricrin (AMLo) identifies a high risk AJCC stage IB (AJCC 8th edition) melanoma subgroup. **119**

Figure 4.1: Visual analysis of the IHC expression of epidermal AMBRA1 and tumoural TGF-β2 in AJCC stage I melanomas revealed by DAB counterstaining suggests a potential association between loss of epidermal AMBRA1 and increased tumoural TGF-β2. ..... **130**

Figure 4.2: Loss of epidermal AMBRA1 overlying AJCC stage I melanomas does not correlate with increased tumoural TGF-β2 expression when compared by IHC using DAB counterstaining. **131**

Figure 4.3: IHC expression of tumoural TGF-β2 in AJCC stage I melanomas revealed by VIP counterstaining. **133**

Figure 4.4: Loss of epidermal AMBRA1 overlying AJCC stage I melanomas correlates with increased tumoural TGF-β2 expression revealed by VIP counterstaining. **134**

Figure 4.5: TGF-β2 expression (revealed following bleaching and automated IHC analysis with DAB counterstaining) is increased in high risk AJCC stage 1 melanomas. **136**

Figure 4.6: Tumoural TGF-β2 expression is increased in AJCC stage I melanomas that developed metastatic disease compared to localised tumours.....**137**

Figure 4.7: High risk AJCC stage I melanomas stratified by AMLo display significantly increased TGF-β2 expression compared to AMLo low risk tumours. **138**

Figure 4.8: TGF-β2 mediates the down regulation of AMBRA1 and Loricrin in calcium-induced differentiated primary keratinocytes. **140**

Figure 4.9: TGF-β2 induces the down regulation of AMBRA1 and junctional protein expression in HUVEC endothelial cells. **142**

Figure 4.10: Isolation of human dermal endothelial cells from human foreskin samples using EN4 antibody coated wells results in mixed dermal endothelial cell and fibroblast subpopulations. **143**

Figure 4.11: Isolation of human dermal endothelial cells from donor foreskin samples using human PE anti CD31 antibody with Miltenyi Biotech magnetic columns results in a mixed colony of dermal endothelial cells and fibroblasts. **145**

Figure 4.12: TGF-β2 induces the down regulation of AMBRA1 and Claudin-5 in primary HDLECs. **147**

Figure 4.13: Culture of A375 cells subjected to TGFβ2 modulation in either complete ECCM or DMEM has no effect on cell viability. **149**

Figure 4.14: Treatment of HUVEC cells with TGF-β2-depleted melanoma supernatants derived from A375 melanoma cells with stable TGF-β2 knockdown prevents TGF-β2 induced down regulation of AMBRA1 and Claudin-5.....**150**

Figure 4.15: Knockdown of TGF-β2 in melanoma cells inhibits TGF-β2 –mediated down regulation of AMBRA1 and Claudin-5 in primary HDLECs.....**152**

Figure 4.16: Dual immunofluorescence (IF) expression of AMBRA1 and CD31 in HUVEC endothelial cells. **154**

Figure 4.17: Loss of epidermal AMBRA1 overlying AJCC Stage I melanomas is associated with a concurrent loss in endothelial AMBRA1. .....**155**

Figure 4.18: Endothelial AMBRA1 expression is lost in metastatic AJCC stage I melanomas stratified as high risk by AMLo scoring.....**159**

Figure 5.1: Schematic model for activation of TGF-β2 mediated ALK1 and ALK5 signalling in endothelial cells. **170**

Figure 5.2: Bioinformatics analysis of the AMBRA1 promoter identifies TGF-β responsive elements. **172**

Figure 5.3: ALK1 and ALK5 are differentially expressed by the keratinocyte cell line CCD1106, primary keratinocytes and HUVEC endothelial cells.....**174**

Figure 5.4: Activation of canonical TGF-β signaling in calcium-induced differentiated CCD1106 keratinocytes in response to exogenous TGF-β2. .....**176**

Figure 5.5: TGF-β2 activates both canonical and non-canonical signalling in HUVEC endothelial cells.....**179**

Figure 5.6: Absence of p-Smad 2/3 and the presence of p-Smad 1/5 expression is associated with metastatic AJCC stage I melanomas. **181**

Figure 5.7: ALK5 inhibition results in blockade of canonical TGF-β2-induced down regulation of AMBRA1 in calcium-induced CCD1106 keratinocytes.....**183**

Figure 5.8: ALK5 inhibition sustains TGF-β2 induced Smad 1/5 phosphorylation but does not prevent AMBRA1 down regulation in endothelial cells.....**185**

Figure 5.9: Efficacy of siRNA mediated knockdown of ALK1 in HUVEC endothelial cells. **187**

Figure 5.10: Knockdown of ALK1 prevents TGFβ2-induced Smad 1/5 phosphorylation and loss of endothelial AMBRA1. .....**189**

Figure 5.11: Effect of recombinant TGF-β2 on HUVEC and primary HDLEC endothelial cell proliferation. **191**

Figure 5.12: ALK5 blockade results in increased TGF-β2 induced stimulation of HUVEC endothelial cell proliferation. **193**

Figure 6.1: Hypothesis of the role of Vitamin D in TGF-β2 induced loss of epidermal/endothelial integrity and melanoma metastasis. **211**

Abbreviations

°C	Degrees Centigrade
µl	Microlitre
µm	Micrometre
µM	Micromolar
1°	Primary
ACTH	Adrenocorticotrophic hormone
AJCC	American Joint Committee On Cancer
ALK	Activin receptor-like kinase
AMBRA1	Activating Molecule In Beclin-1 Regulated Autophagy Protein 1
AMP	Adenosine Monophosphate
ANOVA	Analysis Of Variance
Atg	Autophagy Related Protein
BBE	Bovine brain extract
BRAF	V-Raf Murine Sarcoma Viral Oncogene Homolog B1
BS	Buffer solution
BSA	Bovine Standard Albumin
CAMP	Cyclic Adenosine Monophosphate
CDK	Cyclin-dependent kinase
CDK4	Cyclin-Dependent kinase 4

CDKN2A	Cyclin-Dependent Kinase Inhibitor 2A
CI	Confidence Interval
cm	Centimetre
CO_2	Carbon dioxide
CREB	CAMP responsive-element binding protein
CSG	Clinical Studies Group
Ct	Cycle threshold
CTC	Circulating tumour cells
CTLA4	Cytotoxic T-lymphocyte antigen
Ctrl	Control
DAPI	4’,6-diamidino-2-phenylindole
DFS	Disease Free Survival
DMEM	Dulbecco’s Modified Eagle’s Medium
DMSO	Dimethyl Supfoxide
DNA	Deoxyribonucleic Acid
DPX	Distyrene Plasticizer And Xylene
ECCM	Endothelial cell culture media
EDTA	Ethylenediaminetetraacetic acid
EMT	Epithelial-Mesenchymal Transition
EndoMT	Endothelial-mesenchymal transition
EORTC	European Organisation For Research And Treatment Of Cancer

ERK	Extracellular Signal-Regulated Kinase
FCS	Foetal Calf Serum
FDA	Food and Drug Administration of the United States
FFPE	Formalin-Fixed Paraffin-Embedded
FGF	Fibroblast growth factor
GAPDH	Glyceraldehyde 3-phosphate dehydrogenase
GMCSF	Granulocyte-macrophage colony stimulating factor
GTP	Guanosine Triphosphate
HBSS	Hanks' balanced salt solution
Hcl	Hydrochloric
HDEC	Human dermal endothelial cells
HDLEC	Human dermal lymphatic endothelial cells
HEGF	Human epidermal growth factor
HKGS	Human keratinocyte growth supplement
HR	Hazard Ratio
HUVEC	Human Umbilical Vein Endothelial Cell
IF	Immunofluorescence
IHC	Immunohistochemistry
IL	Interleukin
kDA	Kilodalton
LAP	Latency associated proteins

LC3	Microtubule-Associated Protein Light Chain 3
MAPK	Mitogen-Activated Protein Kinase
MC1R	Melanocortin 1 Receptor
MEK	Mitogen Activated Protein Kinase kinase
MIA	Melanoma inhibitory activity
min	Minute
ml	Millilitre
mm	Millimetre
mM	Millimolar
mRNA	Messenger Ribonucleic Acid
MT	Metallothionein
$mTORC_1$	Mammalian Target Of Rapamycin 1
MTS	3-(4,5-Dimethylthiazol-2-yl)-5-(3-Carboxymethoxyphenyl)-2-(4-Sulfophenyl)-2H- Tetrazolium
NaCl	Sodium Chloride
ng	Nanogram
NICE	The National Institute for Health and Care Excellence
NIHR	National Institute for Health Research
NPV	Negative predictive value
NRAS	Neuroblastoma Rat Sarcoma Viral Oncogene Homolog
P/S	Penicillin Streptomycin
PBS	Phosphate Buffered Saline

PBS/T	Phosphate Buffered Saline and Tween
PCR	Polymerase Chain Reaction
PD-1	Programmed death-1
PE	Phosphatidylethanolamine
PE	Phosphatidylethanolamine
PI3K	Phosphatidylinositol 3-Kinase
PPV	Positive predictive value
PVDF	Polyvinylidene difluoride
qPCR	Quantitative Real-time Polymerase Chain Reaction
RAF	V-Raf Murine Sarcoma Viral Oncogene Homolog
RAR	Retinoic acid receptors
RAS	Rat Sarcoma
REMARK	Reporting Recommendations For Tumour Marker Prognostic Studies
RGP	Radial growth phase
RNA	Ribonucleic acid
ROS	Reactive Oxygen Species
SCC	Squamous Cell Carcinoma
SD	Standard Deviation
SDS	Sodium Dodecyl Sulphate
SEM	Standard Error Of The Mean
shRNA	Short-Hairpin Ribonucleic Acid

shRNA	Short-Hairpin Ribonucleic Acid
siRNA	Short Interfering Ribonucleic Acid
SLNB	Sentinel lymph node biopsy
SQSTM1	Sequestasome 1
TBS	Tris-buffered saline
TBS	Tris Buffered Saline
TEM	Trans endothelial migration
TGF-β	Transforming Growth Factor B
TNF-α	Tumour Necrosis Factor A
TNM	Tumour, Node and Metastasis
UV	Ultraviolet
UVR	Ultraviolet Radiation
VDR	Vitamin D receptors
VE	Vascular endothelial
VEGF	Vascular endothelial growth factor
VGP	Vertical growth phase
α-MSH	α-Melanocyte stimulating hormone

Chapter 1

Introduction

1: Introduction

1.1 Melanocyte development and role in melanin synthesis 3

1.2 Cutaneous melanoma: a malignant transformation of melanocytes 5

1.2.1 Melanoma genesis: From melanocytes to metastases 5

1.2.2 Incidence and mortality 10

1.2.3 Genetic and environmental risk factors 12

1.2.4 Oncogenic mutations in BRAF and NRAS 14

1.3 Melanoma Disease Staging, Biomarkers and Targeted therapies 17

1.3.1 The American Joint Committee on Cancer (AJCC) 7th edition melanoma staging criteria 17

1.3.2 The American Joint Committee on Cancer (AJCC) 8th edition staging criteria 21

1.3.3 Epidermal differentiation and tumour ulceration 22

1.3.4 Biomarkers in melanoma 25

1.3.5 Current Pathway Targeted therapies 29

1.4 Pilot data leading to present study: Down regulation of epidermal AMBRA1 and relationship with TGF-β signalling 32

1.4.1 Role of AMBRA1 in cellular differentiation and proliferation 32

1.4.2 TGF-β signalling cascade and implications in melanoma 36

1.4.3 Current strategies to target TGF-β2 signalling in tumourigenesis 44

1.5 Hypothesis, Aims and Objectives 47

1.1 Melanocyte development and role in melanin synthesis

Melanocytes, through production of the pigmented biopolymer melanin, play a crucial role in forming the defence barrier of the skin, particularly providing photo protection from ultraviolet radiation (UVR). In human skin, the degree and type of pigment production manifests as a skin 'photo type', describing skin colour and ease of tanning, which is the most useful predictor of skin cancer risk in the general population [1].

Human melanocytes begin as pluripotent cells of neural crest origin, which dissociate from the developing neural tube and overlying ectoderm in the second month of embryogenesis. Subsets of these cells migrate along the dorsal lateral pathway, differentiate and are specified into melanoblasts, the precursors of melanocytes [2]. Controlled by a variety of signalling pathways, melanoblasts then proliferate and migrate to a range of destinations in the body including the skin, choroid and iris of the eye and leptomeninges of the brain where they undergo terminal differentiation and maturation into melanocytes [1].

The main and most important function of melanocytes is to manufacture melanin (melanogenesis), which protects the skin from damage through its ability to absorb and scatter harmful ultraviolet radiation (UVR). Melanogenesis takes place within melanocytes in cytoplasmic organelles called melanosomes. Pigmentation differences arise from variation in the number, size and composition of melanosomes, with relatively constant melanocyte numbers. Melanosomes are translocated along the dendritic processes of melanocytes before being incorporated into keratinocytes, where in response to UV radiation, melanin granules accumulate over the sun exposed side of nuclei to form cap-like structures [3]. Multiple keratinocytes are supplied by the dendritic processes of melanocytes distributed along the basal layer as part of epidermal melanin units [4] (Figure 1.1). In the skin, melanocytes can also accumulate in clusters as naevi in the basal layer of the epidermis and occasionally in the dermis.

There are two main types of melanin produced – red/yellow pheomelanin and brown/black eumelanin. This process is largely regulated by the melanocortin-1-receptor (MC1R) expressed on melanocytes. MC1R encodes a seven, transmembrane, G-protein-coupled receptor, which in response to UVR is activated by MC1R agonists (peptides derived from the precursor protein proopiomelanocortin), produced in the pituitary and skin in response to UVR) [5]. Activation of MC1R induces cyclic AMP (cAMP) production leading to phosphorylation of cAMP responsive-element binding protein (CREB) transcription factor family members, ultimately leading to activation of various genes and transcription factors pivotal to the expression of pigment enzymes [1]. Agonists of human MC1R including α-melanocyte stimulating hormone (α–MSH) and adrenocorticotropic hormone (ACTH) lead to an increase in photoprotective eumelanin production. Polymorphisms of the MC1R gene however, lead to a relative increase in pheomelanin production, a less photoprotective melanin subtype responsible for the red-hair and fair skin phenotype. Such individuals have a higher susceptibility to UVR damage and a higher risk of developing melanoma and other non-melanoma skin cancers [6].

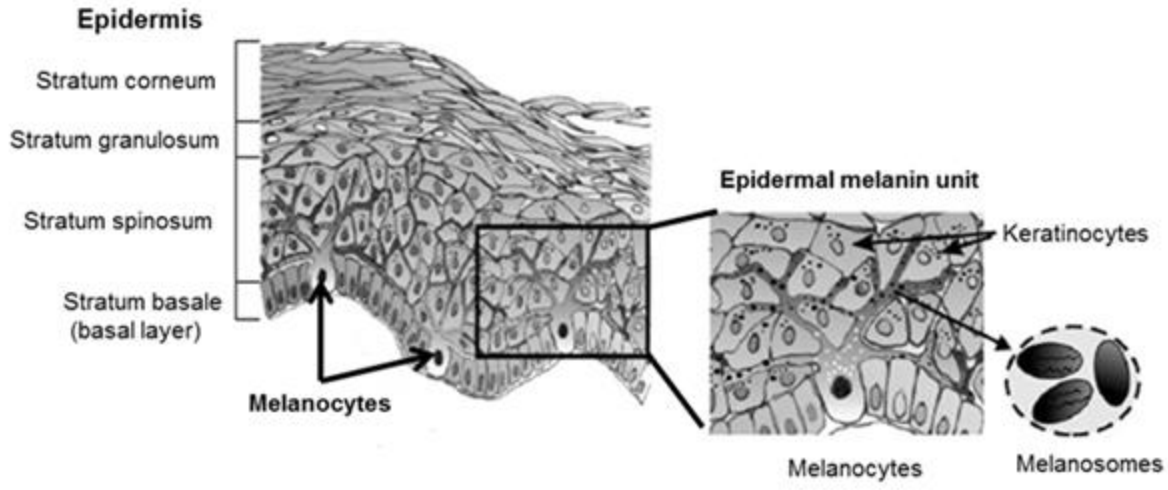

Figure 1.1: Schematic of an epidermal melanin unit. Melanocytes in the basal layer of the epidermis, through their dendritic processes, translocate melanosomes to supply several keratinocytes as part of epidermal melanin units. Adapted: Chichorek et al, 2013 [7].

1.2 Cutaneous melanoma: a malignant transformation of melanocytes

1.2.1 Melanoma genesis: From melanocytes to metastases

Malignant melanoma arises from the malignant transformation of melanocytes and this process is often modelled by a stepwise progression beginning with *in situ* neoplastic transformation of cutaneous melanocytes, followed by invasion and subsequent metastases. Disrupted intracellular signalling regulating melanocyte proliferation and spread leads to naevi formation. Melanocytic naevi are generally benign but can become dysplastic and/or undergo malignant transformation to melanoma. However, it has been observed that only 20 – 30% of melanomas arise in histological association with melanocytic naevi, indicating that a large percentage arise *de novo* [8, 9].

Melanomas begin in a radial growth phase (RGP) which is localised within the epidermis (*in situ* disease), followed by a vertical-growth phase (VGP) where melanoma cells cross the basement membrane and invade the dermis with higher metastatic potential (Figure 1.2 A – C) [10-13]. In VGP melanomas, accumulation of genetic mutations such as BRAF further facilitates progression to metastatic disease. [14]. However, not all melanomas progress through these sequential phases and RGP or VGP melanomas may both progress directly to metastatic disease [15].

Metastatic melanoma evolves when tumour cells spread through the lymph nodes to distant sites in the body. Tumour cells in invasive melanoma, via the dermal microvasculature and lymphatics, can spread to lymph nodes and subsequently distant sites (Figure 1.2 D), accelerated by alterations in the melanoma tumour microenvironment which include immune cell recruitment and angiogenesis. Angiogenesis is crucial for tumour growth and progression where several angiogenic growth factors such as vascular endothelial growth factor (VEGF), interleukin-8 or fibroblast growth factor (FGF) secreted by tumour-recruited mast cells or macrophages have been implicated in this process [16].

In addition, a process of epithelial – mesenchymal transition (EMT) has been well described in metastatic melanoma where tumour cells switch to a phenotype that exhibits higher migratory and invasive properties with alterations in the integrity of cell-cell junctions resulting in loss of contact between neighbouring cells, thereby acquiring the ability to invade surrounding tissues or migrate to secondary sites of metastasis [17].

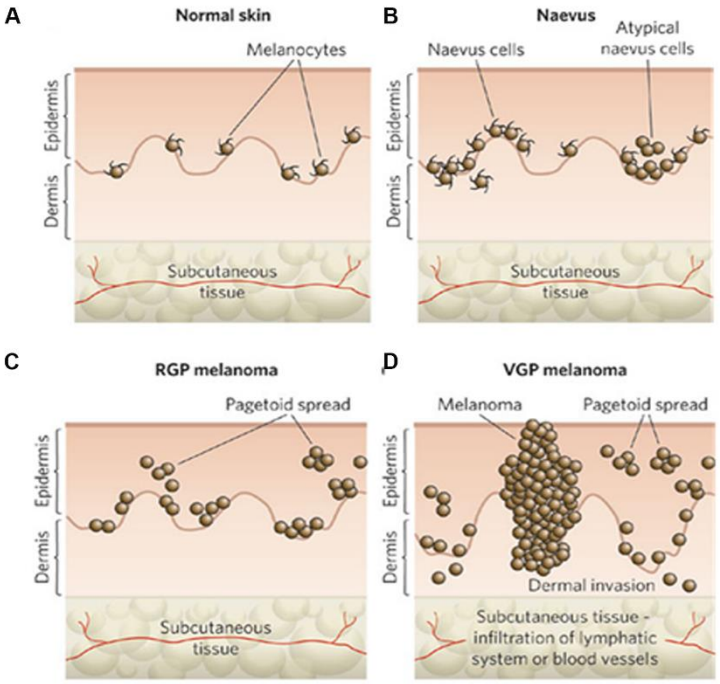

Figure 1.2: Model of melanocyte transformation and melanoma invasion. A Normal skin showing even distribution of melanocytes within the epidermal basal layer. **B** Naevi formation following proliferation of melanocytes, of which some are dysplastic with morphological atypia. **C** RGP melanoma confined to the epidermis exhibiting upward migration or pagetoid spread. **D** VGP melanoma invading the dermis with malignant potential via infiltration of the vascular and lymphatic systems. Adapted: Gray-Schopfer et al, 2007 [13]

Melanoma dissemination and metastasis is dependent on disruption of endothelial cell junctions.

Tumour induced angiogenesis results in formation of new blood vessels that have weak intercellular junctions, where barrier function is further reduced by locally secreted factors within the tumour microenvironment, enabling tumour cell entry into the vasculature [18]. During metastatic dissemination, melanoma cells can enter the circulation by direct migration through endothelial cell junctions, a process termed intravasation(Figure 1.3) [19]. Intravasation of cancer cells mainly occurs through endothelial cell junctions (paracellular transendothelial migration) [20] but can also occur transcellularly [21]. Paracellular TEM is facilitated by secretory factors from cancer cells or macrophages such as VEGF or transforming growth factor-β (TGF-β) that induce remodelling of endothelial junctions or cleavage of vascular endothelial Cadherin (VE-Cadherin), leading to the opening of endothelial cell junctions and loss of endothelial integrity (Figure 1.3) [22, 23]. Once within the vasculature, should these melanoma cells survive immune surveillance, they circulate through the bloodstream to potential secondary tumour sites where they leave the circulation by extravasation. During extravasation, cancer cells interact with platelets and leukocytes to facilitate adherence to endothelial cells and transmigration through the endothelial barrier after which they exit the circulation by invading the basement membrane [19, 24-26]. Following this, cancer cells can either proliferate within their new microenvironment giving rise to micro and macrometastases or equally can remain dormant or undergo cell death [19]. Both the processes of intravasation and extravasation of cancer cells require disruption of endothelial junctions to enable migration across the endothelium.

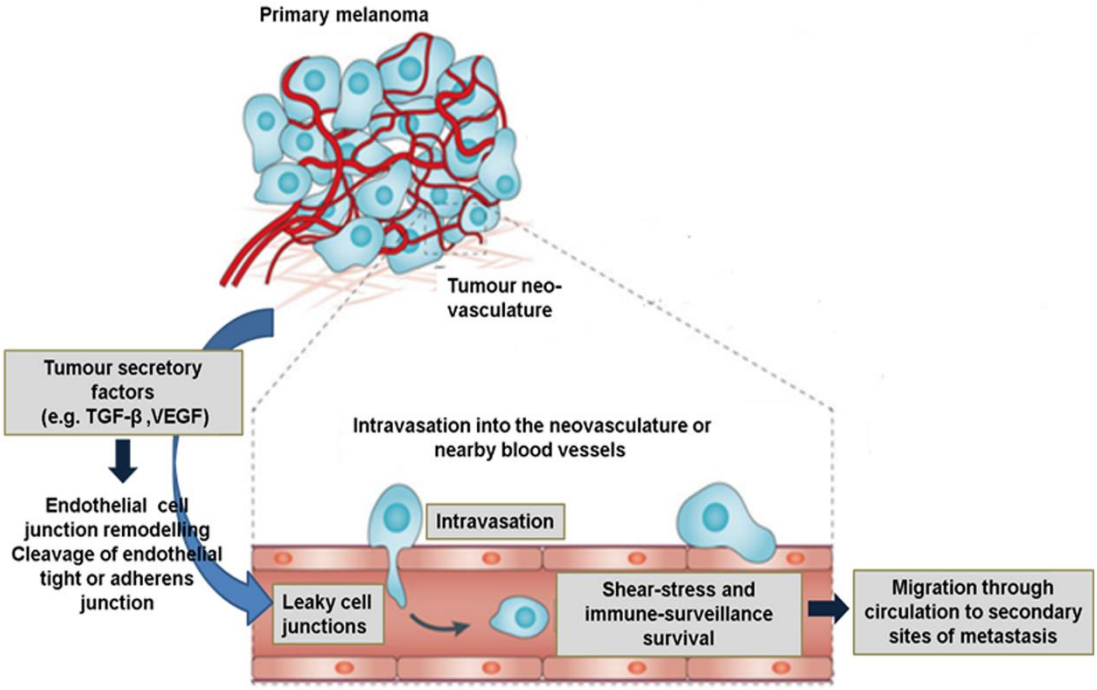

Figure 1.3: Mechanism of melanoma cell entry into the vasculature for dissemination to secondary sites of metastasis. Neovascularisation induced locally by melanoma tumours result in the formation of new blood vessels with weak intercellular junctions reduced barrier function. This is further exacerbated by tumour or tumour related secretory factors such as TGF-β or VEGF that induce opening of the endothelial cell junctions leading to endothelial cell junction remodelling or cleavage of tight and adherens junction proteins such as VE-Cadherin, resulting in reduced barrier endothelial function in the neovasculature or existing nearby blood vessels. Tumour cells may then enter the vasculature by intravasation through weakened endothelial cell junctions (paracellular transendothelial migration) and should they survive the shear-stress of immune-surveillance, migrate through the circulation to secondary sites of metastasis. Adapted: Reymond et al, 2013 [19].

Crosstalk between tight and adherens junctions in maintenance of endothelial barrier integrity.

In endothelial cells, tight and adherens junctions are intermingled throughout cell-cell contact areas where their functional interaction is required for formation, maintenance and remodelling of barrier integrity in these areas [27]. As such, endothelial barrier function requires the functional adhesive activity of VE-Cadherin and Claudin-5, two proteins that are key components of adherens and tight junctions respectively. VE-Cadherin and Claudin-5 expression are highly restricted to endothelial cell lineage where Claudin-5 represents the major claudin expressed in normal endothelial cells. VE-Cadherin has been demonstrated to be directly involved in the control of Claudin-5 expression where it prevents the nuclear accumulation of Claudin-5 repressors Fox01 and β-catenin [28] suggesting that any alterations in VE-Cadherin function will also impact on tight junction function and overall barrier integrity. In addition, endothelial growth factors such as VEGF have been shown to reversibly disrupt VE-Cadherin adhesion leading to subsequent disorganisation of tight junctions, where the chronic exposure (such as in a cancer tumour microenvironment) may lead to severe disruption of the endothelial barrier due to compromise of Claudin-5 expression [29, 30]. Equally, tight junctional molecules have also been shown to regulate cadherin-mediated adhesion in endothelial cells [31]. This interaction between VE-Cadherin and Claudin-5 expression further reinforces the functional relationship between tight and adherens junctions in maintaining endothelial barrier integrity.

1.2.2 Incidence and mortality

Malignant melanoma is an increasing public health concern worldwide and now represents the fifth most common cancer in the United Kingdom, with over 14,000 new cases diagnosed in 2013, an incidence that has more doubled over the last decade [32]. In the UK alone, the incidence of malignant melanoma is predicted to increase overall by 7% by 2035 [32], with increasing rates of up to 5.5% per year in the 20 – 45 year old age group - the 3rd highest internationally [33]. The incidence in males, particularly over the age of 65, is increasing faster than that of females with age standardised incidence rates in England (2007 – 2009) for males and females being 16.6 and 17 per 100,000 respectively (Figure 1.4) [34]. This trend is also observed worldwide with incidence rates doubling every 10-20 years in countries with white populations, faster than any other cancer type [35].

As the most aggressive form of skin cancer, malignant melanoma accounts for 75% of all skin cancer deaths, with steadily rising mortality rates in the UK. Metastatic disease carries an extremely poor prognosis with 5 year survival rates of only 5 – 15%; equating to 2500 melanoma associated deaths in the UK annually [32]. In both males and females, malignant melanoma is the 16th most common cause of cancer death, accounting for 2% of all male cancer deaths in the UK [32]. Highest mortality rates of malignant melanoma are in older males and females, with 54% of melanoma deaths per year occurring in people aged 70 or over [32, 34]. Cutaneous melanoma is also the most common cause of cancer related deaths in young individuals between 20 – 35 years of age [36].

While early stage melanomas is largely curative by surgical excision, metastatic disease represents the cause of death from melanoma in the vast majority of cases as there is still lack of consistently beneficial treatment regimens, resulting in 10 year survival rates of less than 15% [37] and emphasising the urgent need for credible biomarkers to identify high risk tumour subgroups as well as the stratification of such patients for more efficacious therapeutic approaches.

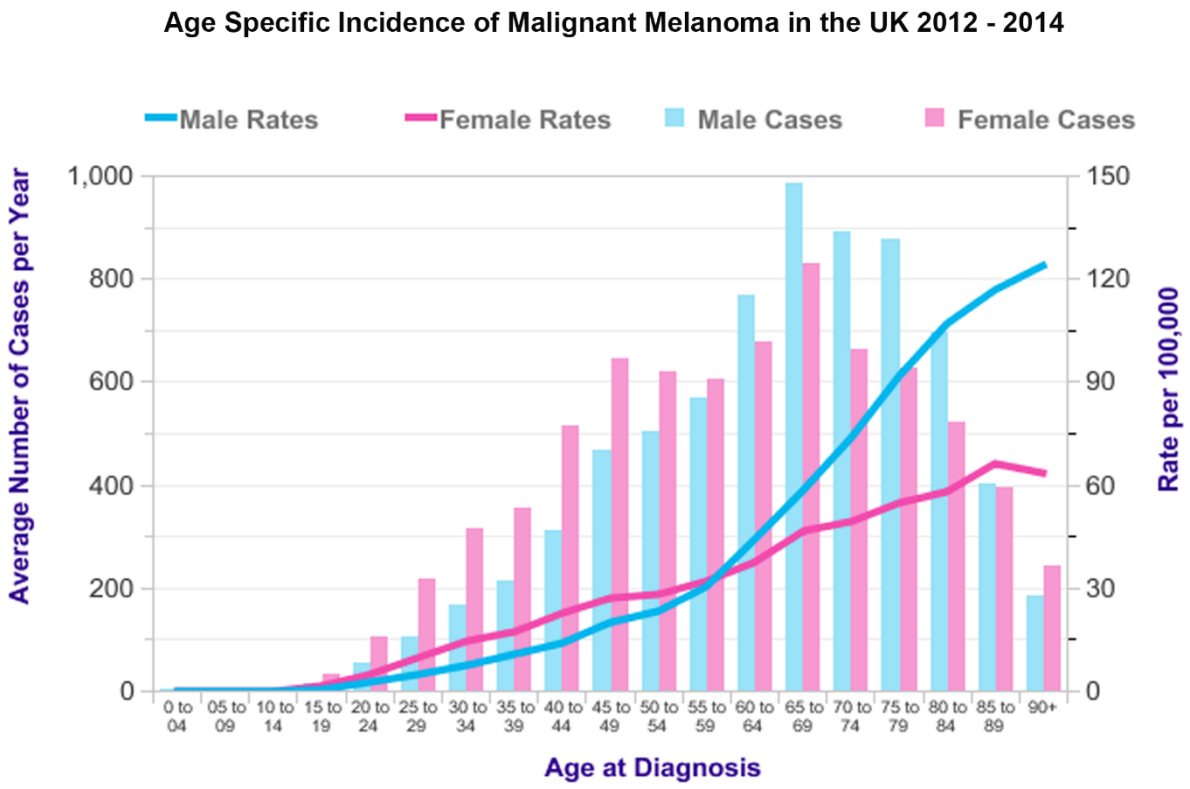

Figure 1.4: Age specific incidence of malignant melanoma in the UK 2012 – 2014. Average number of new cases per year and age specific incidence rates of malignant melanoma per 100,000 population, UK. Source: Cancer Research UK (CRUK) [32].

1.2.3 Genetic and environmental risk factors

The genesis of melanoma consists of a complex interplay of several genetic and environmental factors. Through various epidemiology studies, several predisposing factors associated with increased melanoma risk have been established (Table 1.1). Exposure to UVR remains the strongest causative link with severe episodic sunburn in early life correlating best with melanoma risk [38, 39]. Furthermore, there is evidence that that use of indoor artificial tanning devices, which deliver UVR to the skin, is also linked to melanoma risk in a dose dependent manner [40]. This corresponds with the observation that Queensland, Australia, due to its geographical location exposing its predominantly fair skin population to intense UVR has the highest rate of melanoma. Exposure of children to intense UVR also resulted in the development of melanocytic naevi early in life and in large numbers [41]. However, until recently relatively few studies have shed light on the precise molecular mechanisms by which UVR induces acquired naevi formation or drives melanoma genesis.

It is now known that heritable mutations in the cell cycle regulatory genes CDKN2A and CDK4 increases melanoma susceptibility more than tenfold, with a higher incidence in people living at lower latitudes, indicating close interactions between genetic susceptibility and UV exposure [42]. Moreover, recently, TP53 tumour suppressor (a UVR target gene in non-melanoma skin cancers) mutations have been linked to UVR-induced DNA damage in human melanoma with mutations in Trp53/TP53 accelerating $BRAF^{V600E}$-driven melanoma genesis [43] and providing novel insight into the link between UVR and melanocytic naevi formation and how in the presence of genetic susceptibility (i.e. $BRAF^{V600E}$ mutation), can lead to the induction of melanoma.

Genetic
Strong family history (≥ 3 first degree relatives affected)
Mutations in NRAS, BRAF, cKIT, cyclin-dependent kinase (CDK) and tumour suppressors such as CDKN2A and p53 [44-46]
Naevi
Multiple benign naevi (>100)
Multiple atypical naevi
Previous skin cancer
Previous melanoma
Previous non-melanoma skin cancer
Immunosuppression
Transplant recipients
Patients with AIDS
Surrogates of sun sensitivity
Type 1 skin (burns without tanning)
Freckling
Blue eyes
Red hair
UV exposure
History of blistering sunburn
Use of artificial tanning devices [40]

Table 1.1: Risk factors for melanoma. Adapted: Thomson et al, 2005 [47].

1.2.4 Oncogenic mutations in BRAF and NRAS

Perhaps one of the greatest risk factors described for cutaneous melanoma is the presence of an oncogenic mutation in the BRAF protein kinase, resulting in constitutive activation of the growth mitogen-activated protein kinase (MAPK)/extracellular signal-regulated kinase (ERK) pathway, essential in the regulation of cell proliferation, differentiation, senescence and cell survival.

The MAPK pathway is activated in response to extra cellular signalling from hormones, cytokines and growth factors [48]. These extra cellular signals activate the small GTP-proteins of the RAS family, which in turn recruit RAF protein kinases to the cell membrane, leading to activation of MEK1/2 and ERK1/2 and their downstream effectors which regulate gene expression via a variety of nuclear and cytoplasmic targets [49] (Figure 1.5).

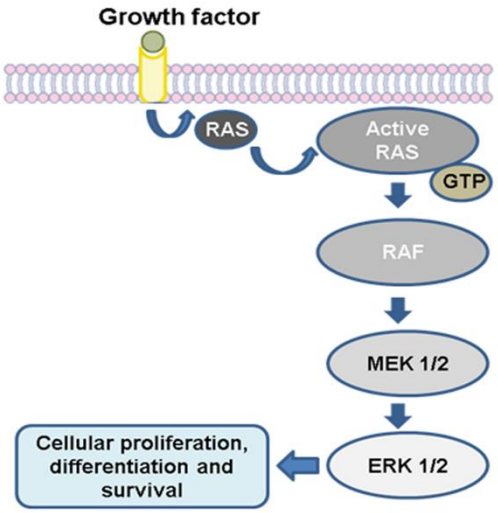

Figure 1.5: Schematic representation of the MAPK signalling cascade. RAS is activated to its GTP-bound form by extracellular signals from hormones, cytokines and growth factors. This in turn recruits RAF protein kinases leading to activation of MEK 1/2 and ERK 1/2 and their downstream effectors which regulate gene expression controlling cellular proliferation, differentiation and cell survival.

BRAF, as a member of the RAF family of serine/threonine protein kinases is the most potent activator of MEK in the MAPK/ERK pathway, initiating a kinase cascade that acts through ERK1/2 (Figure 1.5) [48]. Constitutively activating BRAF mutations may occur in approximately 40% of all primary cutaneous melanomas which lead to the hyper activation of MAPK signalling, promoting tumour proliferation, survival and resistance to apoptosis (Figure 1.6). The most common mutation in BRAF involves a thymidine to adenosine transversion at nucleotide 1799 in exon 15 of the gene, causing a V600E valine with glutamic acid substitution at amino acid 600 ($BRAF^{V600E}$ mutation) which accounts for up to 90% of all BRAF mutations [50].

RAS proteins cycle between an inactive GDP-bound form and an active GTP-bound form, thus functioning as a molecular switch for transmission of regulatory signals [51]. Approximately 20% of human cancers bear an activating RAS point mutation, mainly in codons 12,13 or 61 [52] which like mutations in BRAF, also result in MAPK hyper activation (Figure 1.6). In the context of melanoma, although 15-20% of tumours are reported to bear NRAS mutations, these are mutually exclusive and rarely is a primary NRAS and BRAF mutation observed within the same tumour [53-57].

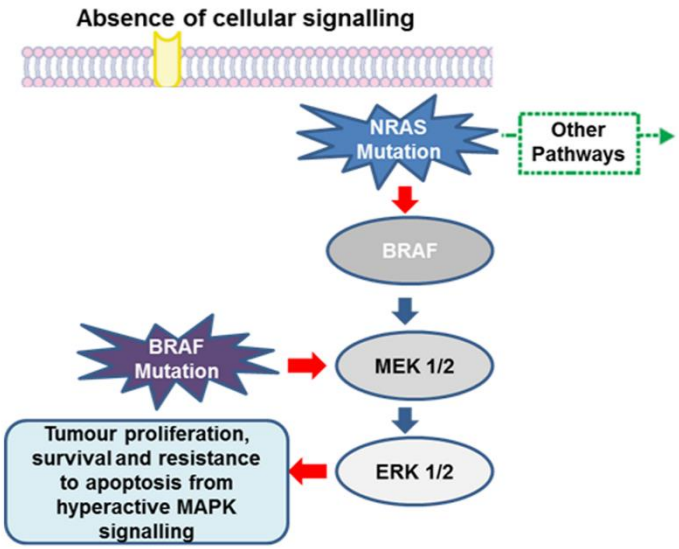

Figure 1.6: Mutations in BRAF or NRAS lead to constitutive activation of the MAPK signalling pathway. BRAF and NRAS mutations are mutually exclusive and rarely occur within the same tumour. $BRAF^{V600E}$ and NRAS mutations constitutively activate MEK and ERK in the absence of extracellular signalling, leading to hyper activation of MAPK signalling promoting tumour proliferation, survival and resistance to apoptosis. While BRAF relies on the MEK/ERK pathway for signalling, mutant NRAS can also act through other pathways.

1.3 Melanoma Disease Staging, Biomarkers and Targeted therapies

1.3.1 The American Joint Committee on Cancer (AJCC) 7th edition melanoma staging criteria

The 2009 AJCC melanoma 7th edition melanoma staging criteria is the most comprehensive staging system to date and remains the international standard for melanoma disease staging. It is the most widely used staging system to stratify patients diagnosed with melanoma according to prognosis and to guide management.

AJCC staging combines several prognostic factors known in melanoma, including the depth of invasion of tumour, rate of mitoses, presence of ulceration, evidence of metastatic spread and changes in serum lactate dehydrogenase (LDH) to allow risk stratification of morbidity and mortality at initial diagnosis.

Breslow Depth and TNM Staging Classification

In 1970, the pathologist Alexander Breslow reported that the depth of invasion was a prognostic factor in melanoma associated with disease progression in a cohort of 98 patients [58]. This has been reinforced by several studies, including a study cohort by the AJCC of 38,900 patients of varying melanoma disease stage showing that increasing Breslow depth was significantly associated with a decreased 10 year survival, re-enforcing its use as a principle tool to stratify disease risk [37]. The eponym ‘Breslow depth” has since been formalised to describe the measurement of melanoma tumour thickness from the top of the epidermal granular layer to the deepest point of invasion [59]. This has been further refined to allow classification under (T) of the TNM system of cancer staging (Table 1.2).

(T) Classification	Tumour thickness (mm)	10-year survival (%)
Tis (in situ)	Confined to epidermis	100
T1	≤1.00	92
T2	1.01 – 2.00	80
T3	2.01 – 4.00	63
T4	>4.00	50

Table 1.2: Tumour thickness (T) classification in TNM staging with associated 10-year survival. Adapted: Balch et al., 2009 [37].

The TNM Staging System was developed and is maintained by the AJCC to facilitate an international standardised system amongst different cancer types and was incorporated into the AJCC 7th edition staging system for melanoma. Alongside tumour thickness (T), TNM describes the extent of spread to the lymph nodes (N) and the presence of metastasis (M) [60].

Mitotic count and tumour ulceration

The presence of mitotic activity and tumour ulceration has been used to further subdivide the (T) staging into Ta and Tb. Increased mitotic rate constitutes the second strongest predictor of survival after tumour thickness, with the most significant threshold being 1-mitosis per mm^2 [37]. In the AJCC 7th edition staging system, the presence of ≥1 per mm^2 of mitoses increases the staging of tumours ≤1 mm thick from T1a to T1b.

The presence of loss of epidermal integrity overlying resected melanoma tumours (ulceration) has been shown to adversely affect outcome [37] with the 5-year survival of patients with melanoma deposits in >4 regional lymph nodes disease but with no

ulceration of the primary tumour dropping from 45.4% to 29.2% if ulceration is present. [61]. Its significance is highlighted in AJCC staging whereby in defining (T) stage, the presence of ulceration increases (T) staging from Ta to Tb, resulting in an increase of overall AJCC clinical stage to a category with poorer prognosis compared to a non-ulcerated tumour of same thickness [37] (Table 1.3).

AJCC Stage	TNM Stage	5-year survival rate (%)
0	Tis	100
IA	T1a	95
IB	T1b – T2a	89 – 91
IIA	T2b – T3a	77 – 79
IIB	T3b – T4a	63 – 67
IIC	T4b	45

Table 1.3: AJCC 2009 Melanoma Staging and 5-year overall survival for stage I-II disease. Adapted: Balch et al., 2009 [37].

Regional and distant metastases

While early stage localised melanoma is largely curative with surgical excision, the presence of any regional or distant site metastases (AJCC Stage III and IV) results in a significant drop in survival rates (Table 1.4). The (N) category of TNM reflects the presence of regional nodal metastases where the number of lymph node involves determines the stage. The presence of 'micrometastases' (detected using immunohistochemistry after sentinel lymph node biopsy) confers a slightly better

outcome than ‘macrometastases’, which are clinically detectable and confirmed histologically. Distant metastases are categorised as M1a – distant skin, subcutaneous, or nodal metastases, M1b – lung metastases and M1c – all other visceral metastases. Elevation of serum LDH in any metastatic disease confers a worse prognosis and automatically elevates any distant metastases regardless of site into category M1c.

AJCC Stage	TNM Stage	5-year survival rate (%)
IIIA	**T**1 – 4a **N**1a / 2a **M**0	63 – 69
IIIB	**T**1 – 4b **N**1a / 2a **M**0 **T**1 – 4a **N**1b / 2b / 2c **M**0	30 – 53
IIIC	**T**1 – 4a / b **N**1b / 2b / 2c / 3 **M**0	27 – 29
IV	**T** – Any **N**-Any **M**1a/1b/1c	9 – 19

Table 1.4: AJCC 2009 Melanoma Staging and 5-year overall survival for stage III-IV disease. Adapted: Balch et al., 2009 [37].

1.3.2 The American Joint Committee on Cancer (AJCC) 8th edition staging criteria

The AJCC 8th edition staging manual was published at the end of 2016, heralding changes in staging criteria for cutaneous melanoma of the skin which will formally come into effect at the beginning of 2018. A significant change in melanoma staging in the 8th edition manual is the classification of a melanoma as T1a if non-ulcerated and <0.8 mm in thickness and T1b if it is 0.8-1.0 mm thick or <0.8 mm with ulceration, with tumour mitotic rate being dropped completely as a staging criterion for T1 tumours [62, 63]. In addition, tumour thickness measurements will be rounded to the closest 0.1 mm as opposed to the closest 0.01 mm as in the 7th edition guidelines to accommodate the inherent lack of precision in measuring melanoma tumours. There has also been expansion of the N and M categorization of TNM with changes in N categorization leading to 4 pathological AJCC stage III subgroups (AJCC stage III A – D) rather than 3 (AJCC stage III A – C) as previously [62, 63]. With regards to N staging as well, the term micrometastasis has been dropped and replaced by “clinically occult disease as detected by sentinel lymph node biopsy (SLNB)” [62]. To date however, there is conflicting evidence on the mortality benefit of SLNB and its impact on overall survival is yet to be determined [64, 65].

Despite the impending changes in melanoma tumour staging brought about by the updated 8th edition AJCC staging criteria, data from biomarker studies presented in the result chapters will be based on the 2009 7th edition AJCC staging criteria unless indicated otherwise.

1.3.3 Epidermal differentiation and tumour ulceration

Epidermal differentiation, associated markers and role in tumour ulceration

The epidermis is the outermost functional barrier of the skin and is formed from tightly packed layers of stratified squamous epithelium, consisting predominantly of keratinocytes that make up 90% of epidermal cells, melanocytes and Langerhans cells. Keratinocytes undergo an ordered process of cornification, beginning with proliferation and differentiation of epidermal stem cells located in the *stratum basale* (the innermost layer of the epidermis) [66]. A process of graduated differentiation continues as these cells migrate supra-basally to become part of *stratum spinosum*, *granulosum* and finally, fully-differentiated corneocytes that are eventually shed through desquamation [67]. This process of keratinocyte renewal can be mapped through the epidermis via expression of proteins synthesised by keratinocytes at each level of differentiation, which form epidermal differentiation markers. These include Cytokeratins 1, 5, 10 and 14, keratinocyte transglutaminases 1 and 5 and terminal differentiation markers Involucrin and Loricrin [68, 69] (Figure 1.7). Deregulation of the sequential process of differentiation can lead to barrier dysfunction contributing to skin disease such as psoriasis and eczema, or in the case of skin neoplasms: tumour ulceration.

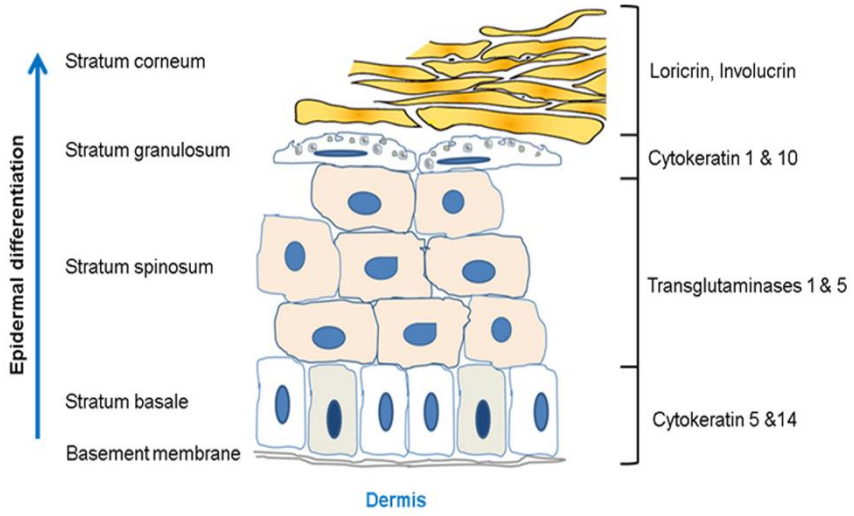

Figure 1.7: Epidermal differentiation markers expression at different layers of the epidermis. Keratinocytes undergo a graduated process of differentiation, moving up the epidermis towards the *stratum corneum* where they become terminally differentiated corneocytes which are eventually shed. This process can be mapped by the expression of proteins synthesised by keratinocytes at each level: Cytokeratin 5 and 14 in the *stratum basale*, transglutaminases 1 and 5 in the *stratum spinosum*, Cytokeratin 1 and 10 in the *stratum granulosum*, Loricrin and Involucrin in the *stratum corneum*.

Tumour Ulceration

Ulceration of a primary melanoma has been defined as an absence of an intact epidermis with reactive changes in the skin [70]. It is an independent histological prognostic marker associated with thicker melanomas and poor survival where 5 year survival rate is reduced from 80% to 55% in ulcerated stage I melanomas and from 53% to 12% for stage II melanomas [71]. The importance of tumour ulceration as a prognosticator for melanoma is reflected by its incorporation in the AJCC 2009 7th edition staging criteria and maintenance in the impending AJCC 8th edition guidelines when categorising patients into TNM stage [37, 62].

It is still unclear however, if the enigma of tumour ulceration represents the effect of an innately more aggressive and metastatic tumour phenotype expanding and breaching the top layers of the epidermis causing ulceration or if ulcerated tumours results in an increased likelihood of spread.

Paradoxically, the European Organisation for Research and Treatment of Cancer (EORTC) 18991 and 18952 trials demonstrated that patients with ulcerated primary melanomas had greater benefit with an increase in recurrence-free survival following adjuvant treatment with PEGylated interferon α-2b compared to non-ulcerated matched controls [72, 73]. This preferential benefit of treatment seen in ulcerated tumours suggests an underlying tumour secretory process leading to direct effects on the surrounding epithelium contributing to ulceration that is modified in some way by interferon-α.

1.3.4 Biomarkers in melanoma

With the emergence of novel targeted and immunotherapies for malignant melanoma, current interest is focused on the discovery of prognostic and predictive biomarkers. A biomarker refers to “any measurable diagnostic indicator that is used to assess the risk or presence of disease” [74].

Predictive biomarkers are able to indicate which patient subgroups are likely to benefit from certain treatments [75]. The best example of this in melanoma is the BRAF mutational status of a tumour where the presence of a B^{V600E} or B^{V600K} mutation acts as a biomarker in predicting responsiveness to BRAF or MEK inhibition to stratify patients for treatment with such inhibitors. BRAF status however, is neither diagnostic nor prognostic as the mutation is also present in benign naevi and there is no evidence that it has any effect on overall survival [55].

Prognostic markers are able to stratify patients at initial diagnosis according to eventual outcome and can be used clinically to guide management including earlier initiation of adjuvant therapies in patients at high risk of disease progression, potentially preventing the development of untreatable metastatic disease [76].

In melanoma, some of the best established prognostic biomarkers seen in solid tumours have been incorporated in the AJCC 2009 staging criteria. These include Breslow depth, presence of mitoses and tumour ulceration. A systemic review and meta-analysis performed by Gould Rothberg and his colleagues identified 101 immunohistochemistry-based proteins with prognostic biomarker potential in melanoma. Unfortunately, many of these tumour marker studies lacked sufficient information for adequate assessment of quality and applicability [76].

Serological biomarkers

In the recent years, there has been much focus on serum Vitamin D levels as a prognosticator in melanoma leading to its recent incorporation into the 2015 NICE guidelines on assessment and management of melanoma [77]. Low levels of serum 25-hydroxyvitamin D at primary melanoma diagnosis has been associated with high risk melanomas with thicker primaries, tumour ulceration and poorer melanoma specific survival despite conflicting evidence on overall survival and insufficient evidence to establish cause-effect [78-82]. To date, serum LDH is still the only established serological prognostic biomarker routinely used in clinical practice and incorporated into AJCC staging [83].

A systemic review on emerging biomarkers in melanoma describes other serological biomarkers including S100, Melanoma Inhibitory Activity (MIA) protein, vascular endothelial growth factor (VEGF) and microRNAs [84]. However to date, there is still no substantial evidence to validate their prognostic use in melanoma. Other prognostic biomarkers reported include the detection of circulating cancer cells (CTC) and cancer stem cell (melanoma initiating cells) markers, metallothionein (MT) expression in tumour cells and tumour lymph angiogenesis [84]. Although promising with many showing significant survival differences, to date none have undergone large rigorous prospective trials with multivariate analysis for full validation for clinical application.

Molecular predictors

More recently, there has been emergence of molecular predictors utilising melanoma gene expression profiling with evidence that gene expression phenotypes hold prognostic information and predict survival outcome in metastatic melanoma [85-87]. DecisionDX by Castle Biosciences determines metastatic risk of AJCC stage I and II cutaneous melanomas by measuring gene signatures of 31 genes on FFPE melanoma tissue with validation based on an original data set of 164 patients and a further cohort of 101 patients with 5 years follow up on outcome [88-90]. The clinical utility of DecisionDx and many other molecular predictors however, remain uncertain given they do not form companion biomarkers i.e. there is lack of a therapeutic target for intervention.

Autophagy biomarkers

Autophagy is a hot topic in cancer medicine and observations of deregulation in melanoma as well as novel therapeutic approaches through which to harness its modulation for therapeutic benefit have brought its potential as a biomarker for melanoma to the forefront of current research. Key regulatory proteins, including Atg8/microtubule-associated light chain 3 (LC3) and BECN1 (Beclin 1) have been proposed as potential prognostic biomarkers [91, 92]. However, given the dynamic nature of autophagy, their expression *in vitro* does not translate to their use as a prognostic biomarker for melanoma *in vivo* [93]. More recently, the expression of the autophagy shuttled protein Sequestosome1/SQSTM1 (p62) has been defined as an independent prognostic biomarker for AJCC stage II melanoma, where its biphasic expression reflects the paradoxical role of autophagy in melanoma [94].

In addition, expression of p62 may represent a companion biomarker of response to autophagy modulation *in vivo,* an important concept in view of emerging autophagy modulator therapies [95] and their potential to improve overall clinical outcome for patients with metastatic melanoma.

Current practice of malignant melanoma is to treat all patients with surgical excision and surveillance until metastasis ensues. However, with still no consistently beneficial treatments for metastatic melanoma, there is a push towards informing the clinical decisions, at the outset. Despite its comprehensiveness, the role of AJCC staging as a prognostic biomarker is still limited by the fact that it is unable to identify tumours that will go on to progress and metastasise, especially seemingly 'low risk' tumours of stage I disease. This emphasises the acute need for novel companion biomarkers to more accurately stratify this subset of patients at risk of disease progression for potential early targeted therapeutic intervention, preferably prior to the development of metastasis.

1.3.5 Current Pathway Targeted therapies

The discovery of activating mutations in the MAPK pathway has undoubtedly revolutionised therapy for melanoma, leading to the development of new generation BRAF and MEK inhibitors, that for patients stratified by the presence of a BRAF mutation now form main line therapy for metastatic disease for which the BRAF mutational status of an individual tumour is perhaps the best example of a companion biomarker [96].

Initial therapy with BRAF inhibitors Vemurafenib (Zelboraf®, Roche, Basel, Switzerland) and Dabrafenib (Tafinlar®, GlaxoSmithKline, Brentford, UK) results in dramatic antitumor activity [97-99], increasing progression free survival by up to 6 months. However, the beneficial effects of BRAF inhibition are short lived, and after a matter of months, the development of acquired resistance is inevitable in most patients [96, 100]. Re-activation of the MAP kinase pathway is thought to be mediated by the acquisition of an additional NRASQ61 mutation or several MEK1 mutations [101], providing the rationale for the clinical use of MEK inhibitors.

More recently, two different combinations of BRAF inhibitors plus MEK inhibitors (Dabrafenib plus Trametinib (Mekinist®, GlaxoSmithKline) and Vemurafenib plus Cobimetinib (COTELLIC®, Roche) have shown higher response rate, longer progression-free survival and overall survival compared with BRAF inhibition alone in phase III clinical trials [102-105]. Treatment with combined BRAF plus MEK inhibitors however was associated with a higher toxicity profile and increased incidence of adverse events compared to monotherapy of either drug alone [104]. Due to significantly better survival outcomes, combination therapy remains mainstay therapy for BRAF V^{600} melanoma however, clinician awareness of the specific set of associated adverse events ultimately determines the use of combination therapy over monotherapy [104].

Overall however, growing concerns over drug resistance to molecular targeted therapies still exists and the optimal treatment approach for management of patients with disease progression while on treatment with BRAF/MEK inhibitors remains under active investigation [106]. In addition, not all melanomas harbour a BRAF mutation and equally not all BRAF mutant melanomas response to targeted therapies with BRAF/MEK inhibition. The rational combination of BRAF/MEK targeted therapies to address resistance or combining BRAF inhibition with other effective therapies such as immunotherapy may therefore improve overall outcome [107].

The introduction of immune modulating antibodies has further improved the outlook for patients with metastatic melanoma. Ipilimumab (Yervoy®, Bristol-Myers Squibb, NY, USA) a cytotoxic T-lymphocyte antigen (CTLA4) blocking antibody, was the first checkpoint inhibitor to be approved by the FDA in 2011 for the treatment of metastatic melanoma following significantly improved median overall survival compared to the control arms in randomised clinical trials [108, 109]. In 2014, Pembrolizumab (Keytruda®, Merck, NJ, USA) a programmed death-1 (PD-1) checkpoint inhibitor was approved for the treatment of BRAF mutated metastatic melanoma that has progressed on treatment with Ipilimumab and BRAF inhibitors, following results of a randomised clinical trial demonstrating increased overall response rates with tumour shrinkage following treatment with Pembrolizumab [110]. Another PD-1 inhibitor, Nivolumab (Opdivo®, Bristol-Myers Squibb) demonstrated improved overall survival, progression free survival and a comparable side effect profile in comparison with Dacarbazine for the treatment of previously untreated melanomas without a BRAF mutation, leading to FDA approval in 2014 [111].

The emergence of BRAF/MEK targeted therapies and immunotherapies have undeniably revolutionised treatment of metastatic melanoma, particularly in the last decade. The impressive initial responses seen following treatment with BRAF inhibitors coupled with prolonged duration of response seen with immunotherapy has driven a move towards combination therapy to further improve outcome with several clinical trials (NCT02130466 and NCT02027961) currently evaluating PDL1/PD1 antibodies combined with BRAF and/or MEK inhibitors [112].

Despite significant breakthroughs in the treatment of metastatic melanoma, there is as of yet still no consistently effective method to determine metastatic risk in early AJCC stage melanomas at time of primary diagnosis, nor any method of adjuvant therapy to prevent disease progression of high risk tumours. Moreover, with increasing focus on personalised medicine and targeted therapy, there is an urgent need for companion biomarkers to enable stratification of high risk patients for early adjuvant therapies to prevent the development of metastasis.

1.4 Pilot data leading to present study: Down regulation of epidermal AMBRA1 and relationship with TGF-β signalling

1.4.1 Role of AMBRA1 in cellular differentiation and proliferation

The process of cellular differentiation is an energy consuming process with oxidative mitochondrial metabolism shown to regulate keratinocyte differentiation [113, 114]. Autophagy, as the principle catabolic process for lysosomal mediated degradation and recycling of damaged organelles and excess proteins has energy providing capacity, supporting its role in differentiation. Activating molecule in Beclin 1 regulated protein 1 (AMBRA1) is a component of the Beclin 1/VPS34 complex and involved in the formation of PI3K rich membranes during the nucleation phase of autophagy [115]. As a key autophagy initiating regulatory protein, AMBRA1 represents a potential marker of autophagy induction as well as a possible therapeutic target for autophagy inhibition. However, in addition to its functional role in autophagy, a growing body of evidence supports a role for AMBRA1 in cellular differentiation [113, 114], with evidence that the protein plays a role in early neuronal differentiation of stem cells which activate autophagy to fulfil their high energy demands [116]. AMBRA1 has also been shown to regulate cell proliferation with Ambra1$^{+/gt}$ heterozygous mice having a three-fold increase in cancer susceptibility and AMBRA1 deficient tumour cells having increased growth capability [117]. This highlights the role of AMBRA1 in cellular differentiation and proliferation, where when dysregulated is pro-tumorigenic and in the context of epidermal differentiation, may promote tumour ulceration.

In line with these findings, pilot data leading up to the present study has demonstrated the role of AMBRA1 in epidermal differentiation with expression *in vivo* increasing in line with keratinocyte differentiation from the basal layer of the epidermis to the uppermost layer, the *stratum corneum* (Figure 1.8) [118].

In addition, knockdown of ATG7 (an alternative autophagy regulatory protein) in calcium-induced differentiated primary keratinocytes *in vitro* demonstrated impaired autophagy with no effect on Loricrin upregulation. In contrast, in addition to impairment of LC3-II induction, siRNA mediated knockdown of AMBRA1 resulted in the significant down regulation of Loricrin suggesting that the role of AMBRA1 in keratinocyte differentiation is independent of its pro-autophagy role, or at least independent of Atg7 (Ellis and Lovat, unpublished data).

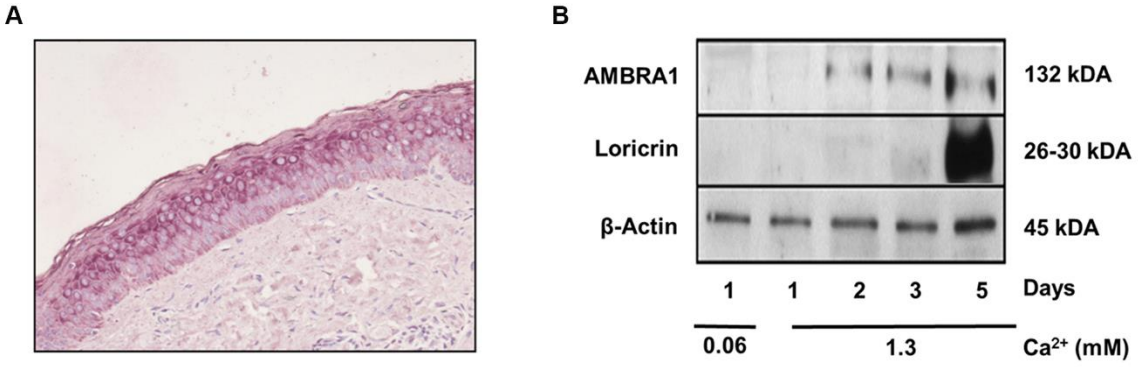

Figure 1.8: Epidermal differentiation is associated with increased expression of AMBRA1. **A** Expression of AMBRA1 increases in line with keratinocyte differentiation from the basal layer of the epidermis to the *stratum corneum.* **B** Representative western blot for the expression of AMBRA1 (132 kDA), Loricrin (26-30 kDA) and β-Actin (45 kDA) depicting concurrent increase in the expression of terminal differentiation marker Loricrin, with increased AMBRA1 expression when primary keratinocytes were cultured in high calcium conditions to induce differentiation (Ellis & Lovat, unpublished data).

More strikingly, AMBRA1 expression was observed to be lost in the epidermis overlying many cutaneous melanomas (Figure 1.9 A) which did not correlate with the degree of epidermal invasion (Figure 1.9 B) and was not observed in benign nevi (Ellis and Lovat, unpublished data). These data suggest that the expression of AMBRA1 in the melanoma microenvironment may have prognostic potential. In addition, there was no correlation with Breslow depth, suggesting that epidermal AMBRA1 expression may represent a biologically distinct biomarker (Ellis and Lovat, unpublished data).

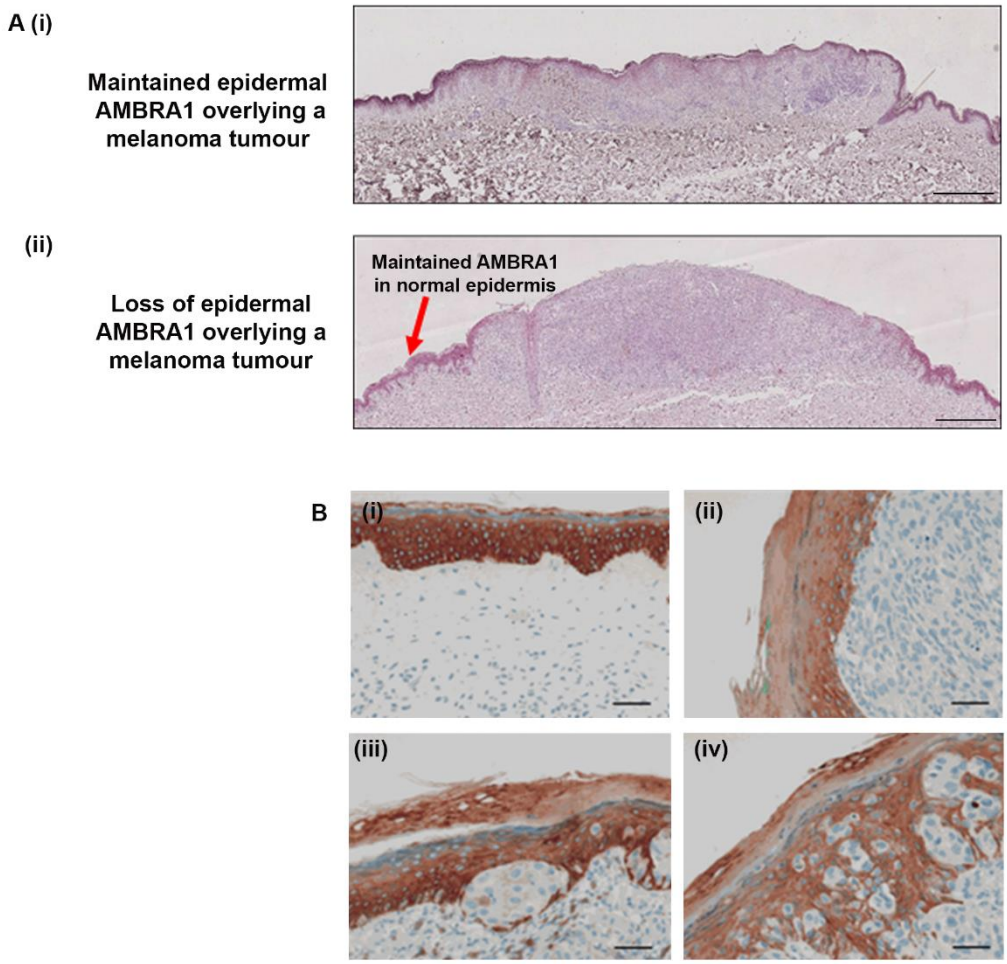

Figure 1.9: Epidermal AMBRA1 loss is not associated with the degree of tumour invasion. A Representative IHC images of AMBRA1 expression revealed by VIP counterstaining (pink) depicting **(i)** maintained and **(ii)** loss of epidermal AMBRA1 expression overlying 2 separate melanoma tumours compared with that of the normal adjacent epidermis. Scale bar =100 μm. **B** Representative IHC images of Cytokeratin 5/6 expression in epidermis with melanoma tumour invasion present revealed by DAB counterstaining (brown). Cytokeratin 5/6 expression levels shown are associated with correlating epidermal AMBRA1 expression levels: **(i)** no AMBRA1 loss, **(ii)** some AMBRA1 loss or **(iii & iv)** complete AMBRA1 loss, depicting no correlation between epidermal invasion and epidermal AMBRA1 expression. Scale bar =50 μm (Ellis and Lovat, unpublished data).

The presence of epidermal hyperplasia and hyperkeratosis observed in melanoma tumours that have lost epidermal AMBRA1 expression (Ellis and Lovat, unpublished data), coupled with the lack of association between AMBRA1 expression and epidermal tumour invasion suggests that these morphological changes are due to a chronic, tumour secretory process, rather than direct tumour invasion of the basal cell layer, a process subsequently shown to be significantly associated with increased tumour expression of transforming growth factor (TGF)-β2 (TGF-β2) (Ellis and Lovat, unpublished data).

1.4.2 TGF-β signalling cascade and implications in melanoma

The secretory polypeptide TGF-β, represented by three isoforms, TGF-β2, TGF-β2 and TGF-β3, signals via receptor serine/threonine kinases and intracellular Smad effectors, exerting multiple effects on numerous biological functions including cellular proliferation, differentiation and apoptosis. TGF-β is initially synthesised in an inactive form, associated with latency associated proteins (LAPs) in a large latent complex (LLC) [119]. Latent TGF-β can be activated in several ways including conformational change of LAPs induced by thrombospondin-1 (TSP-1), upregulation of alpha v beta 6 ($\alpha_v\beta_6$) integrin, mechanical contraction of stromal myofibroblasts and also in response to low pH levels in the environment or the production of irradiation-induced reactive oxygen species (ROS) [120]. These result in proteolytic cleavage of the latent complex and the release of active TGF-β, which binds to TGF-β receptors, propagating downstream signalling.

Active TGFβ ligands transduce signalling via three types of TGF-β receptors (TGF-βR), TGF-βRI (also known as activin receptor-like kinase 1-7 (ALK1-7), TGF-βRII, and TGFβRIII (betaglycan, endoglin in endothelial cells) [121]. In most tissues, TGF-β ligands form heterotetrameric TGF-βRII/ALK5 complexes between two TGF-βRIs and two TGF-βRIIs where TGFβ-RII phosphorylates and activates TGF-βRI, which then interacts with R-Smads, resulting in their phosphorylation [122]. Phosphorylated Smads form heterotrimeric complexes with co-Smads: coactivators (Smad4) or co-repressors (C-SKI, SNON) which translocate into nuclei of cells to modulate gene expression (Figure 1.10) [123].

TGF-β signalling is balanced by a negative feedback loop mediated by the inhibitory Smad7, which can bind to TGF-βRI to prevent Smad activation as well as recruit protein phosphatase PP1/GADD34 which dephosphorylates TGF-β receptors or E3 ubiquitin ligases SMURF1 and 2 which induces proteosomal degradation of the receptors (Figure 1.10) [124-127].

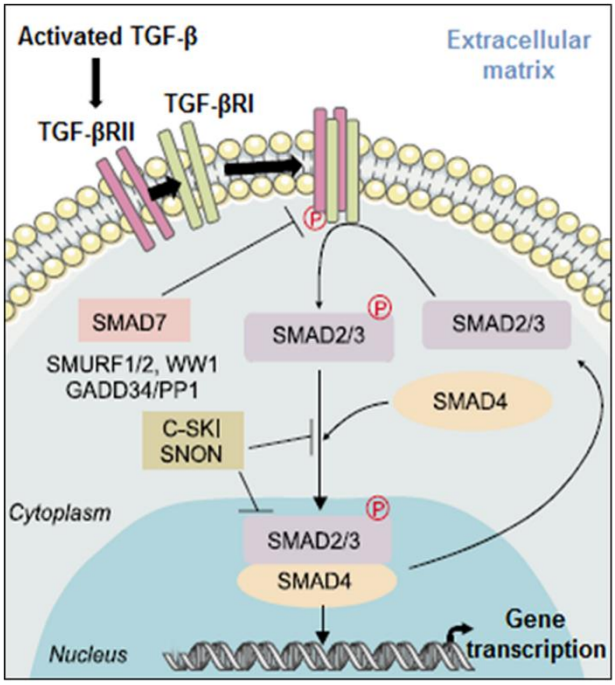

Figure 1.10: The canonical TGF-β/Smad signalling pathway. Activated TGF-β ligands bind to TGF-βRII, which recruits, phosphorylates and activates TGF-βRI (ALK5), forming heterotetrameric TGF-βRII/ALK5 complexes. TGF-βRI interacts and phosphorylates R-Smads (Smad2/3) which associate with co-Smads (Smad4) to form complexes that are translocated into cell nuclei to regulate target gene transcription. Inhibitory Smad7 binds to TGF-βRI to prevent Smad activation or recruit PP1/GADD34 and E3 ubiquitin ligases (SMURF1/2) to degrade or dephosphorylate the TGF-β receptor. C-SKI and SNON function as transcriptional co-repressors to repress TGF-β/Smad driven transcription. Adapted: Perrot et al, 2013 [127].

TGF-βII/ALK5 is the predominant receptor complex responsible for signal transduction in most cell types. It activates Smad2 and 3 as part of the canonical TGF-β/Smad-dependent signalling pathway whereas ALK1, with predominant expression in endothelial cells and sites of epithelial-mesenchymal interactions, activates Smad1 and Smad5 [128-131]. In endothelial cells, TGF-β can transduce signals via ALK1 and 5 with both pathways having opposing effects. ALK5 inhibits endothelial cell migration and proliferation whereas ALK1 stimulates both these processes [129, 132] (Figure 1.11). However, it is important to note that TGF-β signalling can also be transduced

through activation of other non-Smad pathways such as PI3 K/Akt, RhoGTPase, Mek/Erk and p38/MAPK pathways [120].

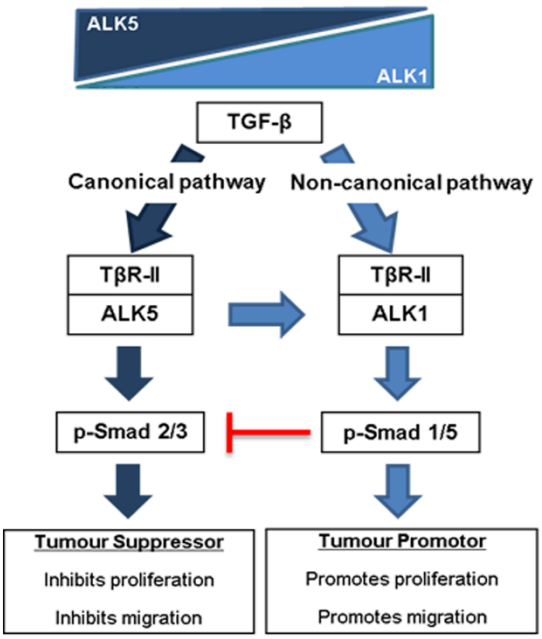

Figure 1.11: Schematic model for activation of TGF-β mediated ALK 1 and 5 signalling in endothelial cells. Active TGF-β binds to TGF-βRII which recruits, phosphorylates and activates ALK5 and signalling down the canonical pathway. TGF-β can also signal down the non-canonical pathway through ALK1 which also can be recruited by ALK5 into the complex. Activated ALK1 and 5 phosphorylates Smad 1/5 and 2/3 respectively with opposing effects in endothelial cells. ALK5 inhibits endothelial cell migration and proliferation whereas ALK1 stimulates both these processes. The preferential activation of either canonical or non-canonical TGF-β signalling determines if TGF-β functions as a tumour suppressor or promoter of tumour progression. Adapted: Goumans et al, 2003 [129].

TGF-β2 signalling in melanoma

The role of TGF-β in carcinogenesis and tumour progression is complex with its effects known to be highly cell-type specific and context dependent. For instance, TGF-β is known to act as a tumour suppressor in early tumorigenesis however may promote tumour invasiveness and metastasis in later stage disease [127, 133].

In melanoma, autonomous activation of the TGF-β/Smad pathway has been well documented [134, 135] with TGF-β secretion by melanoma cells exerting both autocrine and paracrine effects that are cytostatic in early stages but coupled with its effect on the tumour microenvironment, promote tumour invasion and progression in advanced stages (Figure 1.12) [127]. The TGF-β pathway has also been shown to promote an epithelial to mesenchymal transition (EMT), allowing cancer cells to become metastatic and this is believed to be similar to the process melanoma cells undergo during transition from radial to vertical growth phases [136, 137].

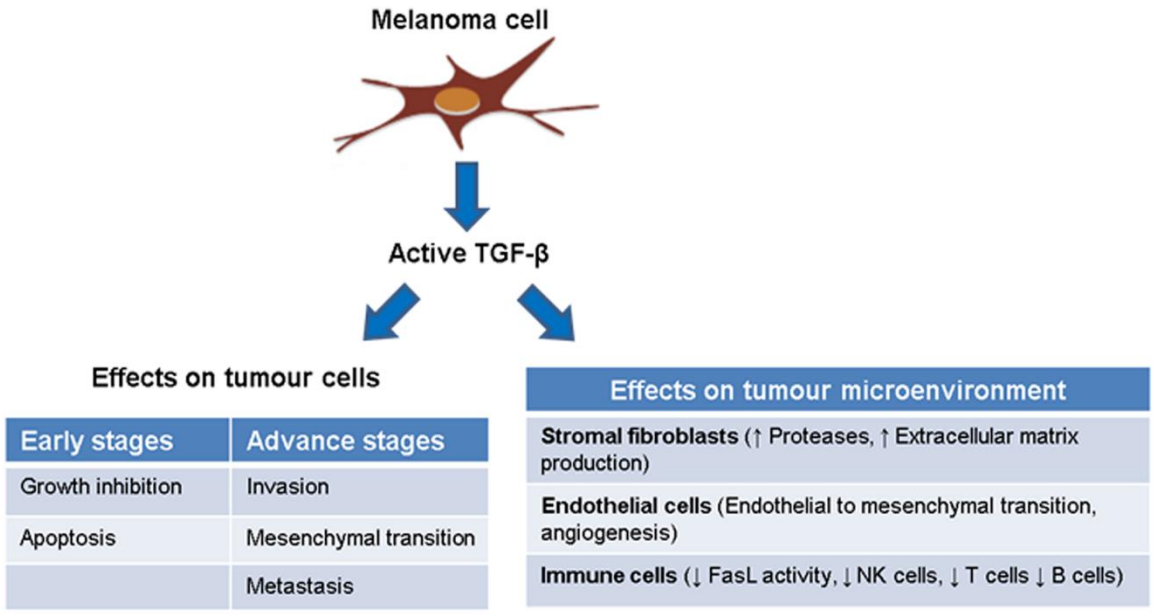

Figure 1.12: Effects of TGF-β on melanoma cells and the tumour microenvironment. High levels of TGF-β expressed and secreted by melanoma cells exert cytostatic effects on early stage tumours however, switches to a tumour promoter role in advanced melanoma. TGF-β secreted also affects stromal fibroblasts, endothelial cells and immune cells in the tumour microenvironment, acting to promote tumour growth, invasion and angiogenesis with reduced immune surveillance. Adapted: Perrot et al, 2013 [127].

In addition, studies have demonstrated that TGF-β induces the expression of interleukin-8, a factor well documented to be involved in angiogenesis, growth and melanoma metastasis [138, 139] and that stable overexpression of inhibitory Smad7 in human melanoma cells inhibits tumourigenesis both *in vitro* and *in vivo* in mice models [140], reinforcing the importance of TGF-β signalling in melanoma metastasis.

Despite high levels of nuclear phosphorylated Smad2 found in benign melanocytic naevi, melanomas in situ and primary invasive melanomas (confirming hyperactivation of the TGF-β/Smad pathway in melanocytic tumours), phospho-Smad2 positivity was associated with low tumour thickness and did not correlate with survival or metastases [141]. This is in keeping with the observation that melanoma cells exhibit a variable degree of resistance to the anti-proliferative action of TGF-β and that this may be further attenuated in advanced disease, the mechanisms of which still remain elusive [142]). A review of proposed mechanisms for the resistance of melanomas to TGF-β-mediated tumour suppression included deregulation of transcription factors-coactivator repressors (Ski/SnoN upregulation, c-myc upregulation, Smad 2/3 linker phosphorylation), cell cycle G_1 – S effectors (Cyclin D1 overexpression, activating mutations in CDK4 or downregulation of p15, p21 or p27), upregulation of MIA or loss of Filamin expression, and suggested that different mechanisms or a combination of these different mechanism may propagate resistance, specific to different melanoma tumours and their unique tumour microenvironment [142]. This suggests that an 'invasive switch' that may be responsible for the critical switch from RGP to VGP and subsequent progression may be via a non-canonical Smad signalling pathway (Figure 1.11).

In vitro studies on melanoma cell lines have shown that there is increased expression of TGF-β2 and 3 isoforms with little or no expression in normal melanocytes [143]. While the TGF-β1 isoform is primarily associated with tumour progression in human cancers, increased levels of TGF-β2 have been measured in the plasma of patients with metastatic melanoma with *in vivo* studies demonstrating that increased secretion of TGF-β2 and 3 in particular, is associated with melanoma progression and metastases [144-147] and that TGF-β2 expression also correlates with tumour thickness and invasiveness [148].

In addition, melanoma cells have been shown to switch between high and low melanin pigment states during metastasis where microarray analysis demonstrated upregulation of TGF-β2 in a subpopulation of poorly pigmented cells within a melanoma tumour, with *in vitro* studies confirming that TGF-β2 signalling induced hypopigmentation and hypermotility in these cells, enabling entry into blood vessels [149].

In line with this, preliminary results leading up to the present study has demonstrated a significant association between increased isoform specific tumoural TGF-β2 and not TGF-β3 expression with loss of epidermal AMBRA1 in all AJCC stage melanomas (Ellis and Lovat, unpublished data, Figure 1.13). Moreover, highest expression of tumoural TGF-β2 was observed in ulcerated melanoma tumours known to be associated with a worse prognosis. Collectively, these data suggest that the specific expression or enhanced secretion of TGF-β2 by primary melanomas may lead to down regulation of epidermal AMBRA1 and in turn, loss of epidermal integrity with potentially a similar process leading to endothelial breach, paving a route for melanoma ulceration and metastasis. The targeting of TGF-β2 signalling may therefore prove a viable therapeutic strategy to prevent the development of melanoma metastasis, for which the epidermal loss of AMBRA1 may be a companion biomarker.

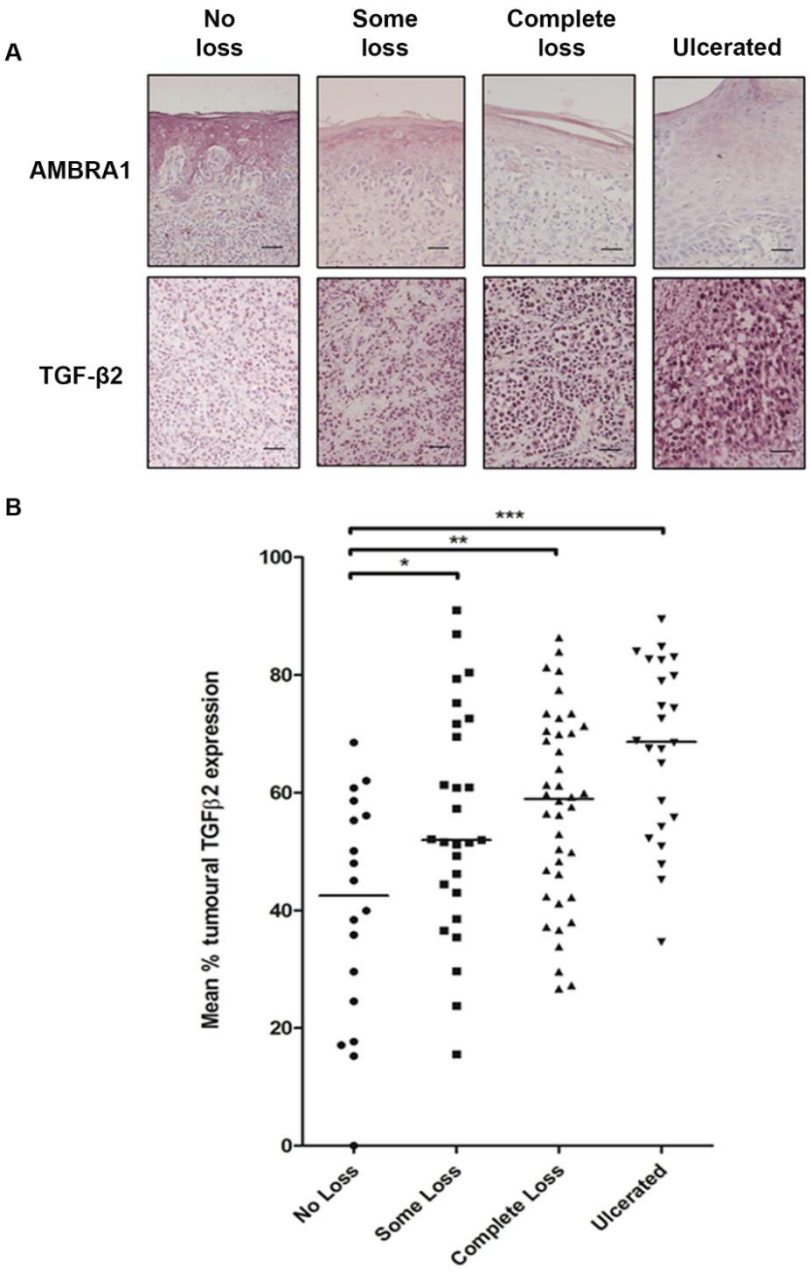

Figure 1.13: Loss of Epidermal AMBRA1 overlying primary cutaneous melanomas correlates with increased tumoural secretion of TGF-β2. A Representative IHC photomicrographs depicting no loss, some loss or complete loss of epidermal AMBRA1 expression overlying the tumour or in the adjacent epidermis of ulcerated melanomas of varying AJCC disease stage in association with tumoural expression of TGF-β2. Scale bar =50 μm. **B** Scatter graph depicting mean % tumoural TGF-β2 expression levels in 109 melanomas of varying AJCC stages where there was no, some or complete loss of epidermal AMBRA1 expression or where the epidermis was ulcerated. Each point represents % tumoural TGF-β2 expression levels derived from analysis of 10 representative 200x magnification microscope fields of vision using Leica QWin image analysis software. Horizontal line represents mean % tumoural TGFβ2 expression levels. One-way ANOVA with Tukey's post hoc correction, * P <0.05, ** P <0.01, **** P <0.0001 (Ellis and Lovat, unpublished data).

1.4.3 Current strategies to target TGF-β2 signalling in tumourigenesis

Several TGF-β inhibitors have been developed for cancer therapy and demonstrated efficacy in preclinical trials but none have been approved for clinical use to date. Generally, these agents target TGF-β signalling at three levels: the ligand, the receptors or down-stream signal transduction and include ligand traps (monoclonal neutralizing antibodies against TGF-β, soluble TGF-β receptors and TGF-β receptor antibodies), antisense oligonucleotides blocking TGF-β ligand production and receptor kinase inhibitors [150].

In the context of pan-TGF-β inhibition, Fresolimumab (GC1008), a monoclonal antibody that neutralizes all isoforms of TGF-β, has been evaluated in advanced melanoma patients with phase I/II trials demonstrating evidence of anti-tumour activity [151]. Its use however, was associated with the development of eruptive keratoacanthomas/SCCs, possibly due to its non-specific pan-inhibitory effects on TGF-β signalling [152].

With regards to specific targeting of TGF-β2 signalling, Lucanix™ (Belangenpumatucel-L, NovaRx, San Diego, CA, USA), a TGF-β2 antisense vaccine has reached phase III trials in advanced stage non-small cell lung cancer with suggested survival benefits [153]. Trabedersen (AP12009, Antisense Pharma, Munich, Germany), an antisense oligonucleotide targeting TGF-β2 has shown encouraging survival results in phase I/II clinical trials for advanced pancreatic cancer, metastatic melanoma and glioblastoma [154, 155]. Its use however, was limited by off-target toxicity and challenges faced in achieving direct delivery of the drug to tumours to avoid this [156, 157]. The FANG™ vaccine (rhGMCSF/shRNAFurin, Gradalis, Tx, USA), an autologous tumor-based product incorporating a plasmid encoding granulocyte-macrophage colony-stimulating factor (GMCSF) and a novel bi-functional short hairpin RNAi (bi-shRNAi) targeting furin convertase, targets TGF-β1 and 2 and has entered phase II clinical trials for treatment of advanced melanoma (NCT01453361), colorectal carcinoma (NCT01505166) and ovarian cancer

(NCT01309230) following initial trial results demonstrating prolonged survival in advanced solid tumours [158].

Alternatively, specific targeting of the TGF-β receptor complex (i.e. targeting ALK5 or ALK1) may prove to be a more efficacious approach to minimise off target effects seen in pan-TGF-β2 inhibition. In addition, despite ligand inhibitors limiting the bioavailability of active TGF-β ligands, they may fail to effectively block downstream receptor signalling. Given this, small molecule inhibition of receptor kinases has been an emerging area of experimental cancer drug development in the recent years as these agents are easy and economical to produce as well as practical as they are stable when delivered orally [159].

To date, Galunisertib (LY2157299, Eli Lilly, Indianapolis, USA), a small molecule inhibitor of TGF-βRI (ALK5), is the most advanced TGF-β signalling inhibitor in clinical which in phase II clinical trials has shown improvement in overall survival in advanced hepatocellular carcinoma patients with normal alpha-fetoprotein (AFP) and reduced serum TGF-β1 following treatment [160]. Galunisertib has also entered/is emerging from phase II clinical trials for treatment of pancreatic cancer, glioma and glioblastoma [161]. Similarly, TEW-7917 (MedPacto, Suwon, South Korea), another small moledule inhibitor of ALK5 has entered phase I clinical trials for the treatment of advance stage solid tumours (NCT02160106) [161].

More recently, specific receptor targeting of the TGF-β/ALK complex with ALK1 inhibitors has emerged as a target for antiangiogenic cancer therapy and is currently evaluated in various malignancies (advanced solid tumours and refractory multiple myeloma)[162]. Dalantercept (Acceleron Pharma, MA, USA) an ALK1 ligand trap that inhibits activation of endogenous ALK1 by binding with high affinity to the ligands bone morphogenetic proteins (BMP 9 and 10), was initially evaluated for clinical use in head and neck and renal carcinomas but failed to progress through phase II clinical trials due to lack of efficacy [163-165].

PF03446962 (Pfizer, NY, USA) a monoclonal antibody targeting ALK1 has emerged from phase I clinical trials with encouraging results observed in solid tumours and hepatocellular carcinoma with good side effect profile and tolerability [166, 167] however, to date the therapeutic use of ALK1 inhibitors has not been evaluated in malignant melanoma [162].

1.5 Hypothesis, Aims and Objectives

While novel targeted and immunotherapies have revolutionised therapeutic approaches in malignant melanoma, unfortunately there is still lack of consistently beneficial treatments and moreover, no credible biomarkers able to predict disease progression of high risk tumours.

Despite its comprehensiveness, the role of AJCC staging as a prognostic biomarker is still limited by the fact that it is unable to identify tumours that will go on to progress and metastasise, especially seemingly 'low risk' tumours of stage I disease. This emphasises the acute need for novel companion biomarkers to more accurately stratify this subset of patients at risk of disease progression for potentially earlier and more efficacious precision based therapies.

Work leading up to this study suggests that the combined loss of epidermal AMBRA1 and Loricrin overlying AJCC stage I melanoma tumours defines a high risk subgroup for which a patent has been filed (**UK Patent 2014:** 1419976.4.4, Inventors RE Ellis, M Labus and PE Lovat). The primary aim of this study is therefore to refine and validate the prognostic potential of epidermal AMBRA1 and Loricrin expression in an independent powered cohort of AJCC stage I melanomas.

Key pilot data (as described in section 1.4) demonstrated that treatment of primary keratinocytes cultured in high calcium medium to induce differentiation, with recombinant TGF-β2 results in the down regulation of AMBRA1 and Loricrin, suggesting that TGF-β2-mediated de-regulated epidermal differentiation may be a pivotal process in melanoma ulceration (Ellis and Lovat, unpublished data). As well as further exploring the signalling mechanisms (specifically the contribution of canonical or non-canonical TGF-β2 signalling) by which melanoma specific secretion of TGF-β2 mediates loss of epidermal integrity, this study additionally aimed to test the hypothesis that a similar mechanism mediates the loss of endothelial integrity whereby the down regulation of endothelial AMBRA1 and cell junctional protein expression leads to

endothelial breach and metastatic spread (Figure 1.14), for which combined epidermal AMBRA1 and Loricrin expression may represent a companion biomarker to stratify patients for potential novel adjuvant TGF-β targeted therapy at the time of primary excision.

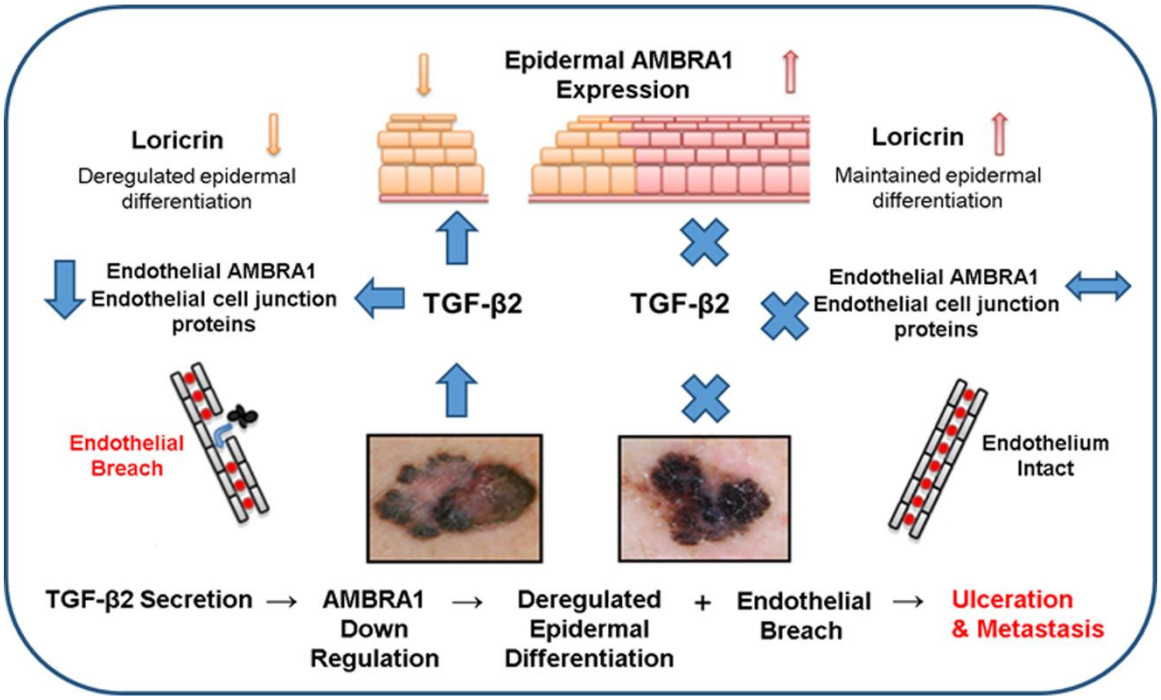

Figure 1.14: Hypothesis for TGF-β2 mediated AMBRA1 down regulation, loss of epidermal and endothelial integrity, tumour ulceration and metastasis. TGF-β2 secretion by some melanomas results in down regulation of AMBRA1 leading to deregulated epidermal differentiation, marked by loss of Loricrin expression. A similar mechanism may exist in the endothelium by which TGF-β2 signalling via ALK1-Smad1/5 mediates down regulation of AMBRA1 which results in endothelial breach, enabling tumour entry and metastatic spread.

To test these hypotheses, the specific objectives of this research project were to:

1. Refine and validate the combined epidermal expression of AMBRA1 and Loricrin as prognostic biomarkers for AJCC stage I melanomas.
2. Confirm the association of increased TGF-β2 expression with loss of epidermal Loricrin and epidermal/endothelial AMBRA1 expression in an independent cohort of AJCC stage I melanomas.
3. Define the mechanisms mediating TGF-β2-induced loss of epidermal and endothelial integrity.
4. Inform the development of novel stratified TGF-β2 targeted adjuvant therapies to prevent melanoma metastasis at the time of primary excision with the use of combined epidermal AMBRA1/Loricrin expression as a companion biomarker

Chapter 2

Materials and Methods

2: Materials and Methods

2.1 Growth and maintenance of primary human keratinocytes, endothelial cells, human endothelial and melanoma cell line 53

2.1.1 Human Umbilical Vein Endothelial Cells (HUVEC) 53

2.1.2 Primary Human Dermal Lymphatic Endothelial Cells (HDLEC) 53

2.1.3 CCD1106 Keratinocytes 54

2.1.4 Human A375 melanoma cells pre subjected to stable knockdown of TGF-β2 54

2.2 Isolation, growth and calcium induced differentiation of primary human keratinocytes 55

2.3 Isolation of primary human dermal endothelial (HDEC) cells 56

2.3.1 Isolation of HDEC using endothelial cell-specific antibody EN4 coated wells.....56

2.3.2 Isolation of HDEC using PE anti human CD31 antibody and Miltenyi Biotech Magnetic Columns 57

2.4 Treatment of HUVEC, HDLEC cells and CCD1106 keratinocytes with human recombinant TGF-β2 in the presence or absence of an ALK5 inhibitor 58

2.5 Treatment of HUVECs and HDLECs with TGF-β2 rich melanoma supernatants or supernatants derived from melanoma cells in which TGF-β2 has been stably knocked down 59

2.6 CellTiter 96® Aqueous Non-Radioactive Cell Proliferation Assay (MTS).....60

2.7 siRNA-mediated knockdown of ALK1 in HUVEC cells 61

2.8 Real Time Reverse Transcriptase Polymerase Chain Reaction (qPCR).....63

2.9 Western blotting 67

2.10 Immunohistochemistry for formalin fixed paraffin embedded (FFPE) tissue 70

2.10.1 Immunohistochemistry for AMBRA1, Loricrin, CD31 and TGF-β2 using DAB counterstaining 70

2.10.2 Bleaching of FFPE melanoma tissue prior to analysis of TGF-β2 using DAB counterstaining 72

2.10.3 Immunohistochemistry for AMBRA1 and TGF-β2 using VIP counterstaining 72

2.11 Immunofluorescence for AMBRA1 and CD31 expression in FFPE HUVEC cell pellets and melanoma tissue 74

2.12 Patient Cohort Selection and Database development 76

2.13 Analysis of Immunohistochemistry by Slide Scanner 80

2.13.1 Analysis and scoring of epidermal and endothelial AMBRA1 expression 80

2.13.2 Analysis and scoring of epidermal Loricrin expression 84

2.13.3 Analysis of tumoural TGF-β2 expression 85

2.14 Statistics and Bioinformatics Analysis 86

2.1 Growth and maintenance of primary human keratinocytes, endothelial cells, human endothelial and melanoma cell line

2.1.1 Human Umbilical Vein Endothelial Cells (HUVEC)

The endothelial cell line HUVEC (ATCC, Middlesex, UK) was cultured in T75 tissue culture flasks (Corning, Flintshire, UK) pre-coated with 0.2% gelatin (Sigma-Aldrich; Poole, UK) and maintained at 37°C in 10ml of Endothelial Cell Basal Medium (Lonza, Walkersville, USA) supplemented with Endothelial Growth Medium Bullet Supplement (Lonza, USA; comprising bovine brain extract (BBE), human epidermal growth factor (HEGF), hydrocortisone, ascorbic acid, Gentamicin, Amphotericin B and foetal bovine serum), $5x10^{-5}$ M N-6,2'-O-dibutyryl-adenosine 3', 5'-cyclic monophosphate (Sigma-Aldrich), 1 µg/ml hydrocortisone acetate (Sigma-Aldrich), 5% Penicillin-Streptomycin (10,000 U/ml Penicillin, 10mg/ml Streptomycin (PS); Sigma-Aldrich) and 10% foetal calf serum (FCS; Sigma-Aldrich) (complete ECCM), in a humidified atmosphere of 5% CO_2 in air. Cells were passaged every 2 – 3 days at approximately 70% confluency by detaching with Trypsin EDTA (TE; Sigma-Aldrich) as previously described [168] and cultured for up to a maximum of 50 passages at which point fresh cells were taken from frozen stocks, with a change in culture flask every 3 passages.

2.1.2 Primary Human Dermal Lymphatic Endothelial Cells (HDLEC)

Primary HDLECs (Promocell, Heidelberg, Germany) were cultured in T75 tissue culture flasks pre-coated with 0.2% gelatin and maintained in 10ml of complete ECCM, at 37°C in a humidified atmosphere of 5% CO_2 in air. Cells were passaged every 5 days at approximately 80 – 90% confluency by detaching with TE as previously described [168] and cultured for up to a maximum passage number of 5, with a change of culture flask at every passage.

2.1.3 CCD1106 Keratinocytes

The retrovirus vector transformed human keratinocyte cell line CCD1106 (ATCC) was cultured in 10 ml of Epilife Medium (ThermoFisher Scientific, Loughborough, UK) supplemented with 5ml of Human Keratinocyte Growth Supplement (HKGS; ThermoFisher Scientific) and 1% PS (complete Epilife) in T75 tissue culture flasks and maintained at 37°C in a humidified atmosphere of 5% CO_2 in air. Cells were passaged every 2 – 3 days at 70 – 80% confluency and cultured for up to a maximum passage number of 8 at which point fresh cells were taken from frozen stocks, with a change of culture flask every 3 passages.

2.1.4 Human A375 melanoma cells pre subjected to stable knockdown of TGF-β2

Stable knockdown of TGF-β2 using short hairpin RNA (shRNA or using a control short hairpin RNA) was performed in human cutaneous A375 melanoma cells by Dr Marco Corazzari, University of Tor Vergata Rome, Italy. TGF-β2 knockdown in A375 cells was confirmed by Real Time Reverse Transcriptase Polymerase Chain Reaction (qPCR) and control (A375 shControl) or A375 cells in which TGF-β2 expression had been depleted (A375 shTGF-β2) were cultured and maintained in T75 tissue culture flasks in 10 ml of Dulbecco's Modified Eagle Medium (DMEM; Lonza, Slough, UK) supplemented with 10% FCS and 1% PS (complete DMEM) at 37°C in a humidified atmosphere of 5% CO_2 in air and passaged every 2 – 3 days at 80% confluency. To prevent genetic drifts and other morphological changes in cells, all modified A375 melanoma cell lines were not passaged beyond 10 passages before replacing with frozen stocks.

2.2 Isolation, growth and calcium induced differentiation of primary human keratinocytes

Primary human keratinocytes were isolated from human foreskin samples obtained from routine circumcision with informed patient consent. Ethical approval was granted by Newcastle and North Tyneside Research Ethics Committee (Ref: 08/H0906/95+5_Lovat) and sponsored by The Newcastle Upon Tyne NHS Foundation Trust (Ref 4775).

Foreskin samples were rinsed with phosphate buffered saline (PBS; Sigma-Aldrich) containing 5% Penicillin-Streptomycin-Amphotericin (10,000 U/ml Penicillin, 10 µg/ml Streptomycin and 25 µg/ml Amphotericin B (PSA; Lonza, UK) in 10 cm petri dishes (Corning). Following removal and disposal of subcutaneous tissue, the epidermis of the remaining sample was scored using a blade prior to overnight incubation in PBS with 10% Dispase II (Sigma-Aldrich) and 10% PSA at 4°C to facilitate epidermal-dermal separation. The epidermis was then peeled off, incubated in TE at 37°C for 5 minutes, neutralised in DMEM with 10% FCS, and centrifuged at 330 g for 5 minutes. The keratinocyte cell pellet derived from this was re-suspended and cultured in 20 ml of Complete Epilife, in T150 – T175 tissue culture flasks, maintained at 37°C in a humidified atmosphere of 5% CO_2 in air.

Primary keratinocytes were passaged at approximately 80% confluency by detaching with TE as previously described [168] and used for subsequent experiments between passages 1 – 5 in the presence or absence of differentiation which was induced by switching culture medium to Epilife medium containing 1.3 mM of Calcium Chloride ($CaCl_2$; Sigma-Aldrich) for 5 days.

2.3 Isolation of primary human dermal endothelial (HDEC) cells

2.3.1 Isolation of HDEC using endothelial cell-specific antibody EN4 coated wells

Human dermal endothelial cells (HDEC) were isolated from the remaining dermis of human foreskin samples, following processing and peeling of the epidermal layer as described in 1.2. After removal of the epidermis, a cell scraper (Corning) was used to remove cells from the top layer of the dermis into complete ECCM. This dermal cell suspension was then filtered through a sterile 100 µm cell strainer (Corning), centrifuged at 330 g for 5 minutes and the cell pellet re-suspended in 4 – 6 ml of complete ECCM, prior to seeding 2 x 10^4 cells/cm^2 in a volume of 2 ml of complete ECCM per well of a 6 well tissue culture plate (Corning) pre-coated with 0.2% gelatin. Cells were cultured at 37°C in a humidified atmosphere of 5% CO_2 in air, with media changes every 2 – 3 days and upon reaching 70% confluency, detached with TE as previously described [168].

To eliminate contaminating cells such as dermal fibroblasts, detached cells at passage 0 were incubated overnight at 37°C in 0.5 ml of complete ECCM in endothelial cell-specific antibody EN4 (Monosan, Newmarket, UK) coated 24 well tissue culture wells (Corning) as previously described [169]. Briefly, EN4 antibody coated wells were pre-prepared by incubating 200 µl of EN4 antibody diluted 1:6 in Hanks' balanced salt solution (HBSS; Sigma-Aldrich) with 1 mM $CaCl_2$ in each well of a 24 well tissue culture plate for 3 hours at 37°C, followed by blocking of non-specific antibody binding with 1% Bovine Serum Albumin (BSA; Bioscience, Nottingham, UK) for 1 hour at 37°C. Following overnight incubation of detached passage 0 cells as described above, non-adherent cells were removed with x3 PBS washes. Adherent isolated endothelial cells were then detached using TE, pooled together and cultured in 3 ml of complete ECCM in a T25 0.2% gelatin coated tissue culture flask with culture medium changes every 2 – 3 days.

2.3.2 Isolation of HDEC using PE anti human CD31 antibody and Miltenyi Biotech Magnetic Columns

To eliminate contaminating cells such as dermal fibroblasts, HDEC cell selection was also attempted using a human Phycoerythrin (PE) anti CD31 antibody (CD31-PE; Miltenyi Biotec, Surrey UK) with Miltenyi Biotech Magnetic Columns (Miltenyi Biotec). Following initial isolation and culture as described in 1.3.1, passage 0 primary endothelial cells with fibroblast contamination were detached with TE at 80% confluency [168]. 5 x 10^6 cells were suspended in 2 ml of complete ECCM and centrifuged 330 g for 5 minutes, after which the supernatant was discarded, the cell pellet re-suspended in 5 ml of PBS and passed through a 30 µm CellTrics mesh filter (Sysmex, Milton-Keynes, UK) to form a single cell suspension which was then centrifuged again for 5 minutes at 330 g. The cell pellet obtained was re-suspended in 40 µl of buffer solution (BS) consisting of PBS with 0.5% BSA and 2 mM Ethylenediaminetetraacetic acid (EDTA; Sigma-Aldrich) followed by addition of 5 µl of FcR blocking reagent (Miltenyi Biotec) and 5 µl of CD31-PE antibody with gentle mixing every 2 – 3 minutes for 10 minutes at 4°C. After x2 washes with 0.5 ml of BS and centrifugation for 5 minutes at 330 g, the cell pellet derived was re-suspended in 35 µl of BS with addition of 5 µl of FcR blocking reagent and 10 µl of anti-PE microbeads (Miltenyi Biotec) and gently mixed for 15 minutes at 4°C. Following x2 washes in 500 µl BS and centrifugation at 330 g, the resulting cell pellet was then resuspended in 500 µl of BS and passed through an MS MACS column (Miltenyi Biotec) with an attached MiniMACS Separator magnet (Miltenyi Biotec). The collected eluate was labelled as the negative population. The MS column was then washed a further x3 with 500 µl BS and the negative population effluent discarded. Finally, the MS column was detached from the magnet, 1 ml of BS added and a plunger firmly applied to expel CD31 positive endothelial cells into a new collection tube. Collected cells were suspended in 5 ml of complete ECCM and cultured in T25 cell culture flasks pre-coated with 0.2% gelatin at 37°C in a humidified atmosphere of 5% CO_2 in air, with media changes every 2 – 3 days.

2.4 Treatment of HUVEC, HDLEC cells and CCD1106 keratinocytes with human recombinant TGF-β2 in the presence or absence of an ALK5 inhibitor

Human recombinant TGF-β2 (Sigma-Aldrich) was reconstituted with sterile 4 nM Hydrochloric Acid (VWR, Lutterworth, UK) containing 0.1% BSA to produce a stock concentration of 1 µg/ml and stored in working aliquots of 6 µl or 20 µl at -20°C. At 90 – 100% confluency, HUVEC or HDLEC cells were detached with TE as previously described [168], seeded onto 0.2% gelatin coated 60 mm cell culture dishes at a density of 2 x 10^5 cells/dish in 3 ml of complete ECCM and left overnight to attach at 37°C in a humidified atmosphere of 5% CO_2 in air before subsequent treatment and continued incubation with 10 ng/ml human recombinant TGF-β2 (diluted in complete culture medium) for 24, 48 or 72 hours or an equal volume of vehicle (complete culture medium) control prior to processing for Western Blot analysis

Primary keratinocytes were seeded at 2.4 x 10^4 cells/well in 6 well tissue culture plates and maintained until 100% confluency in 2 ml/well of Complete Epilife, then switched to culture in Complete Epilife with high $CaCl_2$ (1.3 nM) for 5 days to induce differentiation prior to the addition of 10 ng/ml human recombinant TGF-β2 for the final 24 – 48 hours of incubation.

5 mg ALK5 inhibitor II (Santa Cruz Biotechnology, Heidelberg, Germany) was reconstituted with 5 ml of 100% Dimethyl Sulfoxide (DMSO; Fisher Scientific, Loughborough, UK) and 12.4 ml of sterile H_20 to produce a stock concentration of 1 mM and stored in working aliquots of 30 µl at -20°C. HUVEC cells were seeded onto 0.2% gelatin coated 60 mm cell culture dishes at a density of 2 x 10^5 cells/dish in 3 ml of complete ECCM, co-treated with 10 ng/ml of human recombinant TGF-β2 in the presence or absence of 10 µM ALK5 inhibitor II (again further diluted in complete culture medium) or an equal volume of culture medium vehicle control for 24 hours prior to processing for Western blot analysis or RNA extraction.

2.5 Treatment of HUVECs and HDLECs with TGF-β2 rich melanoma supernatants or supernatants derived from melanoma cells in which TGF-β2 has been stably knocked down

At 80% confluency, high TGF-β2 secreting A375 melanoma cells (A375 shControl) and melanoma cells in which TGF-β2 has been stably knocked down (A375 shTGF-β2) were detached with TE as previously described [168], seeded at 2.4 x 10^4 cells/well in 6 well tissue culture plates and cultured in either 2 ml/well of complete DMEM or complete ECCM for 72 hours. The effect of culture in complete DMEM or ECCM on cell proliferation was then assessed by manual cell counting using a haemocytometer.

Supernatants derived from A375 shControl and A375 shTGF-β2 melanoma cell lines pre-cultured to confluency in complete ECCM for 72 hours were then collected and used as the culture medium for HUVEC or HDLEC cells for 72 hours in replacement of complete ECCM and with daily changes with fresh supernatants to account for nutrient depletion.

The effects on AMBRA1 and Claudin-5 expression in HUVEC and HDLEC cells treated with either supernatants or complete ECCM (negative control) or ECCM containing 10 ng/ml of recombinant TGF-β2 was evaluated by western blotting or a commercial cell viability assay as described in 1.6.

2.6 CellTiter 96® Aqueous Non-Radioactive Cell Proliferation Assay (MTS)

HUVECs or primary HDLECs were seeded at a density of 0.5 x 10^5 cells/well in 0.2% pre-coated gelatin 96 flat well tissue culture plates (Corning) with 4 replicates per treatment condition, in a volume of 200 µl/well of complete ECCM and allowed to attach overnight at 37ºC in a humidified atmosphere of 5% CO_2 in air. The following day, medium from each well was replaced with fresh complete ECCM, complete ECCM medium containing 10.0 ng/ml and 20.0 ng/ml human recombinant TGF-β2 or A375 shControl or shTGF-β2 cell supernatants for 24, 48 or 72 hours. Additionally, the effect on HUVEC cell proliferation in the presence of an ALK5 inhibitor was assessed by the concurrent addition of 10 µM ALK5 inhibitor II and 10.0 ng/ml of human recombinant TGF-β2 or an equal volume of vehicle control added to control for 72 hours.

Cell viability was assessed by the addition of 20 µl of CellTiter 96 Aqueous Assay Reagent (Promega, Southampton, UK) for 3 hours at 37ºC and measuring the absorbance at 490 nm with a SpectraMAX 250 plate reader (Molecules Devices Ltd, Wokingham, UK).

2.7 siRNA-mediated knockdown of ALK1 in HUVEC cells

To transiently knock down the expression of ALK1 in HUVEC endothelial cells, 3 different siRNAs oligoribonucleotides targeting human ALK1 (Invitrogen, Carlsbad, CA, USA, Table 2.1) were evaluated against a non-targeting scrambled siRNA control (Invitrogen).

ALK1 siRNA	Sequence	
ACVRL1HSS100150	1	5’ – UCAAGAGCCGCAAUGUGCUGGUCAA – 3’
	2	5’ – UUGACCAGCACAUUGCGGCUCUUGA – 3’
ACVRL1HSS100151	1	5’ – GGAGGACUAUAGACCACCCUUCUAU – 3’
	2	5’ – AUAGAAGGGUGGUCUAUAGUCCUCC – 3’
ACVRL1HSS100152	1	5’ – CCAGAGAAGCCUAAAGUGAUUCAAU – 3’
	2	5’ – AUUGAAUCACUUUAGGCUUCUCUGG – 3’

Table 2.1: Duplex siRNA oligoribonucleotides targeting human ALK1.

6 x 10^5 HUVEC cells were seeded into 60 mm tissue culture petri dishes pre-coated with 0.2% gelatin, in a volume of 3 ml of complete ECCM and allowed to attach overnight. The following day, a pre-transfection mix consisting of 20 μM of each pool siRNA and 8 μl of Lipofectamine RNAi Max (Invitrogen), was prepared in 3 ml/dish of complete ECCM in absence of PSA and Gentamicin, per transfection condition with 30 minutes incubation at room temperature. In the meantime, adhered HUVEC cells were rinsed in PBS prior to addition of 3 ml of the siRNA/lipofectamine mix and continued

incubation for 24 hours at 37°C in a humidified atmosphere of 5% $C0_2$. Each transfection was then repeated for a further 24 hours to increase efficacy.

Cells were then trypsinised, resuspended in 3 ml of complete ECCM, and seeded at 3 x 10^5 cells/well in 6 well flat bottom cell culture plates pre-coated with 0.2% gelatin in a volume of 2 ml of complete ECCM and incubated overnight at 37°C to allow attachment. The following day, cells were treated with human recombinant TGF-β2 (Sigma-Aldrich) at 10 ng/ml for 2 or 24 hours with an equal volume of vehicle control added to no treatment control cultures. Cells were then harvested and processed for western blot analysis as previously described [170] or for RNA extraction as described in section 2.8 with lysates/RNA additionally derived from cells in absence of TGF-β2 treatment as a control.

2.8 Real Time Reverse Transcriptase Polymerase Chain Reaction (qPCR)

Real Time Reverse Transcriptase Polymerase Chain Reaction (qPCR) was used to quantify AMBRA1, ALK1 and ALK5 mRNA expression in HUVEC cells and CCD1106 keratinocyte cells as well as verify siRNA-mediated knockdown of ALK1 in HUVEC cells.

All cell lines were seeded at 3 x 10^5 cells/well in a volume of 3 ml/well of their respective cell culture medium, in 6 well flat bottom cell culture plates pre-coated with 0.2% gelatin for 24 hours prior to RNA extraction. Extraction of RNA was performed using TRIzol Reagent (Invitrogen, Carlsbad, CA, USA) according to the manufacturer specifications. Total RNA for each sample was quantified using a NanoDrop 2000 Spectrophotometer and its accompanying software (Thermo Scientific, Waltham, Massachusetts, USA). RNA was then stored at -80°C prior to conversion to single stranded cDNA using a Reverse Transcription Kit (Promega, Madison, Wisconsin, USA) as per manufacturer's recommendations. 20 µl of PCR reverse transcription reactions (first-strand cDNA synthesis) were prepared for each sample as detailed in Table 2.2. cDNA from the first-strand reverse transcription reaction was then diluted to 100 µl with Nuclease-Free water for PCR amplification.

Reverse Transcription Reaction (Promega)	
Component	**Amount**
Magnesium Chloride 25mM	4µl
10X Reverse Transcription Buffer	2µl
dNTP Mix (10mM)	2µl
Recombinant RNAsin Ribonuclease Inhibitor	0.5µl
AMV Reverse Transcriptase HC (25u/µl)	0.6µl
RT Random Primers (0.5µg/µl)	1µl
Total RNA	2µg
Nuclease-Free Water	to 20µl
Total volume	**20µl**

Table 2.2: Constituents of a single Reverse Transcription Reaction.

PCR reactions for cDNA amplification were then performed using a Veriti 96-well Thermal Cycler (Applied Biosystems, Foster City, CA, USA) at conditions of 10 minutes at 70°C, 45 minutes at 45°C, 5 minutes at 95°C prior to a cooling cycle at 4°C. cDNA was stored short term at 4°C or -20°C long term.

The expression levels of AMBRA1, ALK1 and ALK5 mRNA relative to the housekeeping control of L34 mRNA were subsequently measured using qPCR. A Maxima SYBR Green Master Mix (Thermo Scientific) was used to produce fluorescently labelled PCR products during repetitive cycling of the amplification

reaction with the melting curve protocol adopted to verify probe specificity as described previously [170]. Primer sets for all amplicons were designed using the Primer Express 1.0 software system (Roche, Basel, Switzerland) as detailed in Table 2.3. Master reaction mixes were prepared for each gene sequence of interest to a volume of 25 µl/well in a 96-well PCR plate (Thermo Scientific) according to the manufacturer's recommendations, and as detailed in Table 2.4. Each qPCR reaction was prepared in replicates of three. qPCR was performed using a Rotor-Gene 6000 Real-Time PCR Machine (Corbett Research Ltd, Cambridgeshire, UK). The thermocycling program consisted of one cycle at 50°C for 2 minutes (pre-treatment) followed by 95°C for 10 minutes (initial denaturation) and 40 cycles at 95°C for 15 seconds (denaturation) and 60°C for 1 min (annealing/extension).

Amplicon	**Primer sequence**	
L34	Forward	5'-GTCCCGAACCCCTGGTAATAGA-3'
	Reverse	5'-GGCCCTGCTGACATGTTTCTT-3'
ALK1	Forward	5'-CATCGTGAATGGCATCGT-3'
	Reverse	5'-CACACACACCACCTTCTTC-3'
ALK5	Forward	5'-GCCTTGAGAGTAATGGCTAAA-3'
	Reverse	5'-CCTTCCTGTTGACTGAGTTG-3'
AMBRA1	Forward	5'-AACCCTCCACTGCGAGTTGA-3'
	Reverse	5'-TCTACCTGTTCCGTGGTTCTCC-3'

Table 2.3: Primer sets for amplification of L34, ALK1, ALK5 and AMBRA1 gene sequences.

Maxima SYBR Green Master Mix	
Component	**Amount**
Maxima SYBR Green Master Mix for qPCR	12.5µl
Forward Primer	0.2 µl
Reverse Primer	0.2µl
cDNA	5µl
Nuclease-Free Water	7.1µl
Total volume	25µl

Table 2.4: Constituents of a single qPCR reaction using the Maxima SYBR Green Assay.

Real time mRNA expression was analysed using the accompanying Rotor-Gene 6000 software (Corbett Research Ltd). The result of the fluorescent PCR was expressed as the threshold cycle (CT). CT values for each sample was normalized to the reference mRNA, L34 to obtain a ΔCT value which is the difference between the CT for the specific mRNA and the CT for L34. The fold change in ALK1 and ALK5 gene expression was calculated using the comparative 2-ΔΔCT method where 2 was raised to the power of ΔΔCT (the difference between the ΔCT from treated cells and the CT from untreated cells) [170].

2.9 Western blotting

Total protein was extracted from cells at the end of experimental treatment by direct lysis of cell pellets, derived from initial seeding of 6 x 10^5 cells in 60 mm cell culture plates per treatment condition, in 150 µl of cell lysis buffer (0.1 M Tris-Hcl pH 7.4, 25 mM NaF, 1 mM benzamidine, 2 mM EDTA, 0.1 mM sodium orthovanadate, 0.1% Triton X-100) containing 150 µl/ml of protease inhibitor cocktail (Promega, Southampton, UK). Cell lysates were incubated on ice for 20 minutes prior to sonication with a probe sonicator, using 3 pulses of 5 seconds each, at an amplitude of 7 microns (Soniprep 150, MSE, UK).

Protein concentration was quantified using a commercial Bradford assay (Pierce Biotech, Rockford, USA) following the manufacturers specification and protein absorbance was measured at a wavelength of 595 nm using a SpectraMAX 250 plate reader (Molecular Devices Ltd, Wokingham, UK). Protein lysates were then diluted 1:3 in 4x sample buffer (0.25 M Tris-HCL (pH 8.0), 8% sodium dodecyl sulphate (SDS), 40% glycerol, 10% β-mercaptoethanol and bromophenol blue) and denatured by heating to 95°C for 5 minutes. Proteins were separated by gel electrophoresis through Bio-Rad 4 – 20% tris-glycine gels (Bio-Rad Laboratories Inc., CA, USA) with running buffer (Tris-Base 250 nM, Glycine 1.9 M, 1% SDS; pH 8.5) using a XCell *Sure*lock apparatus (Novel Experimental Tech; San Diego, CA, USA). Transfer of separated proteins to PVDF membranes was performed using a Trans-Blot Turbo™ Transfer System (1.3 A, 25 V, Bio-Rad, California, USA) with Bio-Rad Trans-Blot Turbo™ Transfer Packs (Bio-Rad,) for 15 minutes. Membranes were then washed briefly in 1x Tris-buffered saline (TBS; 10x stock 200mM Tris-Base, 1.37M Sodium Chloride; pH 7.6) containing 0.1% Tween 20 (ThermoFisher Scientific) (TBS/T) and incubated for 1 hour in TBS containing 5% non-fat milk (Oxoid Ltd, Basingstoke, UK) to block non-specific antibody binding prior to overnight incubation with primary antibodies at 4°C as detailed in Table 2.5.

Membranes were then given 3 x 15 minute washes in TBS/T prior to incubation for 1 hour at room temperature with horseradish peroxidase-conjugated secondary antibodies as detailed in Table 2.5. Finally, following 3 x 15 minute washes in PBS/T, protein expression was revealed using Clarity™ Western ECL Substrate (Bio-Rad, California) for 5 minutes according to the manufacturers specifications followed by visualisation with a LI-COR Odyssey Fc Imager and its accompanying Image Studio Software (LI-COR Biosciences, Cambridge, UK) and quantification by densitometry.

1° Antibody (Supplier)	Species (Molecular Weight)	1° Antibody Dilution	2° Antibody Dilution
AMBRA1 (Novus Biologics, Abingdon, UK)	Rabbit Polyclonal (132 kDA)	1:1000 5% non-fat milk TBS/T	Anti-rabbit 1:2500 5% non-fat milk in TBS/T
Claudin-5 (Abcam, Cambridge, UK)	Rabbit Monoclonal (24 kDA)	1:2000 5% non-fat milk in TBS/T	Anti-rabbit 1:2500 5% non-fat milk in TBS/T
VE-Cadherin (Cell Signalling, Leiden, The Netherlands)	Rabbit Monoclonal (130-140 kDA)	1:1000 5% non-fat milk in TBS/T	Anti-rabbit 1:2500 5% non-fat milk in TBS/T
Phospho-Smad 1/5/9 (Cell Signalling)	Rabbit Monoclonal (60 kDA)	1:1000 5% non-fat milk in TBS/T	Anti-rabbit 1:2500 5% non-fat milk in TBS/T
Phospho-Smad 3 (Cell Signalling)	Rabbit Monoclonal (52-60 kDA)	1:500 5% non-fat milk in TBS/T	Anti-rabbit 1:2500 5% non-fat milk in TBS/T
Phospho-Smad 2 (Cell Signalling)	Rabbit Polyclonal (60 kDA)	1:500 5% non-fat milk in TBS/T	Anti-rabbit 1:2500 5% non-fat milk in TBS/T
Total Smad 1 (Cell Signalling)	Rabbit Polyclonal (58-60 kDA)	1:500 5% non-fat milk in TBS/T	Anti-rabbit 1:2500 5% non-fat milk in TBS/T

Total Smad 5 (Cell Signalling)	Rabbit Monoclonal (60 kDA)	1:500 5% non-fat milk in TBS/T	Anti-rabbit 1:2500 5% non-fat milk in TBS/T
Total Smad 3 (Cell Signalling)	Rabbit Monoclonal (52 kDA)	1:500 5% non-fat milk in TBS/T	Anti-rabbit 1:2500 5% non-fat milk in TBS/T
Loricrin (Biolegend, London, UK)	Rabbit Polyclonal (26-30 kDA)	1:10,000 5% BSA in TBS/T	Anti-rabbit 1:20,000 in 5% BSA in TBS/T
β-Actin (Sigma-Aldrich)	Mouse Monoclonal (45 kDA)	1:40,000 5% non-fat milk in TBS/T	Anti-mouse 1:2500 5% non-fat milk in TBS/T
GAPDH (Cell Signalling)	Rabbit Monoclonal (37 kDA)	1:5000 5% BSA in TBS/T	Anti-rabbit 1:2500 5% BSA in TBS/T

Table 2.5: Optimal primary and secondary antibody conditions for respective western blot analysis.

2.10 Immunohistochemistry for formalin fixed paraffin embedded (FFPE) tissue

2.10.1 Immunohistochemistry for AMBRA1, Loricrin, CD31 and TGF-β2 using DAB counterstaining

5 µm FFPE tissue sections were derived from an independent cohort of AJCC stage I melanomas from the James Cook University Hospital (JCUH), Middlesbrough with ethical permission (Ref 08/H0906/95+5_Lovat).

Antigen retrieval conditions and antibody dilutions for the automated immunohistochemical (IHC) detection of AMBRA, Loricrin and TGF-β2 was optimised using a Ventana Benchmark XT automated IHC staining instrument (Ventana Medical Systems Inc., Tucson, AZ, USA) with antibody binding visualised either with an Optiview DAB Detection Kit (Ventana Medical Systems Inc., Tucson, AZ, USA) or an ultraView Universal DAB Detection Kit (Ventana Medical Systems Inc., Tucson, AZ, USA), according to the manufacturers specifications. All antibodies were optimised by Miss Alison Greenwood at the JCUH pathology lab using control human tissue sample sections known to positively express each antibody.

Following validation of consistent AMBRA1, Loricrin, CD31 and TGF-β2 expression using the Ventana automated system, the following conditions were used to detect these antibodies in tissue cohort samples in the Pathology department of JCUH (Table 2.6) with final counterstaining in haematoxylin for 8 minutes at room temperature. All IHC stained sections were digitally imaged using automated scanning of slides on a digital slide scanner (see section 2.13) for subsequent visual and semi-quantitative analysis.

1° Antibody (Supplier)	Species	Antigen retrieval	1° Antibody dilution	1° Antibody incubation time	Automated DAB detection kit
AMBRA1 (Abcam)	Rabbit Polyclonal	Cell Conditioning 1 (CC1) Solution (Ventana)	1:300	16 minutes	Optiview (Ventana)
Loricrin (Abcam)	Rabbit Polyclonal	EZprep Solution (950-102, Ventana)	1:1000	32 minutes	ultraView Universal (Ventana)
CD31 (Abcam)	Mouse Monoclonal	CC1 Solution (Ventana)	1:200	32 minutes	Optiview (Ventana)
TGF-β2 (R&D Systems, Minneapolis, USA)	Mouse Monoclonal	CC1 Solution (Ventana)	1:200	32 minutes	ultraView Universal (Ventana)

Table 2.6: Optimal conditions for AMBRA1, Loricrin, CD31 and TGF-β2 detection using the Ventana Benchmark XT automated IHC system.

2.10.2 Bleaching of FFPE melanoma tissue prior to analysis of TGF-β2 using DAB counterstaining

To eliminate error in quantifying staining intensity for TGF-β2 expression with DAB counterstaining where there was difficulty in discriminating between melanin staining with that of true TGF-β2 staining, melanoma tumour sections were bleached prior to the automated IHC detection of TGF-β2 as described in 2.10.1. 5 µm FFPE melanoma tissue sections were incubated for 10 minutes in 30% H_20_2 diluted in PBS followed by x3 washes with tap water prior to being loaded onto the Ventana Benchmark XT automated IHC staining instrument.

2.10.3 Immunohistochemistry for AMBRA1 and TGF-β2 using VIP counterstaining

5 µm sections of FFPE tissue samples of melanoma tumours were cut onto X-tra microscope slides (Leica Microsystems, Milton Keynes, UK) prior to incubation in Histoclear (Sigma) for 20 minutes, followed by rehydration of tissue sections through graded ethanol solutions (100%, 75%, 50%) and a wash in distilled water for 5 seconds each. Antigen retrieval was undertaken by microwave heating of slides, incubated in preheated 10 mM Tris-Hcl (pH 9.0) (TGF-β2) or 10 mM Tris-Hcl (pH 7.6)(AMBRA1), for 16 minutes with buffer top up at 8 minutes, followed by cooling at room temperature for 20 minutes. An area of staining for each tissue section was marked using an ImmEdge hydrophobic pen (Vector Laboratories Inc., Burlingame, USA) followed by 3 minute rehydration in PBS containing 0.05% Tween 20 (ThermoFisher Scientific) (PBS/T). Sections were then permeabilised by 10 minute incubation in 0.2% Triton X-100 (Sigma-Aldrich), briefly washed in PBS/T then incubated in 3% H_20_2 (Sigma-Aldrich) in water for 10 minutes at room temperature to block endogenous peroxidase. After another brief wash with PBS/T, endogenous Avidin was blocked with the Avidin solution from an Avidin/Biotin Blocking kit (Vector Laboratories) for 15 minutes,

followed by another brief PBS/T wash and incubation with the Biotin solution from the same kit for a further 15 minutes; again all steps were performed at room temperature. Protein blocking was performed by incubating the sections in 2% blocking serum from an animal specific Vectastain Elite (Vector Laboratories) for 20 minutes, followed by a brief wash in PBS/T. Sections were then incubated for 1 hour at room temperature with a pre-validated TGF-β2 purified mouse monoclonal antibody (R&D Systems; diluted 1:40 in PBS + 2% BSA) or AMBRA1 rabbit polyclonal antibody (Abcam; diluted 1:200 in PBS + 2% BSA) before washing x3 in PBS/T, followed by incubation in biotinylated animal specific secondary antibody from the same Vectastain Elite kit (Vector Laboratories; diluted 1:200 in 2% blocking serum + PBS/T) for 30 minutes. Staining was revealed by incubating sections for 30 minutes in ABC reagent from the Vectastain Elite kit (Vector Laboratories), premixed according to the manufacturers' specifications and left at room temperature for 30 minutes prior to use. Following 3 further washes in PBS/T, sections were next incubated for 10 minutes at room temperature in VIP solution (Vector Laboratories), followed by immersion in tap water for 5 minutes to stop the peroxidase reaction and prior to counter staining with haemotoxylin (Sigma) for 2 minutes. Following several rinses with tap water over 10 minutes, sections were then dehydrated through 75% and 100% ethanol for 5 seconds each, cleared for 2 minutes in Histoclear (Sigma) and finally left to dry at room temperature before mounting with a glass coverslip with DPX mounting medium (VWR International Ltd., Poole, UK).

2.11 Immunofluorescence for AMBRA1 and CD31 expression in FFPE HUVEC cell pellets and melanoma tissue

5 µm sections of HUVEC FFPE cell pellets or FFPE sections derived from the JCUH cohort of AJCC stage I melanomas were incubated in Histoclear for 20 minutes, followed by rehydration of tissue sections through graded ethanol solutions (100%, 75%, 50%) and a wash in distilled water for 5 seconds each. Antigen retrieval was undertaken by microwave heating of slides in preheated 10 mM Tris-Hcl (pH 9.0) for 16 minutes with buffer top up after 8 minutes, followed by cooling at room temperature for 20 minutes. An area of staining for each tissue section was marked using an ImmEdge hydrophobic pen (Vector Laboratories), followed by 3 minute rehydration in PBS/T. Sections were then permeabilised by incubation in 0.2% Triton X-100 (Sigma-Aldrich) for 10 minutes, briefly washed in PBS/T, then incubated for 20 minutes at room temperature in 2% horse serum in PBS/2% BSA for protein blocking. Following a brief wash in PBS/T, sections were then incubated for 1 hour at room temperature with primary AMBRA1, CD31 (alone or together) or null primary antibody control (PBS/2% BSA) in optimal conditions as detailed in Table 2.7. Sections were then given x3 PBS/T washes and incubated in secondary fluorescent antibodies detailed in Table 2.7 for 1 hour in the dark at room temperature, with 4’6-Diamidino-2-Phenylindole dye (DAPI; Thermo Fisher Scientific) diluted 1:1000 in 2% horse serum in PBS/2% BSA to detect nuclear staining. Following x3 further washes in PBS/T, sections were dehydrated through 75% and 100% ethanol for 5 seconds each, cleaned for 2 minutes in Histoclear (Sigma Aldrich) and finally left to dry at room temperature before mounting with a glass coverslip using Vectashield hard set mountant (Vector Laboratories). Slides were finally visualised and images captured using a Leica TC2 SP2 UV AOBS MP Upright Confocal Microscope (Leica Microsystems, Milton Keynes, UK) and analysed using Volocity imaging software (PerkinElmer, Wokingham, UK).

1° Antibody	Species	Antigen Retrieval	1° Antibody dilution	2° Antibody	2° Antibody dilution
AMBRA1 (Abcam)	Rabbit Polyclonal	Tris Hcl (pH 9)	1:200 PBS/2% BSA	Alexa Fluor 568 anti-rabbit	1:250 2% horse serum in PBS/2% BSA
CD31 (Abcam)	Mouse Monoclonal	Tris Hcl (pH 9)	1:25 PBS/2% BSA	Alexa Flour 488 anti-mouse	1:250 2% horse serum in PBS/2% BSA

Table 2.7: Optimal primary and secondary antibody conditions for immunofluorescence detection of AMBRA1 and CD31 expression.

2.12 Patient Cohort Selection and Database development

Ethical permission was obtained from the Newcastle and North Tyneside research ethics committee (REF 08/H0906/95+5) with associated material transfer agreements to enable the collation of patient tissue from JCUH into the Newcastle University Dermatology Biobank.

Suitable tissue was identified from the Department of Plastic & Reconstructive Surgery's melanoma skin cancer database at the JCUH. All melanomas with Breslow depth ≤2 mm diagnosed pre September 2006 were included in the search criteria to allow a minimum of 8 year follow up on outcome. Information obtained from this database included age of patient at diagnosis, date of initial diagnosis, subtype of melanoma, Breslow depth of tumours at diagnosis, occurrence of nodal or metastatic spread to date, patient's co-morbidities including details of other cancers and date and cause of patient's death where applicable (Table 2.8).

The stage of disease at diagnosis (to include only AJCC stage I melanomas) was re-confirmed from initial pathology reports, accessed via the JCUH's results administration systems - APEX and WINPATH. Further searches of the pathology and radiology results reporting system were also conducted to extrapolate any extra information regarding nodal or metastatic spread. Given that our melanoma cohort was derived pre-2006 when mitotic rate was often not reported as it was not a factor discerning TNM stage T1a (AJCC stage IA) and T1b (AJCC stage IB), we did not further stratify our AJCC stage I melanoma cohort into stage IA or IB in our biomarker validation. Exclusion criteria for our study cohort included: unavailable or damaged FFPE tissue blocks from JCUH pathology stores, tumour samples where the epidermis was lost/ulcerated or where there was no melanoma tumour tissue visible (Figure 2.1).

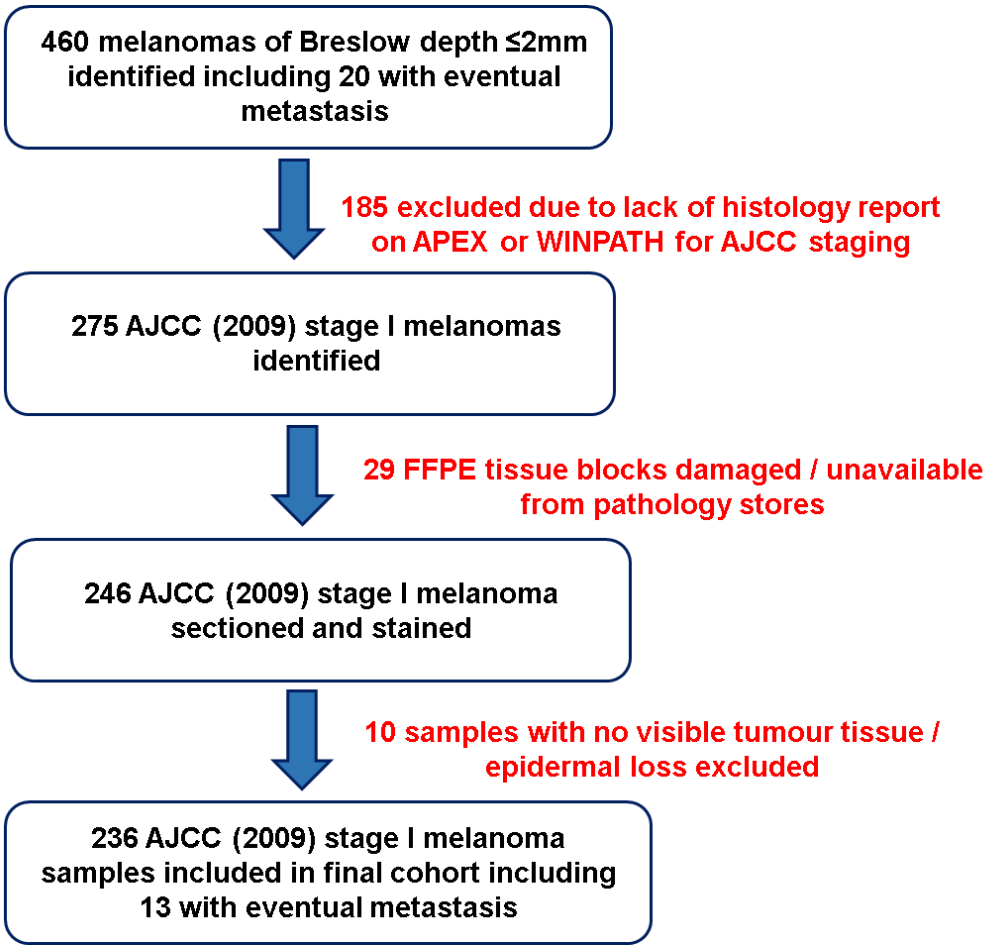

Figure 2.1: Graphical illustration of exclusion of samples from initial identification of potential samples using the JCUH Department of Plastic and Reconstructive surgery melanoma database, to inclusion in the final biomarker validation study cohort.

All information obtained was amalgamated into a Microsoft Access template, creating a bio-bank database for this JCUH melanoma cohort within the central Dermatology Biobank database. The template allows simplified storage and analysis of patient demographics and disease characteristics. All data was link anonymised and stored on a secure University computer, backed up every 24 hours.

Relevant FFPE tissue blocks of identified melanoma tumours were retrieved by Ms Alison Greenwood, a biomedical scientist based at the JCUH pathology laboratory, who performed IHC staining for AMBRA1, Loricrin, CD31, TGF-β2 using their Ventana Benchmark XT automated IHC staining system (Ventana) described in section 2.10.1. In addition, 20 additional 5 µm tissue sections were cut onto X-tra microscope slides (Leica) for additional manual staining for other biomarkers. These were then logged into the above database and transferred to the Newcastle University laboratory bio-bank.

JCUH Cohort of AJCC Stage I Melanomas	
Number of patients	236
Male: Female	83:153
Median age at diagnosis (range)	55 (13-94)
Eventual AJCC Stage (8 year follow up)	
I/II	223
III	6
IV	7
Total number of metastases	13
Melanoma subtype	
Superficial Spreading	139
Nodular	12
Other (lentigo maligna melanoma, naevoid, etc.)	85
Median Breslow depth (range)	0.8 (0.1-2) mm

Table 2.8: Study cohort patient demographics.

2.13 Analysis of Immunohistochemistry by Slide Scanner

All IHC stained sections were digitally imaged using automated scanning of slides on a Leica SCN400 digital slide scanner (Leica Biosystems, Milton Keynes, UK) within the Newcastle University Biobank. These were then visualised using Leica Biosystems Digital Image Hub software (Leica Biosystems), allowing visual analysis of biomarker expression as well as the semi quantitative calculation of percentage staining intensity.

2.13.1 Analysis and scoring of epidermal and endothelial AMBRA1 expression

IHC staining of epidermal AMBRA1 expression was analysed visually using the Leica Digital Image Hub software (Leica Biosystems) by two independent dermatologists. Each tumour was assigned a score (Table 2.9) based on the perceived degree of loss of epidermal AMBRA1 expression overlying it compared to normal epidermis within the same tumour section (Figure 2.2, depicting example of intensity staining).

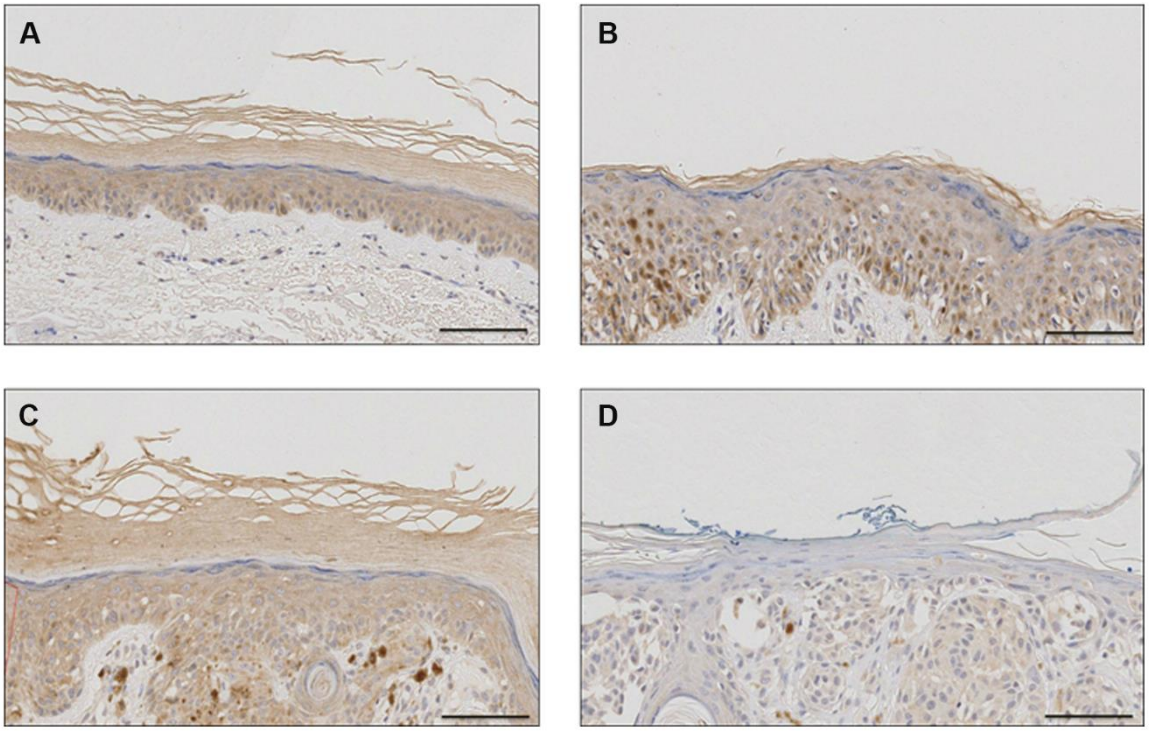

Figure 2.2: AMBRA1 expression in normal epidermis and the epidermis overlying primary AJCC stage I melanomas. Photomicrographs depicting expression of AMBRA1 with DAB (brown) counterstain in **A** normal epidermis, or in the epidermis overlying a stage 1 melanoma **(B – D)** in which epidermal AMBRA1 expression was either maintained **(A, B)** decreased **(C)** or completely lost **(D)**. Scale bar = 100 µm.

	Score
No loss	0
Some loss	1
Complete loss	2

Table 2.9: Visual scores of epidermal AMBRA1 expression/staining intensity overlying primary melanomas.

As it was potentially difficult to clearly discriminate between expression levels of epidermal AMBRA1 by eye, the robustness of visual scoring was next assessed by comparing expression levels scored qualitatively “by eye” with those derived from semi-quantitative analysis of epidermal AMBRA1 staining intensity using the previously validated Leica Biosystems Digital Image Hub software (Leica Biosystems). 5 representative areas of normal epidermis were selected at 200x magnification and the mean percentage of DAB positive pixels were obtained for each tumour. This was compared to the mean percentage of DAB positive pixels in a minimum of 5 representative areas of epidermis overlying each tumour at 200x magnification. The overall percentage decrease in AMBRA1 expression/staining intensity between the epidermis overlying each tumour and that of the corresponding normal epidermis was then calculated and compared with visual scores.

IHC expression of peri-tumoural endothelial AMBRA1 was analysed qualitatively using the Leica Digital Image Hub software (Leica Biosystems) in conjunction with endothelial cell marker CD31 expression in the same field of vision to highlight endothelial cells, both revealed by DAB counterstaining pre-optimised on the Ventana automated platform as described in 2.10.1. Loss of endothelial AMBRA1 expression was depicted by the absence of brown DAB staining whereas maintained endothelial AMBRA1 expression was depicted by the presence of brown DAB staining in the peri-tumoural endothelium, in the same field of vision where brown staining for CD31 expression highlighting endothelial cells was present (Figure 2.3).

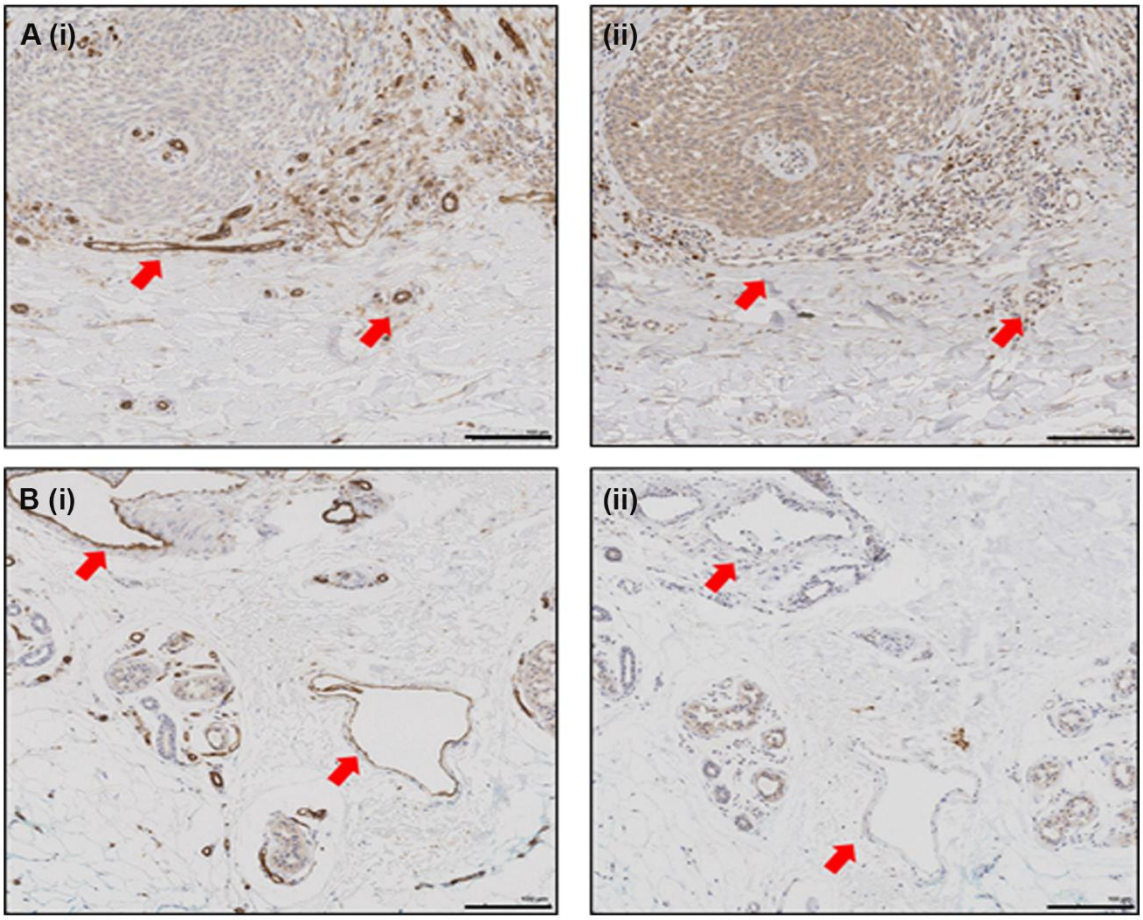

Figure 2.3: Peri-tumoural AMBRA1 and CD31 expression in primary AJCC stage I melanomas. Photomicrographs depicting expression of **A – B (i)** CD31 highlighting the endothelium, in an AJCC stage I melanoma with **A (ii)** maintained AMBRA1 expression or an AJCC stage I melanoma with **B (ii)** loss of AMBRA1 expression in the peri-tumoural endothelium, revealed by DAB counterstaining (brown). Red arrows indicate the endothelium in matched fields of vision. Scale bar = 100 μm.

2.13.2 Analysis and scoring of epidermal Loricrin expression

IHC staining of epidermal Loricrin expression was also visually assessed by two independent dermatologists, using the Leica Digital Image Hub software (Leica Biosystems). Any break in the continuity of Loricrin staining in the epidermis overlying the tumour that was not due to direct tumour invasion of the upper epidermis was scored as Loricrin loss. Unlike AMBRA1, semi-quantitative analysis of Loricrin expression was not deemed necessary as in this case the visual analysis assessment was clear-cut, i.e. it was either expressed continuously or not in the epidermis overlying any evaluated melanoma (Figure 2.4).

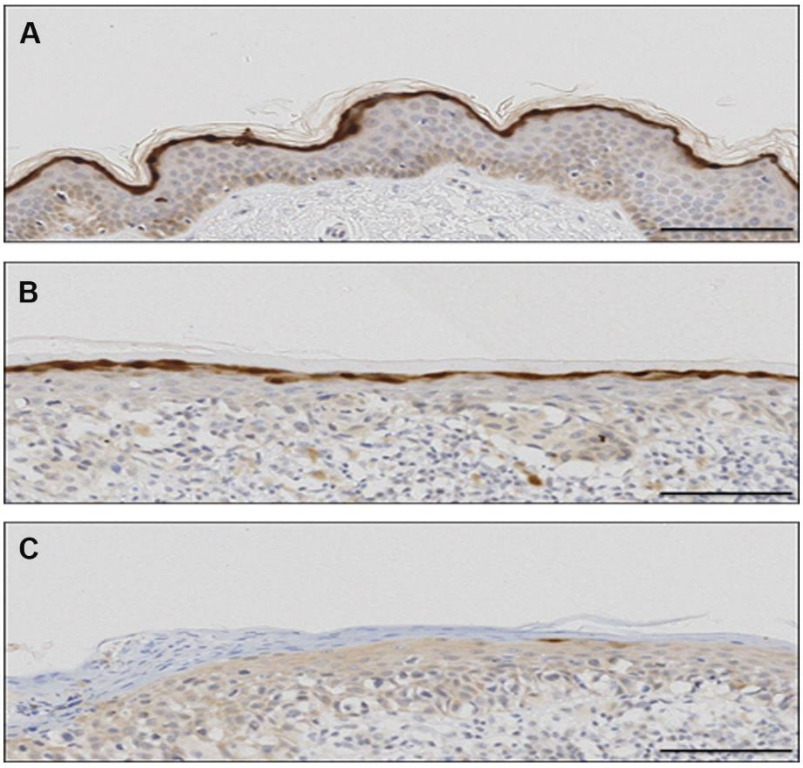

Figure 2.4: Loricrin expression in normal epidermis and the epidermis overlying primary melanomas. Photomicrographs of Loricrin expression with DAB counterstain in **A** normal epidermis, or **B & C** in the epidermis overlying two differing AJCC stage I melanomas, depicting maintained expression in image **B** and complete loss of expression in image **C**. Scale bar = 100 µm.

2.13.3 Analysis of tumoural TGF-β2 expression

IHC staining of tumoural TGF-β2 expression (revealed with both DAB and VIP counterstaining) was visually analysed and staining intensity was measured semi quantitatively using the Leica Digital Image Hub software (Leica). 5 representative areas of normal epidermis were selected at 200x magnification and the mean percentage of DAB positive pixels were obtained for each tumour for correlation analyses.

2.14 Statistics and Bioinformatics Analysis

GraphPad Prism 6 (GraphPad Software Inc; San Diego, USA) statistical analysis software was used for all statistical analysis and the generation of graphical images unless otherwise stated.

Quantification of protein expression *in vitro* via Western blotting was derived from densitometry analysis of at least 3 replicate experiments with absolute expression levels acquired using LI-COR Image Studio Software. Western blot band intensity of respective protein expression was normalised to corresponding β-actin or GAPDH housekeeping gene expression and expressed relative to the mean protein/β-Actin value for each experiment. Data presented are the mean ± SD from 3 independent biological replicates unless otherwise stated In the text. Statistical variation in protein expression levels between two groups were compared using the unpaired t Test whereas variation between more than two groups was compared using one way ANOVA with Dunnett's multiple comparison test (when comparing differences in protein expression against a control) or one way ANOVA with Tukey's multiple comparisons test (when comparing differences between all treatment groups). *P* values of <0.05 were considered as significant.

Quantification of cell viability was derived from the readings of a SpectraMAX 250 plate reader (Molecules Devices Ltd) at 490 nm and expressed as the mean of 3 replicate experiments ± SD and normalised to respective vehicle control. Statistical variation in cell viability was derived using One-way ANOVA with Dunn's multiple comparisons test. *P* values of <0.05 were considered as significant.

To test the robustness of visual scoring in evaluating epidermal AMBRA1 expression, qualitative visual scores of epidermal AMBRA1 expression (no loss, some loss or complete loss) were compared to semi-quantitative calculation of the percentage decrease in staining intensity overlying each tumour with that of adjacent normal epidermis. D'Agostino and Pearson omnibus normality test revealed all groups had a Gaussian distribution; one-way analysis of variance (ANOVA) testing was undertaken

to determine statistical variance between the means of all groups, as well as Dunn's multiple comparison test to calculate differences between the means of each individual pair within the group.

Power calculations to determine sample size were undertaken with the assumptions of an Alpha score (probability of a type 1 (false positive) error) of 0.05, and a power (ability to detect a difference between groups) of 90% and performed in collaboration with Mr Stuart Horswell, Senior biostatistician, The CRICK Institute, UK. The anticipated incidence of metastases was based on the rate of metastases seen in AJCC stage I disease in the general population as described in the 2009 AJCC staging criteria [37]. Based on hazard ratios derived from survival curve analysis of AMLo expression in the pilot Newcastle Hospitals NHS Trust cohort, this gave a minimum sample size of 133, with at least 8 metastatic samples to be included in subsequent biomarker validation studies.

To assess the validity of combined epidermal AMBRA1 and Loricrin expression as a prognostic biomarker, tumours were stratified into "high risk" and "low risk" groups. A 'high risk' tumour was defined as one in which AMBRA1 expression in the overlying tumour epidermis was completely lost AND with any break in the continuity of overlying epidermal Loricrin expression. Any other combination of variables e.g. where epidermal AMBRA1 expression was completely lost but where Loricrin expression was maintained, or where epidermal AMBRA1 expression was maintained with only expression of Loricrin lost, were stratified as 'low risk'.

All univariate (analysis of data based on the biomarker expression as the only variable) and multivariate analysis (when pre-stratified by AJCC stage of disease) of study variables for disease free survival (DFS) were undertaken using Kaplan-Meier curve constructions against 10 year follow up, as well as log-rank (Mantel-Cox) analysis of the comparative data. The Mantel-Cox log-rank test is a non-parametric hypothesis test to compare survival distributions of two samples.

Positive predictive values (PPV) are the proportion of true positives within all positive results whereas negative predictive values (NPV) are the proportion of true negative results within all negative results. PPVs and NPVs describe the accuracy of a diagnostic test or statistical measure [171]. These were calculated as follows:

$$PPV = \frac{\text{No.of high risk tumours that metastasised}}{\text{No.of high risk tumours that metastasised+No.of high risk tumours that did not metastasise}}$$

$$NPV = \frac{\text{No.of low risk tumours that did not metastasise}}{\text{No.of low risk tumours that did not metastasise+No.of low risk tumours that metastasised}}$$

Sensitivity is defined as the proportion of true positives that are correctly identified by a test, where a negative result in a test with high sensitivity is useful for ruling out disease. A positive result however, is not necessarily significant and would need to be looked at in the context of how specific a test is [172]. Specificity is the proportion of true negatives that are correctly identified by a test where a positive result in a test with high specificity signifies a high probability of the presence of disease but a negative test does necessarily rule this out [172]. Sensitivity and specificity were calculated as follows:

$$Sensitivity = \frac{\text{No.of high risk tumours that metastasised}}{\text{No.of high risk of tumours that metastasised+No.of low risk tumours that metastasised}}$$

$$Specificity = \frac{\text{No.of low risk tumours that did not metastasise}}{\text{No.of low risk tumours that did not metastasise+No.of high risk tumours that did not metastasise}}$$

Bioinformatics analysis of the upstream AMBRA1 promoter (Figure 2.5) was undertaken in collaboration with Dr Marco Corazzari, University of Rome 'Tor Vergata' in which the MatInspector (Genomatix, Munich, Germany) matrix library tool was used to identify putative TGF-β2 related transcription factor binding sites/responsive elements by locating matches in DNA sequences. Confidence matrix simetry values of >0.8 were considered significant.

TGAGTAGTGGGGAAGGGTGTAAACCTCCCTAGGAGCAGGTAAGGTAGACTATGATTGCTCACAATTGGTA
ACCATACTTGCAGTGATCTTTGTGATTTATTGAATCACATCTAGGATGTACATATTAATCCATATTTGTGCTG
AGCATATTCATTTATCAACTAAGAGACTACAGAAAAAAGCCATTGTTGTGGTGATGAAAATGTCAACACTTT
ATCAGGTTCTGAACCCAAAGAGACTTTTGCTTATTATGTAAGAAGCACACCTGTGGCTCTAGGCCTTTGGA
AGAAAATAAAAGAGAAAAGCAATCCGTGTGCTTTTTTTCCCCCTGCCTTAAGGTCAGGCTACATAATTCTG
GGTTTTCCCAGCTTCTCTTGGTCATGCTTTGTGGGGACTAAACTGGAGCTTTTACGTAGACTGTTCATTTTGT
TCCTCAGCTTGAATTCTCTCTCGTTTTCTGTCTCTATGATTTTTAATTCCCCTCACTGCTCTGTTAGGAAACTA
AGGGTCAAATGAGGTTAACTAATTTGCTCAATTGGGATAAAGAGTGTTGGGAGTCCATAGAACAGTTGGG
GGACTATAGTTACACAACAAGTGTTATTGCGCTATGATTTGATCTTCAACACATTCACGAGAAACTCCAGTT
CTCTAAAGAACTTTAACAGCCGGCGACCCACAGAAAATGGCAGAAGTGCAGGCTCTTTTTTAACCCGTGG
CTTATGATCTGGGTTTGTTTATTTACGCCTCAGACAGGAGCCGGACCTTGAGTAGGAGTTGAGCTGTTTTTC
GGCGCTCGGCTGTGGTTCCTTGAACGATTGCTTGGGCGTTCCTCCTTTGATGTCTGGGGCGTTCTTGTATTC
GGTGATCTTTTGCGCCGTCTTCTTGCTTGATGTCTCCTGAGCGGCGGCGGCGCCGGGTCGAGGGCTGAGT
TGTCCGCGAGGCCCCGCGCTCAAGCCGCCTTCTCCTGCCGGTCGGTAGAACGGACCCCTTCCTTTA

Figure 2.5: AMBRA1 upstream promoter sequence.

Chapter 3

Combined loss of epidermal AMBRA1 and Loricrin (AMLo): A novel prognostic biomarker for AJCC Stage I melanomas

3: Combined loss of epidermal AMBRA1 and Loricrin (AMLo): A novel prognostic biomarker for AJCC Stage I melanomas

3.1 Introduction 92

3.2 Results 95

3.2.1 Loss of AMBRA1 in the overlying AJCC stage I melanomas is a putative prognostic biomarker 95

3.2.2 Loss of Loricrin in the epidermis overlying AJCC stage I melanomas is a putative prognostic biomarker 99

3.2.3 Validation of visual analysis of epidermal AMBRA1 expression as a robust mean of identifying 'loss of AMBRA1 expression' in AJCC stage I melanomas 105

3.2.4 Combined loss of epidermal AMBRA1 and Loricrin (AmLo) identifies a high risk AJCC stage I melanoma subgroup 110

3.2.5 Combined loss of epidermal AMBRA1 and Loricrin (AmLo) identifies a high risk AJCC stage IB (AJCC 8th edition) melanoma subgroup. 116

3.3 Discussion 120

3.1 Introduction

Activating molecule in Beclin 1 regulated protein 1 (AMBRA1) is a component of the Beclin 1/VPS34 complex and involved in the formation of PI3K rich membranes during the nucleation phase of autophagy [115]. As a key autophagy initiating regulatory protein, AMBRA1 represents a potential marker of autophagy induction as well as a possible therapeutic target for autophagy inhibition. In addition to its functional role in autophagy, a growing body of evidence however, supports the role of AMBRA1 as an important regulator of cellular differentiation [113, 114] including in the early stages of differentiation in neuronal stem cells, during which autophagy is activated to fulfil the high energy demands of this process [115, 116]. Furthermore, functional inactivation of AMBRA1 results in epithelial hyper-proliferation, as well as dysregulated differentiation [173] however, the precise role autophagy plays within the differentiation process is yet to be fully elucidated [174].

Preliminary observations leading up to the present study support the role of AMBRA1 in epidermal differentiation with an observed increase in AMBRA1 expression in the epidermis of normal skin *in vivo* in line with keratinocyte differentiation [118]. However, knockdown of ATG7 (an alternative autophagy regulatory protein) in calcium-induced differentiated primary keratinocytes *in vitro* demonstrated impaired autophagy with no effect on Loricrin upregulation. In contrast, in addition to impairment of LC3-II induction, siRNA mediated knockdown of AMBRA1 resulted in the significant down regulation of Loricrin suggesting that the role of AMBRA1 in keratinocyte differentiation is independent of its pro-autophagy role, or at least independent of Atg7 (Ellis & Lovat, unpublished data).

The observed decrease, or even complete loss of AMBRA1 expression in the epidermis overlying numerous cutaneous melanomas revealed by IHC [118], further suggested that the expression of AMBRA1 in the melanoma microenvironment may have prognostic potential. Preliminary analysis of the IHC expression of epidermal AMBRA1 overlying 111 all AJCC stage primary melanomas derived retrospectively from the Newcastle Hospitals NHS Trust demonstrated that decreased or complete loss of epidermal AMBRA1 expression was indeed associated with significantly decreased disease free survival (DFS) which when stratified by AJCC stage, was also significant for AJCC stage I disease (Ellis & Lovat, unpublished data). However, although AMBRA1 expression alone was able to detect all primary melanomas that went on to develop metastases, the specificity of AMBRA1 alone as a prognostic biomarker, required further improvement to be clinically relevant. Specificity in this context is defined as the proportion of truly low risk tumours without subsequent metastases that were correctly identified by epidermal AMBRA1 expression; a high degree of test specificity in this context signifies a high probability of eventual metastases when epidermal AMBRA1 expression is decreased or completely lost. Consequently these studies led to the investigation of other markers of epidermal differentiation to aid the improved specificity of epidermal AMBRA1 expression as a single prognostic biomarker.

Expression of Loricrin in the *stratum corneum* of the epidermis represents a marker of keratinocyte terminal differentiation and in normal skin is revealed by IHC staining as a clear-cut “line” of expression in contrast to other potential IHC markers of differentiation with less clear cut pan-epidermal IHC staining (involucrin), or where genetic variability in expression exists across patients i.e. filaggrin [175]. Preliminary analysis of the epidermal IHC expression of Loricrin overlying a small cohort of 14 AJCC Stage I melanoma tumours derived from the Newcastle Hospitals demonstrated that loss of epidermal Loricrin was indeed associated with decreased disease free survival.

However in contrast to AMBRA1 expression, epidermal Loricin alone was associated with poor sensitivity i.e. the proportion of high risk tumours with eventual metastases that were correctly identified by epidermal Loricrin loss (Ellis, Tang and Lovat, unpublished data) was relatively insensitive.

However, when loss of epidermal Loricrin overlying primary AJCC stage I melanomas was combined with the analysis of epidermal AMBRA1 loss, this resulted in the significant enhancement of prognostic potential and the prediction of disease free survival for AJCC stage I melanomas, with an assay specificity and sensitivity of 100% (Ellis and Lovat, unpublished data), and leading to the current studies and primary aim of the current chapter, to validate combined loss of AMBRA1 and Loricin (AMLo) as a prognostic biomarker for AJCC stage I melanoma.

3.2 Results

Data presented in this chapter was derived from an extension of the initial Newcastle Hospitals NHS Trust melanoma cohort (up to 129 patients) and validation of both biomarkers in a further independent retrospective cohort of AJCC stage I melanomas derived from the James Cook University Hospital NHS Trust with 8 year follow up on outcome. All biomarker studies and data presented within this chapter were performed in line the "Reporting Recommendations for Tumour Marker Prognostic Studies" (REMARK) guidelines released on behalf of the National Cancer Institute – European Organisation for Research and Treatment of Cancer (NCI-EORTC) that gives guidance on preferred methods on biomarker data analysis and presentation (Appendix 1) [75].

3.2.1 Loss of AMBRA1 in the overlying AJCC stage I melanomas is a putative prognostic biomarker

To determine the potential role of AMBRA1 expression as an independent biomarker for melanoma progression, qualitative visual analysis of its expression was performed in an initial retrospective cohort of 129 all AJCC stage melanomas derived from Newcastle Hospitals NHS Trust with at least 8 years follow up data. Following optimised IHC detection of epidermal AMBRA1 (see section 2.10.1), each slide was imaged using a Leica SCN400 digital slide scanner software (Leica Biosystems). Analysis of peri-tumoural epidermal AMBRA1 expression was scored qualitatively "by eye" as being 'maintained', 'decreased', 'completely lost' or 'ulcerated' when compared to the normal epidermis adjacent to the tumour which acted as an internal control. Three independent observers; two dermatologists and a histopathologist undertook independent analysis. Univariate analysis comparing epidermal AMBRA1 expression scores with time to metastases development (disease free survival (DFS)) over an 8

year follow up period was performed using Kaplan-Meier survival analysis. This revealed a significant step-wise reduction in DFS from 100% survival in tumours with maintained epidermal AMBRA1 expression, to 72.2% survival for patients in which AMBRA1 expression in the overlying epidermis was 'decreased' or 'completely lost', to only 35.7% in frankly ulcerated tumours (where the epidermis overlying the tumour had been lost or breached by the tumour; Log-Rank (Mantel-Cox) Test $P < 0.0001$, Figure 3.1). Of note, ulcerated tumours are unable to be analysed via AMBRA1 expression as, by definition, the epidermis is not present in the sample and so cannot be assessed.

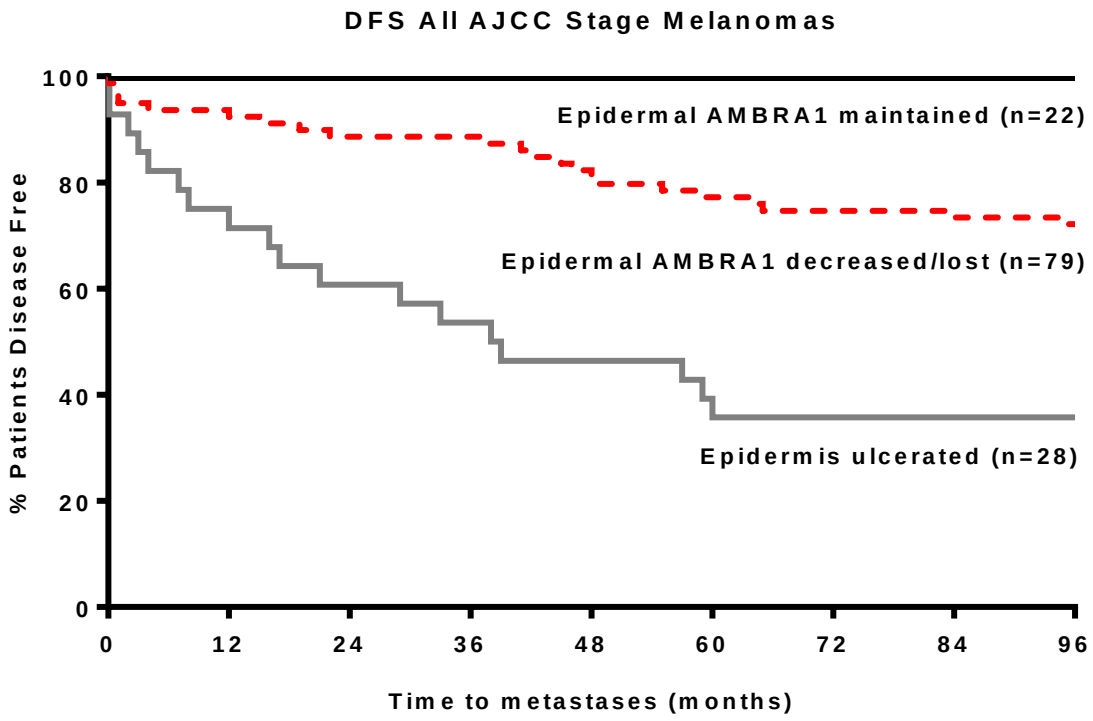

Figure 3.1: Loss of epidermal AMBRA1 expression overlying tumours correlates with decreased disease free survival in all AJCC stage melanomas. Kaplan-Meier curve showing a 27.8% decrease in 8 year DFS (months until metastases first detected) in 79 primary AJCC stage I melanomas with decreased or completely lost epidermal AMBRA1 expression (red line, DFS 72.2%) and a 64.3% decrease in DFS in 28 tumours with epidermal ulceration (grey line, DFS 35.7%) compared to 22 primary tumours in which epidermal AMBRA1 expression was maintained (black line, DFS 100%). Log-Rank (Mantel-Cox) Test P <0.0001.

To further test the utility of AMBRA1 as a prognostic biomarker in early stage disease, sub-cohort multivariate analysis of this initial retrospective cohort was undertaken to assess epidermal AMBRA1 expression levels overlying the tumours, pre-stratified by AJCC stage of disease at diagnosis. Results highlighted a significant association between decreased DFS and decreased/lost epidermal AMBRA1 in AJCC stage I melanomas, with a DFS of 100% associated with no loss of epidermal AMBRA1 expression, compared to a DFS of 80.8% in the decreased/lost AMBRA1 sub-group (Log-Rank (Mantel-Cox) Test *P* <0.03, HR 4.3 (95% CI 1.14 – 16.51), Figure 3.2), suggesting that loss of epidermal AMBRA1 expression overlying stage I melanomas may represent a putative biomarker of disease progression.

However, although loss of epidermal AMBRA1 expression overlying tumours was associated with the development of metastasis with 100% sensitivity in this cohort i.e. all tumours that metastasised were correctly identified, the specificity was not particularly high at 34.3%. This translates to 65.7% of melanoma tumours identified as high risk by epidermal AMBRA1 loss not actually developing metastasis (Figure 3.2). To improve assay specificity, we hypothesised that expression of the terminal differentiation marker Loricrin is altered overlying high risk melanoma tumours in line with the down regulation of epidermal AMBRA1 expression, which could then be used in conjunction with epidermal AMBRA1 expression to increase assay validity.

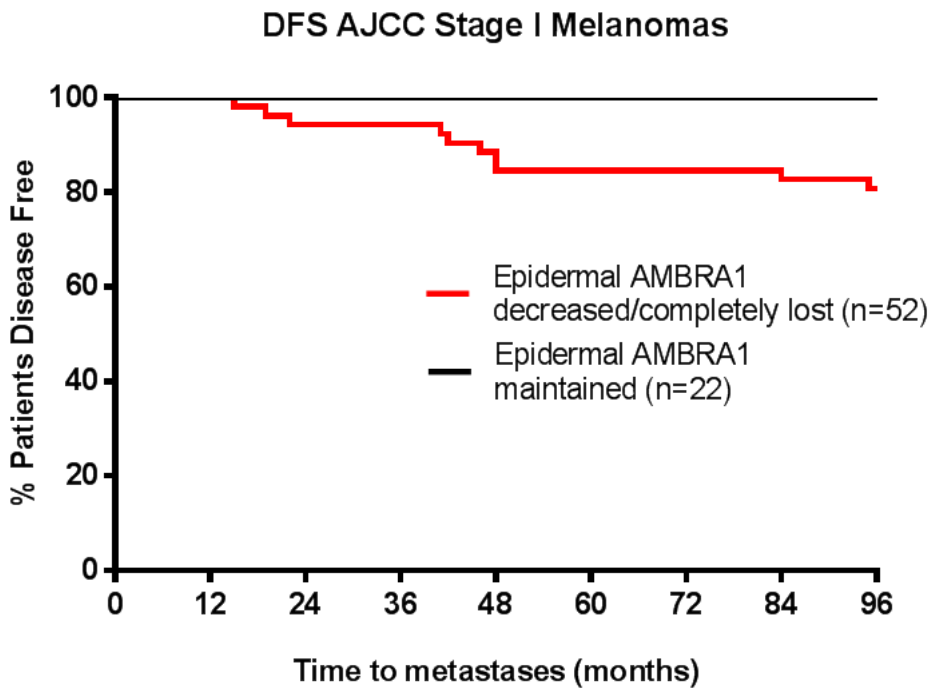

Sensitivity	Specificity	PPV	NPV
100%	34.3%	19.2%	100%

Figure 3.2: Loss of AMBRA1 expression in the epidermis overlying AJCC stage I melanomas correlates with decreased disease free survival. Kaplan-Meier curve showing a 19.2% decrease in 8 year DFS in 52 AJCC stage I melanomas in which epidermal AMBRA1 expression was decreased or lost (red line, DFS 80.8%) as compared with 22 tumours in which epidermal AMBRA1 overlying tumours was maintained (black line, DFS 100%). Log-Rank (Mantel-Cox) Test *P* <0.03, HR 4.3 (95% CI 1.14 – 16.51). AMBRA1 as a prognostic biomarker in this Newcastle Hospitals derived cohort demonstrates 100% sensitivity and NPV; however is only 34.3% specific with a PPV of 19.2%.

3.2.2 Loss of Loricrin in the epidermis overlying AJCC stage I melanomas is a putative prognostic biomarker

Epidermal expression of Loricrin overlying 20 all AJCC stage melanomas derived from the Newcastle Hospitals NHS Trust retrospective cohort was analysed using an optimised IHC assay (section 2.10.1). Sections were visualised and scored as having either maintained or lost epidermal Loricrin expression using Leica Digital Image Hub software (Leica) as previously described in section 2.13.2.

Univariate analysis comparing peri-tumoural epidermal Loricrin expression scores with DFS over a 8 year follow up period was performed using Kaplan-Meier survival analysis, revealing a significant reduction in DFS from 69.2% in tumours with maintained epidermal Loricrin expression to 0% in tumours with any break in continuous expression (Log-Rank (Mantel-Cox) Test *P* =0.0006, HR 18.40 (95% CI 3.52 – 96.21), Figure 3.3). Loss of Loricrin in the overlying tumour epidermis was also associated with the development of metastasis with 100% specificity in this cohort however; sensitivity was only 63.6% with a NPV of 69.2%.

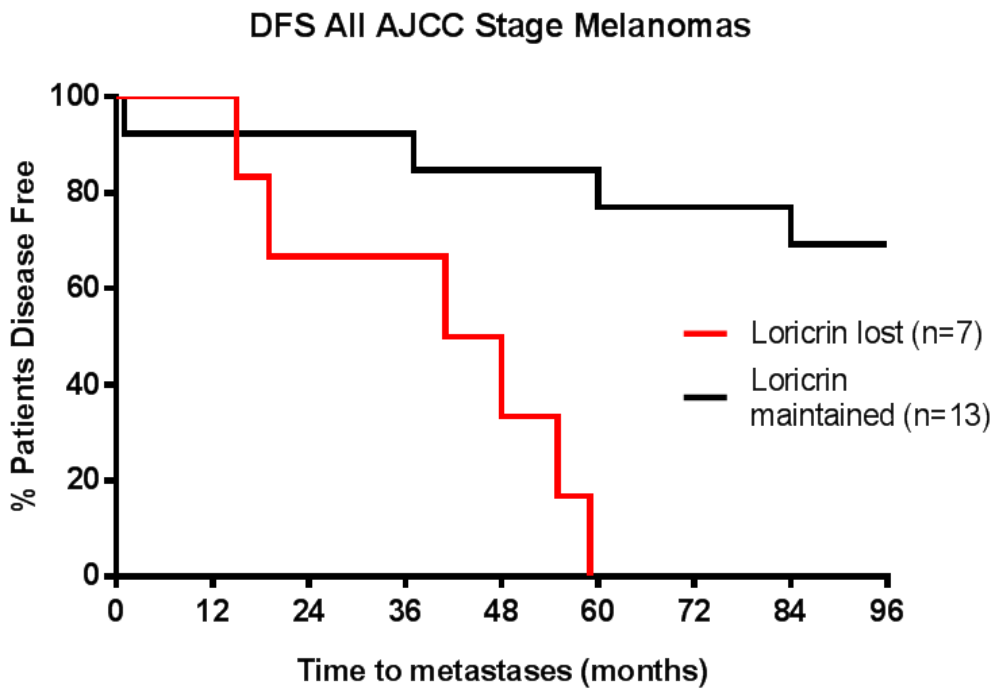

Sensitivity	Specificity	PPV	NPV
63.6%	100%	100%	69.2%

Figure 3.3: Loss of Loricrin expression overlying primary melanomas of differing AJCC stage correlates with decreased disease free survival. Kaplan-Meier curve showing a 69.2% decrease in 8 year DFS in 7differing AJCC stage primary melanomas (derived from the Newcastle Hospitals cohort) with loss of epidermal Loricrin expression (red line, DFS 0%) compared to 7 tumours in which expression was maintained (black line, DFS 69.2%). Log-Rank (Mantel-Cox) Test *P* =0.0006, HR 18.4 (95% CI 3.52 – 96.21). Loricrin as a prognostic biomarker in this Newcastle Hospitals derived cohort is highly specific (specificity of 100%) but lacks sensitivity at 63.6%. PPV and NPV were 100% and 69.2% respectively.

When stratifying for AJCC stage I disease in 14 primary melanoma from this initial cohort, multivariate analysis demonstrated a significant reduction in DFS which dropped from 90% in tumours where epidermal Loricrin expression was maintained to 0% in tumours with loss of expression (Log-Rank (Mantel-Cox) Test *P* <0.0001, HR 210.3 (95% CI 16.86 – 2624), Figure 3.4). In this context, the assay sensitivity for the

IHC analysis of epidermal Loricrin improved to 80% with a maintained specificity of 100% (Figure 3.4), collectively suggesting that similarly to AMBRA1 expression, the loss of Loricrin expression in the epidermis overlying AJCC stage I primary melanomas is also associated with an increased risk of metastasis in AJCC stage I melanomas.

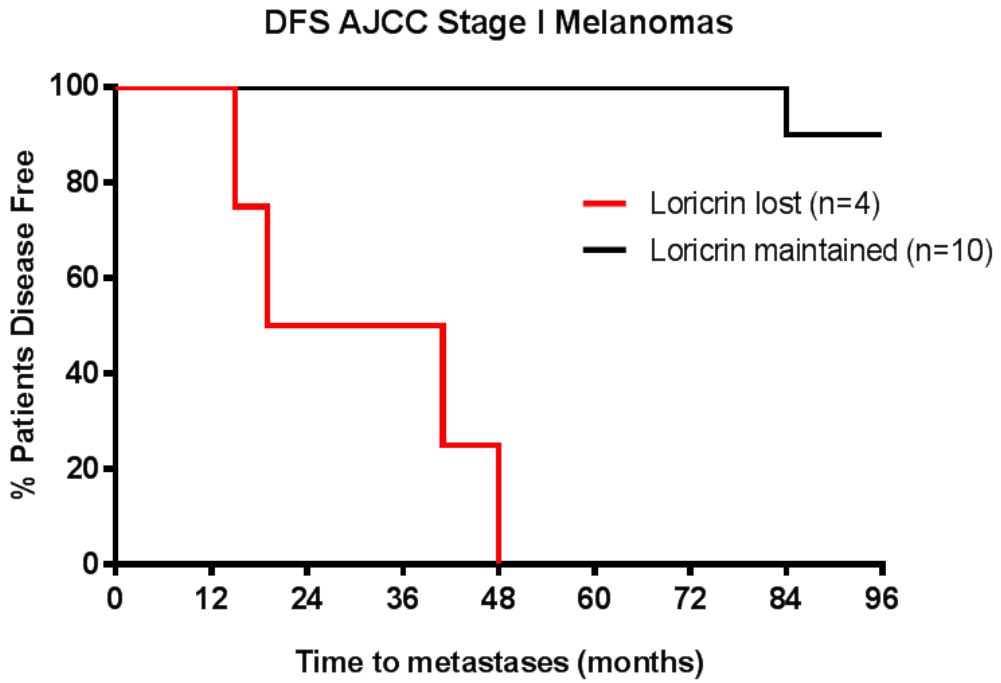

Sensitivity	Specificity	PPV	NPV
80.0%	100%	100%	90.0%

Figure 3.4: Loss of Loricrin expression in the epidermis overlying primary AJCC stage I melanomas correlates with decreased disease free survival. Kaplan-Meier curve showing a 90% decrease in 8 year DFS in 4 primary AJCC stage I melanomas (Newcastle Hospitals Cohort) in which epidermal Loricrin was lost (red line, DFS 0%) compared to 10 primary tumours in which epidermal Loricrin was maintained (black line, DFS 90%). Log-Rank (Mantel-Cox) Test *P* <0.0001, HR 210.3 (95% CI 16.86 – 2624). Table indicating 100% assay specificity and PPV for the IHC detection of epidermal Loricrin with 80% sensitivity and a 90% NPV.

Given the high assay sensitivity for the detection of epidermal AMBRA1 and high specificity for the detection of epidermal Loricrin at predicting DFS in AJCC stage I melanomas, subsequent studies explored the potential for the combined expression as a means to improve both assay sensitivity and specificity and the utility of combined epidermal AMBRA1 and Loricrin as an independent prognostic biomarker for AJCC stage I melanomas.

Multivariate analysis comparing combined AMBRA1 and Loricrin expression scores with DFS in a sub-cohort of 12 AJCC stage I melanomas derived from the Newcastle Hospitals cohort revealed a highly significant decrease in DFS from 100% in tumours where expression of both proteins in the overlying epidermis was maintained to 0% in tumours in which both epidermal AMBRA1 and Loricrin expression were lost. (Log-Rank (Mantel-Cox) Test *P* =0.0002, HR 93.5 (95% CI 8.67 – 1008), Figure 3.5).

Furthermore using combined analysis of epidermal AMBRA1 and Loricrin in these studies resulted in the improvement of both assay sensitivity and specificity to 100%, thereby underpinning the utility of combined expression as a prognostic biomarker, over and above the expression of either epidermal AMBRA1 or Loricrin alone.

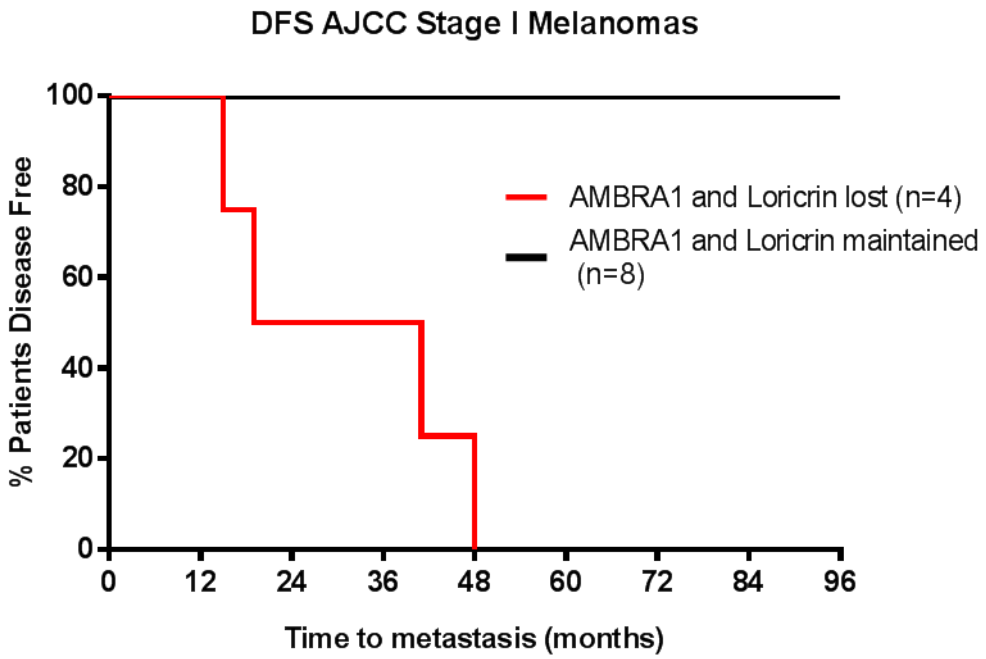

Sensitivity	Specificity	PPV	NPV
100%	100%	100%	90.0%

Figure 3.5: Combined loss of AMBRA1 and Loricrin expression overlying primary melanomas is a highly sensitive and specific prognostic biomarker for the prediction of disease free survival in AJCC stage I melanomas. Kaplan-Meier curve showing % decrease in DFS of 12 patients diagnosed with AJCC stage I melanomas (Newcastle Hospitals Cohort) over 8 years according to the loss (red line) or maintenance (black line) of epidermal AMBRA1 and Loricrin expression and indicating the significant correlation of reduced DFS from 100% to 0% in patients with tumours in which the expression of AMBRA1 and Loricin overlying the primary tumour was lost. Log-Rank (Mantel-Cox) Test *P* =0.0002, HR 93.5 (95% CI 8.67 – 1008). Table indicating the 100% assay specificity and sensitivity and, NPV and PPV values of 90 and 100% respectively.

To further validate the prognostic value of combined epidermal expression of AMBRA1 and Loricrin, expression levels subsequent studies were undertaken in an independent powered, retrospective cohort of AJCC stage I melanomas derived from the James Cook University Hospital (JCUH), Middlesbrough 8 year follow up on outcome.

Power calculations to determine sample size were undertaken with the assumptions of an Alpha score (probability of a type 1 (false positive) error) of 0.05, and a power (ability) to detect a difference between groups) of 90%. The anticipated incidence of metastases was based on the rate of metastases seen in AJCC stage I disease in the general population as described in the 2009 AJCC staging criteria [37]. Based on hazard ratios derived from survival curve analysis of AMLo expression in the pilot Newcastle Hospitals NHS Trust cohort, this gave a minimum sample size of 133, with at least 8 metastatic samples to be included. In line with this, 460 potential AJCC stage I melanomas including 20 metastatic samples were initially identified from the JCUH Plastic Surgery Department melanoma database of which 224 were excluded as detailed in section 2.12, leaving 236 including 13 metastatic samples (5.5% prevalence of metastases) making up the final cohort.

Prior to further biomarker validation work, initial studies were undertaken to validate qualitative visual analysis of epidermal AMBRA1 expression as a robust mean of identifying ‘loss of AMBRA1 expression’ in AJCC stage I melanomas for subsequent scoring of melanoma tumours as high risk or low risk based on the combined loss of epidermal AMBRA1 and Loricrin expression.

3.2.3 Validation of visual analysis of epidermal AMBRA1 expression as a robust mean of identifying 'loss of AMBRA1 expression' in AJCC stage I melanomas

While visual assessment of the maintenance or loss of epidermal Loricrin was clear cut, i.e. expression was continuous throughout the epidermis over lying primary AJCC stage I melanomas or not, this was less apparent with AMBRA1 expression where more subtle differences in epidermal expression were apparent and as such, making it potentially more difficult to visually discriminate between relatively small differences in staining intensity. Prior to further combined analysis of AMBRA1 and Loricrin in the independent retrospective JCUH melanoma cohort of AJCC stage I melanomas, the optimal means of scoring epidermal AMBRA1 expression and the robustness of scoring this by eye was thus evaluated.

Qualitative visual assessment of staining intensity (scored as no loss, some or complete loss of staining intensity) was compared with semi-quantitative expression analysis using the Leica SCN400 digital slide scanner software (Leica) in order to calculate the overall percentage decrease between the staining intensity for AMBRA1 in the epidermis overlying a melanoma with that in the normal adjacent epidermis. Analysis of 101 AJCC stage I melanomas from the JCUH cohort demonstrated that "by eye" scoring of epidermal AMBRA1 staining revealed a significant step wise correlation with semi-quantitative scoring (D'Agostino-Pearson omnibus normality test revealed normal distribution of the data, thereby enabling the application of One Way ANOVA with Dunn's multiple post hoc correction for statistical comparison between groups). This confirmed a highly significant difference in percentage decrease of epidermal AMBRA1 staining intensity derived semi-quantitatively between tumours scored visually as having 'no loss', 'some loss' and 'complete loss' of epidermal AMBRA1 expression (*** P =0.0001(no loss vs. some loss), **** P <0.0002 (no and some loss vs. complete loss), Figure 3.6).

However, despite a stepwise correlation, there was broad crossover between the percentage decrease of epidermal AMBRA1 staining intensity derived semi-quantitatively falling within the ‘no loss’ and ‘some loss’ groups (‘no loss’ median percentage quantitative expression loss 12.43 (25^{th} percentile 2.19, 75^{th} percentile 30.88), and ‘some loss’ median quantitative expression loss 37.41 (25^{th} percentile 25.84, 75^{th} percentile 52.02) which reduced the sensitivity of visual scoring between these groups. Visual scoring of ‘complete loss’ however, was highly statistically separate with a median percentage quantitative score of 89.10 (25^{th} percentile 58.52, 75^{th} percentile 95.76) (Figure 3.6).

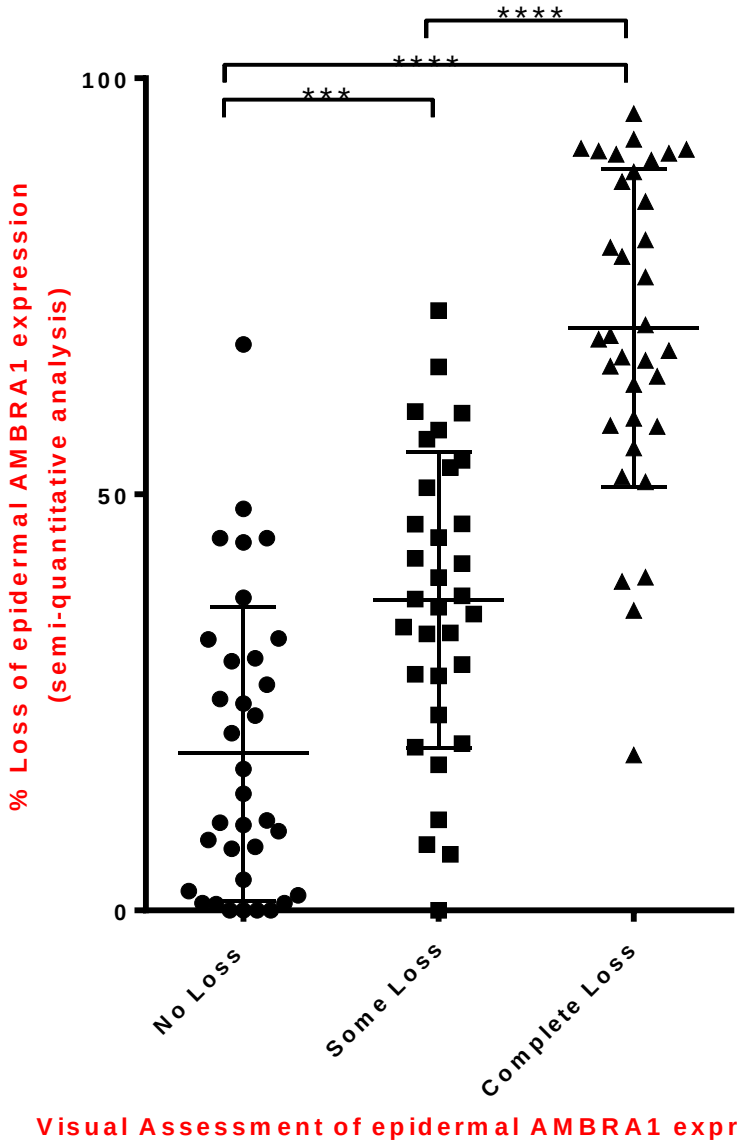

Figure 3.6: Correlation of qualitative visual scoring of epidermal AMBRA1 expression with semi-quantitative scoring. Scatter graph representing the mean % decrease of epidermal AMBRA1 staining intensity in the epidermis overlying 101 primary AJCC stage I melanomas (JCUH cohort, semi-quantitative analysis) compared with qualitative visual assessment in the same tumour group scored as 'no loss' (n=34), 'some loss' (n=33) or 'complete loss' (n=34). Each point is the mean % decrease in AMBRA1 staining intensity from 10 fields of vision compared with staining intensity in the normal adjacent epidermis. Horizontal bars represent the mean % decrease in AMBRA1 staining intensity for each group ± SEM. One Way ANOVA with Dunn's multiple post hoc correction *** P =0.0001, **** P <0.0002.

The statistical difference of ‘complete loss’ to ‘no loss’ and ‘some loss’ of epidermal AMBRA1 overlying primary AJCC stage I melanomas as determined by visual analysis was further assessed by comparing ‘complete loss’ with a combination of ‘no or some loss’. Direct comparison of the combination of ‘no or some loss’, with ‘complete loss’ visual loss of AMBRA1 epidermal expression overlying tumours revealed a highly significant difference in percentage quantitative scoring values, as well as minimal overlap of percentiles (‘no/some’ loss median percentage quantitative staining 28.38, 25th percentile 9.52, 75th percentile 44.24 versus ‘complete loss’ median percentage quantitative staining 68.85, 25th percentile 58.25, 75th percentile 89.10) (Mann-Whitney P <0.0001, Figure 3.7). The clear-cut difference between visual staining assessment of ‘no or some loss’ versus ‘complete loss’ of AMBRA1 expression suggested that only tumours in which there is complete loss of epidermal AMBRA1 expression can be defined ‘high risk’ and hence this scoring was applied to all subsequent analysis.

Collectively these data thus validated visual scoring as a robust and reliable method for analysing IHC epidermal AMBRA1 expression levels, also providing a simple and cheap as well as a favourable method for pathologists over complex scoring algorithms used in other biomarker studies.

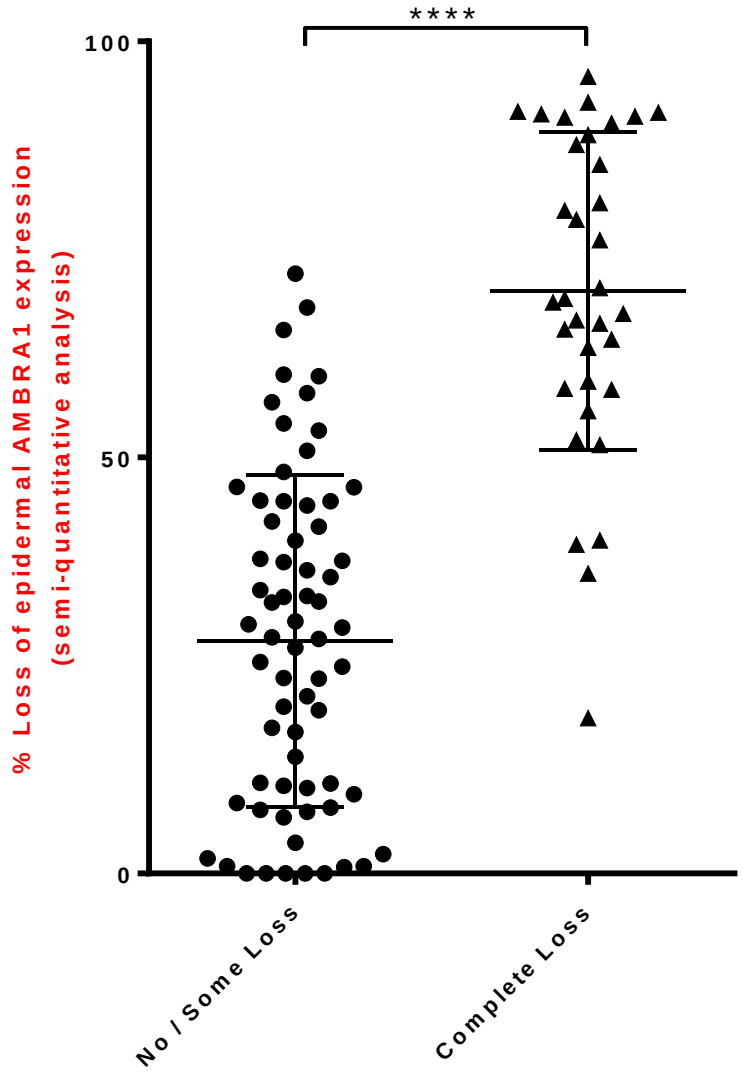

Figure 3.7: Comparison of 'complete loss' with a combination of 'no or some loss' of AMBRA1 expression in the epidermis overlying AJCC stage I melanomas with semi-quantitative analysis. Scatter graph representing the mean % decrease of epidermal AMBRA1 staining intensity in the epidermis overlying 101 primary AJCC stage I melanomas (JCUH cohort, semi-quantitative analysis) compared with qualitative visual assessment in the same tumour group scored as 'no or some loss' (n=67) or 'complete loss' (n=34). Each point is the mean % decrease in AMBRA1 staining intensity from 10 fields of vision compared with staining intensity in the normal adjacent epidermis. Horizontal bars represent the mean % decrease in AMBRA1 staining intensity for each group ± SEM. Mann-Whitney *P* <0.0001.

3.2.4 Combined loss of epidermal AMBRA1 and Loricrin (AmLo) identifies a high risk AJCC stage I melanoma subgroup

To validate the prognostic value of combined epidermal AMBRA1 and Loricrin expression for AJCC stage I melanomas, analysis of the expression of each protein individually was initially performed in a further retrospective cohort of 236 stage I melanomas derived from the JCUH NHS Foundation Trust with at least 8 years follow up data and for which all analysis was performed by visual assessment. Power calculations were performed in conjunction with the study biostatistician Mr Stuart Horswell (Cancer Research UK, London) to determine how many AJCC stage I tumours would be required in a valid independent retrospective cohort. The anticipated incidence of metastases was based on the rate of melanoma metastases seen in AJCC stage I disease in the general population as described in the 2009 AJCC staging criteria [37] and power calculations were based on hazard ratios derived from survival curve analysis of AMLo expression in the pilot Newcastle Hospitals NHS Trust cohort, which revealed a minimum sample size of 133, with at least 8 metastatic samples to be included, as described above.

Multivariate analysis comparing epidermal AMBRA1 expression scores with time to metastatic development over an 8 year follow up period was performed using Kaplan-Meier survival analysis. In line with the results from the Newcastle Hospitals cohort, analysis of 236 stage I melanoma tumours revealed a significant step-wise reduction in DFS from 98.1% survival in AJCC stage I melanoma tumours with maintained or decreased epidermal AMBRA1 expression to 87.8% in tumours with complete loss of epidermal AMBRA1 expression in the overlying epidermis (Log-Rank (Mantel-Cox) Test $P \leq 0.001$, HR 6.9 (95% CI 2.17 – 21.62), Figure 3.8), thus suggesting AMBRA1 as an independent putative biomarker for AJCC stage I melanoma. However once again, although loss of epidermal AMBRA1 expression overlying tumours associated with the development of metastasis with 76.9% sensitivity, the specificity for predicting metastasis was only 63.2% with a positive predictive value of 10.9% (Figure 3.8).

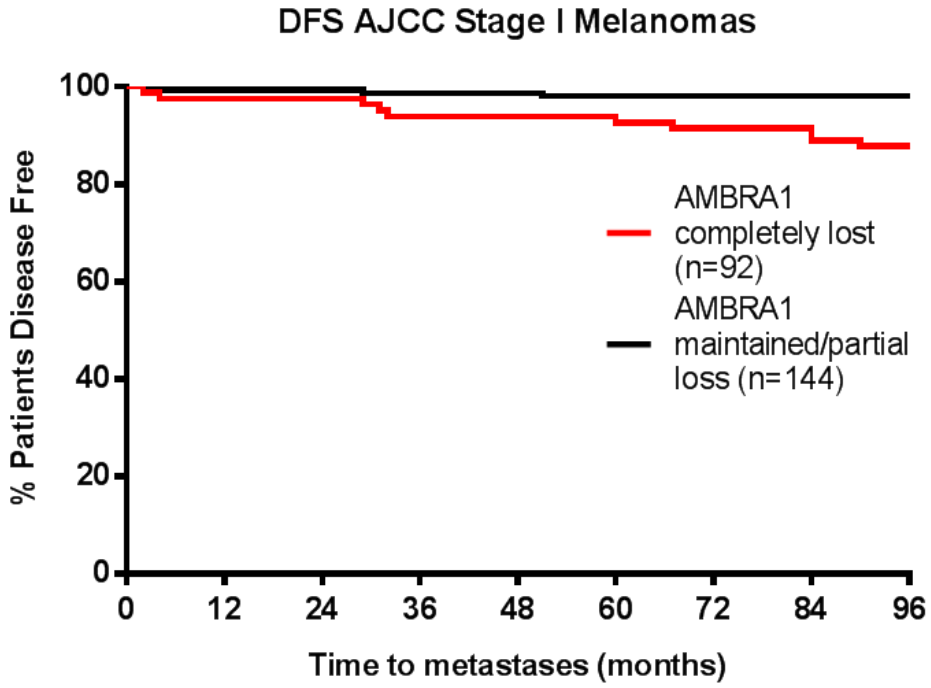

Sensitivity	Specificity	PPV	NPV
76.9%	63.2%	10.9%	97.9%

Figure 3.8: Loss of AMBRA1 expression in the epidermis overlying AJCC stage I melanomas is associated with decreased disease free survival. Kaplan-Meier curve showing a 10.3% decrease in DFS over 8 years of 236 patients diagnosed with AJCC Stage I melanomas (JCUH cohort) in which epidermal AMBRA1 was completely lost overlying 92 tumours (red line) as compared with 144 tumours (black line) in which epidermal AMBRA1 overlying tumours was partially lost or maintained. Log-Rank (Mantel-Cox) Test $P \leq 0.001$, HR 6.9 (95% CI 2.17 – 21.62). AMBRA1 as a prognostic biomarker in these studies revealed an assay sensitivity of 76.9% sensitivity, 63.2% specificity and PPV and NPV values of 10.0% and 97.9% respectively.

Validation of the prognostic potential of Loricrin as an independent biomarker for AJCC stage I melanoma was also undertaken in the JCUH melanoma cohort. IHC epidermal expression of Loricrin overlying 236 stage I melanoma tumours was analysed and scored as described previously. Multivariate analysis comparing Loricrin expression scores with DFS using Kaplan-Meier survival analysis in this cohort also demonstrated a significant reduction in DFS, which dropped from 99.1% in tumours in which epidermal Loricrin expression was maintained to 90.2% in tumours with loss of expression (Log-Rank (Mantel-Cox) Test $P \leq 0.002$, HR 5.3 (95% CI 1.79 – 15.77), Figure 3.9). Loricrin as a biomarker to detect metastasis in these studies was thus more sensitive than AMBRA1 (92.3% sensitive) but the IHC assay in this context lacked specificity (50.7% specific). Nevertheless, these results again show the loss of Loricrin expression in the epidermis overlying primary AJCC stage I melanomas is associated with increased risk of metastasis and further guided the evaluation in combination with the loss of epidermal AMBRA1 expression to test the prognostic value of both biomarkers.

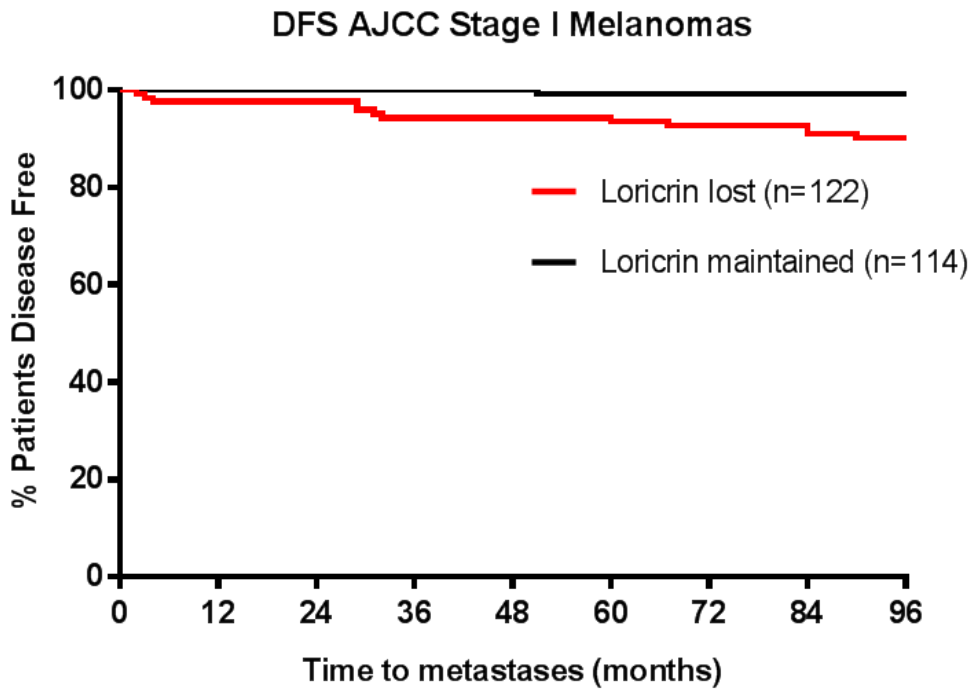

Sensitivity	Specificity	PPV	NPV
92.3%	50.7%	9.8%	99.1%

Figure 3.9: Loss of Loricrin expression in the overlying AJCC stage I melanomas is associated with decreased disease free survival. Kaplan-Meier curve showing an 8.2% decrease in DFS of 236 patients diagnosed with AJCC stage I melanomas (JCUH cohort) over 8 years in 122 tumours in which the expression of epidermal Loricrin was lost (red line, DFS 90.2%) compared to 114 tumours in which expression was maintained (black line, DFS 99.1%). Log-Rank (Mantel-Cox) Test $P \leq 0.002$, HR 5.3 (95% CI 1.79 – 15.77). Loricrin as a prognostic biomarker in these studies was 92.3% sensitive, with an assay specificity of 50.7% and PPV and NPV values of 9.8% and 99.1% respectively.

To validate the prognostic value of combined epidermal Loricrin and AMBRA1 expression for AJCC stage I melanomas, 236 stage I tumours from the JCUH cohort were pre-stratified into 'high risk' and 'low risk subgroups'. A 'high risk' tumour was defined as one in which AMBRA1 expression in the overlying tumour epidermis was completely lost AND with any break in the continuity of overlying Loricrin expression. Any other combination of variables e.g. where epidermal AMBRA1 expression was completely lost but where Loricrin expression was maintained, or where epidermal AMBRA1 expression was maintained with only expression of Loricrin lost, were stratified as 'low risk'.

Multivariate analysis of 236 tumours comparing high risk and low risk tumour subgroups with DFS using Kaplan-Meier survival analysis revealed a significant decrease in DFS in high risk tumours (DFS of 85.1%) as compared to 98.2% DFS in tumours where expression of both epidermal AMBRA1 and Loricrin were maintained (Log-Rank (Mantel-Cox) Test P <0.0001, HR 12.2 (95% CI 3.59 – 41.18), Figure 3.10). The use of this combined assay as a prognostic biomarker results in improved overall sensitivity of 76.9%, specificity of 74.4%, NPV of 98.2% and PPV of 14.9%, collectively validating loss of epidermal AMBRA1 and Loricrin (AMLo) as a novel independent prognostic biomarker for AJCC stage I melanomas.

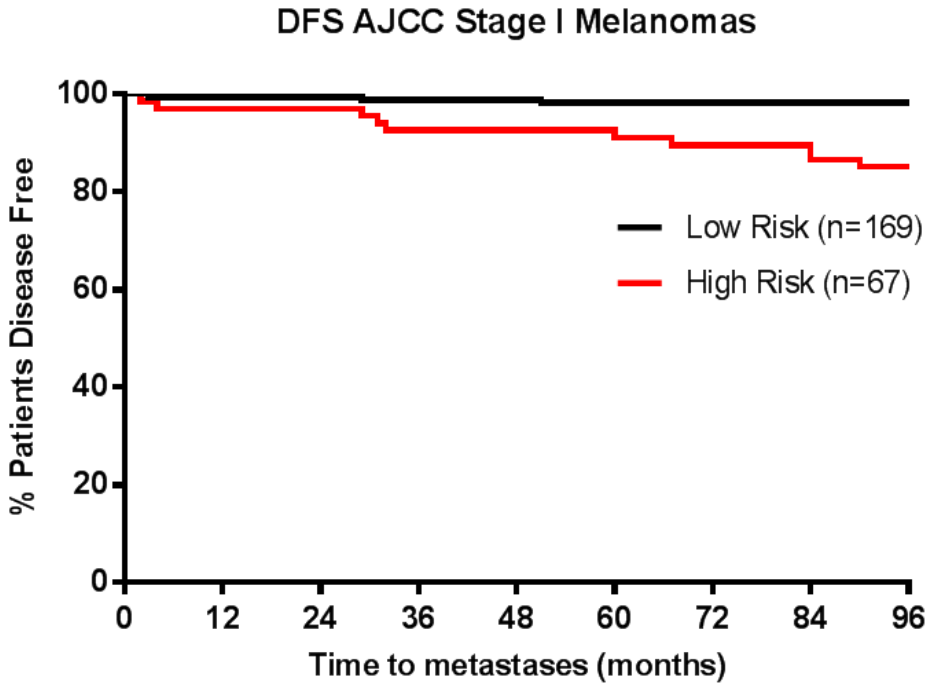

Sensitivity	Specificity	PPV	NPV
76.9%	74.4%	14.9%	98.2%

Figure 3.10: Combined loss of epidermal AMBRA1 and Loricrin (AMLo) expression in the epidermis overlying AJCC stage I melanomas identifies a high risk sub group. Kaplan-Meier curve showing a 13.1% decrease in DFS of 236 patients diagnosed with AJCC stage I melanomas over 8 years stratified as high risk (red line, DFS 98.2%) or low risk (black line, DFS 85.1%). Log-Rank (Mantel-Cox) Test *P* <0.0001, HR 12.2 (95% CI 3.59 – 41.18). Combined analysis of AMLo in these studies revealed an assay sensitivity of 76.9%, and a specificity of 74.4%, with PPV and NPV values of 14.9% and 98.2% respectively.

3.2.5 Combined loss of epidermal AMBRA1 and Loricrin (AmLo) identifies a high risk AJCC stage IB (AJCC 8th edition) melanoma subgroup.

With changes in classification of melanoma staging being brought in by the updated 8th Edition of the AJCC Staging Manual, which comes into effect in January 2018, the implications on the prognostic effect of AMLo in accordance with the updated guidelines were additionally assessed. A significant change in melanoma staging in the 8th edition is the classification of a melanoma as T1a if non-ulcerated and <0.8 mm in thickness and T1b if it is 0.8-1.0 mm thick or <0.8 mm with ulceration, with tumour mitotic rate additionally being dropped completely as a staging criterion for T1 tumours [176]. The implications of this on the present study cohort of melanomas diagnosed as AJCC stage I on the basis of the 7th edition of AJCC staging criteria is that a significant proportion of tumours given a TNM score of T1a or T1b will fall into the T2a category based on the 8th edition guidelines. However, overall, these changes in AJCC staging criteria will have minimal impact on the validity of AMLo as a prognostic biomarker for AJCC stage I melanoma as the present cohort of T1 – T2a melanoma tumours will still fall within AJCC stage I criteria. Nevertheless, given that the JCUH AJCC stage I melanoma cohort was derived pre-2006 when mitotic rate was not a factor discerning TNM stage T1a (AJCC stage IA) and T1b (AJCC stage IB), adequate information for further stratification of tumours into stage IA or IB was lacking for the present study biomarker validation. As mitotic rate will no longer be taken into consideration in the 8th edition AJCC staging criteria, the prognostic impact of AMLo in stage IA melanomas defined by the updated guidelines (i.e. melanoma tumours <0.8 mm in thickness) was therefore further assessed.

Multivariate analysis of 98 tumours with a Breslow thickness of <0.8mm, comparing AMLo high risk and low risk scores with DFS using Kaplain-Meier survival analysis, demonstrated a significant decrease in DFS between tumours that have been scored as AMLo high risk (DFS of 90%) compared to tumours scored as AMLo low risk (DFS of 100%). The combined assay of AMLo loss as a prognostic biomarker in AJCC stage IA within the JCUH cohort revealed extremely high sensitivity and a NPV of 100%, specificity of 90.72 and a PPV of 10% (Log-Rank (Mantel-Cox) Test *P* =0.003, HR 18034 (95% CI 27.8 – 11699018), Figure 3.11).

Similarly, multivariate analysis of 138 AJCC stage I melanomas within the JCUH cohort reclassified as stage IB melanoma subgroup according to the AJCC (8^{th} edition) staging criteria, comparing AMLo high risk and low risk scores with DFS, demonstrated a highly significant decrease in DFS in high risk tumours (DFS of 81.7%) as compared to 98.7% DFS in low risk tumours (Log-Rank (Mantel-Cox) Test *P* =0.0004, HR 7.981 (95% CI 2.526 – 25.21), Figure 3.12). The use of combined AMLo analysis in this context was associated with an assay sensitivity of 91.7%, specificity of 56.5%, NPV of 98.7% and PPV of 15.5%.

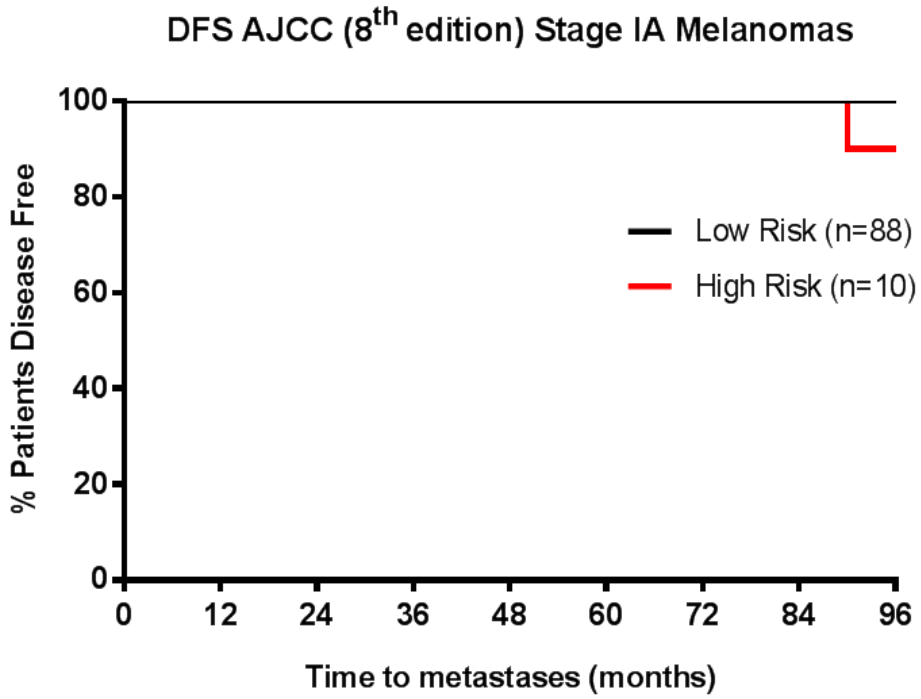

Sensitivity	Specificity	PPV	NPV
100%	90.72%	10%	100%

Figure 3.11: Combined loss of epidermal AMLo expression is a prognostic biomarker in AJCC 8th edition criteria stage IA melanomas. Kaplan-Meier curve showing % DFS over 8 years of 98 patients diagnosed with AJCC stage I melanomas reclassified as AJCC stage IA according to the 8th edition AJCC staging criteria, revealing a significant decrease in DFS from 100% in AMLo low risk tumours (black line) to 90% DFS in AMLo high risk (red line) tumours. Use of the combined assay in this subgroup resulted in high sensitivity and NPV of 100% and was also highly specific as a prognostic biomarker with specificity of 90.72% and a PPV of 10%. Log-Rank (Mantel-Cox) Test *P* =0.003, HR 18034 (95% CI 27.8 – 11699018).

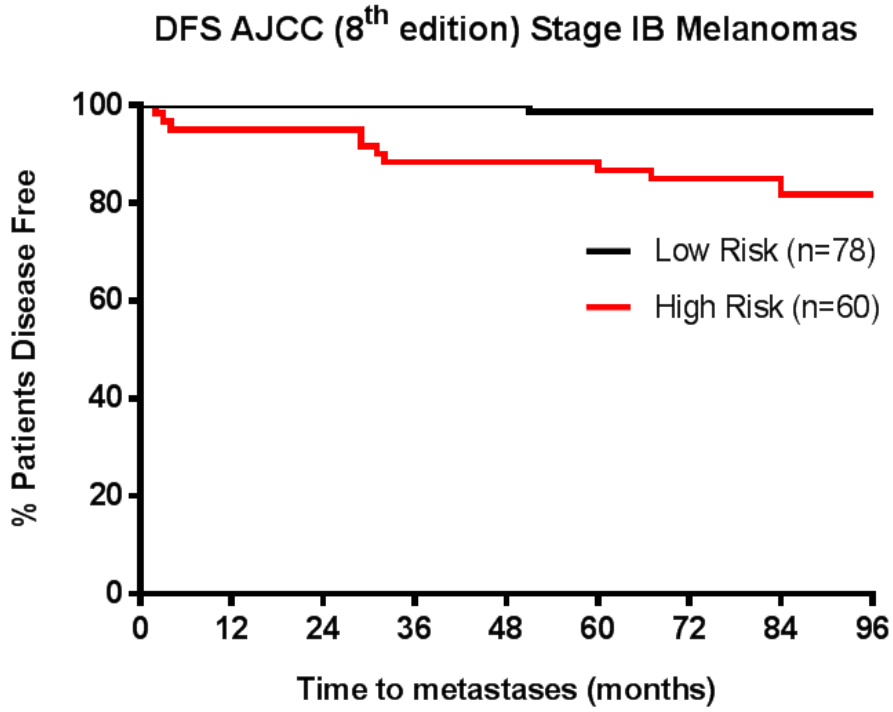

Sensitivity	Specificity	PPV	NPV
91.7%	56.5%	15.5%	98.7%

Figure 3.12: Combined loss of epidermal AMBRA1 and Loricrin (AMLo) identifies a high risk AJCC stage IB (AJCC 8th edition) melanoma subgroup. Kaplan-Meier curve showing % DFS over 8 years of 138 patients diagnosed with AJCC stage I melanomas (JCUH cohort) reclassified as AJCC stage IB melanoma, revealing a significant decrease in DFS from 98.7% in tumours scored as AMLo high risk to 81.7% in tumours scored as AMLo low risk. Log-Rank (Mantel-Cox) Test *P* =0.0004, HR 7.981 (95% CI 2.526 – 25.21). The combined loss of AMLo.as a prognostic biomarker results in overall improved sensitivity of 91.7%, NPV of 98.7% and PPV of 15.1% in AJCC stage IB melanomas.

Collectively, these data underpin the prognostic impact of AMLo as a powerful prognostic biomarker for AJCC stage IA and IB melanomas classified by the AJCC 8th edition staging criteria.

3.3 Discussion

The current and universally adopted 7th edition AJCC staging system (AJCC 2009) [37] provides a relatively accurate means through which to stage melanomas and guide some treatment approaches, however, the criteria within this staging system are unable to specifically identify those seemingly 'low risk' early stage melanomas at the highest risk of disease progression. In this case, such tumours are identified after the onset of disease progression at which point systemic treatment is required, which although increasingly effective, still lacks consistent clinical benefit and is associated with high morbidity and mortality and thereby emphasising the acute need for novel credible biomarkers to identify high risk tumour subsets and enable earlier patient follow up and the implementation of more efficacious personalised treatment.

The incidence of melanoma is increasing worldwide, which in the UK alone is predicted to increase overall by 7% by 2035 [32], with increasing rates of up to 5.5% per year in the 20 – 45 year old age group - the 3rd highest internationally [33]. In the UK, up to 91% of all melanomas are diagnosed at an early stage (stage I or II), each requiring follow up between 1 – 5 years however, there is lack of consistent evidence for the effectiveness of surveillance in these groups and to date, no internationally accepted standardised model of patient follow up [177, 178]. This inadvertently puts an increasing burden on already increasing healthcare costs and underpins the demand for more accurate biomarkers of genuinely low risk tumours to enable earlier patient discharge.

Prior to biomarker validation studies within the JCUH cohort, results derived from the comparison of qualitative visual assessment of AMBRA1 expression with semi-quantitative staining intensities for expression, validated visual assessment as a robust and reliable method for IHC analysis of epidermal AMBRA1 expression levels and identified tumours with complete loss of epidermal AMBRA1 expression as a distinct high risk subgroup. Adoption of this simple method of visual analysis of epidermal

AMBRA1 expression will thus provide a simple and cheap as well as a favourable method for pathologists for future utility, over and above other currently used complex scoring algorithms in other biomarker studies.

Confirming preliminary observations leading up to the present validation study of AMBRA1 and Loricrin as prognostic biomarkers in AJCC stage I melanoma, results derived from multivariate survival curve analysis comparing visual scores of epidermal AMBRA1 expression against DFS in the JCUH melanoma cohort, confirmed loss of AMBRA1 loss as an independent prognostic biomarker able to predict risk of metastasis with reasonable sensitivity and specificity. Similarly, results derived from multivariate survival curve analysis comparing visual scores of Loricrin expression against DFS also validated Loricrin as a highly sensitive putative prognostic biomarker, however its expression alone over lying AJCC stage I melanomas was not highly specific, thereby limiting its prognostic impact as a single biomarker. Importantly however, when epidermal Loricrin expression was evaluated in combination with loss of epidermal AMBRA1 expression (AMLo), the combined assay resulted in improved overall sensitivity, specificity and PPV, while retaining a high NPV above the utility of either biomarker alone, collectively validating the combined loss of epidermal AMBRA1 and Loricrin (AMLo) as a novel independent prognostic biomarker for AJCC stage I melanomas.

Despite impending changes in melanoma tumour staging brought about by the updated 8th edition AJCC staging criteria (due to be implemented in January 2018), overall this will have minimal impact on the results derived from biomarker validation studies of AMBRA1 and Loricrin to date, since the study cohorts (both Newcastle Hospitals & JCUH) would remain classified as AJCC stage I tumours. However, with mitotic rate being omitted completely as a factor discerning TNM stage T1a and T1b (T1a distinguishes AJCC stage IA from AJCC stage IB which includes T1b and T2a melanomas) in the AJCC 8th edition guidelines, it was possible to further stratify the current AJCC stage I melanoma cohort into stage IA and IB in order to evaluate the prognostic impact of epidermal AMLo loss in each subgroup.

Results derived from multivariate survival curve analysis comparing AMLo high risk and low risk scores with DFS in AJCC (8th edition) stage IA melanomas not only validated the significant prognostic utility of AMLo scoring in predicting DFS in this subgroup in line with the new staging guidelines, but also highlighted an extremely high NPV of 100% associated with high sensitivity. Similarly, multivariate survival curve analysis comparing AMLo high risk and low risk scores with DFS in AJCC (8th edition) stage IB melanomas, demonstrated that epidermal AMLo loss in this subgroup was a highly sensitive prognostic biomarker with improved sensitivity, specificity and PPV while maintaining a high NPV, compared to the initial analyses in all AJCC stage I melanomas without differentiation of stages IA and IB.

AJCC stage IA and IB melanomas represent the thinnest tumours with the lowest associated mortality risk of ~ 14% over 10 years [37]. With low rates of metastases of tumours at an early physiological stage development, more stratified follow up strategies in these groups would potentially allow the greatest benefit for health economics, with some evidence suggesting that patients at the lowest risk of disease recurrence may not need intensive clinician follow-up as is generally recommended [179]. Currently in the UK, patients diagnosed with AJCC stage IA melanomas are followed-up at 3 – 4 monthly intervals for up to a year. However, as these tumours are regarded to be at the lowest risk of disease progression, the high NPV afforded by AMLo as a prognostic biomarker could translate to the future earlier discharge of patients diagnosed with AMLo low risk AJCC stage IA melanomas following surgical excision of the primary tumour. Patients diagnosed with stage IB melanomas on the other hand, are currently followed up at 3 – 6 monthly intervals for up to 5 years as they understandably make up a higher risk group compared to thinner stage IA tumours. Within this subgroup, AMLo as a prognostic biomarker may inform on the need for closer clinical or radiological surveillance and investigation following primary excision in melanomas scored as AMLo high risk and equally, reduce the need for frequent and prolonged follow up for melanomas stratified as AMLo low risk.

At present, there are no robust validated biomarkers in routine use to guide clinical management of AJCC stage I melanomas or predict risk of metastases. DecisionDX by Castle Biosciences measures gene signatures of 28 genes on FFPE melanoma tissue based on an original data set of 164 patients and validation in 101 with 5 years follow up on outcome [88, 89]. The test however, has a 2 – 3 week turnaround and is costly at up to $7,918 per test and as a prognostic biomarker only affords an NPV of 89% [88, 89] compared to AMLo which has a 5 hour test turnaround with an NPV of 98.7% and estimated cost of £150 pounds per test.

Overall, results from our biomarker validation studies suggest that going forwards with the staging changes brought in by the new 8th edition AJCC guidelines, the combined loss of AMLo overlying melanoma tumours as a prognostic biomarker will in fact enable prognostic evaluation of both AJCC stage IA and IB melanomas, supporting future validation work in a further independent "prospective retrospective" cohort. Completion of these studies will hopefully support future adoption of AMLo as a prognostic biomarker into NICE guidelines and eventual incorporation as a prognosticator in AJCC staging criteria for melanoma, facilitating its use in a wider context. More detailed evaluation of the proposed changes however, will be required when the full and finalised AJCC 8th edition guidelines are implemented in 2018.

Given that results from this chapter clearly identifies AMLo as a powerful prognostic biomarker enabling the identification of high risk tumour subsets, it is therefore important to consider the underlying mechanisms contributing to loss of either protein expression and to the loss of epidermal integrity as well as any impact on the loss of endothelial integrity, allowing for the identification of a drug-able target for which AMLo may serve as a companion biomarker to stratify patients for novel adjuvant therapy. These questions are addressed in the subsequent chapter.

Summary

- Loss of epidermal AMBRA1 expression overlying AJCC stage I melanomas is an independent prognostic biomarker identifying a high risk AJCC stage I melanoma subgroup; revealed by an assay with relatively high sensitivity but less specificity in predicting disease free survival.
- Loss of epidermal Loricrin expression overlying AJCC stage I melanomas is a prognostic biomarker; revealed by an assay with high sensitivity but which lacks specificity in predicting disease free survival.
- The combined loss of epidermal AMBRA1 and Loricrin (AMLo) expression overlying tumours is a novel prognostic biomarker for AJCC stage I melanomas allowing the identification of high risk tumour subgroups.
- AMLo as a prognostic biomarker allows evaluation of AJCC stage IA melanomas with a very high NPV, which could translate to the future earlier discharge of stage IA melanomas scored as AMLo low risk following surgical excision of the primary tumour.
- AMLo as a prognostic biomarker in AJCC stage IB melanomas may inform on the need for closer clinical or radiological surveillance and investigation following primary excision in tumours scored as AMLo high risk and equally, reduce the need for frequent and prolonged follow up for tumours stratified as AMLo low risk.

Chapter 4

Melanoma secretion of TGF-β2 mediates the down regulation of epidermal and endothelial integrity

4: Melanoma secretion of TGF-β2 mediates the down regulation of epidermal and endothelial integrity

4.1 Introduction 127

4.2 Results 129

4.2.1 Increased TGF-β2 by AJCC stage I melanomas correlates with the decreased expression of epidermal AMBRA1 129

4.2.2 High Risk AJCC stage I melanomas are associated with increased tumoural TGF-β2 135

4.2.3 TGF-β2 induces the down regulation of calcium-induced differentiation of primary keratinocytes 139

4.2.4 TGF-β2 induces the down regulation of AMBRA1 and junctional proteins in endothelial cells 141

4.2.5 Knockdown of TGF-β2 in metastatic melanoma cell lines prevents TGF-β2-induced down regulation of AMBRA1 and Claudin-5 in endothelial cells 148

4.2.6 Loss of endothelial AMBRA1 is associated with high risk AJCC stage I melanomas 153

4.3 Discussion 160

4.1 Introduction

Ulceration of a primary melanoma has been defined as an absence of an intact epidermis with reactive changes in the skin [70] and is an independent histological prognostic marker associated with poor survival [37]. However, the underlying biology of ulceration is still unclear and whether it represents the effect of an innately more aggressive and metastatic tumour phenotype expanding and breaching the top layers of the epidermis, or if ulcerated tumours result from a secretory factor mediating the loss of epidermal differentiation, leading to loss of integrity remains undefined.

Pilot data demonstrating a lack of association between epidermal AMBRA1 levels and degree of epidermal tumour invasion raises the possibility of a localised, tumour derived secretory process, mediating the loss of epidermal differentiation leading to ulceration (Ellis and Lovat, unpublished data). The loss in expression of epidermal AMBRA1 or Loricrin overlying melanoma tumours may therefore be key factors leading to tumour ulceration and as such, may define a surrogate marker of incipient melanoma ulceration that identifies a 'high risk' subgroup of patients associated with poorer prognosis.

The preferential benefit of treatment with interferon α-2b seen in ulcerated melanoma tumours (demonstrated by the EORTC 18991 and 18952 trials) further supports the existence of an underlying tumour secretory process leading to direct effects on the surrounding epithelium, contributing to ulceration [72] that is modified in some way by interferon-α. Interestingly, interferon α-2b has been shown to modulate TGF-β signalling where it enhances the secretion and pro-apoptotic effects of TGF-β1 in pre-neoplastic liver cells, preventing hepatocellular carcinogenesis [180]. This suggests that the paradoxical benefit following treatment with interferon α-2b in ulcerated melanoma may also be linked to TGF-β signalling.

In melanoma, autonomous activation of the TGF-β pathway has been well documented [134, 135] with TGF-β secretion by melanoma cells exerting cytostatic effects in early stages but coupled with its effect on the tumour microenvironment, promote tumour invasion and progression in advanced stages [127]. These findings are further supported by *in vitro* observations of increased TGF-β2 expression by melanoma cell lines compared to normal melanocytes [143] and *in vivo* studies demonstrating increased TGF-β2 expression correlates with tumour thickness and invasiveness [148] and that an increase in the secretion of both TGF- β2 and TGF-β3 is associated with melanoma progression and metastasis [144-147].

Preliminary results leading up to the present study demonstrated a significant association between increased secretion of isoform specific tumoural TGF-β2 and not TGF-β3 expression and the loss of epidermal AMBRA1 expression in all AJCC stage melanomas (Ellis and Lovat, unpublished data), suggesting that enhanced tumoural TGF-β2 secretion mediates loss of epidermal integrity leading to tumour ulceration. As the endothelium of blood and lymphatic vessels represent an epithelial structure like the epidermis, this also raises the possibility that enhanced or increased melanoma TGF-β2 secretion may mediate the loss of endothelial integrity and provide a route for tumour cell entry and subsequent metastasis. To test this hypothesis, the aim of the current chapter was to validate the correlation of increased tumoural TGF-β2 and decreased AMBRA1 expression *in vivo* specifically in AJCC stage I melanomas and any association with high risk tumours stratified as high or low risk by AMLo expression as well as evaluate the specific effect of TGF-β2 on endothelial AMBRA1 and endothelial cell junction proteins expression with the ultimate aim of defining a drug-able novel target to prevent the metastasis of high risk tumour subsets for which AMLo may serve as a companion biomarker.

4.2 Results

4.2.1 Increased TGF-β2 by AJCC stage I melanomas correlates with the decreased expression of epidermal AMBRA1

Pilot data leading to the present study demonstrated in a cohort of all AJCC stage melanomas that loss of epidermal AMBRA1 overlying primary tumours correlated with increased tumoural TGF-β2 expression (Ellis and Lovat, unpublished data). To evaluate this potential correlation in AJCC stage I melanomas alone, semi quantitative analysis of tumoural TGF-β2 expression in 76 AJCC stage I melanomas derived from the present study JCUH cohort was undertaken by automated IHC analysis using DAB counterstaining and results compared with epidermal AMLo expression defined in chapter 2.

Results revealed a trend for decreased epidermal AMBRA1 expression with the increased expression of tumoural TGF-β2 (Figure 4.1). However, semi-quantitative analysis of 76 AJCC stage I melanomas comparing mean percentage tumoural TGF-β2 staining intensity of each tumour with percentage decrease in epidermal AMBRA1 staining intensity overlying the same tumour compared with the normal adjacent epidermis, revealed no significant correlation between percentage decrease in epidermal AMBRA1 expression and increased tumoural TGF-β2 expression (Figure 4.2).

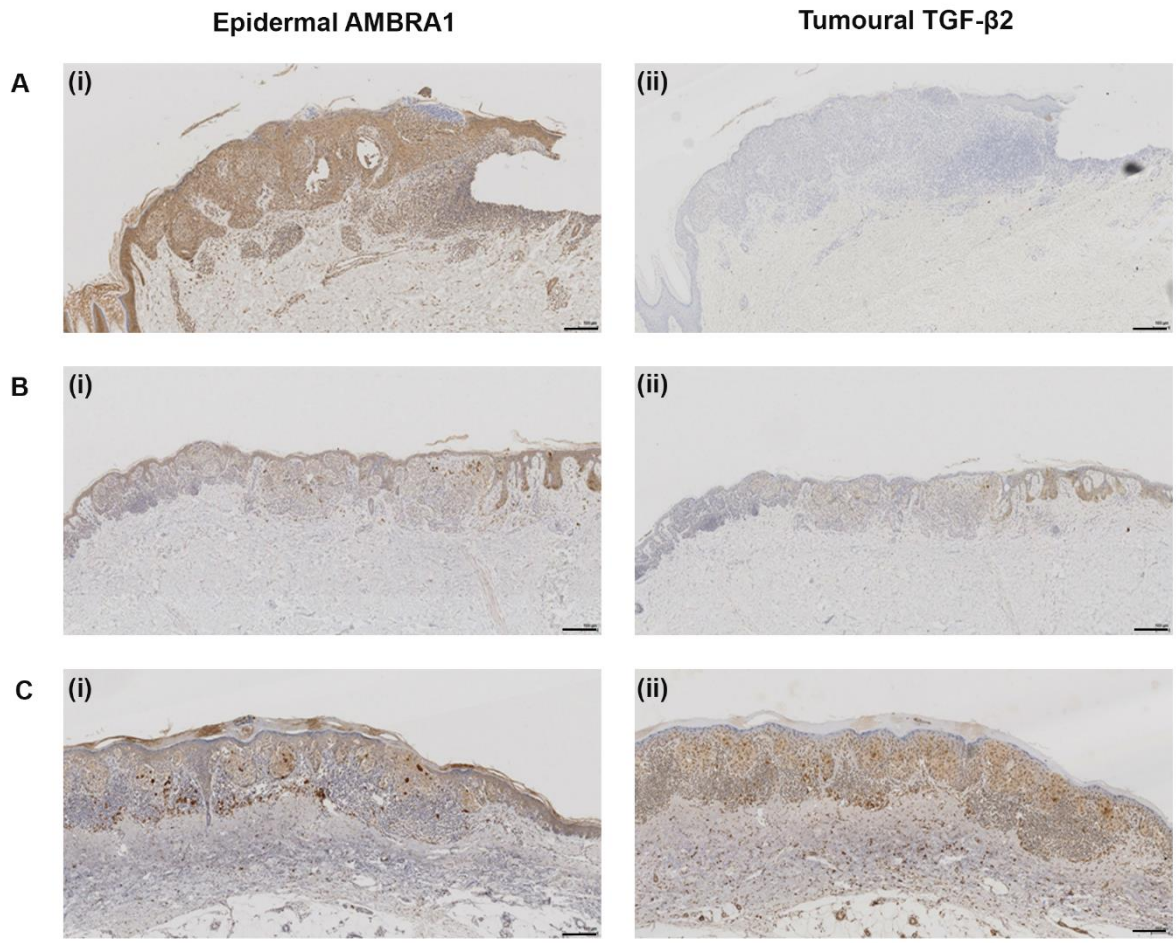

Figure 4.1: Visual analysis of the IHC expression of epidermal AMBRA1 and tumoural TGF-β2 in AJCC stage I melanomas revealed by DAB counterstaining suggests a potential association between loss of epidermal AMBRA1 and increased tumoural TGF-β2. Representative IHC photomicrographs of 3 AJCC stage I melanomas **(A – C)**: depicting **A (i)** maintained, **B (i)** some loss or **C (i)** complete loss of epidermal AMBRA1 associated with **A (ii)** lack of, **B (ii)** some or **C (ii)** high tumoural TGF-β2 expression in the corresponding tumour, revealed by DAB counterstaining (brown). Scale bar = 100 μm.

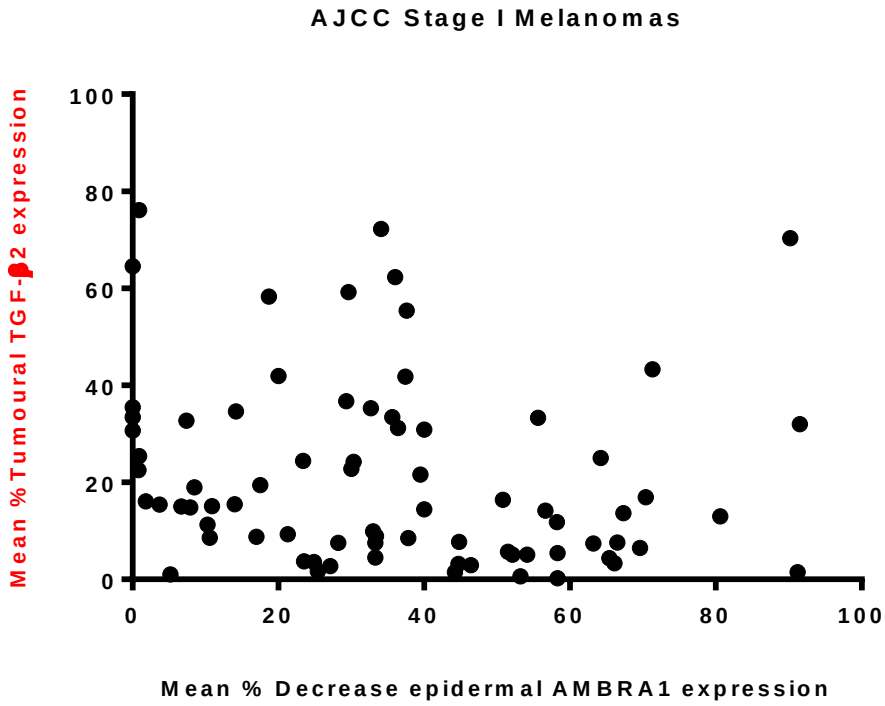

Figure 4.2: Loss of epidermal AMBRA1 overlying AJCC stage I melanomas does not correlate with increased tumoural TGF-β2 expression when compared by IHC using DAB counterstaining. Scatter graph of semi-quantitative IHC analyses in 76 AJCC stage I melanomas demonstrating no significant correlation between mean % tumoural TGF-β2 expression and mean % decrease in epidermal AMBRA1 expression revealed by DAB counter staining. Each point represents the matched mean % positive TGF-β2 staining intensity (derived from 10 fields of vision) against the mean % decrease in epidermal AMBRA1 expression overlying the tumour compared with that of the adjacent epidermis (derived from 10 fields of vision).

Unlike AMBRA1 which is only expressed in the epidermis, one of the main issues faced with IHC analysis of tumoural TGF-β2 expression using DAB counterstaining was the difficulty in discriminating between melanin staining with that of true TGF-β2 protein expression, likely accounting for inconsistent data derived from the semi-quantitative analysis (Figure 4.2) and providing a possible explanation for the lack of association between increasing tumoural TGF-β2 expression with loss of epidermal AMBRA1 overlying AJCC stage I melanomas that was observed by visual analysis. To eliminate this error, staining of tumoural TGF-β2 expression using VIP counterstaining was subsequently undertaken and semi-quantitative analyses repeated and correlated in the same way, with epidermal AMBRA1 expression in the same tumour revealed by DAB counterstaining. Using this method, both visual (Figure 4.3) and semi-quantitative analysis of tumoural TGF-β2 IHC expression revealed by VIP counterstaining in 21 AJCC stage I melanomas revealed a significant correlation between the mean % increase in tumoural TGF-β2 expression and the mean % decrease in epidermal AMBRA1 expression (Spearman's r= 0.711, 95% CI 0.412 – 0.872, *P* =0.0001, Figure 4.4).

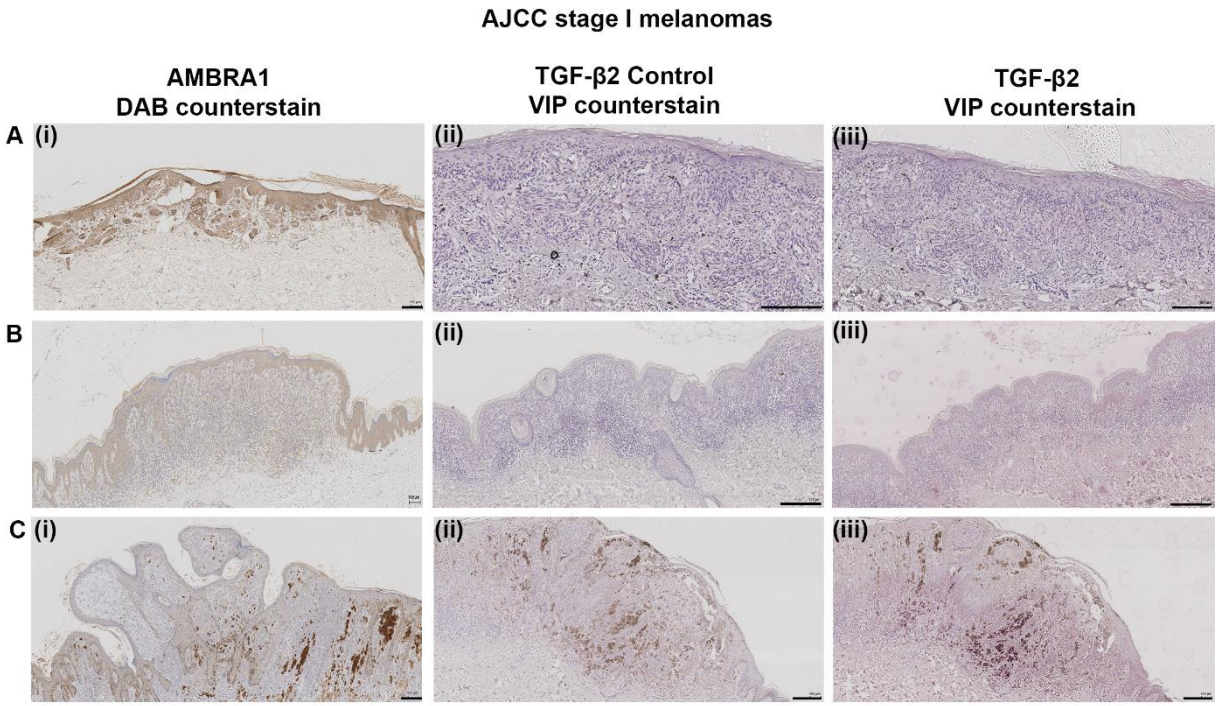

Figure 4.3: IHC expression of tumoural TGF-β2 in AJCC stage I melanomas revealed by VIP counterstaining. Representative IHC photomicrographs of 3 AJCC stage I melanomas depicting **A (i)** maintained, **B (i)** partial loss or **C (i)** complete loss of epidermal AMBRA1 expression revealed by DAB counterstain (brown) and corresponding tumoural TGF-β2 basal expression levels showing **A (iii)** absent **B (iii)** some or **C (iii)** increased TGF-β2 positive staining revealed by VIP counterstaining (pink) compared with matched negative controls **A – C (ii)** in the absence of TGF- β2 primary antibody. Scale bar = 100 μm.

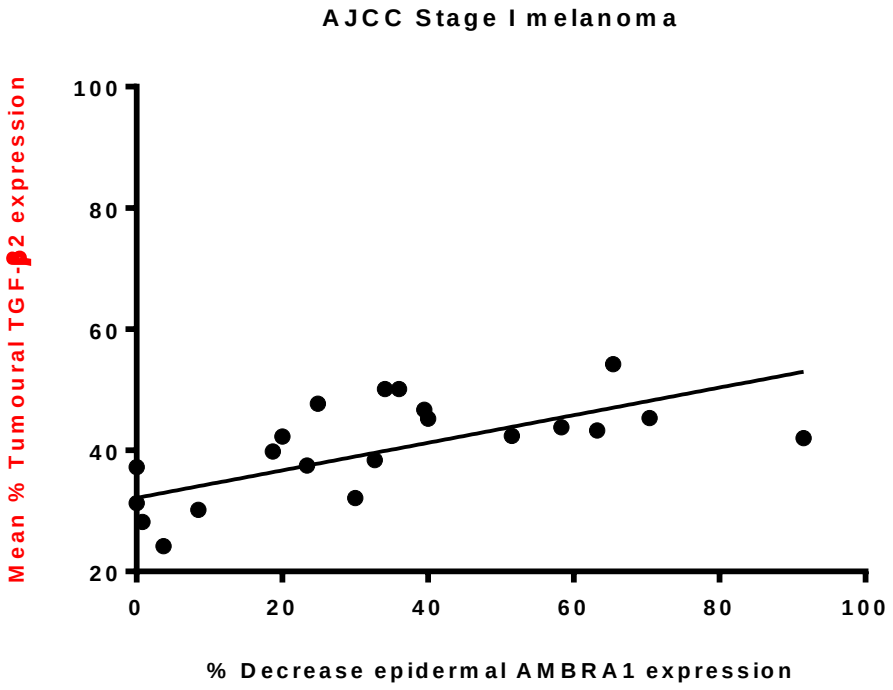

Figure 4.4: Loss of epidermal AMBRA1 overlying AJCC stage I melanomas correlates with increased tumoural TGF-β2 expression revealed by VIP counterstaining. Scatter graph of semi-quantitative IHC analyses in 21 AJCC stage I melanomas demonstrating a positive correlation between mean % tumoural TGF-β2 expression revealed by VIP counterstaining and mean % decrease in epidermal AMBRA1 expression revealed by DAB counterstaining. Each point represents the matched mean positive TGF-β2 staining intensity (derived from 10 fields of vision) against the mean % decrease in epidermal AMBRA1 staining intensity overlying the tumour compared with that of the normal adjacent epidermis (derived from 10 fields of vision). Spearman's r= 0.711, 95% CI 0.412 – 0.872, *P* =0.0001).

4.2.2 High Risk AJCC stage I melanomas are associated with increased tumoural TGF-β2

To test the hypothesis that high risk AJCC stage I melanomas at risk of developing metastases display increased expression of tumoural TGF-β2, correlation of the combined loss of epidermal AMBRA1 and Loricrin expression (AMLo) with tumoural TGF-β2 expression in AJCC stage I melanomas was assessed. Given that IHC staining for AMBRA1 and Loricrin in the JCUH study cohort was performed using DAB counterstaining on the Ventana automated platform, IHC staining for TGF-β2 expression was once again performed using this method in attempt to standardise the semi-quantitative analysis and correlation of tumoural TGF-β2 with epidermal AMBRA1 and Loricrin loss. To eliminate the issue associated with difficulty in discerning between true TGF-β2 staining with that of melanin, FFPE melanoma tumour sections were bleached prior to IHC staining for TGF-β2 with DAB counterstaining on the Ventana platform as described in section 2.10.2.

Qualitative visual analysis of 29 AJCC stage I melanomas using this methodology revealed a trend for increased tumoural TGF-β2 staining intensity in tumours that subsequently developed metastatic disease compared to tumours that remained localised (example indicated by Figure 4.5). This observation was further supported by semi-quantitative analysis of mean percentage tumoural TGF-β2 in 10 AJCC stage I melanomas that subsequently developed metastasis (Mean 63.8 ± 2.497 SEM) with mean percentage tumoural TGF-β2 expression in 19 tumours that remained localised, revealing significantly increased TGF-β2 expression by the high risk tumour subset (Mean 50.68 ± 2.943 SEM; Unpaired t test $^{**}P$ =0.007, 95% CI (3.959 – 22.27), Figure 4.6).

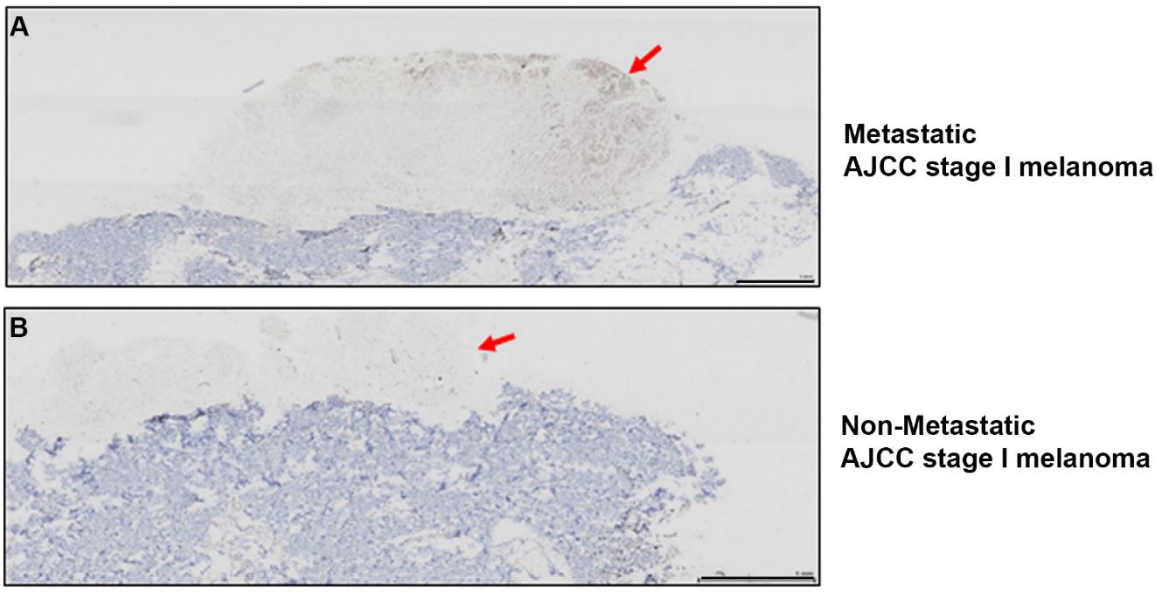

Figure 4.5: TGF-β2 expression (revealed following bleaching and automated IHC analysis with DAB counterstaining) is increased in high risk AJCC stage 1 melanomas. Representative IHC photomicrographs of tumoural TGF-β2 basal expression expression (revealed by DAB counterstaining) in bleached AJCC stage I melanoma tumour sections depicting **A** increased tumoural TGF-β2 expression in a tumour that subsequently metastasised compared to **B** reduced tumoural TGF-β2 expression in a tumour that remained localised. Upper margin of tumour bulk indicated by red arrows. Scale bar =100 μm.

In addition, semi-quantitative analysis of the mean percentage tumoural TGF-β2 expression levels in these 29 tumours AJCC stage I melanomas demonstrated a significant increase in the mean percentage tumoural expression of TGF-β2 by tumours stratified as high risk by AMLo analysis (Mean % 59.52 ± 2.44 SEM) compared with those stratified as AMLo low risk (Mean % 49.1 ± 4.14; Unpaired t test **P* =0.02, 95% CI (1.136-19.7), Figure 4.7). Collectively, these results suggest that high risk AJCC stage I melanoma tumours that go on to develop metastasis have increased basal expression levels of TGF-β2 for which the loss of epidermal AMLo is a predictive biomarker.

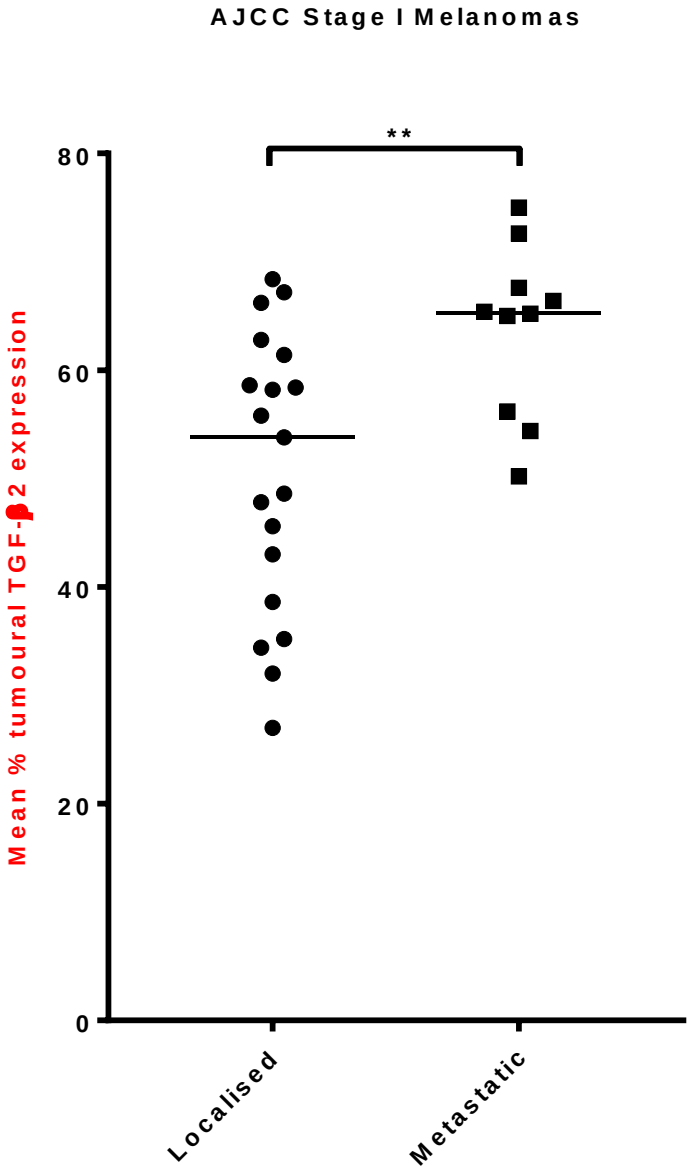

Figure 4.6: Tumoural TGF-β2 expression is increased in AJCC stage I melanomas that developed metastatic disease compared to localised tumours. Scatter graph representing the mean % tumoural TGF-β2 expression in 19 primary AJCC stage I melanomas that remained localised compared to expression in 10 melanomas that eventually developed metastases. Each point is the mean % tumoural TGF-β2 staining intensity from 5 fields of vision. Horizontal bars represent the mean % tumoural TGF-β2 staining intensity for each group ± SEM demonstrating significantly higher mean % tumoural TGF-β2 expression in AJCC stage I melanomas that develop metastases. Unpaired t test ***P* =0.007, 95% CI (3.959 – 22.27).

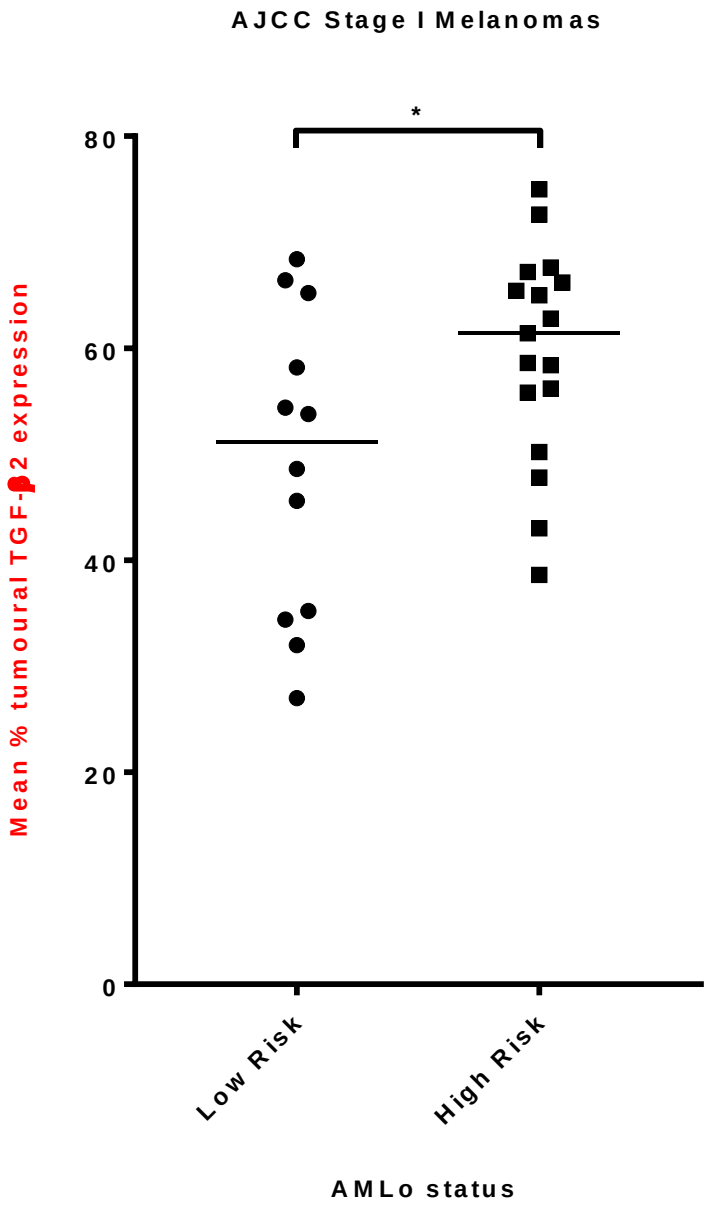

Figure 4.7: High risk AJCC stage I melanomas stratified by AMLo display significantly increased TGF-β2 expression compared to AMLo low risk tumours. Scatter graph representing the mean % tumoural TGF-β2 expression in 12 primary AJCC stage I melanomas stratified as AMLo low risk compared to expression in 17 AMLo high risk tumours. Each point is the mean % tumoural TGF-β2 staining intensity derived from 5 fields of vision. Horizontal bars represent the mean % tumoural TGF-β2 staining intensity for each group ± SEM demonstrating significantly higher mean % tumoural TGF-β2 expression in AMLo high risk AJCC stage I melanomas. Unpaired t test *P =0.02, 95% CI (1.136 – 19.7).

4.2.3 TGF-β2 induces the down regulation of calcium-induced differentiation of primary keratinocytes

Preliminary data leading up to the present study demonstrated the integral role of AMBRA1 in epidermal differentiation, with expression *in vivo* increasing in line with keratinocyte differentiation from the basal layer to the *stratum corneum*, and which in *in vitro* studies of calcium-induced differentiation of primary keratinocytes is reflected by a concurrent increase in the terminal differentiation marker Loricrin (Ellis and Lovat, unpublished data). In addition, the lack of association between AMBRA1 expression and epidermal tumour invasion in the presence of epidermal hyperplasia suggests the presence of an underlying chronic, tumour secretory process (Ellis and Lovat, unpublished data). These findings coupled with the preferential benefit of interferon-α treatment seen in ulcerated tumours [72, 73] and studies demonstrating that increased secretion of TGF-β2 is associated with melanoma progression and metastasis [144-147] led to the hypothesis that melanoma secretion of TGF-β2 leads to epidermal AMBRA1 down regulation and in turn, loss of epidermal integrity and tumour ulceration, conferring a worse prognosis.

To test this hypothesis, primary keratinocytes were subjected to calcium-induced differentiation by culture for 5 days in high calcium medium (1.3 mM Calcium Chloride) in the presence or absence of 0.3, 1 or 10 ng/ml recombinant TGF-β2 or an equal volume of vehicle control (4 mM Hcl + 0.1% BSA), prior to western blotting for the expression of AMBRA1, Loricrin and β-Actin as a loading control. Results demonstrated increased expression of both AMBRA1 and Loricrin following 5 days culture of primary keratinocytes in medium with high calcium (Figure 4.8). However, culture for 5 days in high calcium media in the presence of recombinant TGF-β2 resulted in the dose dependent down regulation of both AMBRA1 and Loricin (Figure 4.8), collectively suggesting TGF-β2 secretion by melanoma cells leads to dysregulated differentiation and epidermal ulceration in ‘high risk’ tumours, associated with poorer prognosis.

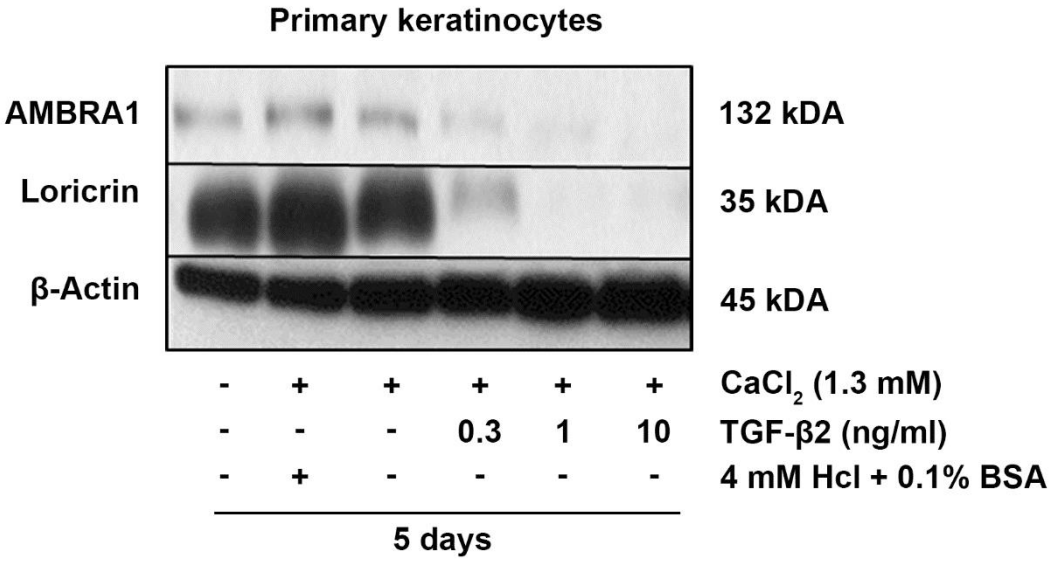

Figure 4.8: TGF-β2 mediates the down regulation of AMBRA1 and Loricrin in calcium-induced differentiated primary keratinocytes. Representative western blot for the expression of AMBRA1 (132 kDA), Loricrin (35 kDA) or β-Actin loading control (45 kDA) in primary keratinocytes in which differentiation was induced by culture in high calcium medium (1.3 mM Calcium Chloride) in the presence or absence of either 0.3, 1.0 or 10.0 ng/ml of human recombinant TGF-β2 or vehicle control over 5 days.

In the management of malignant melanoma however, as the whole tumour along with the overlying epidermis is removed at the time of primary excision, the potential effects of tumoural secretion of TGF-β2 are more pertinent to endothelial and endo-lymphatic integrity, disruption of which provides a route for subsequent tumour invasion and metastasis. Subsequent studies were therefore focused towards evaluating the impact of TGF-β2 secretion by primary melanomas on endothelial integrity.

4.2.4 TGF-β2 induces the down regulation of AMBRA1 and junctional proteins in endothelial cells

Since the epidermis is an epithelial structure, the morphological changes that occur in the epidermis brought about by melanoma TGF-β2 secretion that lead to deregulated epidermal differentiation and ulceration are similarly, likely to occur in the surrounding endothelium. To test the hypothesis that TGF-β2 secretion by melanomas cells mediates down regulation of AMBRA1 and vascular endothelial integrity, model HUVEC endothelial cells were first cultured in the presence or absence of 10 ng/ml recombinant TGF-β2 for 24, 48 and 72 hours prior to the analysis of AMBRA1 and endothelial junctional proteins Claudin-5 and VE-Cadherin expression by western blotting. Results demonstrated the time dependent down regulation of AMBRA1 and Claudin-5 (Figure 4.9 A), with significant down regulation of AMBRA1 observed following 48 and 72 hours culture in the presence 10 ng/ml recombinant TGF-β2 compared to expression in vehicle treated control HUVEC cells (One way ANOVA with Dunnett's post-test correction *P <0.02, **P <0.001, Figure 4.9 B) and significant down regulation of Claudin-5 observed after 48 and 72 hours culture in the presence of recombinant TGF-β2 (One way ANOVA with Dunnett's post-test correction ***P <0.0001, Figure 4.9 D). A similar trend for time-dependent TGF-β2-induced down regulation of VE Cadherin was also observed (Figure 4.9 A and C), however this effect across 3 independent experiments was not significant.

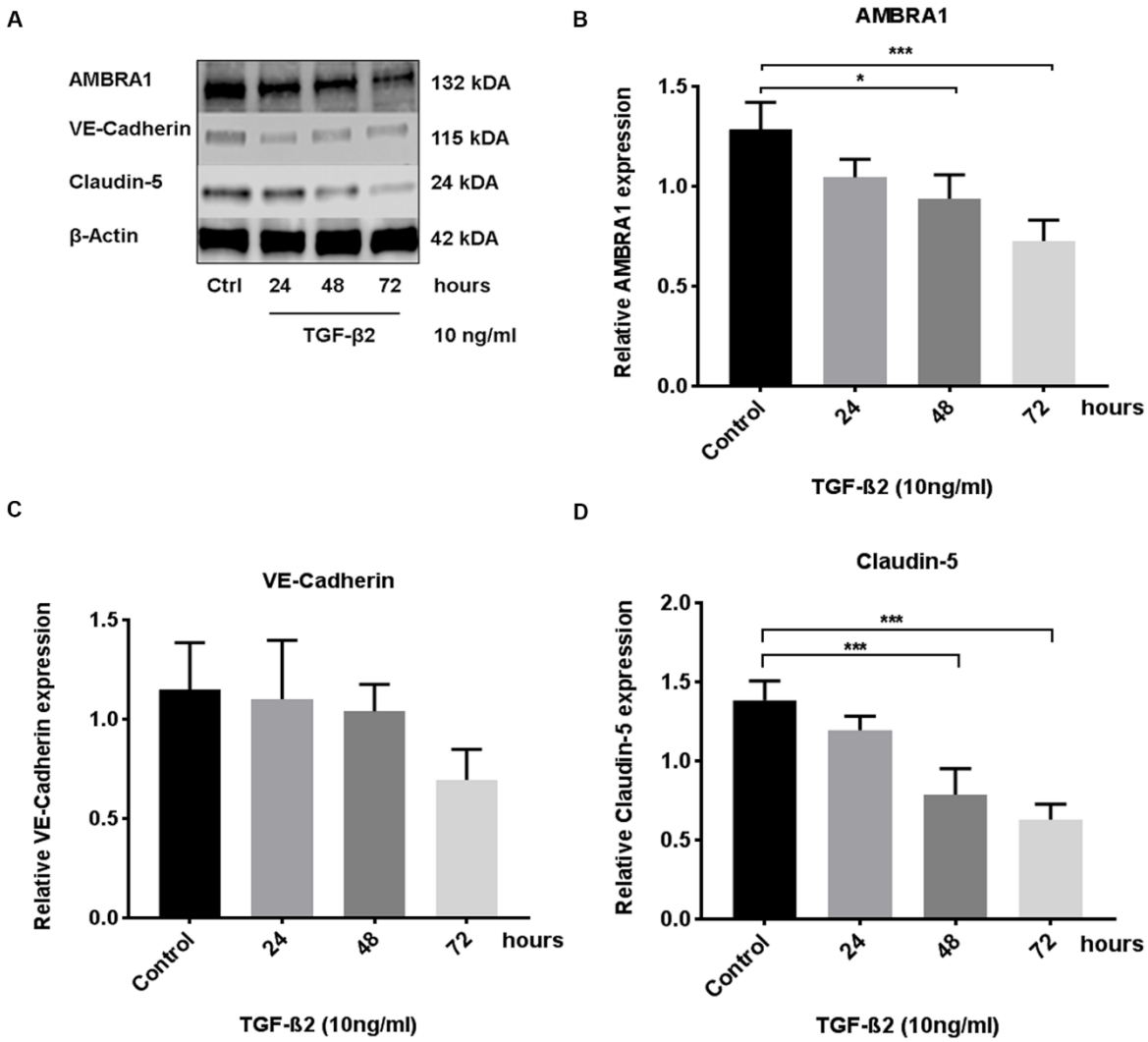

Figure 4.9: TGF-β2 induces the down regulation of AMBRA1 and junctional protein expression in HUVEC endothelial cells. A Representative western blot for the expression of AMBRA1 (132 kDA), VE-Cadherin (115 kDA), Claudin-5 (24 kDA) and β-Actin (42 kDA) loading control in HUVEC cells following culture in the absence (Ctrl) or presence of 10 ng/ml recombinant TGF-β2 for 24, 48 and 72 hours. **B** Relative protein expression (quantified by densitometry) of AMBRA1, **C** VE-Cadherin or **D** Claudin-5 normalised to β-Actin and expressed relative to the mean protein/β-Actin value for each experiment, following treatment of HUVECs for 24, 48 and 72 hours with 10 ng/ml recombinant TGF-β2. Each bar represents the mean ± SD of 3 replicate experiments. One way ANOVA with Dunnett's post-test correction *P <0.02, ***P <0.001.

To further evaluate the potential for TGF-β2-mediated down-regulation of endothelial AMBRA1 and junctional proteins and the impact of melanoma secretion of TGF-β2 on the endothelial integrity, identical experiments were performed in primary human dermal lymphatic endothelial cells to more accurately represent an *in vivo* setting.

Isolation of primary human dermal endothelial cells (HDEC) from the dermis of redundant adult foreskin samples was initially attempted using an endothelial cell specific EN4 antibody as described in section 2.3.1. However, use of this method resulted in very low endothelial cell yield in which selected cells failed to expand or achieve confluency despite 21 days of culture. Furthermore, analysis of selected endothelial cell populations following 21 days subsequent culture in endothelial specific culture media revealed significant fibroblast contamination (Figure 4.10).

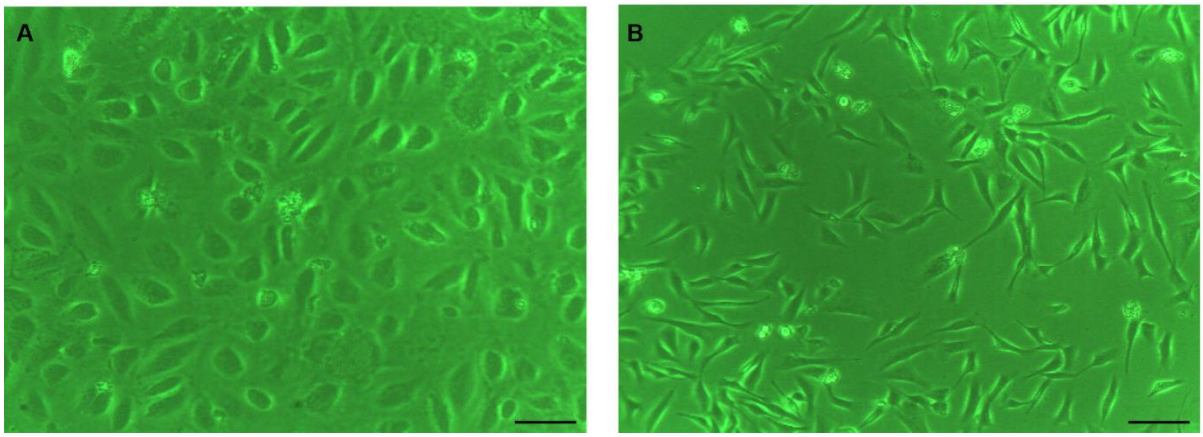

Figure 4.10: Isolation of human dermal endothelial cells from human foreskin samples using EN4 antibody coated wells results in mixed dermal endothelial cell and fibroblast subpopulations. Representative photomicrographs of EN4 endothelial cell antibody selected primary dermal subpopulations following 21 days culture and depicting two distinct cell colonies of **A** dermal microvascular endothelial cells that grow in pebble-patterned circular colonies and **B** dermal fibroblasts that grow as spindle-shaped clusters. Scale bar =50 μm.

Isolation of primary human HDECs was also attempted using human Phycoerythrin (PE) anti CD31 antibody with Miltenyi Biotech magnetic columns as described in section 2.3.2. Using this method of endothelial cell selection resulted in culture of relatively pure endothelial cell colonies at passage 1 that grew in circular clusters and expanded to achieve confluency after 21 days of culture. At day 14 of culture however, there was once again evidence of fibroblast contamination that rapidly expanded to form independent colonies at day 21 (Figure 4.11).

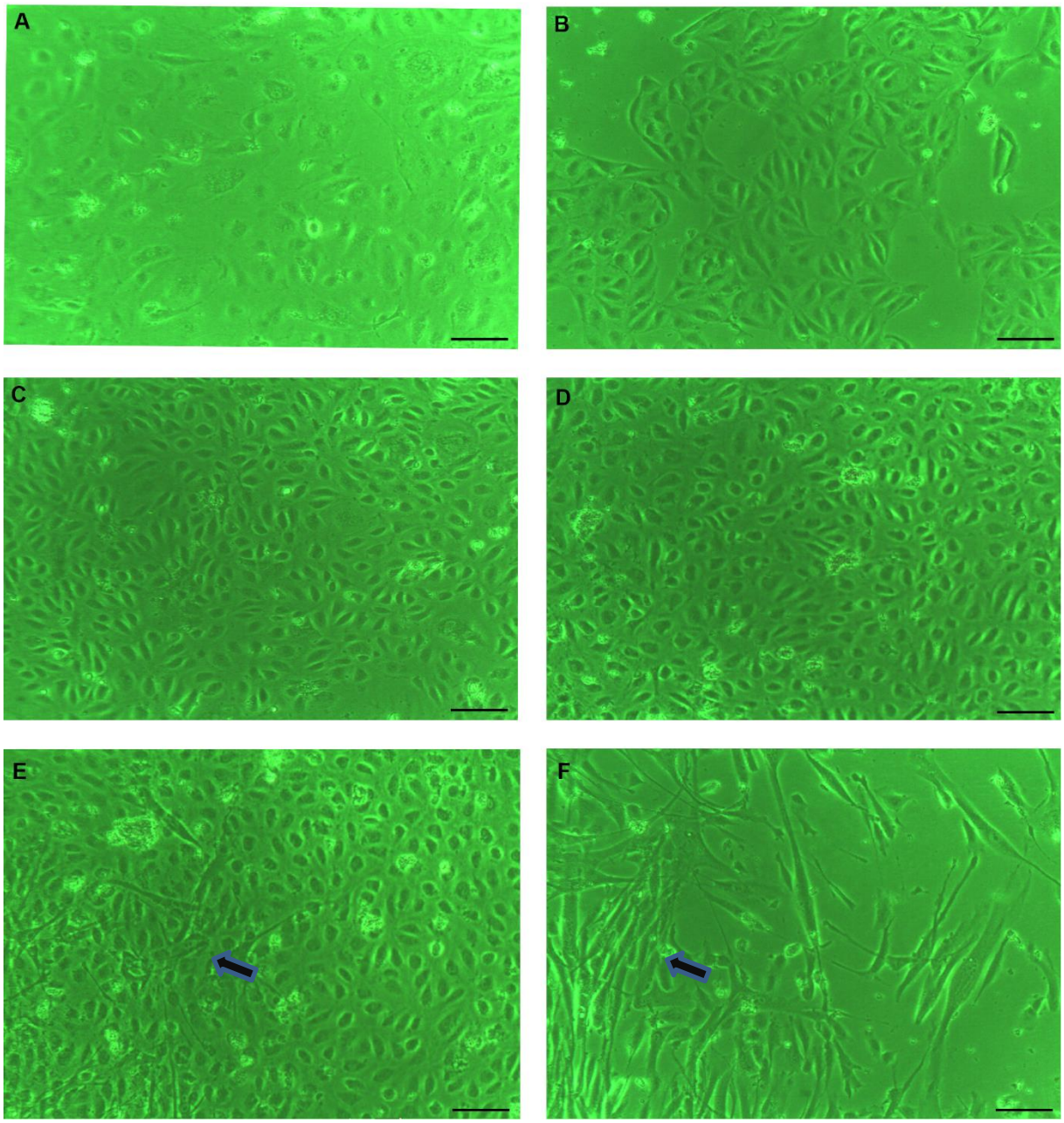

Figure 4.11: Isolation of human dermal endothelial cells from donor foreskin samples using human PE anti CD31 antibody with Miltenyi Biotech magnetic columns results in a mixed colony of dermal endothelial cells and fibroblasts. Representative photomicrographs of **A** an initial mixed colony of dermal endothelial cells and fibroblasts derived from a donor foreskin sample at passage 0, or dermal endothelial cells after anti CD31 cell selection (passage 1) following **B** 7 days, **C** 14 days or **D** 21 days of culture and depicting the increasing presence of contaminating fibroblasts after **E** 14 days or **F** 21 days of maintained culture. Black arrows indicate fibroblasts. Scale bar =100 μm.

Due to the inability to isolate and culture pure populations of primary dermal endothelial cells, human dermal lymphatic endothelial cells (HDLEC) isolated from juvenile foreskin were subsequently obtained from PromoCell as detailed in section 2.1.2 in order to determine the impact of melanoma TGF-β2 secretion on primary endothelial AMBRA1 and endothelial junctional protein expression. Dermal lymphatic endothelial cells were chosen over dermal microvascular endothelial cells as in an *in vivo* setting, the lymphatics represent one of the earliest potential points for tumour cell entry with metastases from melanoma most commonly first presenting at regional lymph nodes [181].

To test the hypothesis that TGF-β2 secretion by melanoma tumour cells mediates down regulation of AMBRA1 resulting in loss of lymphatic endothelium integrity, HDLECs were treated with 10 ng/ml recombinant TGF-β2 for 24, 48 and 72 hours prior to the analysis of AMBRA1 and Claudin-5 expression by western blotting. As with the observed results in studies in HUVEC cells, results demonstrated significant TGF-β2-induced down regulation of AMBRA1 and Claudin-5 following 72 hours culture of HDLECs in the presence of 10 ng/ml recombinant TGF-β2 compared to expression in vehicle treated control HDLECs (Unpaired t Test $*P$ <0.04 AMBRA1, $**P$ <0.001 Claudin-5, Figure 4.12).

Collectively, these results suggest that melanoma secretion of TGF-β2 induces the down regulation of endothelial AMBRA1 and endothelial junctional protein expression thereby facilitating tumour metastasis by disrupting vascular and lymphatic endothelium integrity, leading to alterations in barrier function and the creation of an entry point for tumour cells into the wider circulation.

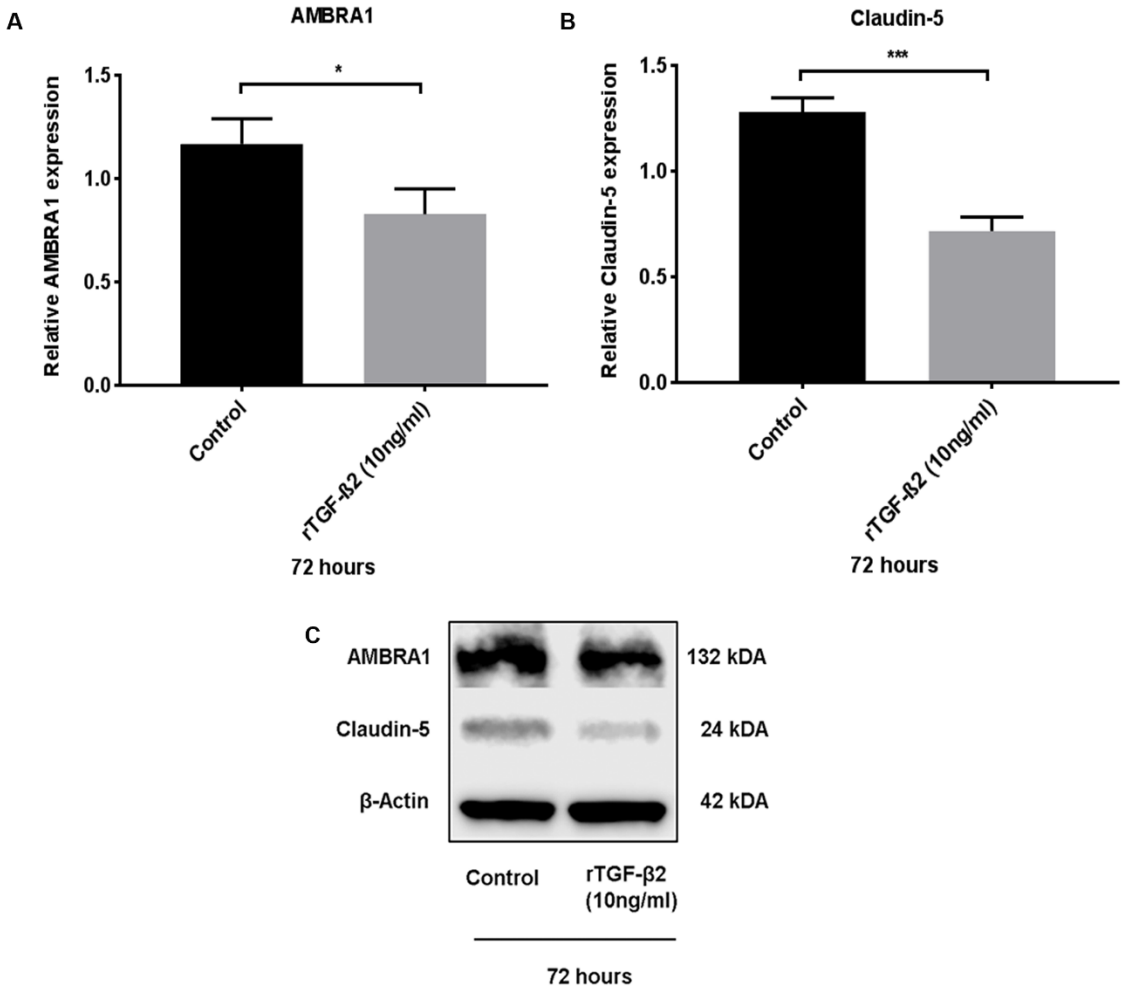

Figure 4.12: TGF-β2 induces the down regulation of AMBRA1 and Claudin-5 in primary HDLECs. Relative protein expression (quantified by densitometry) of **A** AMBRA1 and **B** Claudin-5 normalised to β-Actin and expressed relative to the mean protein/β-Actin value for each experiment, following treatment of HDLECs for 72 hours with 10 ng/ml recombinant TGF-β2. Each bar represents the mean ± SD of 3 replicate experiments. Unpaired t Test *P <0.04 (AMBRA1), ***P <0.001 (Claudin-5). **C** Representative western blot for the expression of AMBRA1 (132 kDA), Claudin-5 (24 kDA) and β-Actin (42 kDA) loading control in HDLECs following treatment with 10 ng/ml recombinant TGF-β2 for 72 hours or an equal volume of vehicle control for 72 hours in control no treatment cells.

4.2.5 Knockdown of TGF-β2 in metastatic melanoma cell lines prevents TGF-β2-induced down regulation of AMBRA1 and Claudin-5 in endothelial cells

Preliminary data leading up to the present study also demonstrated the increased expression of TGF-β2 mRNA as well as increased secretion of TGF-β2 by metastatic melanoma cell lines SK-Mel-28, A375 and MeWo (Lovat et al, unpublished data). To test the hypothesis that metastatic melanoma secretion of TGF-β2 results in the down regulation of endothelial AMBRA1 and endothelial junctional proteins, HUVEC cells were subjected to culture with supernatants derived from A375 melanoma cells previously stably transfected with control (A375 shControl) or supernatants derived from A735 melanoma cells where TGF-β2 has been stably knocked down (A375 shTGF-β2), prior to western blotting for AMBRA1 and Claudin-5.

As HUVEC cells require culture only in complete ECCM whereas A375 melanoma cells are routinely maintained in DMEM, supernatants derived from A375 shControl and A375 shTGF-β2 melanoma cells used to treat HUVEC cells would need to consist of complete ECCM. As such, prior to the treatment of HUVECs with A375 melanoma cell supernatants subjected to TGF-β2 modulation, the cell viability of A375 shControl and shTGF-β2 melanoma cells cultured in complete ECCM was initially compared with the cell viability of cells cultured in complete DMEM, by manual cell counting following culture in either cell media for 72 hrs.

Results confirmed no significant difference between the cell viability of either cell line cultured in either ECCM or DMEM (Figure 4.13) and hence for all subsequent experiments comparing the effect of A375 shControl or A375 shTGF-β2 melanoma supernatants on endothelial AMBRA1 or junctional protein expression, both melanoma cell lines were cultured in complete ECCM prior to collection and use of supernatants to treat HUVEC or HDLECs.

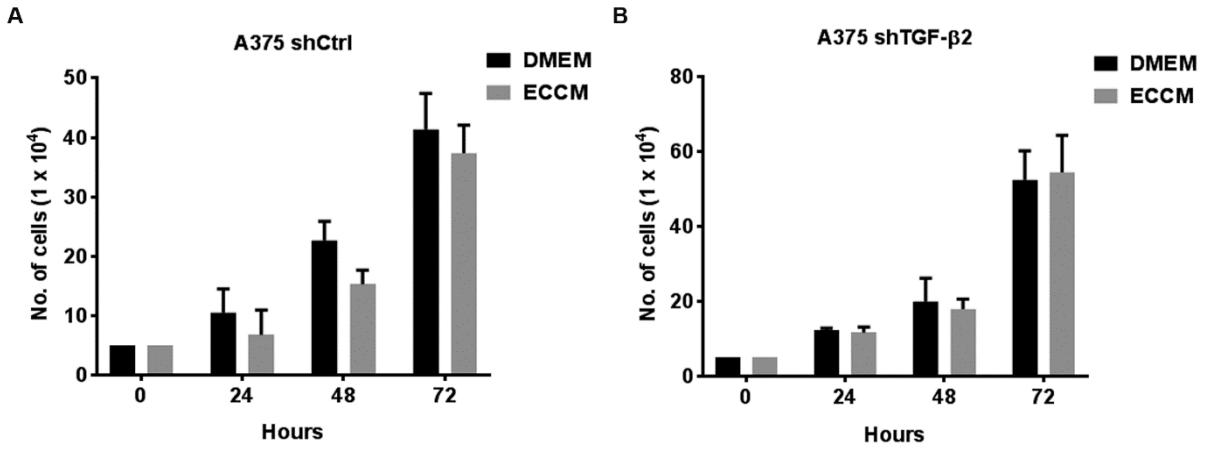

Figure 4.13: Culture of A375 cells subjected to TGFβ2 modulation in either complete ECCM or DMEM has no effect on cell viability. Cell viability of **A** A375 shControl or **B** shTGF-β2 melanoma cells following growth in ECCM or DMEM for 24, 48 and 72 hours. Each bar is the mean of 3 replicate experiments ± SD.

To assess the effect of modulating TGFB 2 expression in melanoma cells on endothelial AMBRA1 and junctional protein expression, HUVEC cells were first subjected to culture for 72 hours in either complete ECCM or supernatants derived from A375 shControl or A375 shTGF-β2 melanoma cells prior to western blot analysis for the expression of AMBRA1and Claudin-5. Where control A375 melanoma cell supernatants were used as culture media, media changes were conducted daily to account for depleted nutrient content. Results demonstrated the significant down regulation of both AMBRA1 and Claudin-5, following culture in TGF-β2-rich A375 melanoma supernatant (One way ANOVA with Dunnett's post-test correction, ***P =0.001 for AMBRA1 (Figure 4.14 A and B), and **P <0.01 for Claudin-5 (Figure 4.14 A and C) and partial rescue of TGF-β2-induced AMBRA1 and Claudin-5 down regulation (Figure 4.14 B & C) in HUVEC cells subjected to culture in TGF-β2 depleted A375 melanoma supernatants.

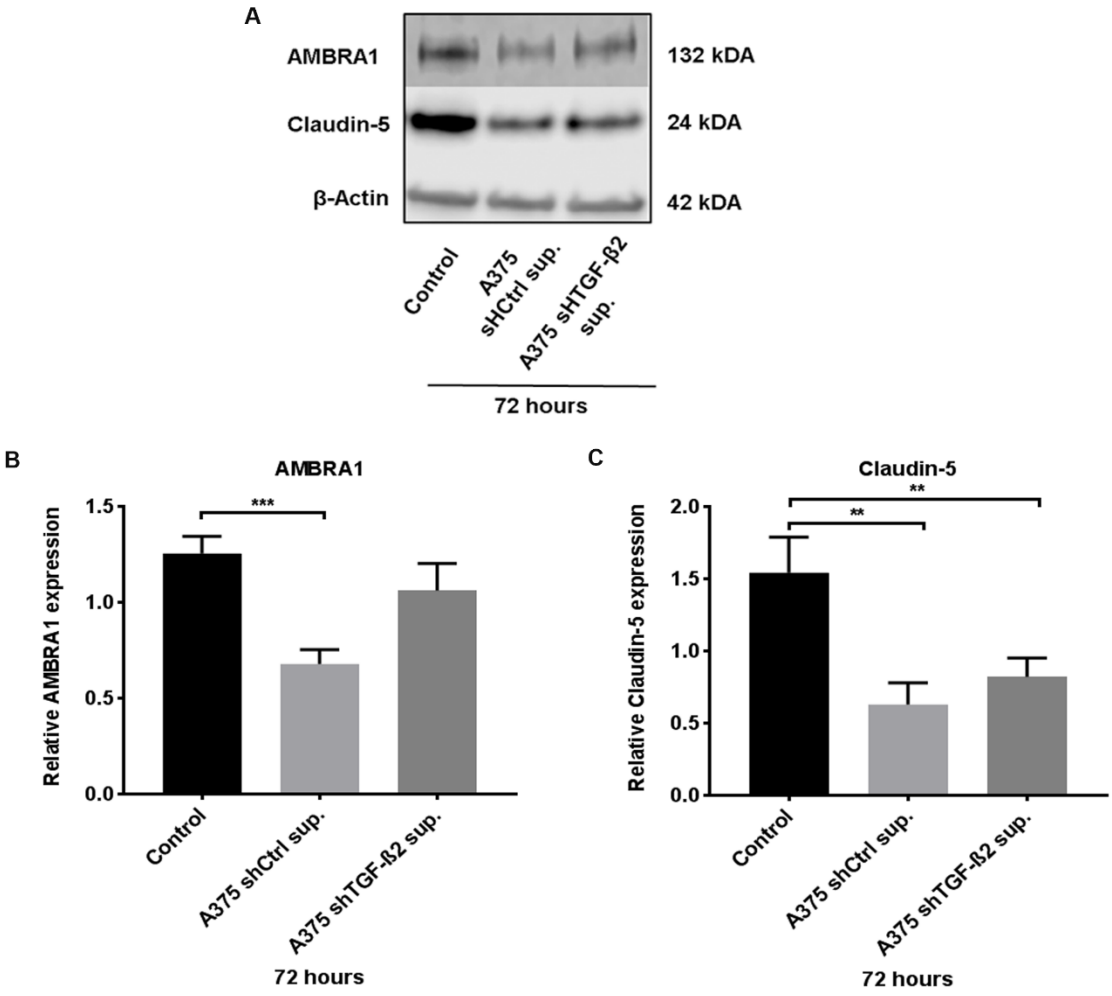

Figure 4.14: Treatment of HUVEC cells with TGF-β2-depleted melanoma supernatants derived from A375 melanoma cells with stable TGF-β2 knockdown prevents TGF-β2 induced down regulation of AMBRA1 and Claudin-5. A Representative western blot for the expression of AMBRA1 (132 kDA), Claudin-5 (24 kDA) or β-Actin (42 kDA) loading control in HUVECs cultured in ECCM vehicle control or HUVECs following culture for 72 hours in supernatants derived from A375 shControl (A375 shCtrl sup) or A375 shTGF-β2 (A375 shTGF-β2 sup) melanoma cells. **B** Relative protein expression (quantified by densitometry) of AMBRA1 and **C** Claudin-5 normalised to β-Actin and expressed relative to the mean protein/β-Actin value for each experiment, following culture of HUVECs for 72 hours in ECCM (vehicle control) or supernatants derived from A375 shControl or A375 shTGF-β2 melanoma cells. Each bar represents the mean ± SD of 3 replicate experiments. One way ANOVA with Dunnett's post-test correction ****P* =0.001 (AMBRA1), ***P* <0.01 (Claudin-5).

To test whether melanoma TGF-β2 mediated down regulation of AMBRA1 and junctional protein expression may also be prevented in primary human dermal lymphatic endothelial cells by modulation of TGF-β2 expression in melanoma cells, HDLECs were also subjected to culture for 72 hours in supernatants derived from A375 shControl or shTGF-β2 melanoma cells, prior to western blot analysis of AMBRA1 and Claudin-5 expression. Results clearly demonstrated the significant down regulation of AMBRA1 in HDLECs following culture for 72 hours in TGF-β2-rich A375 shControl melanoma supernatant (One way ANOVA with Dunnett's post-test correction $^{**}P$ <0.01, $^{***}P$ <0.001, Figure 4.15 A and B), with partial rescue of TGF-β2-induced AMBRA1 down regulation also observed after 72 hrs culture TGF-β2-depleted A375 shTGF-β2 melanoma supernatant (Figure 4.15 A & B). Similarly, results demonstrated a trend for the down regulation of Claudin-5 expression following culture of HDLECs for 72 hours in TGF-β2-rich A375 melanoma supernatant, with again an observed partial rescue of Claudin-5 expression in HDLECs cultured in supernatants derived from A375 melanoma cells previously subjected to stable knockdown of TGF-β2 (Figure 4.15 A & C).

Collectively, these data suggest that blockade of TGF-β2 secretion by melanoma cells may prevent the down regulation of AMBRA1 and Claudin-5 in both vascular and lymphatic endothelium. The partial rescue of AMBRA1 and Claudin-5 observed in HUVEC cells and HDLECs could be attributed to sub-complete TGF-β2 short hairpin RNA knockdown of the A375 melanoma cell clone used to derive the treatment supernatant (65-70% TGF-β2 knockdown confirmed by qPCR; Lovat et al, unpublished data), where the melanoma cells may still retain some residual TGF-β2 secreting function.

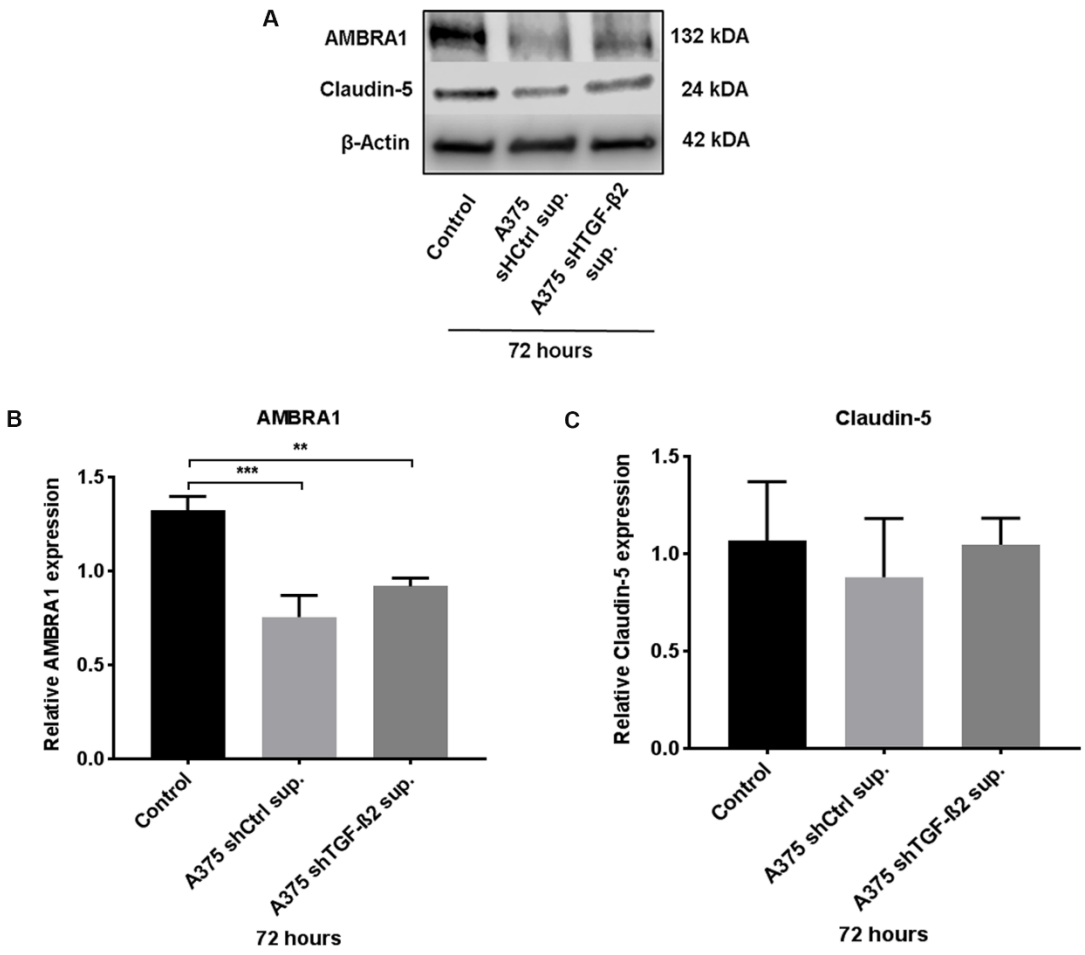

Figure 4.15: Knockdown of TGF-β2 in melanoma cells inhibits TGF-β2 –mediated down regulation of AMBRA1 and Claudin-5 in primary HDLECs. A Representative western blot for expression of AMBRA1 (132 kDA), Claudin-5 (24 kDA) or β-Actin (42 kDA) loading control in control HDLECs (cultured for 72 hours in complete ECCM vehicle control) or HDLECs following culture for 72 hours in supernatants derived from A375 shControl or A375 shTGF-β2 melanoma cells. **B** Relative protein expression of AMBRA1 and **C** Claudin-5 in HDLECs quantified by densitometry (normalised to β-Actin loading control and expressed relative to the mean protein/β-Actin value for each experiment), following culture for 72 hours in ECCM (vehicle control) or supernatants derived from A375 shControl or A375 shTGF-β2 melanoma cells. Each bar represents the mean ± SD of 3 replicate experiments. One way ANOVA with Dunnett's post-test correction ***P* <0.01, ****P* <0.001 (AMBRA1).

4.2.6 Loss of endothelial AMBRA1 is associated with high risk AJCC stage I melanomas

Data in this chapter so far has shown that AJCC stage I melanomas at high risk of metastases express or secrete higher levels of isoform specific TGF-β2 and that TGF-β2 secretion by melanoma cells induces the down regulation of AMBRA1 and endothelial junctional protein expression *in vitro*; an effect that was partially rescued with by blockade of melanoma TGF-β2.

To investigate if endothelial AMBRA1 is concurrently decreased in the melanoma microenvironment of tumours in which AMBRA1 expression in the overlying epidermis is lost, immunofluorescence (IF) analysis for the dual expression of endothelial AMBRA1 and CD31 (an endothelial cell marker expressed by both vascular and lymphatic endothelial cells) was undertaken in FFPE AJCC stage I tumour sections. Pre-assay optimisation was performed using FFPE sections of HUVEC cell pellets, where clear dual expression of AMBRA1 (red) and CD31 (green) was visualised, with DAPI as a stain for cell nuclei (blue) (Figure 4.16).

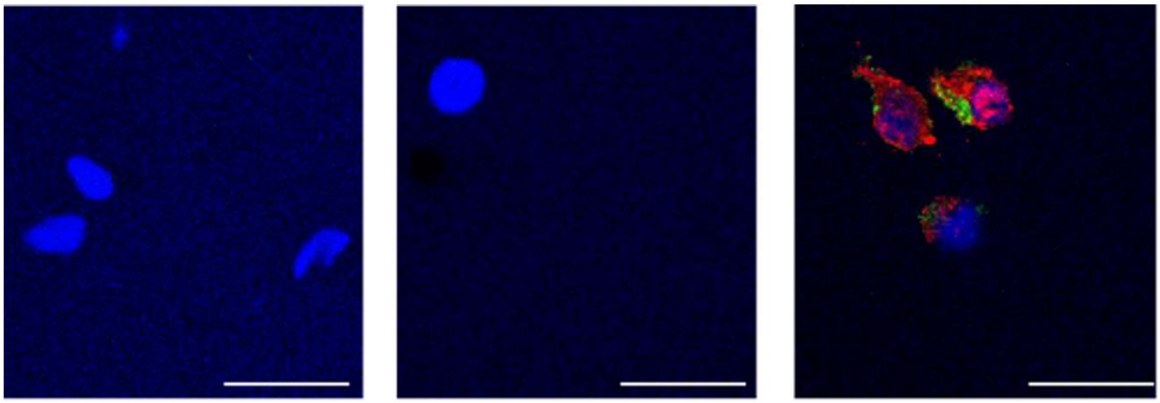

Figure 4.16: Dual immunofluorescence (IF) expression of AMBRA1 and CD31 in HUVEC endothelial cells. Representative images for the IF expression of DAPI (cell nuclei, blue) in the absence of CD31 or AMBRA1 primary antibody **(A & B)** and **C** dual expression of AMBRA1 (red) and CD31 (green) with DAPI in HUVEC cells. Scale bar =23 μm.

Subsequent dual IF analysis of AMBRA1 and CD31 expression in AJCC stage I melanomas with known maintained expression of epidermal AMBRA1, revealed partial maintenance of peri-tumoural endothelial AMBRA1 expression with maintained expression of epidermal AMBRA1 (Figure 4.17 A – B). Moreover, dual IF analysis in an AJCC stage I melanoma with known loss of epidermal AMBRA1 expression revealed concurrent loss of AMBRA1 expression in both the epidermis and endothelium (Figure 4.17 C – D). These preliminary findings thus support the hypothesis that melanoma TGF-β2-mediated down regulation of epidermal AMBRA1 is associated with concurrent loss of endothelial AMBRA1 in the tumour microenvironment.

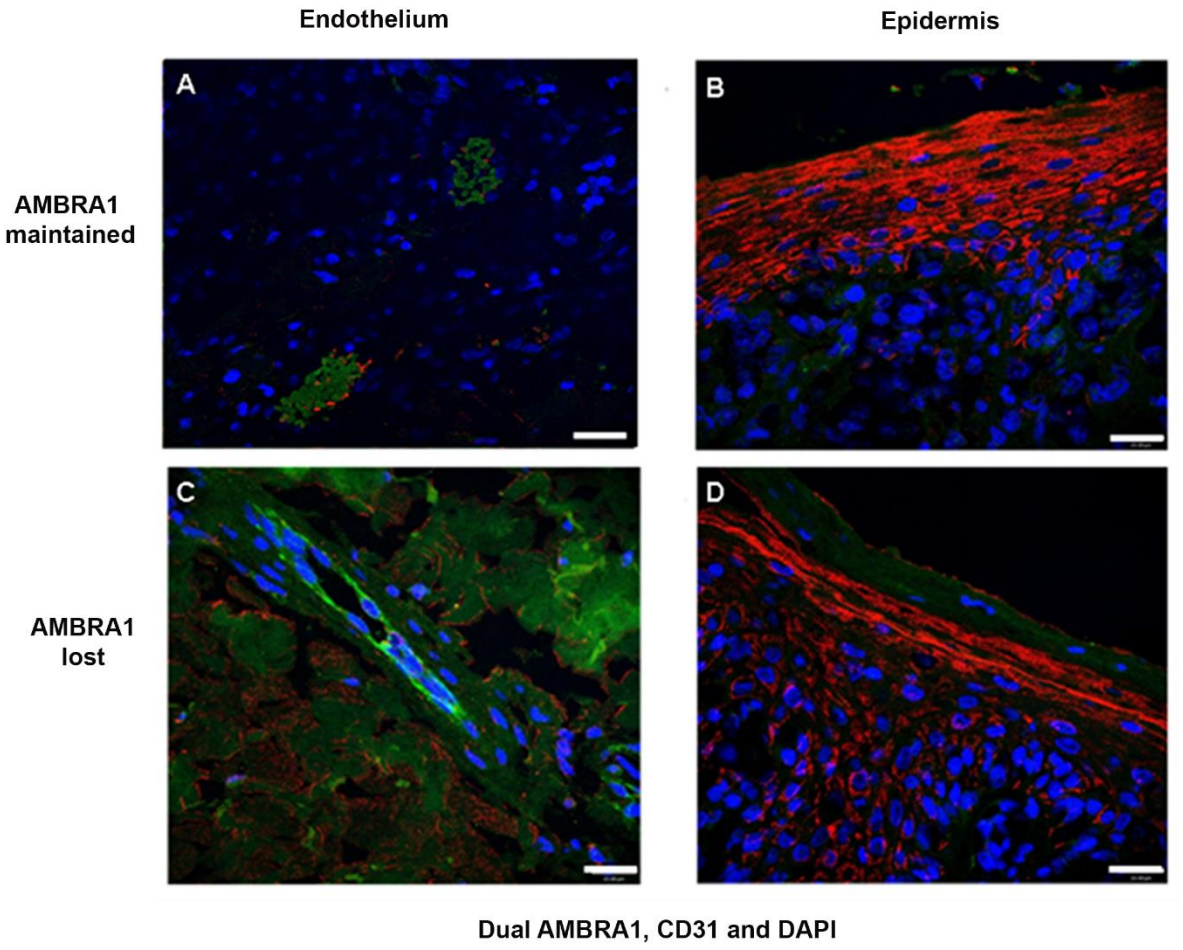

Figure 4.17: Loss of epidermal AMBRA1 overlying AJCC Stage I melanomas is associated with a concurrent loss in endothelial AMBRA1. Representative images for the IF expression of AMBRA1 (red), CD31 (green) or DAPI (cell nuclei, blue) in the **A** endothelium or **B** epidermis of an AJCC stage I melanoma with known epidermal AMBRA1 loss; or in the **C** endothelium or **D** epidermis of an AJCC stage I melanoma with known maintained expression of epidermal AMBRA1. Scale bar =23μm.

To further confirm these findings and test the hypothesis that loss of endothelial AMBRA1 expression is associated with high risk AJCC stage I melanomas, IHC analysis of peri-tumoural endothelial AMBRA1 and CD31 expression (revealed by DAB counterstaining on the Ventana automated platform) was undertaken in 15 primary AJCC stage I melanomas; 4 with known maintained epidermal AMBRA1 expression and 11 in which epidermal AMBRA1 expression was known to be completely lost.

Results revealed that peri-tumoural endothelial expression of AMBRA1 was maintained in all 4 melanomas in which epidermal AMBRA1 was maintained (Table 4.1), suggesting a trend for maintenance of peri-tumoural endothelial AMBRA1 where epidermal AMBRA1 expression overlying the tumour is maintained (Figure 4.18 A – C). Conversely, in 11 melanomas with complete loss of epidermal AMBRA1 expression, 7 had concurrent loss of peri-tumoural endothelial AMBRA1 expression (Figure 4.18 G – I) while peri-tumoural endothelial AMBRA1 expression was maintained in 4 (Figure 4.18 D – F), also suggesting a trend for loss of peri-tumoural endothelial AMBRA1 where epidermal AMBRA1 expression is completely lost (Table 4.1). Interestingly, 6 of the 7 tumours with concurrent loss of epidermal and endothelial AMBRA1 expression eventually developed metastases, whereas all 8 tumours in which peri-tumoural endothelial AMBRA1 expression was maintained, regardless of epidermal AMBRA1 expression, did not metastasise (Table 4.1).

When further stratifying these 15 AJCC stage I melanomas into high or low risk subgroups according to the combined epidermal expression of AMBRA1 and Loricrin (AMLo), all 4 tumours with concurrent maintenance of epidermal and endothelial AMBRA1 expression fell within the AMLo low risk category (Table 4.1). These data suggest that concurrent maintenance of epidermal AMBRA1 expression and endothelial AMBRA1 expression in the tumour microenvironment of AJCC stage I melanomas correlates with AMLo low risk scores and define a subgroup at low risk of developing metastases.

Similarly, all 7 melanomas with concurrent complete loss of epidermal AMBRA1 and peri-tumoural endothelial AMBRA1 expression fell within the AMLo high risk category, of which 6 developed metastases (Table 4.1), suggesting that concurrent loss of epidermal and peri-tumoural endothelial AMBRA1 expression defines a subgroup at high risk of metastases for which AMLo is a biomarker. Interestingly, 4 melanomas with complete loss of epidermal AMBRA1 expression but maintained peri-tumoural endothelial AMBRA1 expression also fell within the AMLo high risk category despite not developing metastases, supporting the hypothesis that endothelial integrity is key

in preventing melanoma metastasis and may explain why not all tumours with complete loss of epidermal AMBRA1 or scored as AMLo high risk develop metastases.

AJCC stage I melanomas	**Epidermal AMBRA1 maintained (n=4)**		**Epidermal AMBRA1 completely lost (n=11)**			
	AMLo Low Risk		AMLo Low Risk		AMLo High Risk	
Peri-tumoural endothelial AMBRA1	Maintained	Lost	Maintained	Lost	Maintained	Lost
Non Metastatic tumours	4	0	0	0	4	1
Metastatic tumours	0	0	0	0	0	6

Table 4.1: Stratification of 15 AJCC stage I melanomas with known epidermal AMBRA1 status according to peri-tumoural endothelial AMBRA1 status, associated AMLo score and eventual outcome.

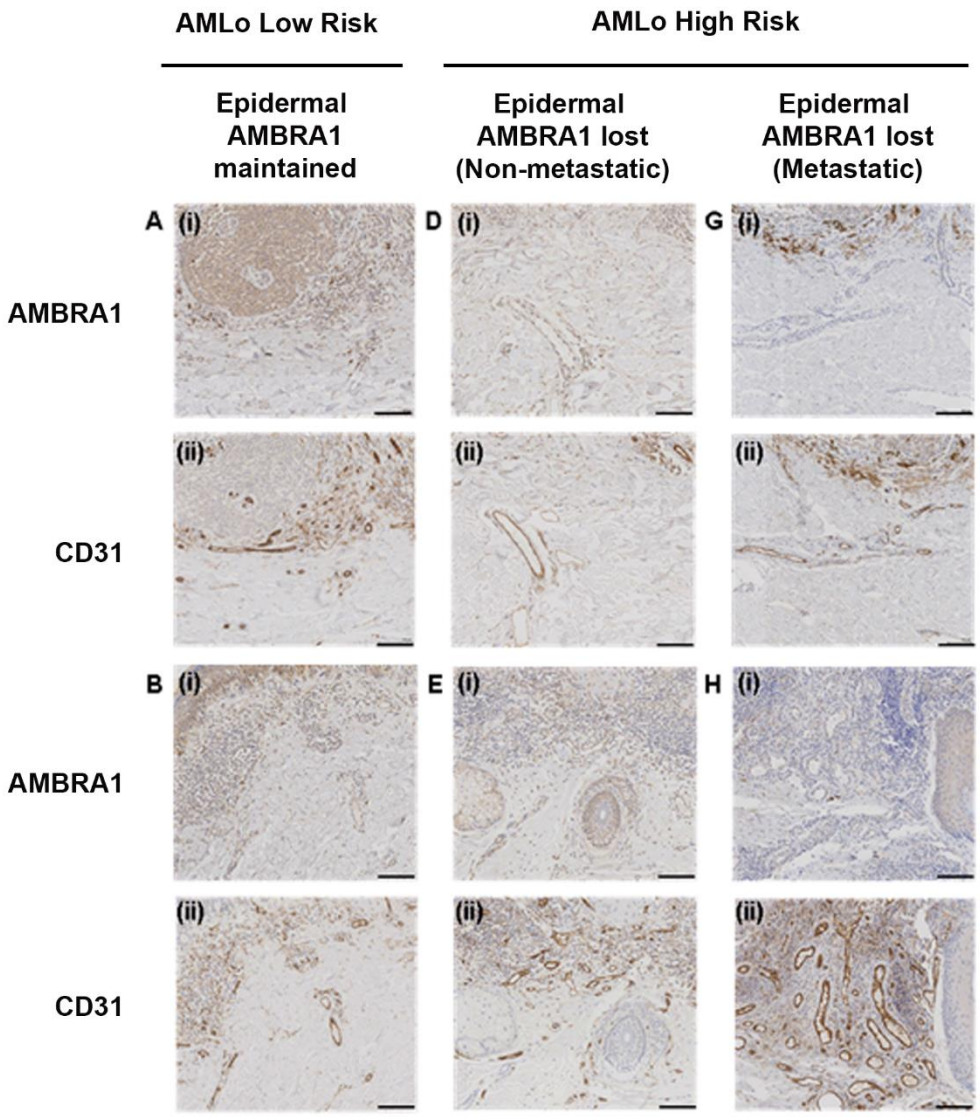
AMLo Low Risk
AMLo High Risk
Epidermal AMBRA1 maintained
Epidermal AMBRA1 lost (Non-metastatic)
Epidermal AMBRA1 lost (Metastatic)
AMBRA1
CD31
AMBRA1
CD31
A
B
D
E
G
H
(i)
(ii)

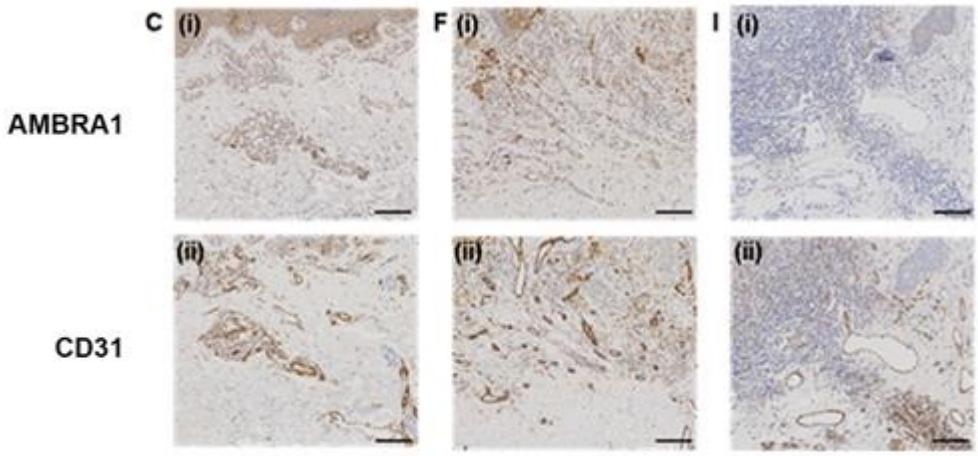

Figure 4.18: Endothelial AMBRA1 expression is lost in metastatic AJCC stage I melanomas stratified as high risk by AMLo scoring. Representative photomicrographs of **A – F (i)** endothelial AMBRA1 expression (brown staining) with **A – F (ii)** corresponding CD31 expression (brown staining highlighting the endothelium) in 3 AMLo low risk AJCC stage I melanoma tumours with maintained epidermal AMBRA1 **(A – C)**, 3 AMLo high risk tumours with complete loss of epidermal AMBRA1 that did not metastasise **(D – F)** and 3 AMLo high risk tumours with complete loss of epidermal AMBRA1 that developed metastasis **(G – I)**. Scale bar = 100 μm.

Collectively, these results suggest that TGF-β2 secretion by high risk AJCC stage I melanomas leads to down regulation of epidermal AMBRA1 expression in the overlying tumour epidermis as well as a trend for concurrent down regulation of endothelial AMBRA1 and junctional proteins, leading to loss of endothelial integrity and a higher risk of tumour metastases. In addition results demonstrate AJCC stage I tumours that retain endothelial AMBRA1 expression, regardless whether epidermal AMBRA1 expression is lost or maintained, are associated with a low risk of metastases; suggesting the existence of idiosyncratic factors exhibited by such tumours that are protective against the pro-metastatic effect of TGF-β2 on the endothelium in the tumour microenvironment.

4.3 Discussion

Presence of ulceration of a primary melanoma is an independent histological prognostic biomarker associated with poor survival [37]. Despite the poorly understood underlying biology of this association, the preferential benefit of treatment with interferon-α seen in ulcerated melanomas [72], support an underlying tumour secretory process having a direct effect on ulceration that is modified in some way by interferon-α. Interestingly, crosstalk between interferon-α and TGF-β signalling has been described by studies showing that interferon-α antagonises TGF-β/Smad-dependent hepatic fibrosis in mice [182] as well as enhances the secretion and pro-apoptotic effects of TGF-β1 in pre-neoplastic liver cells, preventing hepatocellular carcinogenesis [180]. This raises the possibility that ulceration in melanoma may be linked to TGF-β signalling.

Certainly in melanoma, the dual role of TGF-β in tumorigenesis has been well documented with TGF-β secretion by melanoma cells exerting tumour suppressive effects in early stages but promoting tumour invasion and metastasis in advanced stages [127]. Moreover, the isoform specific increased secretion of TGF-β2 has been widely reported to be associated with melanoma progression and confers a worse prognosis [144, 145, 147, 148].

Data from chapter 3 demonstrating the loss of AMBRA1 expression in the epidermis overlying primary AJCC stage I melanomas at high risk of metastases, taken together with preliminary data linking this association to an increase in melanoma secretion of isoform specific TGF-β2, raises the possibility that melanoma TGF-β2 secretion may contribute directly to the down regulation of epidermal AMBRA1, leading to loss of epidermal integrity and ulceration of a higher risk tumour.

Results from the present chapter incorporating analysis of an independent cohort of AJCC stage I melanomas derived from the James Cook University Hospital, Middlesbrough confirmed the correlation between loss of AMBRA1 expression overlying primary AJCC stage I melanomas with increased tumoural expression of TGF-β2. In addition, AJCC stage I melanomas with increased TGF-β2 expression correlated with high risk AMLo scores and were associated with a higher risk of metastases compared to tumours that remained localised. In addition, results demonstrating TGF-β2 mediated down-regulation of AMBRA1 and Loricrin in primary keratinocytes, further support the hypothesis that increased melanoma secretion of TGF-β2 leads to the disrupted epidermal differentiation leading to loss of epidermal integrity and tumour ulceration, conferring a worse prognosis, of which the combined loss of epidermal AMLo expression is a surrogate marker.

As the epidermis is an epithelial structure, the morphological changes that occur in the epidermis brought about by tumoural TGF-β2 secretion leading to dysregulated epidermal differentiation and ulceration are also likely to occur in the endothelium. In addition, TGF-β2 has been also shown to modify the tumour microenvironment via endothelial-mesenchymal transition (EndoMT) in which endothelial cells lose expression of endothelial markers and acquire an invasive phenotype [183, 184].

Supporting the pro-tumorigenic role of TGF-β2 in melanoma progression and metastases, results from the present chapter demonstrated treatment of HUVEC endothelial cells or primary HDLECs with exogenous TGF-β2 induced the down regulation of AMBRA1 and junctional protein expression. To closer represent an *in vivo* setting and test the potential of metastatic melanoma TGF-β2 secretion in disrupting endothelial integrity, HUVEC cells and primary HDLECs were subjected to culture in supernatants derived from the metastatic melanoma cell line A375 known to secrete high levels of TGF-β2 or supernatants derived from A375 melanoma cells in which TGF-β2 had been stably knocked down. Results highlighted the significant down regulation of AMBRA1 and Claudin-5 in HUVECs, with significant down regulation of

AMBRA1 and a trend for down regulation of Claudin-5 in primary HDLECs cultured in TGF-β2 rich A375 melanoma cell supernatant; an effect that was partially reversed by culture in supernatant of A375 melanoma cells in which TGF-β2 has been knocked down. Collectively, these data suggest that melanoma secretion of TGF-β2 leads to loss of endothelial integrity by disrupting endothelial differentiation with down regulation of key cell junctional proteins, thereby facilitating a potential route for tumour cell entry and subsequent metastasis, a process that may be prevented by blockade of TGF-β2 signalling.

Finally, analysis of AMBRA1 expression using CD31 as a marker of endothelial cells in the peri-tumoural endothelium of AJCC stage I melanomas revealed a trend for the concurrent loss of endothelial AMBRA1 where epidermal expression of AMBRA1 overlying the primary tumour was lost, particularly in tumours scored as AMLo high risk that subsequently went on to metastasise. More interesting was the observation that some tumours with loss of epidermal AMBRA1 expression and scored as AMLo high risk, in fact maintained endothelial AMBRA1 expression and did not develop metastases. These findings further support the hypothesis that TGF-β2 secretion by high risk stage I melanoma tumours induce the down regulation of epidermal AMBRA1 leading to epidermal ulceration and in the peri-tumoural endothelium of high risk melanomas, exert the same effect by disrupting endothelial integrity and facilitating melanoma metastases. The enigma remains however, as to how some melanoma tumours with loss of epidermal AMBRA1 expression appear to be protected from the pro-metastatic effects of TGF-β2 in the endothelium and which perhaps explains why some AJCC stage I melanomas defined as high risk by the combined loss of epidermal AMBRA1 and Loricrin expression do not in fact, develop metastases.

In the recent years, Vitamin D in melanoma has received much attention as a key regulator of cell proliferation, differentiation and immunomodulation [185-187], with accumulating evidence that its deficiency may increase the risk of malignancy and cancer outcomes [188]. Vitamin D is primarily synthesised in the skin under the action of ultraviolet B (UVB) light from the sun as Cholecalciferol, which then undergoes

double hydroxylation; first in the liver to form 25-hydroxyvitamin D (25-hydroxycholecalciferol) and finally in the kidneys to form the biologically active form 1-25-dyhydroxycholecalciferol (Calcitriol) [189] which activates vitamin D receptors (VDR). To determine a person's vitamin D status, 25-hydroxyvitamin D is the form measured in serum [190] .

Certainly in melanoma, low levels of serum 25-hydroxyvitamin D at the point of primary melanoma diagnosis have been associated with high risk tumours with thicker primaries and a poorer prognosis, despite conflicting evidence on overall survival and insufficient evidence to establish cause-effect [78-82]. Lower Vitamin D levels have also been associated with ulceration of primary melanomas and poorer melanoma specific survival however, the underlying biology of this remains uncertain. Interestingly, Vitamin D is known to be a regulator of TGF-β signalling [191, 192] where impaired Vitamin D receptor signalling with reduced expression of VDR and decreased levels of its ligand may contribute to enhanced sensitivity to the effects of TGF-β and hyperactive TGF-β signalling [189]. In addition, calcitriol has been shown to inhibit both migration and invasion induced by TGF-β1 and TGF-β2 and regulates TGF-β induced epithelial-mesenchymal (EMT) transition in human airway epithelial cells [193].

In human skin, VDRs are found in the outer root sheath of hair follicles, the basal and upper layer of the epidermis where lack of its expression results in keratinocyte hyper proliferation and decreased epidermal differentiation [194, 195]. This interestingly ties in with the present observations of dysregulated epidermal differentiation with a hyper proliferative epidermis associated with loss epidermal AMBRA1 expression overlying high risk AJCC stage I melanomas. Moreover, this highlights the potential influence of the interaction of Vitamin D with its receptors may have on TGF-β2-induced down regulation of AMBRA1 and melanoma prognosis i.e. peri-tumoural keratinocytes and endothelial cells may have enhanced or reduced sensitivity to the pro-metastatic effects of melanoma TGF-β2 secretion depending on Vitamin D levels and/or receptor status. Therefore, melanomas that secrete high levels of TGF-β2 leading to epidermal AMBRA1 down regulation may be protected against the pro-metastatic effect of TGF-

β2 in the endothelium where there is adequate Vitamin D and receptor status. This may explain why some melanoma tumours scored as AMLo high risk with loss of epidermal AMBRA1 do not lose expression of peri-tumoural endothelial AMBRA1 and do not metastasise. To investigate this association however, further studies of TGF-β signalling and Vitamin D levels and receptor status in melanoma would be required.

Collectively, results in this chapter support the targeting of TGF-β2 signalling as a viable therapeutic strategy to prevent the ulceration and metastases of high risk AJCC stage I melanomas following primary excision. In the management of early AJCC stage I melanoma however, as the whole tumour along with the overlying epidermis is removed at the time of primary excision, the definition of an optimal strategy which to target TGF-β2 signalling in the endothelium is therefore crucial in order to preserve endothelial and endo-lymphatic integrity, which if disrupted, provides a potential route for melanoma metastasis. Further work focussed on TGF-β signalling in the endothelium and the mechanisms leading to endothelial AMBRA1 down regulation are discussed in the following chapter.

Summary

- Loss of epidermal AMBRA1 overlying AJCC stage I melanomas correlates with increased tumoural TGF-β2.
- AJCC stage I melanomas defined as high risk by the combined loss of epidermal AMBRA1 and Loricrin (AMLo) display increased tumoural TGF-β2 expression.
- High risk AJCC stage I melanomas that subsequently develop metastases display higher tumoural TGF-β2 expression compared with tumours that remain localised.
- Treatment of calcium-induced differentiated primary keratinocytes with recombinant TGF-β2 results in the dose dependent down regulation of AMBRA1 and the terminal differentiation marker Loricrin.
- Treatment of HUVEC endothelial cells and primary HDLECs with exogenous TGF-β2 results in the down regulation of AMBRA1 and endothelial cell junctional proteins.
- Treatment of HUVECs and HDLECs with TGF-β2 rich supernatant derived from the melanoma cell line A375 results in the down regulation of AMBRA1 and Claudin-5, an effect that is partially prevented by TGF-β2 blockade in melanoma cells.
- Expression of endothelial AMBRA1 is concurrently lost in AJCC stage I melanomas in which AMBRA1 expression in the overlying tumour epidermis is lost and which go on to develop metastatic disease.
- Expression of endothelial AMBRA1 is lost in metastatic AJCC stage I melanomas stratified as high risk by AMLo scoring.
- Targeting of TGF-β2 signalling may be a viable therapeutic strategy to prevent the ulceration and metastases of high risk AJCC stage I melanomas following primary excision, for which the combined loss of epidermal AMBRA1 and Loricrin (AMLo) expression is a companion biomarker.

Chapter 5

Contribution of canonical and non-canonical TGF-β2 signalling to melanoma metastasis

Chapter 5: Contribution of canonical and non-canonical TGF-β2 signalling to melanoma metastasis

5.1 Introduction 168

5.2 Results 171

5.2.1 Bioinformatics analysis of the AMBRA1 promoter identifies TGF-β2 responsive elements 171

5.2.2 ALK1 and ALK5 are differentially expressed in keratinocytes and endothelial cells 173

5.2.3 TGF-β2-induced deregulation of keratinocyte (CCD1106) differentiation and AMBRA1 down regulation is mediated by canonical TGF-β signalling 175

5.2.4 TGF-β2 induces both canonical and non-canonical signalling in HUVEC endothelial cells 178

5.2.5 Non-canonical TGF-β2 signalling is increased in the endothelium of metastatic AJCC stage I melanomas 180

5.2.6 Inhibition of ALK5 prevents canonical TGF-β2 signalling-mediated down regulation of AMBRA1 in calcium-induced keratinocytes 182

5.2.7 Inhibition of ALK5 in HUVEC endothelial cells exacerbates non-canonical TGF-β2 signalling and does not prevent TGF-β2-induced endothelial AMBRA1 down regulation. 184

5.2.8 SiRNA-mediated knockdown of ALK1 prevents non-canonical TGF-β2 mediated endothelial AMBRA1 downregulation. 186

5.2.9 Inhibition of canonical TGF-β2 signaling by ALK5 inhibition promotes endothelial cell proliferation 190

5.3 Discussion 194

5.1 Introduction

Data presented so far support a pathogenic role for TGF-β2 in melanoma progression, and suggest the targeting of TGF-β2 signalling may prove a valuable therapeutic strategy to prevent the development of metastasis in high risk AJCC stage I melanomas, for which the loss of epidermal AMBRA1 and Loricrin may be a companion biomarker. To date, several approaches have evaluated the potential for targeting TGF-β signalling including agents that inhibit the ligand, receptors or downstream signalling [161]. Fresolimumab (GC1008), a pan inhibitor of TGF-β1, 2 and 3 ligands, has been clinically evaluated in advanced melanoma patients in phase I/II trials. Despite initial evidence for anti-tumour activity [151] however, the use of Fresolimumab was associated with the development of eruptive keratoacanthomas or SCCs, mediated by the inhibition of TGF-β1 [152], further emphasising the need for isoform specific TGF-β inhibitors and specifically a selective inhibitor of TGF-β2 signalling. To this aim a TGF-β2 antisense vaccine, LucanixTM (Belangenpumatucel-L, NovaRx, San Diego, CA, USA), has been developed, for which phase III trials in advanced stage non-small cell lung cancer demonstrated survival benefits, but which to date has not been evaluated in melanoma [153].

Rather than targeting the TGF-β2 ligand, perhaps a more effective approach in melanoma may be to target the TGF-β2 receptor complex thereby preventing non-specific receptor activation, downstream signalling and off target effects. To consider this possibility and inform the design of an appropriate TGF-β2 receptor target, it is important to understand the downstream mechanisms by which tumoural TGF-β2 secretion engages canonical or non-canonical TGF-β2 mediated signalling.

TGF-β Receptor II (TGF-βRII)/ALK5 is the predominant receptor complex responsible for canonical down-stream TGF-β2 mediated signal transduction in most cell types. Canonically TGF-β2 ligand binds to TGF-βRII/ALK5 receptor dimers present on most cells including keratinocytes resulting in activation or phosphorylation of Smad 2 and 3, and evoking downstream signalling mechanisms, which in endothelial cells has been shown to inhibit cell proliferation and migration [129]. In addition, TGF-β2 ligand may also bind to TGF-βRII/ALK1 receptor dimer complexes, activating non-canonical signalling, activation/phosphorylation of Smad 1/5 and which in endothelial cells may promote cell proliferation and migration [129, 132]. Since ALK1 is predominantly expressed in endothelial cells and at sites of epithelial-mesenchymal interactions and is known to activate Smad 1 and Smad 5 [129, 131], this may be the predominant mechanism by which TGF-β2 secreted by melanomas transduces downstream signalling and perhaps the mechanism by which the expression of AMBRA1 in both the epidermis and the endothelium is down regulated (Figure 5.1).

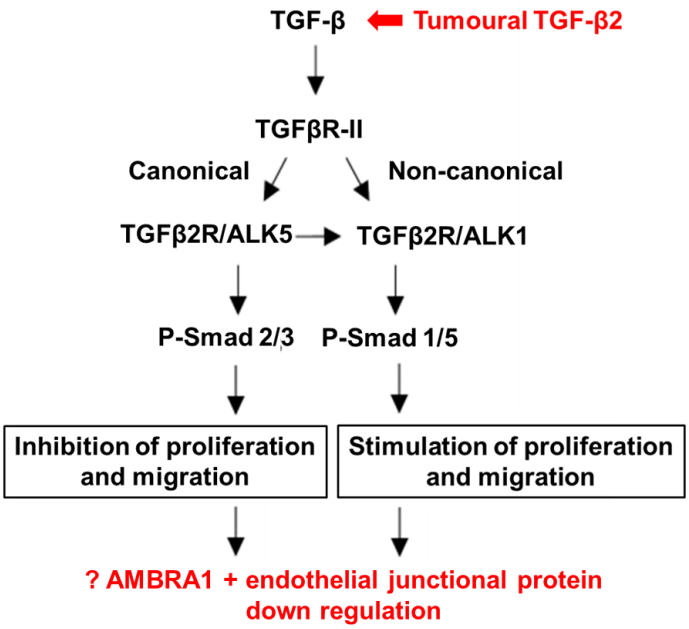

Figure 5.1: Schematic model for activation of TGF-β2 mediated ALK1 and ALK5 signalling in endothelial cells. Active TGF-β2 binds to TGF-βRII, which recruits and activates ALK5, which in turn can recruit ALK1 into the complex. Activated ALK1 and ALK5 phosphorylates Smad 1/5 and Smad 2/3 respectively with opposing downstream effects where ALK 5 inhibits endothelial cell migration and proliferation whereas ALK1 stimulates both these processes [129]. The ratio between their expressions may determine if TGF-β2 functions as a tumour suppressor or promoter of tumour progression leading to the down regulation of AMBRA1 and endothelial junctional proteins [129].

To test these hypotheses, the aim of the present chapter was thus to characterise ALK 1 and ALK5 expression in keratinocytes and endothelial cells and determine the mechanisms by which melanoma secretion of TGF-β2 leads to the down regulation of AMBRA1, resulting in loss of epidermal and endothelial integrity.

5.2 Results

5.2.1 Bioinformatics analysis of the AMBRA1 promoter identifies TGF-β2 responsive elements

To further decipher the downstream signalling evoked by melanoma secretion of TGF-β2 and the mechanisms by which TGF-β2 mediates epidermal and or endothelial AMBRA1 down regulation, a bioinformatics approach was undertaken in collaboration with Dr Marco Corazzari, University of Rome 'Tor Vergata'. Specifically, the on line MatInspector (Genomatix) matrix library tool was used to identify putative TGF-β2 related transcription factor binding sites/responsive elements in the AMBRA1 promotor in which identified DNA sequences with confidence matrix simetry values of >0.8 were considered significant. Results identified responsive elements for Smad 1/5 and Smad 3, further affirming the potential contribution of both canonical or non-canonical TGF-β2 signalling to AMBRA1 down regulation (Figure 5.2).

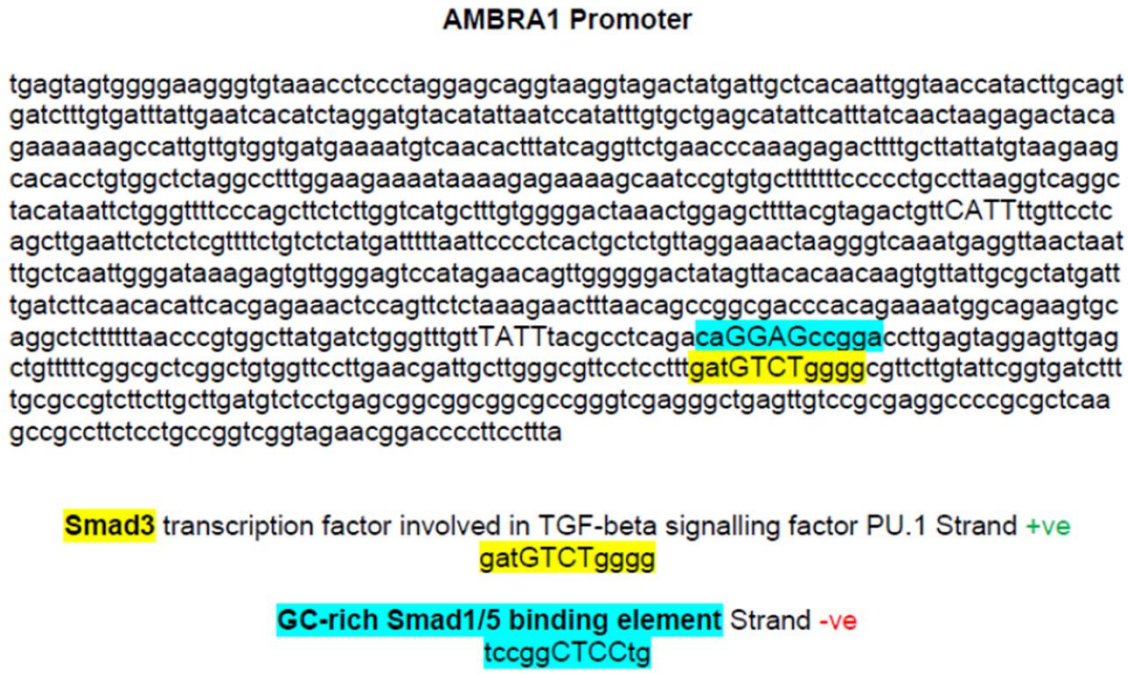

Figure 5.2: Bioinformatics analysis of the AMBRA1 promoter identifies TGF-β responsive elements. AMBRA1 upstream promoter sequence highlighting TGF-β responsive elements for Smad 3 (yellow) and Smad 1/5 (blue), identified following bioinformatics analysis for TGF-β related transcription factor binding sites/responsive elements using the MatInspector matrix library tool.

5.2.2 ALK1 and ALK5 are differentially expressed in keratinocytes and endothelial cells

Following the identification of TGF-β responsive elements for Smad 1/5 and Smad in the AMBRA1 promoter, mRNA expression levels of ALK1 and ALK5 in the retrovirus vector transformed keratinocyte cell line CCD1106 and HUVEC endothelial cells were quantified by qPCR, as well as in primary undifferentiated and calcium-induced differentiated keratinocytes in collaboration with Dr Gareth Inman, University of Dundee, UK.

Results revealed expression of ALK5 by CCD1106 keratinocytes and both primary differentiated and undifferentiated keratinocytes (with no difference in expression between undifferentiated and differentiated primary keratinocytes) while in contrast there was no expression of ALK1 by these cell types (Figure 5.3 A – B). Conversely, qPCR analysis revealed the expression of both ALK 1 and ALK5 mRNA by HUVEC endothelial cells with no significant difference in expression levels between the two receptors (Figure 5.3 C). Collectively, these data suggest that TGF-β2 mediated down regulation of AMBRA1 in the epidermis likely occurs via ALK 5 canonical TGF-β2 signalling whereas in the endothelium, either pathway could be responsible for AMBRA1 down regulation given that both ALK1 and ALK5 are equally expressed.

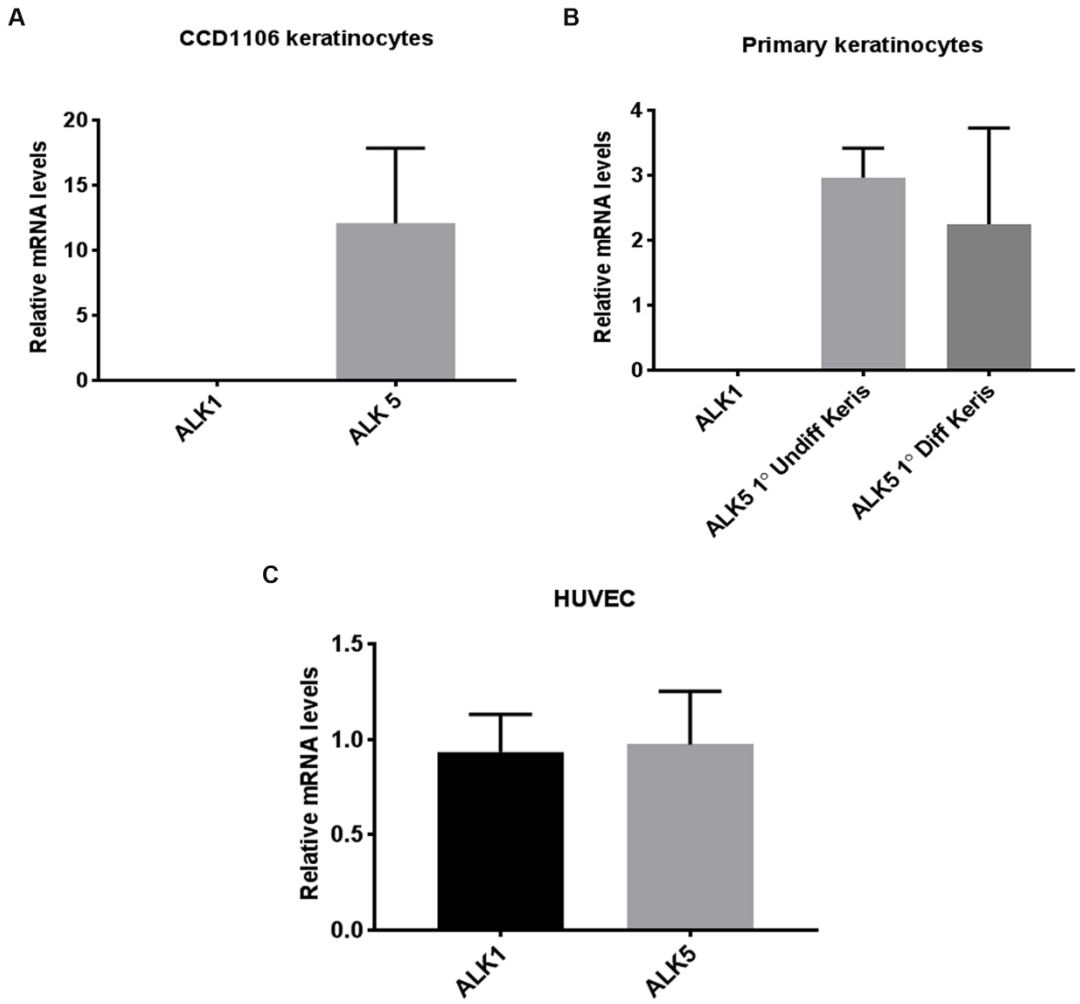

Figure 5.3: ALK1 and ALK5 are differentially expressed by the keratinocyte cell line CCD1106, primary keratinocytes and HUVEC endothelial cells. Relative mRNA levels for the expression of ALK 1 and ALK 5 in **A** CCD1106 keratinocytes, **B** primary undifferentiated and differentiated keratinocytes (differentiated for 5 days by culture in 1.3 mM Calcium Chloride) or **C** HUVEC endothelial cells, normalized to L34 housekeeping gene expression and expressed as the 2-ΔΔCT mRNA fold change demonstrating no expression of ALK1 by CCD1106 or primary keratinocytes and expression of both ALK1 and ALK5 by HUVEC endothelial cells. Each bar represents the mean ± SD of three replicate experiments.

5.2.3 TGF-β2-induced deregulation of keratinocyte (CCD1106) differentiation and AMBRA1 down regulation is mediated by canonical TGF-β signalling

To further characterize the differential contribution of canonical or non-canonical TGF-β signaling to deregulated epidermal differentiation, CCD1106 keratinocytes were subjected to calcium-induced differentiation for 7 days (by switching to culture in Epilife media containing 1.3 mM $CaCl_2$) in the presence of 10 ng/ml of recombinant TGF-β2 for the last 24 hours, prior to the analysis of total or phosphorylated Smad 1, 3 or 5 expression by Western Blotting. Results demonstrated calcium-induced differentiation of CCD1106 cells at 5 and 7 days was accompanied by the reduced expression of phosphorylated Smad 2 and Smad 3, which was then increased by subsequent incubation for 24 hours in the presence of exogenous TGF-β2 (Figure 5.4 A). Conversely, calcium-induced differentiation of CCD1106 cells for 5 or 7 days had no effect on the expression of phosphorylated Smad 1/5, the expression of which was also not altered by co-culture with exogenous TGF-β2 for 24 hours following the induction of differentiation (Figure 5.4 B). Collectively, these results therefore suggest that exogenous TGF-β2 activates evokes canonical TGF-β2 signalling in keratinocytes via binding to the ALK5 receptor complex and inducing the phosphorylation of Smad 2 and Smad 3. Furthermore, these data are consistent with the likelihood of the contribution of TGF-β2-induced Smad 3 phosphorylation to the down regulation of epidermal AMBRA1 and Loricrin and the loss of epidermal integrity mediated by melanoma secretion of TGF-β2.

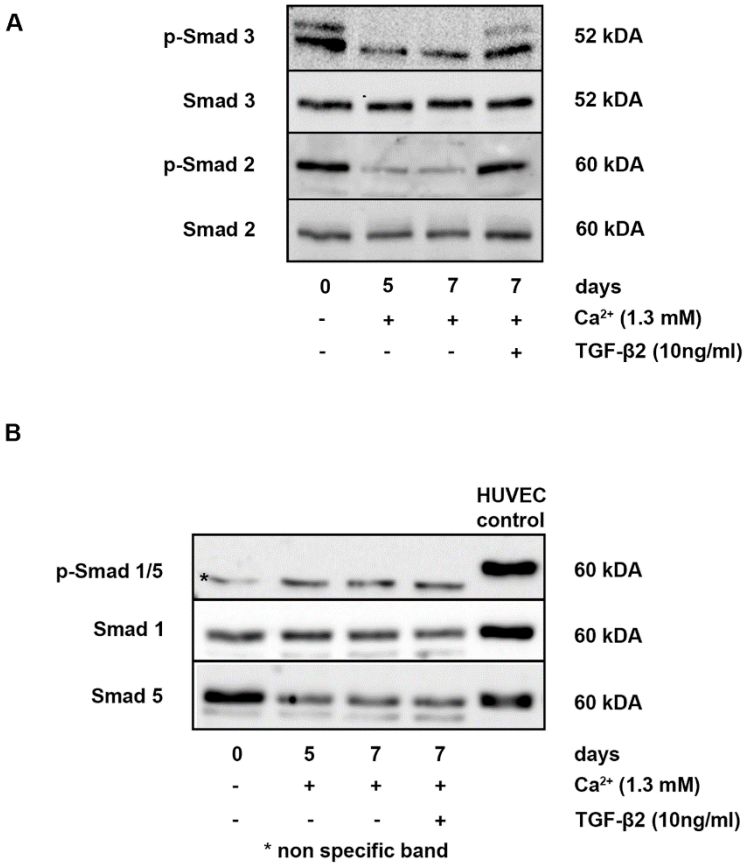

Figure 5.4: Activation of canonical TGF-β signaling in calcium-induced differentiated CCD1106 keratinocytes in response to exogenous TGF-β2. Representative western blot for **A** the expression of p-Smad 2 (60 kDA) and p-Smad 3 (52 kDA), Total Smad 2 (60 kDA) or Smad 3 (60 kDA) or **B**, p-Smad 1/5, total Smad 1 (60 kDA) or Smad 5 (60 kDA) in CCD1106 cells or CCD1106 cells following 5 or 7 days switch to culture in medium with high calcium (1.3 mM Ca^{2+}) in the presence or absence of 10 ng/ml recombinant TGF-β2 for the last 24 hours or p-Smad 1/5, total Smad 1 or total Smad 5 expression in control HUVEC cells

In the clinical context of melanoma management however, the epidermis is removed along with the tumour at primary excision and hence in order to define a potential target to prevent metastasis of high risk AJCC stage I melanomas it is important to consider the signalling mechanisms by which tumoural secretion of TGF-β2 (by any remaining melanoma cells following primary excision) lead to the loss endothelial AMBRA1, and associated loss of junctional protein expression and endothelial integrity. The remaining data are hence focused towards defining the optimal strategy through which to target TGF-β2 signalling in the microvascular or lymphatic endothelium in order to preserve endothelial integrity and prevent melanoma metastasis.

5.2.4 TGF-β2 induces both canonical and non-canonical signalling in HUVEC endothelial cells

Unlike in keratinocytes that only express ALK5, analysis of TGF-βRI expression in HUVEC endothelial cells revealed expression of both ALK1 and ALK5, suggesting melanoma secretion of TGF-β2 may potentially evoke either or both canonical or non-canonical signalling in the endothelium, leading to AMBRA1 down regulation. To further test this hypothesis, HUVEC endothelial cells were treated with 10 ng/ml recombinant TGF-β2 for 2 or 8 hours, prior to western blot analysis for the expression of p-Smad 1/5 and p-Smad 3 or Total Smad 1, 3 or 5. Smad 2 signalling was disregarded since responsive elements for this transcription factor were not revealed in bioinformatics analysis of the AMBRA1 promoter (section 5.2.1). Results revealed recombinant TGF-β2 induced increased early phosphorylation of Smad 1/5 following 2 hours treatment which returned close to basal levels at 8 hours, with no significant change in total Smad 1 or 5 expression (One way ANOVA with Dunnett's post-test correction ***P <0.001; Figure 5.5 A & C). Similarly, treatment of HUVEC endothelial cells with TGF-β2 induced the early phosphorylation of Smad 3 following 2 hours treatment which again returned close to basal levels at 8 hours, with no change in total Smad 3 (One way ANOVA with Dunnett's post-test correction ***P <0.001) and confirming the activation of both canonical and non-canonical TGF-β signalling (Figure 5.5 B & D). Collectively these data suggest melanoma secretion of TGF-β2 results in the activation of both canonical and non-canonical TGF-β2 signalling in endothelial cells.

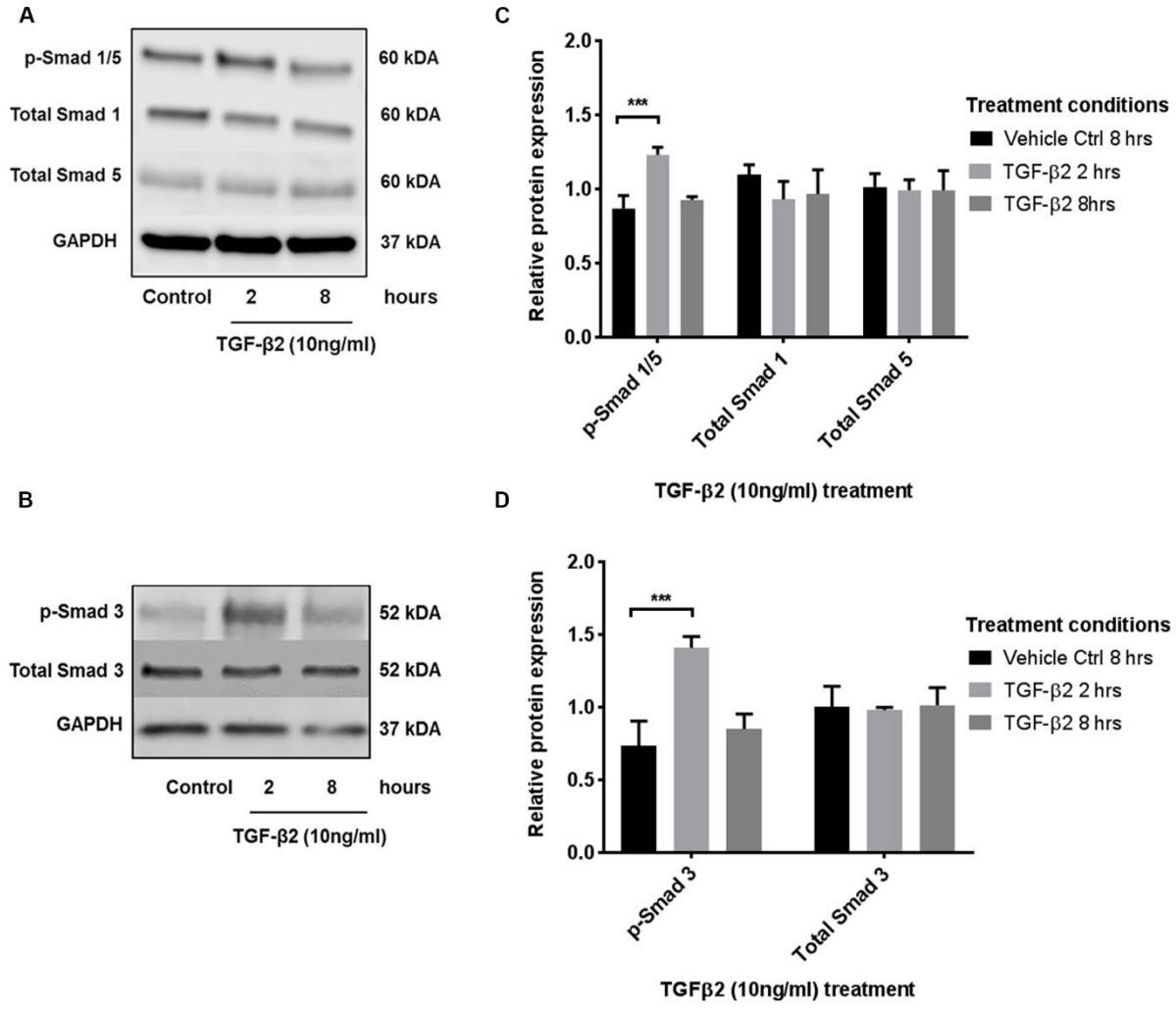

Figure 5.5: TGF-β2 activates both canonical and non-canonical signalling in HUVEC endothelial cells. Representative western blot for the expression of **A** p-Smad 1/5 (60 kDA), Total Smad 1 (60 kDA), Total Smad 5 (60 kDA) and GAPDH (37 kDA) loading control or **B** p-Smad 3 (52 kDA), Total Smad 3 (52 kDA) and GAPDH (37 kDA) loading control in HUVEC endothelial cells following treatment with 10 ng/ml recombinant TGF-β2 or vehicle control for 2 or 8 hours. **C** Relative p-Smad 1/5, Total Smad 1 and Total Smad 5 protein expression or **D** Relative p-Smad 3 and Total Smad 3 protein expression normalised to time matched GAPDH loading control and expressed relative to the mean protein/GAPDH value for each experiment, following treatment for 2 or 8 hours with 10 ng/ml recombinant TGF-β2 or vehicle control. Each bar is the mean ± SD of 3 replicate experiments. One way ANOVA with Dunnett's post-test correction ***P <0.001.

5.2.5 Non-canonical TGF-β2 signalling is increased in the endothelium of metastatic AJCC stage I melanomas

To further characterise whether canonical or non-canonical TGF-β2 signalling is preferentially activated or predominates in the peri-tumoural endothelium of high risk TGF-β2 secreting early stage melanomas, the immunohistochemical expression of p-Smad 3 and p-Smad 1/5 was determined in a sub cohort of AJCC stage I melanomas. Specifically, IHC expression with VIP counterstaining for the expression of p-Smad 2/3 or p-Smad 1/5 was performed manually in 10 AJCC stage I melanomas (6 metastatic and 4 that remained localised. Results revealed a trend for the presence of p-Smad 2/3 expression and the absence of p-Smad 1/5 expression in the peri-tumoural endothelium of non-metastatic AJCC stage I melanomas (Figure 5.6 A). Conversely, the absence of p-Smad 2/3 expression was associated with a marked increase in p-Smad 1/5 expression in the peri-tumoural endothelium of metastatic AJCC stage I melanomas (Figure 5.6 B). These data suggest that non-canonical TGF-β2 signalling is activated or predominates in the endothelium of high risk AJCC stage I melanomas and is associated with melanoma metastasis. Targeting non-canonical TGF-β2 signalling may thus represent a novel adjuvant approach to prevent metastasis of AJCC stage I melanomas identified as high risk by loss of epidermal/endothelial AMBRA1.

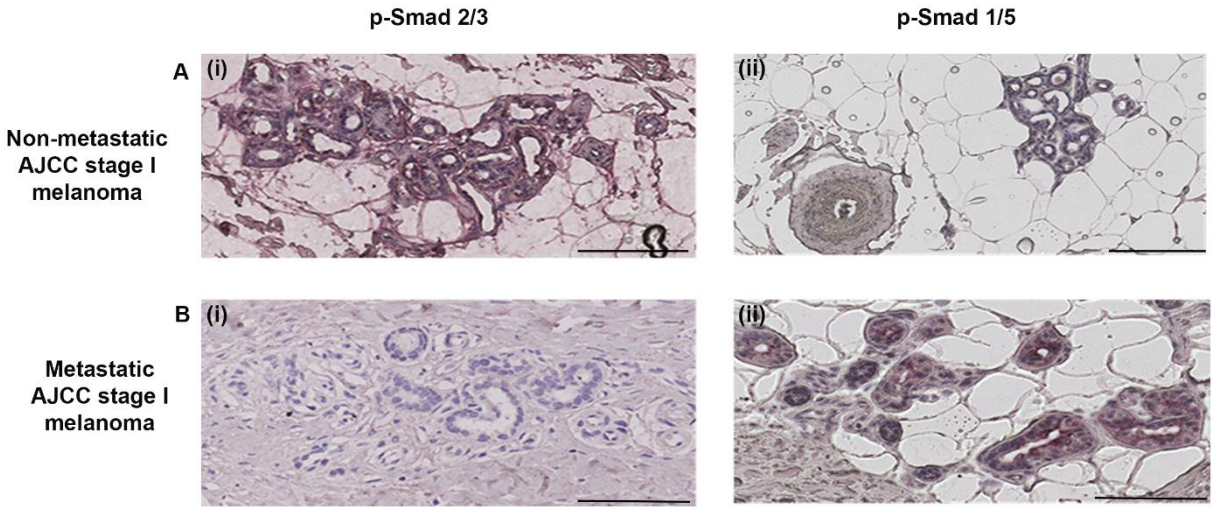

Figure 5.6: Absence of p-Smad 2/3 and the presence of p-Smad 1/5 expression is associated with metastatic AJCC stage I melanomas. Representative IHC photomicrographs of the peri-tumoural endothelium of 2 AJCC stage I melanomas **(A – B)** depicting: **A (i)** positive p-Smad 2/3 staining and **A (ii)** negative p-Smad 1/5 expression in a non-metastatic AJCC stage I melanoma and **B (i)** negative p-Smad 2/3 staining with **B (ii)** positive p-Smad 1/5 expression in a metastatic AJCC stage I melanoma revealed by VIP counterstaining (pink). Scale bar =100 μm.

5.2.6 Inhibition of ALK5 prevents canonical TGF-β2 signalling-mediated down regulation of AMBRA1 in calcium-induced keratinocytes

Data presented so far suggest melanoma secretion of TGF-β2 mediates AMBRA1 down regulation in the epidermis by canonical signalling leading to the loss of epidermal integrity and tumour ulceration. To test the hypothesis that blocking ALK5 in keratinocytes may therefore prevent a means through which to prevent TGF-β2-induced down regulation of AMBRA1 down regulation, CCD1106 keratinocytes were subjected to culture in high calcium medium (1.3 mM Ca^{2+}) for 6 days in the presence or absence of 10 ng/ml recombinant TGF-β2 and or 10 μM of a selective ALK5 inhibitor for the last 24 hours, prior to western blot analysis for the expression of p-Smad 2/3, AMBRA1 and β-Actin loading control. Results revealed and confirmed calcium-induced differentiation of CCD1106 cells was accompanied by an increase in AMBRA1 expression, the effect of which was partially prevented in the presence of 10 ng/ml TGF-β2, with a concurrent increase in the expression of p-Smad 2/3, thereby demonstrating activation of canonical TGF-β signalling. Addition of the ALK5 inhibitor however, prevented TGF-β2-induced p-Smad2/3 with a concurrent rescue of AMBRA1 expression (Figure 5.7), collectively suggesting that blockade of ALK5 signalling in keratinocytes prevents TGF-β2 induced AMBRA1 down regulation, and further supporting the involvement of canonical TGF-β2 signalling in epidermal AMBRA1 down regulation, loss of epidermal integrity and tumour ulceration.

To preserve endothelial AMBRA, endothelial integrity and prevent melanoma metastasis would however require appropriate targeting of TGF-β2 signalling in the microvascular or lymphatic endothelium, for which the potential for inhibition of ALK1 or ALK5 was next investigated and modelled using the HUVEC endothelial cell line.

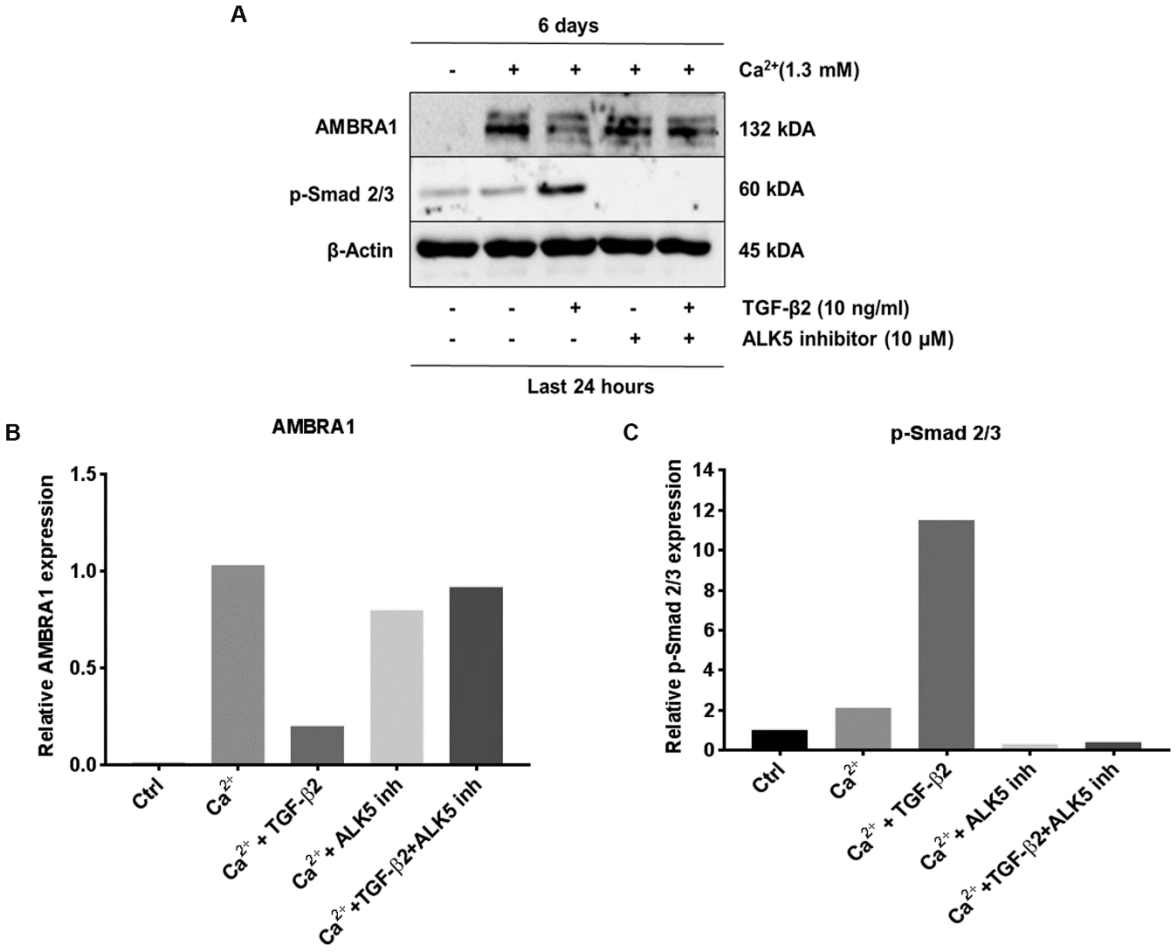

Figure 5.7: ALK5 inhibition results in blockade of canonical TGF-β2-induced down regulation of AMBRA1 in calcium-induced CCD1106 keratinocytes. A Representative western blot for the expression of AMBRA1 (132 kDA), p-Smad 2/3 (60 kDA) and β-Actin (45 kDA) loading control in CCD1106 keratinocytes cultured in Epilife media or induced to differentiate by culture in high calcium media (1.3 mM Ca^{2+}) for 6 days in the presence or absence of 10 ng/ml recombinant TGF-β2 and/or 10 μM ALK5 inhibitor for the last 24 hours of culture. **B** Relative expression of AMBRA1 and **C** p-Smad 2/3 normalised to time matched β-Actin loading control in CCD1106 keratinocytes induced to differentiate by culture for 6 days in high calcium Epilife media (Ca^{2+}) and expressed relative to undifferentiated CCD1106 keratinocytes cultured in Epilife media (vehicle control), following treatment with 10 ng/ml recombinant TGF-β2 or 10 μM ALK5 inhibitor (ALK5 inh) or both for the last 24 hours of culture.

5.2.7 Inhibition of ALK5 in HUVEC endothelial cells exacerbates non-canonical TGF-β2 signalling and does not prevent TGF-β2-induced endothelial AMBRA1 down regulation.

To explore the potential for ALK5 inhibition as a strategy to prevent TGF-β2-induced down regulation of endothelial AMBRA1 expression, HUVEC endothelial cells were treated with 10 μM of a selective ALK5 inhibitor in the presence or absence of 10 ng/ml recombinant TGF-β2 for 2 or 24 hours, prior to western blot analysis for the expression of AMBRA1, p-Smad 3 as well as control p-Smad 1/5. Results demonstrated, relative to GAPDH loading control, that TGF-β2-induced early phosphorylation of Smad 3 and markedly increased phosphorylation of Smad 1/5 at 2 hours in the presence of the ALK5 inhibitor but with no apparent change in AMBRA1 expression. In addition, despite phosphorylation of Smad 1/5 or 3 typically returning back to baseline levels by 24 hours, interestingly phosphorylation of Smad 1/5 was sustained at 24 hours in the presence of the ALK5 inhibitor (Figure 5.8 A). Given in the aforementioned studies (section 4.2.4), significant TGF-β2-induced AMBRA1 down regulation in HUVEC cells was only apparent after 72, possibly accounting for the lack of discernible change in AMBRA1 protein expression in the present results (Figure 5.8 A), qPCR analysis was additionally performed to assess AMBRA1 expression at mRNA level at 2 and 24 hours (Figure 5.8 B). Results revealed a trend for an initial increase in TGF-β2-induced AMBRA1 mRNA expression levels following 2 hours exposure to 10 ng/ml recombinant TGF-β2 with reduced levels at 24 hours, which was significantly decreased in the presence of the ALK5 inhibitor i.e. the decline in AMBRA1 mRNA expression levels following 24 hours exposure to TGF-β2 is enhanced in presence of the ALK5 inhibitor. (One way ANOVA with Tukey's post-test correction *P <0.001, Figure 5.8 B).

Collectively, these data demonstrate inhibition of ALK5 blocks canonical TGF-β2-induced p-Smad3 in endothelial cells, but is accompanied by the concurrent enhancement/exacerbation of non-canonical TGF-β2-induced p-Smad1/5 and the continued down regulation of endothelial AMBRA1 expression thereby suggesting

AMBRA1 down regulation and loss of endothelial integrity is mediated by non-canonical TGF-β2 signalling (Figure 5.8 C).

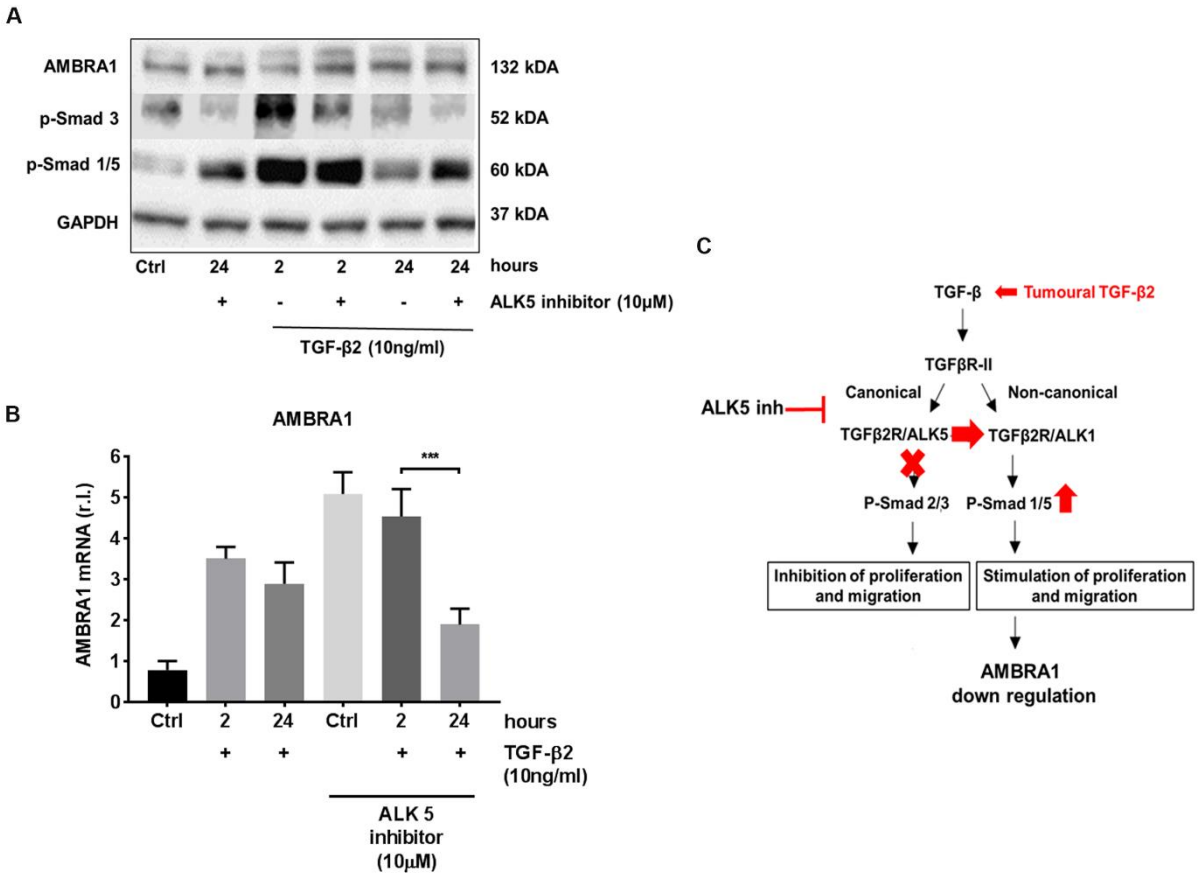

Figure 5.8: ALK5 inhibition sustains TGF-β2 induced Smad 1/5 phosphorylation but does not prevent AMBRA1 down regulation in endothelial cells. A Representative western blot for the expression of AMBRA1 (132 kDA), p-Smad 3 (52 kDA), p-Smad 1/5 (60 kDA) and GAPDH (37 kDA) loading control in HUVEC endothelial cells cultured for 24 hours in the presence or absence of 10 μM ALK5 inhibitor, or HUVEC cells treated with 10 ng/ml recombinant TGF-β2 for 2 hours or 24 hours in the presence or absence of 10 μM ALK5 inhibitor. **B** Relative mRNA levels for the expression of AMBRA1 in HUVEC endothelial cells cultured for 24 hours in the presence or absence of 10 μM ALK5 inhibitor (controls), or HUVEC cells following treatment with 10 ng/ml of recombinant TGF-β2 for 2 hours or 24 hours in the presence or absence of 10 μM ALK5 inhibitor, normalized to L34 housekeeping gene and expressed as the 2-ΔΔCT mRNA fold change relative to siCtrl non treatment cells. Each bar represents 3 replicates ± SD of an experiment. One way ANOVA with Tukey's post-test correction ****P* <0.001. **C** Schematic indicating blockade of canonical TGF-β2 signalling with an ALK5 inhibitor prevents phosphorylation of Smad 3 but exacerbates and sustains phosphorylation of Smad 1/5 and non-canonical TGF-β2 signalling, leading to AMBRA1 down regulation in endothelial cells.

5.2.8 SiRNA-mediated knockdown of ALK1 prevents non-canonical TGF-β2 mediated endothelial AMBRA1 downregulation.

Given lack of commercially available ALK1 inhibitors, to evaluate the potential for ALK1 inhibition as a strategy to prevent canonical TGF-β2-induced down regulation of endothelial AMBRA1, siRNA mediated transient knockdown of ALK1 was performed in HUVEC endothelial cells. 3 different siRNA oligoribonucleotides: ACVRL1HSS100150 (siALK1#150), ACVRL1HSS100151 (siALK1 #151) and ACVRL1HSS100152 (siALK1 #152) targeting human ALK1 and a mixture of all 3 siRNAs were initially evaluated for their potential to knockdown ALK1 expression in HUVEC cells with knockdown efficacy assessed by qPCR in comparison to a non-targeting scrambled siRNA control as described in section 2.7. Successful transient knockdown of ALK1 in HUVEC cells (defined by >50% decrease in ALK1 mRNA by qPCR) was achieved with siALK1 #150 and siALK1 #151 siRNAs (Figure 5.9). For subsequent experiments, siALK1#150 siRNA was selected to assess the potential of transiently knocking down ALK1 to prevent TGF-B2 induced non-canonical signalling and AMBRA1 down regulation in HUVEC endothelial cells.

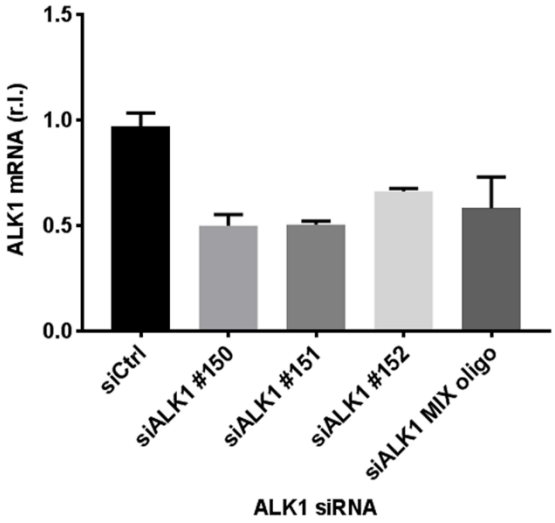

Figure 5.9: Efficacy of siRNA mediated knockdown of ALK1 in HUVEC endothelial cells. Relative mRNA levels of ALK1 in HUVEC endothelial cells following transfection for 48 hours with siCtrl, siALK #150, siALK1 #151, siALK1 #152 or siALK1 MIX of all three siRNAs normalized to L34 housekeeping gene and expressed as 2-ΔΔCT values relative to siCtrl. Each bar represents the mean ± SD of 3 replicate qPCR reactions.

Knockdown of ALK1 using siALK1#150 siRNA (Figure 5.10 B) with subsequent treatment of HUVEC cells with 10 ng/ml recombinant TGF-β2 for 2 hours revealed a reduction in the expression of p-Smad 1/5 with no change in expression of total Smad 1 and 5 as well as the partial rescue of TGF-β2-induced AMBRA1 down regulation, sustained levels of which were still observable after 24 hours (Figure 5.10 A).

To further evaluate the rescue of TGF-β2-induced AMBRA1 down regulation in HUVEC cells by knockdown of ALK1, in line with the early induction of phosphorylated Smad 1/5, AMBRA1 mRNA expression levels were additionally assessed by qPCR. In contrast to data derived by ALK5 blockade, siRNA-mediated knockdown of ALK1 in HUVEC endothelial cells resulted in significant prevention of TGF-β2–induced AMBRA1 down regulation at 24 hours (One way ANOVA with Tukey's multiple comparison test $^{**}P < 0.01$, $^{***}P < 0.001$, Figure 5.10 C).

Coupled with data demonstrating the lack of prevention of TGF-β2 –induced AMBRA1 downregulation by blockade of ALK5 and canonical TGF-β2 signalling (section 5.2.6), these data further suggest the down regulation of endothelial AMBRA1 is mediated by non-canonical ALK1 signalling and that targeting ALK1 may represent a novel therapeutic strategy to prevent loss of endothelial integrity and metastasis in high risk melanomas (Figure 5.10 D). Nevertheless, to confirm this hypothesis, further studies will be required to confirm the effects of ALK 1 blockade on TGF-β2-induced endothelial cell junctional protein expression.

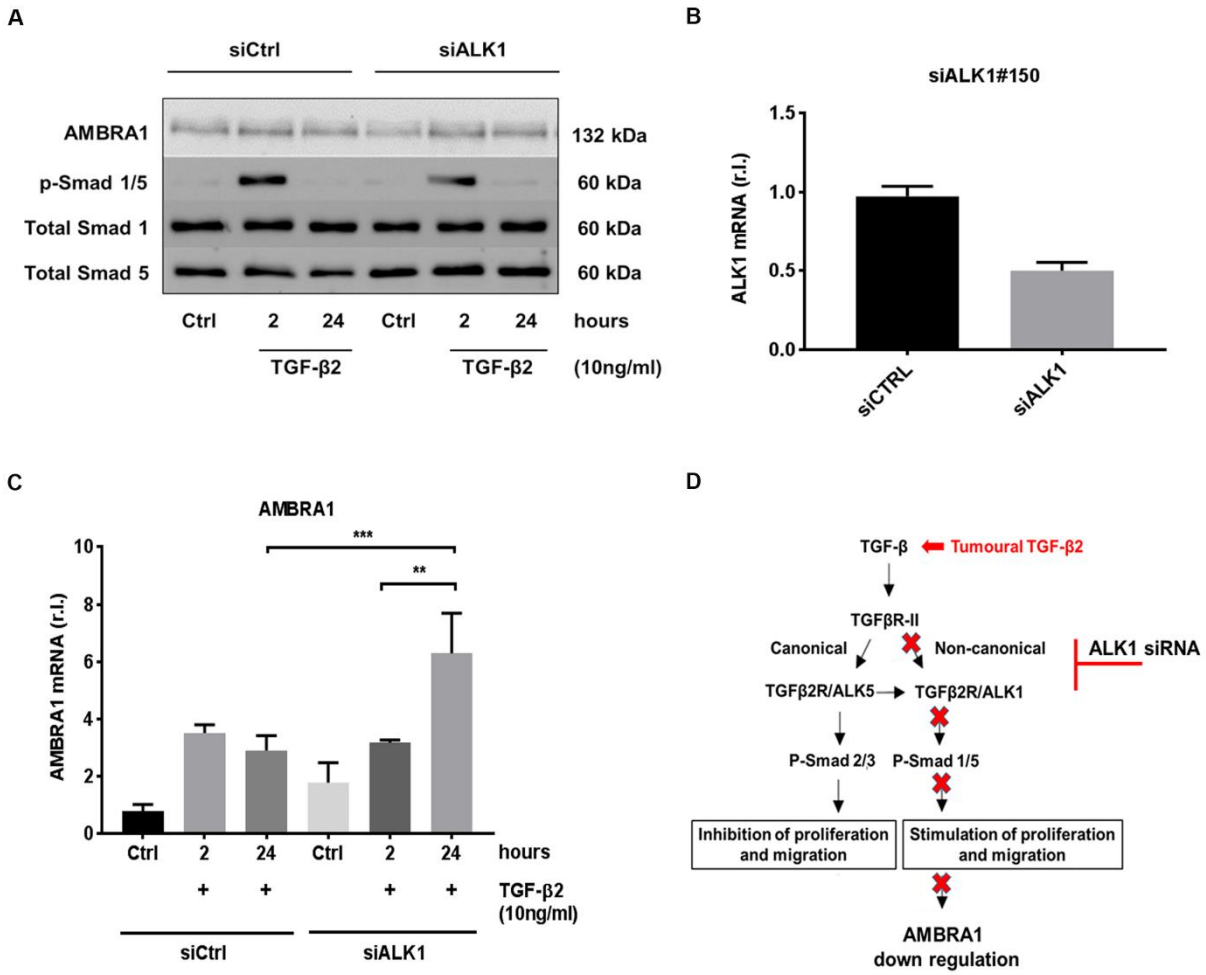

Figure 5.10: Knockdown of ALK1 prevents TGFβ2-induced Smad 1/5 phosphorylation and loss of endothelial AMBRA1. A Representative western blot for the expression of AMBRA1 (132 kDA), p-Smad 1/5 (60 kDA), total Smad 1 (60 kDA) and total Smad 5 (60 kDA) in HUVEC endothelial cells following transfection of siControl (siCtrl) RNA or siALK1 RNA and treatment with 10mg/ml recombinant TGFβ2 for 2 or 24 hours. **B** Relative ALK1 mRNA levels in HUVEC endothelial cells following two transfections with 20 μM siALK1#150 siRNA (siALK1) or ctrl siRNA for 24 hours and confirming >50% knockdown of ALK1. **C** Relative AMBRA1 mRNA in HUVEC cells following transfection with siCtrl or siALK1 in the absence (Ctrl) or presence of treatment with 10ng/ml recombinant TGF-β2 for 2 hours or 24 hours, normalized to L34 housekeeping gene and expressed as the 2-ΔΔCT mRNA fold change relative to siCtrl non treatment HUVEC cells. Each bar represents 3 replicates ± SD of an experiment. One way ANOVA with Tukey's multiple comparison test ***P* <0.01, ****P* <0.001. **D** Schematic indicating blockade of non-canonical TGF-β2 signalling with ALK1 siRNA prevents TGF-β2-induced phosphorylation of Smad 1/5 and partially rescues TGF-β2 induced AMBRA1 down regulation in endothelial cells.

5.2.9 Inhibition of canonical TGF-β2 signaling by ALK5 inhibition promotes endothelial cell proliferation

The formation of neovasculature from pre-existing blood vessels is widely considered an essential process to ensure nutrient and oxygen supply for melanoma tumour survival as well as provide a potential route for tumour cell entry and metastasis [196], a process mediated by several pro-angiogenic factors [197]. In endothelial cells, TGF-β2 has been shown to transduce signals via ALK1 and 5 with both pathways having opposing effects where signalling via ALK5 has been shown to inhibit endothelial cell migration and proliferation whereas ALK1 stimulates both these processes [129, 132]. To test any potential effect of exogenous TGF-β2 on endothelial cell proliferation, HUVEC endothelial cells and primary HDLECs were first treated with 10 ng/ml or 20 ng/ml human recombinant TGF-β2 prior to assessment of cell viability over 72 hours via a commercial MTS cell viability assay. Results demonstrated a significant decrease in HUVEC cell proliferation following treatment with 20 ng/ml recombinant TGF-β2 for 72 hours, however there was no significant difference in HDLEC cell proliferation following 72 hour treatment with either 10 ng/ml or 20 ng/ml recombinant TGF-β2 (One way ANOVA with Dunnett's post-test correction P <0.04, Figure 5.11). Given that TGF-β2 signals via both ALK1 and AK5 in endothelial cells, maintenance of balance between activation of both canonical and non-canonical signalling pathways may have accounted for the lack of effect on endothelial cell proliferation observed.

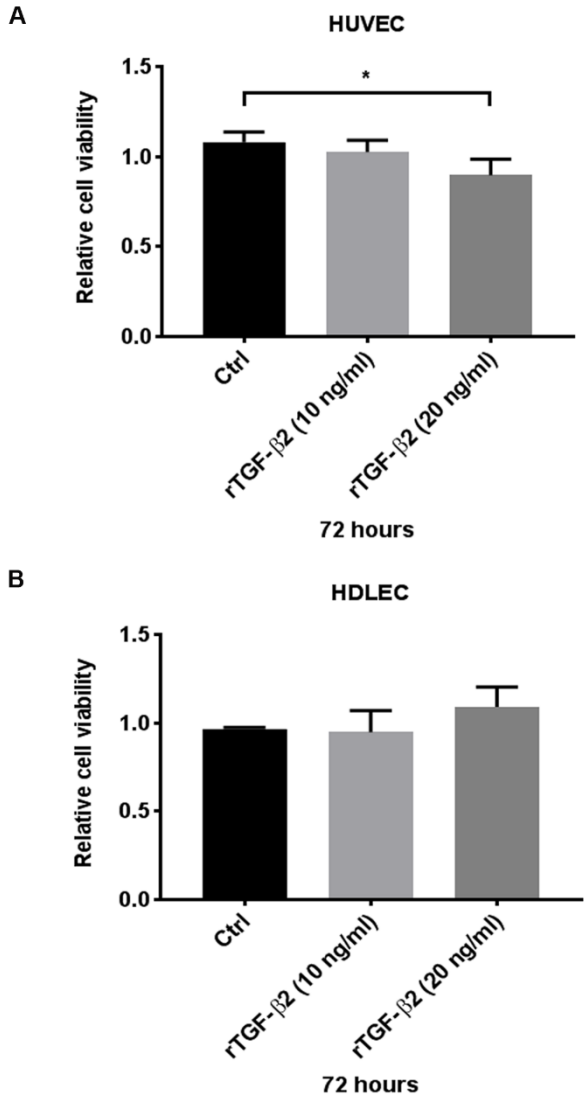

Figure 5.11: Effect of recombinant TGF-β2 on HUVEC and primary HDLEC endothelial cell proliferation. Relative cell viability of **A** HUVEC or **B** HDLEC endothelial cells (presented relative to the mean cell viability value for each experiment) in the presence of treatment for 72 hours with 10 or 20 ng/ml recombinant TGF-β2 or equal volume vehicle control (Ctrl). Each bar represents the mean ± SD of 3 replicate experiments. One way ANOVA with Dunnett's post-test correction *P* <0.04.

Given previous results demonstrating TGF-β2-enhanced Smad 1/5 phosphorylation in HUVEC cells in the presence of ALK5 inhibition, and the possibility that ALK5 inhibition exacerbates non-canonical TGF-β2 signalling, this led to the hypothesis that ALK5 inhibition may in fact drive endothelial cell proliferation. To test this hypothesis, HUVEC cells were next treated with 10 ng/ml recombinant TGF-β2 for 72 hours in the presence or absence of 10 µM ALK5 inhibitor prior to assessing relative cell viability. Results demonstrated, ALK5 inhibition alone did not significantly alter HUVEC cell proliferation, however, in response to treatment with exogenous treatment with TGF-β2 for 72 hours, ALK5 inhibition significantly increased cell proliferation compared to cell viability of control untreated HUVEC cells and cell viability derived by treatment of HUVEC cells treated with 10 ng/ml recombinant TGF-β2 alone (One way ANOVA with Tukey's multiple comparisons test *P <0.05, **P <0.01, Figure 5.12 A).

.

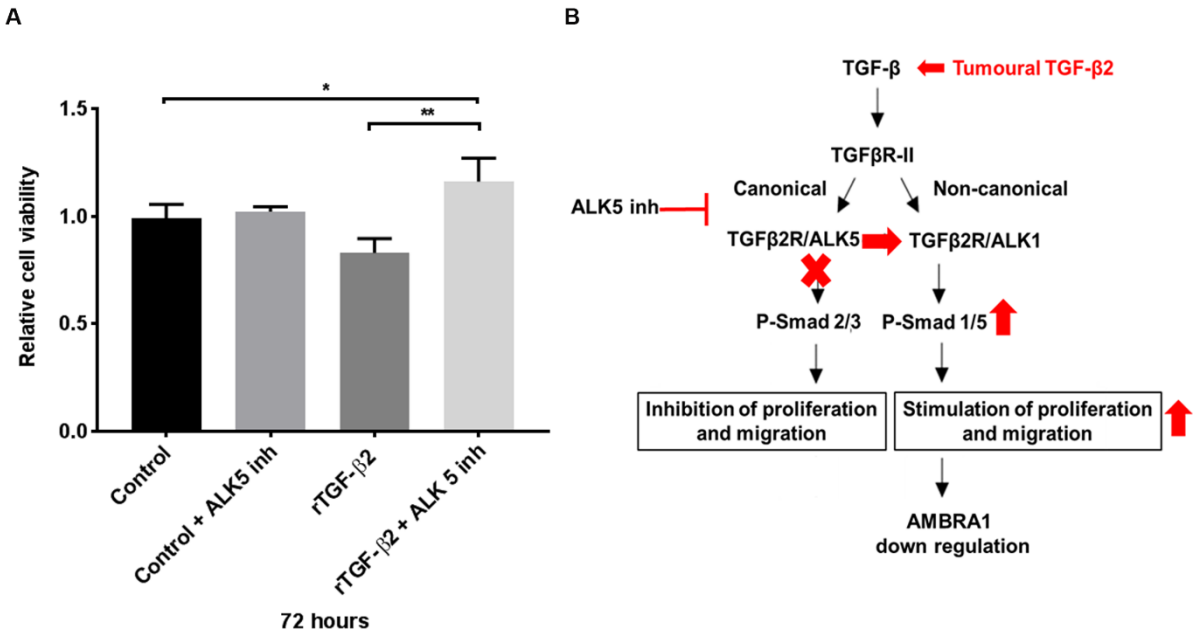

Figure 5.12: ALK5 blockade results in increased TGF-β2 induced stimulation of HUVEC endothelial cell proliferation. A Relative cell viability of HUVEC endothelial cells following treatment with 10 ng/ml recombinant TGF-β2 for 72 hours in the presence or absence of 10 μM ALK5 inhibitor presented relative to the mean cell viability value for each experiment. Each bar represents the mean ± SD of 3 replicate experiments. One way ANOVA with Tukey's multiple comparison test **P* <0.05, ***P* <0.01. **B** Schematic reflecting derived results and ALK5 inhibition-mediated enhanced activation of non-canonical TGF-β2-induced stimulation of HUVEC endothelial cell proliferation.

Collectively, these data thus support the hypothesis that ALK5 blockade results in the enhancement of non-canonical TGF-β2-induced endothelial proliferation (Figure 5.12 B). Studies of the effects of ALK1 inhibition on melanoma TGF-β2 mediated endothelial cell proliferation are nevertheless required to confirm whether or not ALK1 inhibition may specifically inhibit HUVEC or HDLEC cell proliferation.

5.3 Discussion

The secretory polypeptide TGF-β2 exerts multiple effects on numerous key biological functions including cellular proliferation, differentiation and apoptosis [119]. Activated TGF-β2 initiates its signalling cascade via heterotetrameric TGF-β receptor complexes consisting of 2 TGFβ-RIs (ALK 1-7) and 2 TGF-βRIIs which when activated, evoke downstream TGF-β2 signalling through phosphorylation of Smad proteins that translocate into nuclei of cells to modulate gene expression [122, 123]. Despite all 3 isoforms of TGF-β signalling in this manner, there is a distinction in downstream signalling and target effects depending on the composition of the TGF-β receptor complex. In endothelial cells, ALK1 activation phosphorylates Smad 1/5 whereas ALK5 activates Smad 2/3, driving differential responses to TGF-β2 that maintains a homeostatic balance in the endothelium. Disruption to this balance has been shown to exert opposing effects on endothelial cells where preferential canonical signalling via ALK5 inhibits cellular proliferation and migration whereas non-canonical signalling via ALK1 stimulates these processes [120, 129].

Results presented in the previous chapter demonstrated the potential contribution of TGF-β2 secretion by high risk early AJCC stage primary melanomas to AMBRA1 and endothelial junctional protein down regulation leading to loss of epidermal and endothelial integrity, and highlighting the targeting of TGF-β2 signalling as a potential therapeutic strategy to prevent melanoma metastasis within this subgroup. To further understand the mechanisms leading to TGF-β2 mediated AMBRA1 down regulation, bioinformatics analysis of the upstream AMBRA1 promoter was undertaken which identified TGF-β responsive elements for Smads 1/5 and 3 further supporting the involvement of canonical or non-canonical TGF-β2 signalling to AMBRA1 down regulation. This was further characterized by results demonstrating the expression of both ALK1 and ALK5 by endothelial cells while only ALK5 was expressed by keratinocytes and suggesting that TGF-β2 down regulation of AMBRA1 in the

epidermis likely occurs via ALK 5 mediated canonical TGF-β2 signalling whereas in the endothelium, either pathway could be responsible for AMBRA1 down regulation.

To confirm the activation of canonical or non-canonical TGF-β2 signalling in both the epidermis and endothelium in response to exogenous TGF-β2, p-Smad 1/5 or 3 expression was analysed in calcium-induced differentiated CCD1106 keratinocytes and HUVEC endothelial cells following treatment with recombinant TGF-β2. Results revealed activation of canonical signalling via ALK5 in CCD1106 keratinocytes and confirmed the lack of non-canonical signalling due to absence of ALK1 expression. More importantly, the apparent activation of ALK5 signalling was linked to TGF-β2-induced down regulation of AMBRA1 and Loricrin in calcium-induced differentiated CCD1106 keratinocytes, further supporting the contribution of canonical TGF-β2 signalling to the loss of epidermal integrity overlying primary melanomas. In HUVEC endothelial cells however, treatment with recombinant TGF-β2 induced phosphorylation of both Smad 1/5 and Smad 3, suggesting concurrent activation of canonical and non-canonical signalling in response to exogenous TGF-β2. These findings are in line with studies demonstrating TGF-β signalling in endothelial cells occurring via both ubiquitously expressed ALK5 receptors and endothelial cell predominant ALK1 receptors with a fine balance maintained between canonical and non-canonical signalling, where both signalling pathways have opposing effects [162, 198, 199]. TGF-β stimulation of ALK1 has been shown to promote endothelial cell proliferation and migration whereas signalling via ALK5 inhibits these processes [199]. In addition, transcriptional profiling of endothelial cells demonstrated significant differences in the molecular output obtained from ALK1 and ALK5 signalling, further supporting the divergent roles of each receptor in vascular development [200].

To determine the potential contribution of canonical or non-canonical TGF-β2 signalling to loss of integrity of the peri-tumoural endothelium of high risk melanomas that are known to secrete high levels of TGF-β2, the expression of endothelial p-Smad 1/5 and p-Smad 2/3 (Smad 2 and Smad 3 functions as a dimer) were compared in

metastatic and non-metastatic AJCC stage I melanomas *in vivo*. Results revealed a trend for an increase in p-Smad 1/5 but not p-Smad 2/3 in high risk tumours while expression levels of p-Smad 1/5 were minimal in the endothelium surrounding AJCC stage I melanomas that remained localized. These findings hence suggest that non-canonical TGF-β2 signalling rather than canonical TGF-β2 signalling is implicated in the down regulation of endothelial AMBRA1 and junctional protein expression leading to the loss of endo-vascular/lymphatic integrity and highlights the targeting of ALK1 as a potentially viable therapeutic strategy to prevent melanoma metastasis. In addition, given ALK1 is predominantly expressed in endothelial cells and at sites of epithelial-mesenchymal interactions [129, 131] specific targeting of ALK1 in the vascular or lymphatic endothelium may prove an optimal strategy to prevent metastasis in the clinical context of early AJCC stage high risk melanomas, as the tumour along with the overlying epidermis is removed at primary excision. Furthermore, given the wide range of essential cellular processes dependent on TGF-β signalling such as cell proliferation, differentiation, apoptosis and immune suppression [201], inhibition of the TGF-β2 ligand or pan TGF-β receptor complex inhibition would not be ideal strategy to target TGF-β2 signalling due to significant off-target effects.

Finally, supporting a link between the induction of non-canonical TGF-β2 signalling and the down regulation of endothelial AMBRA1, blockade of ALK5 resulted in further and sustained induction of Smad 1/5 phosphorylation and failure to rescue TGF-β2-induced AMBRA1 downregulation thereby suggesting ALK5 blockade exacerbates non-canonical TGF-β2 signalling. Conversely, siRNA mediated ALK1 knockdown in HUVEC endothelial cells resulted in reduced phosphorylation of p-Smad 1/5 and the partial rescue of TGF-β2-induced down regulation of AMBRA1 down regulation, further supporting the notion that the down regulation of endothelial AMBRA1 and endothelial integrity is mediated by non-canonical TGF-β2 signalling, although the effects of ALK1 inhibition on TGF-β2-induced junctional protein expression require further confirmation. Coupled with observations that activated TGF-β/ALK5 signalling in endothelial cells recruits ALK1 and propagates signalling down the non-canonical

pathway, which directly antagonizes ALK5 signalling [129, 199], these results shed light on how non-canonical ALK1 signalling may become predominant in the peri-tumoural endothelium in response to hyperactive or enhanced TGF-β signalling in melanoma, leading to down regulation of AMBRA1 and loss of endothelial integrity.

During metastatic dissemination, melanoma cells enter the circulation by intravasation through endothelial cell junctions [19], facilitated by secretory factors from cancer cells or macrophages such as VEGF or TGF-β that induce remodelling of endothelial junctions or cleavage of vascular endothelial Cadherin (VE-Cadherin), leading to the opening of endothelial cell junctions and loss of endothelial integrity [22, 23]. Endothelial cell junctions are made up of adherens and tight junctions that are intermingled throughout endothelial cell-cell contact areas where their functional interaction is required for maintenance of barrier integrity [27]. As such, intact endothelial barrier function requires the functional adhesive activity of key adherens junction proteins such as VE-Cadherin, where if disrupted, may also result in compromise of tight junctional proteins (Claudin-5), leading to loss of endothelial barrier integrity [29, 30]. Coupled with results in chapter 4 demonstrating down regulation of AMBRA1 and endothelial cell junction proteins VE-Cadherin and Claudin-5 in response to melanoma TGF-β2, results from the present chapter further supports blockade of non-canonical TGF-β2 signalling by targeting ALK1 as a viable therapeutic strategy to prevent endothelial AMBRA and cell junctional protein function and maintain endothelial barrier integrity.

TGF-β2 is known to play a pivotal role in regulating key mechanisms of tumour progression such as proliferation and angiogenesis in a variety of malignant tumours [202]. Tumour induced angiogenesis results in formation of new blood vessels that have weak intercellular junctions, where barrier function is further reduced by locally secreted factors within the tumour microenvironment, enabling tumour cell entry into the vasculature [18]. Despite the apparent lack of any direct effect of exogenous TGF-β2 on enhanced endothelial cell proliferation, blockade of ALK5 enhanced the proliferation of HUVEC cells in the presence of exogenous TGF-β2, which combined

with its effect on increased TGF-β2-induced pSmad 1/5, further supports the role of non-canonical TGF-β2 signalling in melanoma metastasis. Moreover, ALK1 has also been reported to be expressed by lymphatic endothelial cells where inhibition of ALK1 signalling diminishes neonatal lymphangiogenesis [203, 204]. In addition, ALK1 and VEGF receptor-3 signalling has been shown to regulate lymph vessel development [204, 205], likely accounting for the similar effect of TGF-β2-induced AMBRA1 and endothelial junctional protein down regulation in HUVECS also observed in HDLECs, as discussed in chapter 4. Given the lymphatics represent one of the earliest potential points for tumour cell entry with metastases from melanoma most commonly first presenting at regional lymph nodes [181], the potential for TGF-β2 to mediate lymphangiogenesis as well as breach of lymphatic endothelial integrity, further highlight its pro-metastatic role but would warrant further investigation.

Taken together, results from the present chapter suggest that high risk TGF-β2 secreting AJCC stage I melanomas evoke non-canonical TGF-β2 signalling in the peri-tumoural endothelium, resulting in the down regulation of AMBRA1 and junctional protein expression that leads to loss of endothelial integrity as well as increased melanoma neo-vascularisation, increasing the risk of metastasis. Targeting ALK1 may therefore represent an ideal strategy to prevent melanoma metastasis while preserving canonical TGF-β2 signalling.

In the recent years, ALK1 inhibition has gained attention as an attractive therapeutic target in cancer therapy given the presence of its expression and signalling within the vasculature of several tumour types [206]. With regards to specific ALK1 inhibitors, Dalantercept (Acceleron Pharma, MA, USA) an ALK1 ligand trap that inhibits activation of endogenous ALK1 by binding with high affinity to the ligands bone morphogenetic proteins (BMP 9 and 10), was initially evaluated for clinical use in head and neck and renal carcinomas but failed to progress through phase II clinical trials due to lack of efficacy [163-165].

PF03446962 (Pfizer, NY, USA) a monoclonal antibody targeting ALK1 has emerged from phase I clinical trials with encouraging results observed in solid tumours and hepatocellular carcinoma with good side effect profile and tolerability [166, 167] however, to date the therapeutic use of ALK1 inhibitors has not been evaluated in malignant melanoma.

Ultimately, validation of ALK1 as a therapeutic target to prevent metastasis in early AJCC stage high risk melanomas will inform the drug development of novel ALK1 inhibitors for which the combined loss of epidermal AMBRA1 and Loricrin (AMLo) is a companion biomarker. Definition of this targetable pathway will alter the current landscape of the management of early AJCC stage melanomas, which presently lacks novel adjuvant targeted therapy for early stage disease to prevent the development of metastasis.

Summary

- Bioinformatics analysis of the upstream AMBRA1 promoter identified TGF-β signalling responsive elements/binding sites for Smad 1/5 and 3, supporting the role of canonical and non-canonical TGF-β2 signalling in AMBRA1 down regulation and loss of epidermal and endothelial integrity.
- Epidermal AMBRA1 down regulation is mediated by canonical TGF-β2 signalling.
- Endothelial cells express ALK1 and ALK5, mediating activation of both canonical and non-canonical signalling in response to treatment with exogenous TGF-β2.
- Non-canonical TGF-β2 signalling is increased in the endothelium of metastatic AJCC stage I melanomas demonstrated by increased endothelial p-Smad 1/5 and absence of p-Smad 2/3 expression.
- ALK5 inhibition resulted in exacerbated non-canonical TGF-β2 signalling and sustained TGF-β2-induced downregulation of endothelial AMBRA1 expression in HUVEC cells.
- siRNA-mediated knockdown of ALK1 in HUVEC cells resulted in blockade of non-canonical TGF-β2 signaling and the partial rescue of TGF-β2-induced AMBRA1 down regulation
- Enhancement of ALK1 non-canonical TGF-β2 signalling by blockade of ALK5 results in increased HUVEC endothelial cell proliferation.
- Targeting of ALK1 may represent a novel therapeutic strategy to prevent loss of endothelial integrity and melanoma metastasis for which AMLo is a companion biomarker.

Chapter 6

Final discussion and future perspectives

Chapter 6: Final discussion and future perspectives

6.1 AMLo as a follow-up stratification tool for AJCC stage I melanoma following primary melanoma excision 203

6.2 AMLo as a companion biomarker for adjuvant therapy targeting TGF-β2 signalling 206

6.3 The role of Vitamin D in TGF-β2 mediated AMBRA1 down regulation and melanoma metastasis 208

6.1 AMLo as a follow-up stratification tool for AJCC stage I melanoma following primary melanoma excision

To date there is still a lack of evidence based guidelines or an international consensus as to which surveillance strategies are most effective following primary melanoma excision, leading to significant variation in practices worldwide with no internationally accepted standardised model of patient follow up [177, 178]. In view of this, identifying and validating robust, evidence based surveillance programs with an emphasis on efficient prognostication and personalised treatment options for melanoma patients should underpin the focus of future work to translate better outcomes for patients. Current practice is to treat all patients with melanoma by initial surgical excision of the primary tumour with continued surveillance until metastasis ensues. With still no consistently beneficial treatments for metastatic melanoma however, there is a push towards informing clinical decisions at the outset.

The identification and validation of AMLo as a novel prognostic biomarker for early AJCC stage I melanoma addresses an unmet need in melanoma management by enabling risk-stratification of the earliest stage tumours, potentially altering future management and surveillance practices for patients with early stage AJCC melanomas. To date there have been no other accurate means of identifying high risk AJCC stage I melanomas at risk of metastasis, with an umbrella approach of ‘excision followed by watchful waiting’ currently employed by skin cancer services in the management of patients with such tumours. Similarly, as there have also been no previous means of accurately identifying high risk AJCC stage I melanomas, current drug trials for the treatment of melanoma have primarily focussed on the recruitment of patients already with advanced metastatic disease. Instead, utility of AMLo in a clinical setting will henceforth allow a more personalised approach to management of AJCC stage I melanomas, allowing closer surveillance practices, further radiological investigation and longer follow up duration if required for high risk tumours or facilitating discharge following primary excision for low risk tumours, as well as informing and

stratifying patients with high risk tumours for earlier novel targeted adjuvant therapy.

In addition, due to the rapidly increasing incidence of melanoma, NHS costs for all skin cancers are expected to climb from £106 – £112 million in 2008 to over £180 million in 2020 [207], placing increasing burden on an already stretched national health service. The high NPV afforded by AMLo as a prognostic biomarker will therefore potentially have significant positive impact on the cost of skin cancer care by aiding discharge decisions of low risk early stage tumours, given up to 91% of all melanomas are diagnosed in the UK fall within stage I or II, each requiring follow up between 1 – 5 years [32]. Future work will therefore include an application to the National Institute for Health Research (NIHR) health technology assessment programme to determine the prognostic performance of currently available prognostic biomarkers used in risk stratification, surveillance and follow up strategies of patients with AJCC stage I melanoma as well as evaluate the cost-effectiveness of such strategies. Results derived from such studies will further aid the evaluation and potential impact of the clinical utility of AMLo in the management of melanoma on the health economics of skin cancer care.

Overall, results from the present AMLo biomarker validation study presented in chapter 3 suggest that going forwards with the staging changes brought in by the new 8th edition AJCC guidelines, the combined loss of AMLo overlying melanoma tumours will enable prognostic evaluation of both AJCC stage IA and IB melanomas, with further validation work already commenced in a further independent ‘prospective retrospective’ cohort of AJCC stage I melanomas derived from County Durham & Darlington NHS Trust in collaboration with histopathologist Dr Paul Barrett, University Hospital of North Durham, UK.

Based on the recommendations of the REMARK guidelines however, validation of a biomarker should be performed in a large randomised control trial setting(Appendix 1) [75]. Nonetheless, the high prognostic potential of AMLo derived from initial studies in predicting melanoma metastasis will give rise to ethical implications of withholding prognostic information or failure to offer or modify surveillance practices in the management of patients identified as high risk, as would be the case in a randomised prospective study. Given the huge impact the clinical utility of AMLo could potentially afford to melanoma cancer care, it would also be clinically beneficial for rapid validation of AMLo as a prognostic biomarker in AJCC stage I melanoma and incorporation into cancer care guidelines, compared to a prospective trial that will require at least 8 year follow-up data and will require costly funding. In view of this, results derived from AMLo biomarker validation within this study were presented at the National Cancer Research Institute (NCRI) UK Clinical Studies Group (CSG) meeting in November 2016. Feedback obtained from an expert panel recommended clinical validation of the prognostic potential of AMLo in a further independent, geographically distinct cohort of AJCC stage I melanomas, in addition to validation in the County Durham & Darlington NHS Trust melanoma cohort will be required to support application its adoption into NICE clinical guidelines without the need for a prospective clinical trial.

All work to date has employed the use of commercially available research grade antibodies, use of such antibodies is however unsuitable in a clinical test setting. Supporting the continued development of AMLo as a prognostic biomarker for AJCC stage I melanoma, work is therefore already underway to produce recombinant clinical grade antibodies to the same protein epitopes that will validated by comparison with results derived from the present study using research grade antibodies and CE marked to allow their use as a clinical diagnostic tool. Completion of these studies will hopefully support future adoption of AMLo as a prognostic biomarker into NICE guidelines and eventual incorporation as a prognosticator in AJCC staging criteria for melanoma, facilitating its use in a wider context.

6.2 AMLo as a companion biomarker for adjuvant therapy targeting TGF-β2 signalling

In this current era of personalised medicine, there is a constant drive towards identifying novel companion biomarkers to inform and guide targetable therapeutic avenues in cancer care. Companion biomarkers are biomarkers that can be used to prospectively predict likely response, resistance or toxicity risk in combination with specific therapies [208] i.e. biomarkers that are able to predict success of a specific treatment in each individual, enabling rational stratification for therapy. Historically, systemic treatment for advanced melanoma has incorporated chemotherapy with agents such as Dacarbazine or immunotherapy with interleukin-2 with limited success [209, 210], where treatment strategies were largely guided by AJCC staging with other factors such as patient age and performance status taken into consideration. With the advent of novel targeted therapies and immunotherapies for advanced melanoma in the past decade, the importance of companion biomarkers has become more apparent in stratifying patients for the most appropriate systemic therapy. In addition, companion biomarkers may also inform on selection of appropriate therapeutic doses or alert physicians to patients with likelihood of severe toxicity for closer monitoring, forming the basis of personalised medicine i.e. the use of molecular diagnosis of disease to prescribe optimal treatment for the right patient [211].

Two of the best examples where companion biomarkers have been developed in parallel with targeted cancer therapy include stratification of patients with EML4-ALK-positive non-small cell lung cancer for treatment with Crizitonib [212, 213] or the evaluation of $BRAF^{V600}$ mutation status to stratify patients for therapy with BRAF inhibitors [97, 98]. In both these examples, the relevant biomarkers were incorporated in clinical trials at stage I where co-development with drug therapy resulted in rapid approval of their widespread clinical utility [208].

Results presented in chapter 2 demonstrate the targeting of TGF-β2 signalling as a viable therapeutic strategy to prevent ulceration and metastases of high risk AJCC stage I melanomas following primary excision, for which AMLo expression is a companion biomarker. More specifically, studies of TGF-β2 signalling in the endothelium, presented and discussed in chapter 3, suggest the targeting of non-canonical ALK1-mediated TGF-β2 signalling may represent an optimal strategy to inhibit TGF-β2-mediated AMBRA1 and junctional protein down regulation, thereby potentially preventing melanoma metastasis. Given loss of epidermal AMLo overlying AJCC stage I melanomas was found to be associated with loss of peri-tumoural endothelial AMBRA1 expression in metastatic AJCC stage I melanoma as discussed in chapter 2, epidermal AMLo expression may therefore serve as an ideal companion biomarker to stratify patients for adjuvant therapy with ALK1 specific inhibitors. Further studies in a larger AJCC stage I melanoma cohort investigating the correlation between epidermal AMLo expression and endothelial AMBRA1 as well as melanoma prognosis will however, be required to validate this association and ideally can be undertaken in the 'prospective-retrospective' AJCC stage I melanoma cohort derived from Country Durham & Darlington NHS Foundation Trust.

Despite the recent emergence of ALK1 inhibitors as a target for anti-angiogenic cancer therapy with evaluation in several clinical trials for treatment of various malignancies, to date the therapeutic utility of this approach has not been evaluated in malignant melanoma [162]. Future work will hence require further validation of ALK1 as a therapeutic target for drug development in high risk AJCC stage I melanoma using siRNA mediated ALK1 knockdown as well as chemical validation *in vitro* using rationally designed ALK1 inhibitor compounds to evaluate the effect of ALK1 inhibition on AMBRA1 down regulation and endothelial cell junction integrity. In addition, evaluation of the potential for novel ALK1 inhibitors to prevent melanoma invasion in fully humanised melanoma skin equivalents as well as *in vivo* in established xenograft models of human metastatic melanoma will inform novel drug development and ultimately clinical drug trials for which AMLo may serve as a companion biomarker to stratify high risk patient subgroups.

6.3 The role of Vitamin D in TGF-β2 mediated AMBRA1 down regulation and melanoma metastasis

In the recent years, there has been much debate regarding the role of Vitamin D in melanoma progression. Certainly in melanoma, low levels of serum 25-hydroxyvitamin D at primary melanoma diagnosis has been associated with high risk melanomas with thicker primary tumours and a poorer prognosis, despite conflicting evidence on overall survival and insufficient evidence to establish cause-effect [78-82]. However, given vitamin D is primarily synthesised in the skin following exposure to UV exposure which has been historically linked to UVR-induced melanoma genesis, the association between increased vitamin D levels and reduced melanoma risk remains a controversial topic.

Despite lower Vitamin D levels being associated with ulceration of primary melanomas and a poorer melanoma specific survival, the underlying biology of this remains uncertain. Following on from their previous work linking low levels of Vitamin D to melanoma ulceration and poor survival in a melanoma cohort derived from Leeds [78], a further study by Newton-Bishop *et al* recently suggested that the protective effect of Vitamin D may in fact be reduced by high serum Vitamin A (retinoic acid) levels [214].

Interestingly, functional interactions between Vitamin A and TGF-β have long been observed underlying regulatory events controlling cellular proliferation and differentiation [215]. Vitamin A has been shown to regulate TGF-β expression *in vivo*, where basal expression of TGF-β2 was diminished in Vitamin A deficient conditions and treatment with retinoic acid resulted in induction of TGF-β2 and TGF-β3 in the epidermis, tracheobronchial and alveolar epithelium as well as intestinal mucosa [216]. Additionally, retinoic acid receptors have been shown to interfere with the TGF-β/Smad signalling pathway with suggestion that retinoic acid receptors (RAR) may function as co-activators of Smad signalling [217].

A recent study by O'Shea *et al* investigating the enigma of melanoma ulceration and poor melanoma specific survival evaluated gene expression patterns associated with ulceration and demonstrated upregulation of pro-inflammatory cytokines IL-6 and IL-8, as well as establishing an association between co-morbidities associated with systemic inflammation such as smoking, diabetes and obesity with melanoma ulceration, suggesting that ulceration is driven by inflammation [86, 218]. There is also strong evidence in literature linking low Vitamin D levels to higher C-Reactive protein levels (marker of systemic inflammation) [219], further supporting the role of Vitamin D in melanoma ulceration. Interestingly, TGF-β has been reported to be an important regulator of IL-6 and IL-8 production with studies demonstrating that TGF-β can augment or inhibit IL-6 production in human fibroblasts as well as enhance IL-6 secretion by intestinal epithelial cells [220, 221] and induce increased expression of IL-1 and IL-8 in rat alveolar epithelial cells [222] as well as overexpression of IL-8 in human prostate cancer [223]. As previously discussed in chapter 2, Vitamin D is known to be a regulator of TGF-β signalling [191, 192] where impaired Vitamin D receptor signalling with reduced expression of VDR and decreased levels of its ligand have been shown to contribute to enhanced sensitivity of epithelial cells to the effects of TGF-β and result in hyperactive TGF-β signalling [189]. Collectively, this highlights the possibility of interplay between Vitamin D and TGF-β where low levels of Vitamin D or receptor could enhance the effect or increase expression/secretion of melanoma TGF-β2 leading to pro-inflammatory conditions and melanoma ulceration.

Collectively, literature discussed above highlights the potential interaction Vitamin D and its receptor expression may have on TGF-β2-induced down regulation of AMBRA1 and melanoma prognosis observed in the present study cohort where melanomas that secrete high levels of TGF-β2 leading to activation of canonical TGF-β2 signalling and epidermal AMBRA1 down regulation may be protected against the pro-metastatic effect of TGF-β2 in the endothelium where there is adequate Vitamin D and receptor status (Figure 6.1 B). Equally, melanomas that have low Vitamin D or receptor status may display enhanced sensitivity or hyperactive TGF-β signalling resulting in epidermal ulceration, whereby exacerbated canonical signalling in response to TGF-β2 may tip the balance towards favouring non-canonical signalling in the endothelium, resulting in loss of endothelial integrity and metastasis; an effect that will be further compounded in high risk melanomas that secrete higher levels of TGF-β2 (Figure 6.1 A). This may explain why some melanoma tumours within the present study cohort scored as AMLo high risk with loss of epidermal AMBRA1 did not display any loss in expression of peri-tumoural endothelial AMBRA1 and develop metastases and equally why some AMLo low risk melanomas develop metastatic disease. Overall, these findings suggest that it may not only be high levels of TGF-β2 that determine metastatic risk but rather the effect of other factors contributing to enhanced or reduced signalling that determine metastatic risk and emphasising why the expression of tumoural TGF-β2 itself is unsuitable as a biomarker for disease progression.

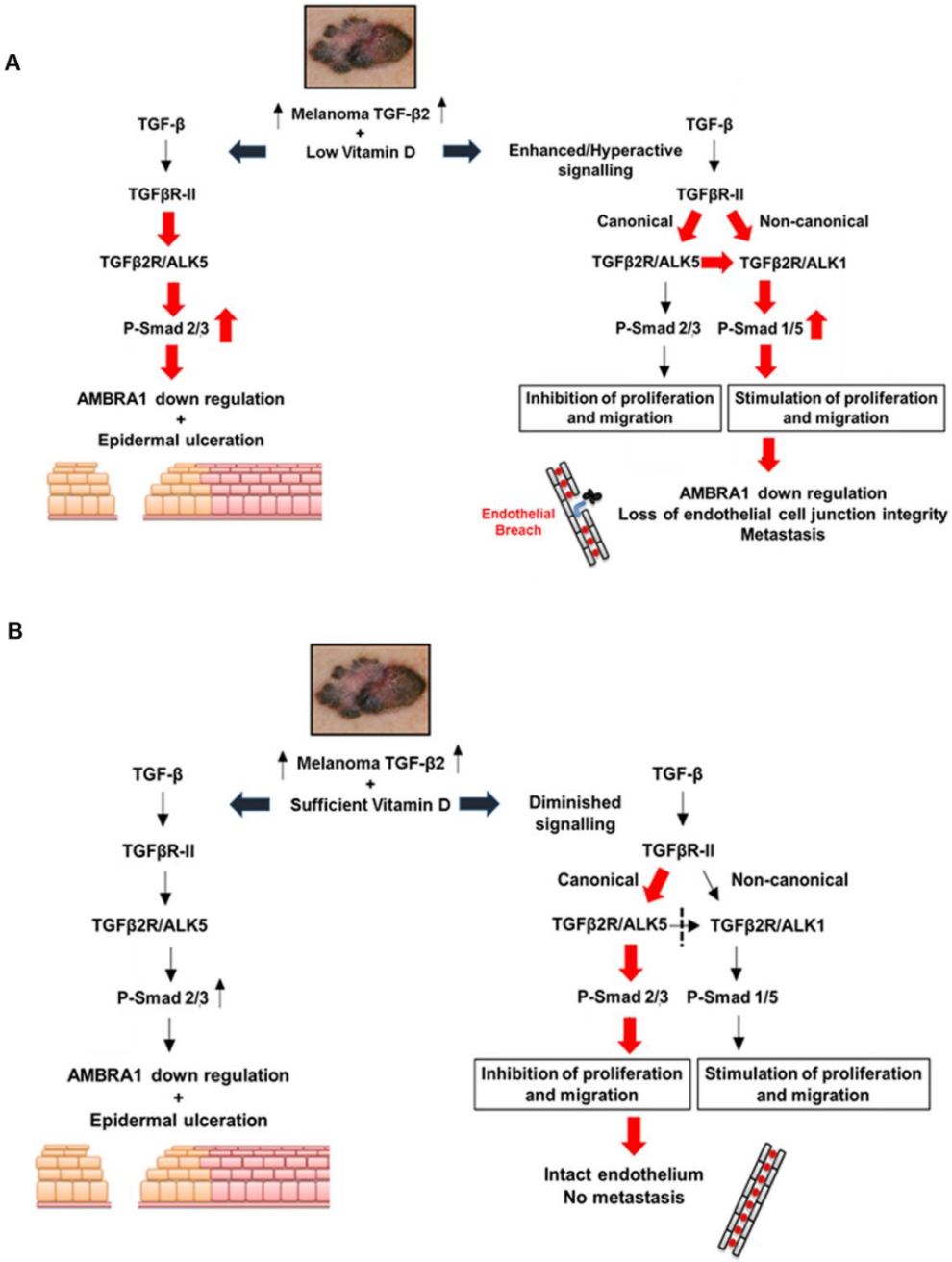

Figure 6.1: Hypothesis of the role of Vitamin D in TGF-β2 induced loss of epidermal/endothelial integrity and melanoma metastasis. A Melanomas that secrete high levels of TGF-β2 have enhanced TGF-β2 signalling in the presence of low Vitamin D levels leading to AMBRA1 downregulation and ulceration in the epidermis. In the endothelium, this results in increased recruitment of ALK1 thereby further enhancing non-canonical TGF-β2 signalling which becomes predominant, leading to stimulation and proliferation of endothelial cells, endothelial AMBRA1 down regulation, loss of endothelial cell integrity, tumour cell entry and metastasis. **B** In the presence of sufficient Vitamin D levels, TGF-β2 signalling is diminished. Here, high levels of TGF-β2 secreted by some melanomas may still be sufficient to down regulate AMBRA1 in the epidermis and cause ulceration however, will not be sufficient to tip the balance of TGF-β2 signalling in the endothelium to favour non-canonical signalling, instead favouring canonical signalling which is protective against metastasis.

In addition reported findings that high Vitamin A levels negate the protective effects of Vitamin D on melanoma survival [214] and that Vitamin A antagonises the effects of Vitamin D *in vivo* [224] but induce TGF-β signalling as discussed above, further highlight the potential crosstalk between these two steroid hormone receptor family members with TGF-β2 signalling and AMBRA1 down regulation. It may be that low risk melanoma tumours that would normally be protected from the pro-metastatic effects of TGF-β2 due to adequate Vitamin D status, lose that protective effect in the presence of high Vitamin A levels (Table 6.1). Future work should therefore incorporate IHC analysis or mRNA expression analysis of Vitamin A and D receptor status in association with TGF-β2 signalling (by IHC expression of p-Smads), analysis of which could be undertaken in the AJCC stage I melanoma cohort derived from County Durham & Darlington NHS Foundation trust in order to further evaluate this link given the possibility that the utility of Vitamin A or D status in conjunction with AMLo as a biomarker may further improve the prognostic potential of AMLo alone.

Equally interesting, is the association of Vitamin D with a plethora of other dermatological conditions such as psoriasis, disorders of keratinisation and skin fibrosis that have been traditionally treated with Vitamin D analogues, where the precise mechanisms underlying their therapeutic efficacy are still not completely understood [225]. The epidermal hyperkeratosis and dysregulated epidermal differentiation observed overlying melanoma tumours with loss of AMBRA1 expression mirrors in some ways, the changes observed in psoriasis and other disorders of keratinisation, shedding light on the potential role of TGF-β2 signalling in these disorders. In addition, the indisputable role TGF-β plays in fibrosis has long led to studies identifying pathways targeting its signalling to prevent fibrosis in a variety of fibrotic diseases such as renal and hepatic fibrosis or fibrosing lung conditions [226-228].

This opens doors to endless possibilities on the potential of targeting TGF-β2 signalling not only in the treatment of high risk melanomas, but also for its widespread application in several other diseases not limited to a dermatology setting. Ultimately, further and more in-depth studies into the relationship between Vitamin A and D and TGF-β2 signalling will be required to understand the precise mechanisms underpinning the interaction between these three very complex signalling pathways.

Prognosis of AJCC stage I melanoma	**High melanoma TGF-β2**				**Low to average melanoma TGF-β2**			
	Vitamin D				**Vitamin D**			
	High		**Low**		**High**		**Low**	
Ulcerated epidermis	Yes		Yes		No		Possible	
Loss of endothelial integrity & metastasis	No		Yes		No		Possible	
Prognosis Incorporating Vitamin A status	**Vitamin A**		**Vitamin A**		**Vitamin A**		**Vitamin A**	
	High	**Low**	**High**	**Low**	**High**	**Low**	**High**	**Low**
Ulcerated epidermis	Yes	Yes	Yes	Yes	Possible	No	Possible	Possible
Loss of endothelial integrity & metastasis	Possible	No	Yes	Yes	Possible	No	Possible	Possible

Table 6.1: Potential effect of Vitamin D and Vitamin A status on prognosis of AJCC stage I melanomas in association with melanoma TGF-β2 secretion.

References

1. Lin, J.Y. and D.E. Fisher, *Melanocyte biology and skin pigmentation.* Nature, 2007. **445**(7130): p. 843-50.
2. Silver, D.L.a.P., W.J., *The Origin and Development of Neural Crest-Derived Melanocytes.* From Melanocytes to Melanoma, 2006. **1**: p. 3-26.
3. Ernfors, P., *Cellular origin and developmental mechanisms during the formation of skin melanocytes.* Exp Cell Res, 2010. **316**(8): p. 1397-407.
4. Fitzpatrick, T.B. and A.S. Breathnach, *[the Epidermal Melanin Unit System].* Dermatol Wochenschr, 1963. **147**: p. 481-9.
5. Tsatmalia, M., et al., *Skin POMC peptides. Their binding affinities and activation of the human MC1 receptor.* Ann N Y Acad Sci, 1999. **885**: p. 466-9.
6. Healy, E., et al., *Functional variation of MC1R alleles from red-haired individuals.* Hum Mol Genet, 2001. **10**(21): p. 2397-402.
7. Cichorek, M., et al., *Skin melanocytes: biology and development.* Postepy Dermatol Alergol, 2013. **30**(1): p. 30-41.
8. Marks, R., A.P. Dorevitch, and G. Mason, *Do all melanomas come from "moles"? A study of the histological association between melanocytic naevi and melanoma.* Australas J Dermatol, 1990. **31**(2): p. 77-80.
9. Bevona, C., et al., *Cutaneous melanomas associated with nevi.* Arch Dermatol, 2003. **139**(12): p. 1620-4; discussion 1624.
10. Rezze, G.G., A. Leon, and J. Duprat, *Dysplastic nevus (atypical nevus).* An Bras Dermatol, 2010. **85**(6): p. 863-71.
11. Guerry, D.t., et al., *Lessons from tumor progression: the invasive radial growth phase of melanoma is common, incapable of metastasis, and indolent.* J Invest Dermatol, 1993. **100**(3): p. 342S-345S.
12. Elder, D.E., *Dysplastic naevi: an update.* Histopathology, 2010. **56**(1): p. 112-20.
13. Gray-Schopfer, V., C. Wellbrock, and R. Marais, *Melanoma biology and new targeted therapy.* Nature, 2007. **445**(7130): p. 851-7.
14. Tas, F., *Metastatic behavior in melanoma: timing, pattern, survival, and influencing factors.* J Oncol, 2012. **2012**: p. 647684.

15. Miller, A.J. and M.C. Mihm, Jr., *Melanoma.* N Engl J Med, 2006. **355**(1): p. 51-65.
16. Regad, T., *Molecular and cellular pathogenesis of melanoma initiation and progression.* Cell Mol Life Sci, 2013. **70**(21): p. 4055-65.
17. Li, F.Z., et al., *Phenotype switching in melanoma: implications for progression and therapy.* Front Oncol, 2015. **5**: p. 31.
18. Weis, S.M. and D.A. Cheresh, *alphaV integrins in angiogenesis and cancer.* Cold Spring Harb Perspect Med, 2011. **1**(1): p. a006478.
19. Reymond, N., B.B. d'Agua, and A.J. Ridley, *Crossing the endothelial barrier during metastasis.* Nat Rev Cancer, 2013. **13**(12): p. 858-70.
20. Vestweber, D., *Relevance of endothelial junctions in leukocyte extravasation and vascular permeability.* Ann N Y Acad Sci, 2012. **1257**: p. 184-92.
21. Carman, C.V. and T.A. Springer, *Trans-cellular migration: cell-cell contacts get intimate.* Curr Opin Cell Biol, 2008. **20**(5): p. 533-40.
22. Hoeben, A., et al., *Vascular endothelial growth factor and angiogenesis.* Pharmacol Rev, 2004. **56**(4): p. 549-80.
23. Drabsch, Y. and P. ten Dijke, *TGF-beta signaling in breast cancer cell invasion and bone metastasis.* J Mammary Gland Biol Neoplasia, 2011. **16**(2): p. 97-108.
24. Bendas, G. and L. Borsig, *Cancer cell adhesion and metastasis: selectins, integrins, and the inhibitory potential of heparins.* Int J Cell Biol, 2012. **2012**: p. 676731.
25. Dong, C., et al., *Melanoma cell extravasation under flow conditions is modulated by leukocytes and endogenously produced interleukin 8.* Mol Cell Biomech, 2005. **2**(3): p. 145-59.
26. Strell, C., et al., *Surface molecules regulating rolling and adhesion to endothelium of neutrophil granulocytes and MDA-MB-468 breast carcinoma cells and their interaction.* Cell Mol Life Sci, 2007. **64**(24): p. 3306-16.
27. Dejana, E., *Endothelial cell-cell junctions: happy together.* Nat Rev Mol Cell Biol, 2004. **5**(4): p. 261-70.
28. Taddei, A., et al., *Endothelial adherens junctions control tight junctions by VE-cadherin-mediated upregulation of claudin-5.* Nature Cell Biology, 2008. **10**(8): p. 923-934.

29. Gavard, J. and J.S. Gutkind, *VEGF controls endothelial-cell permeability by promoting the beta-arrestin-dependent endocytosis of VE-cadherin.* Nat Cell Biol, 2006. **8**(11): p. 1223-34.
30. Gavard, J. and J.S. Gutkind, *VE-cadherin and claudin-5: it takes two to tango.* Nat Cell Biol, 2008. **10**(8): p. 883-5.
31. Orlova, V.V., et al., *Junctional adhesion molecule-C regulates vascular endothelial permeability by modulating VE-cadherin-mediated cell-cell contacts.* J Exp Med, 2006. **203**(12): p. 2703-14.
32. Kingdom, C.R.U., *Skin Cancer Statistics.* Available: http://www.cancerresearchuk.org/health-professional/cancer-statistics/statistics-by-cancer-type/skin-cancer, 2016.
33. Erdmann, F., et al., *International trends in the incidence of malignant melanoma 1953-2008--are recent generations at higher or lower risk?* Int J Cancer, 2013. **132**(2): p. 385-400.
34. *National Cancer Intelligence Network, United Kingdom.* Mortality, Incidence and gender-Malignant Melanoma. Available: http://www.ncin.org.uk/publications/data_briefings/mortality_incidence_and_gender_malignant_melanoma, 2012.
35. Lens, M.B. and M. Dawes, *Global perspectives of contemporary epidemiological trends of cutaneous malignant melanoma.* Br J Dermatol, 2004. **150**(2): p. 179-85.
36. Beddingfield, F.C., 3rd, *The melanoma epidemic: res ipsa loquitur.* Oncologist, 2003. **8**(5): p. 459-65.
37. Balch, C.M., et al., *Final version of 2009 AJCC melanoma staging and classification.* J Clin Oncol, 2009. **27**(36): p. 6199-206.
38. Armstrong, B.K. and A. Kricker, *The epidemiology of UV induced skin cancer.* J Photochem Photobiol B, 2001. **63**(1-3): p. 8-18.
39. Tucker, M.A. and A.M. Goldstein, *Melanoma etiology: where are we?* Oncogene, 2003. **22**(20): p. 3042-52.
40. Boniol, M., et al., *Cutaneous melanoma attributable to sunbed use: systematic review and meta-analysis.* BMJ, 2012. **345**: p. e4757.

41. Harrison, S.L., et al., *Sun exposure and melanocytic naevi in young Australian children.* Lancet, 1994. **344**(8936): p. 1529-32.
42. Bishop, D.T., et al., *Geographical variation in the penetrance of CDKN2A mutations for melanoma.* J Natl Cancer Inst, 2002. **94**(12): p. 894-903.
43. Viros, A., et al., *Ultraviolet radiation accelerates BRAF-driven melanomagenesis by targeting TP53.* Nature, 2014. **511**(7510): p. 478-82.
44. Flaherty, K.T., F.S. Hodi, and D.E. Fisher, *From genes to drugs: targeted strategies for melanoma.* Nat Rev Cancer, 2012. **12**(5): p. 349-61.
45. Tsao, H., et al., *Melanoma: from mutations to medicine.* Genes Dev, 2012. **26**(11): p. 1131-55.
46. Dutton-Regester, K. and N.K. Hayward, *Reviewing the somatic genetics of melanoma: from current to future analytical approaches.* Pigment Cell Melanoma Res, 2012. **25**(2): p. 144-54.
47. Thompson, J.F., R.A. Scolyer, and R.F. Kefford, *Cutaneous melanoma.* Lancet, 2005. **365**(9460): p. 687-701.
48. Cantwell-Dorris, E.R., J.J. O'Leary, and O.M. Sheils, *BRAFV600E: implications for carcinogenesis and molecular therapy.* Mol Cancer Ther, 2011. **10**(3): p. 385-94.
49. Platz, A., et al., *Human cutaneous melanoma; a review of NRAS and BRAF mutation frequencies in relation to histogenetic subclass and body site.* Mol Oncol, 2008. **1**(4): p. 395-405.
50. Lee, J.H., J.W. Choi, and Y.S. Kim, *Frequencies of BRAF and NRAS mutations are different in histological types and sites of origin of cutaneous melanoma: a meta-analysis.* Br J Dermatol, 2011. **164**(4): p. 776-84.
51. Barbacid, M., *ras genes.* Annu Rev Biochem, 1987. **56**: p. 779-827.
52. Downward, J., *Targeting RAS signalling pathways in cancer therapy.* Nat Rev Cancer, 2003. **3**(1): p. 11-22.
53. Padua, R.A., N.C. Barrass, and G.A. Currie, *Activation of N-ras in a human melanoma cell line.* Mol Cell Biol, 1985. **5**(3): p. 582-5.
54. Long, G.V., et al., *Prognostic and clinicopathologic associations of oncogenic BRAF in metastatic melanoma.* J Clin Oncol, 2011. **29**(10): p. 1239-46.

55. Ellerhorst, J.A., et al., *Clinical correlates of NRAS and BRAF mutations in primary human melanoma.* Clin Cancer Res, 2011. **17**(2): p. 229-35.
56. Menzies, A.M., et al., *Distinguishing clinicopathologic features of patients with V600E and V600K BRAF-mutant metastatic melanoma.* Clin Cancer Res, 2012. **18**(12): p. 3242-9.
57. Houben, R., et al., *Constitutive activation of the Ras-Raf signaling pathway in metastatic melanoma is associated with poor prognosis.* J Carcinog, 2004. **3**(1): p. 6.
58. Breslow, A., *Thickness, cross-sectional areas and depth of invasion in the prognosis of cutaneous melanoma.* Ann Surg, 1970. **172**(5): p. 902-8.
59. Breslow, A., *Tumor thickness, level of invasion and node dissection in stage I cutaneous melanoma.* Ann Surg, 1975. **182**(5): p. 572-5.
60. Edge, S.B. and C.C. Compton, *The American Joint Committee on Cancer: the 7th edition of the AJCC cancer staging manual and the future of TNM.* Ann Surg Oncol, 2010. **17**(6): p. 1471-4.
61. Spatz, A., et al., *The biology of melanoma prognostic factors.* Discov Med, 2010. **10**(50): p. 87-93.
62. Amin, M.B., et al., *The Eighth Edition AJCC Cancer Staging Manual.* New York, Springer, 2017.
63. Gershenwald JE, S.R., Hess KR et al., *Melanoma of the skin.* AJCC Cancer Staging Manual: Eighth Edition, Amin MB. (Ed), 2017. **American Joint Committee on Cancer, Chicago 2017**: p. 563.
64. Leiter, U., et al., *Complete lymph node dissection versus no dissection in patients with sentinel lymph node biopsy positive melanoma (DeCOG-SLT): a multicentre, randomised, phase 3 trial.* Lancet Oncol, 2016. **17**(6): p. 757-67.
65. Morton, D.L., et al., *Final trial report of sentinel-node biopsy versus nodal observation in melanoma.* N Engl J Med, 2014. **370**(7): p. 599-609.
66. Abhishek, S. and S. Palamadai Krishnan, *Epidermal Differentiation Complex: A Review on Its Epigenetic Regulation and Potential Drug Targets.* Cell J, 2016. **18**(1): p. 1-6.
67. Houben, E., K. De Paepe, and V. Rogiers, *A keratinocyte's course of life.* Skin Pharmacol Physiol, 2007. **20**(3): p. 122-32.

68. Lourenco, S.V., et al., *Relationship of adhesion molecules expression with epithelial differentiation markers during fetal skin development.* J Cutan Pathol, 2008. **35**(8): p. 731-7.
69. Kypriotou, M., M. Huber, and D. Hohl, *The human epidermal differentiation complex: cornified envelope precursors, S100 proteins and the 'fused genes' family.* Experimental Dermatology, 2012. **21**(9): p. 643-9.
70. Spatz, A., et al., *Interobserver reproducibility of ulceration assessment in primary cutaneous melanomas.* Eur J Cancer, 2003. **39**(13): p. 1861-5.
71. Balch, C.M., et al., *The prognostic significance of ulceration of cutaneous melanoma.* Cancer, 1980. **45**(12): p. 3012-7.
72. Eggermont, A.M., et al., *Long-term results of the randomized phase III trial EORTC 18991 of adjuvant therapy with pegylated interferon alfa-2b versus observation in resected stage III melanoma.* J Clin Oncol, 2012. **30**(31): p. 3810-8.
73. Eggermont, A.M., et al., *Ulceration and stage are predictive of interferon efficacy in melanoma: results of the phase III adjuvant trials EORTC 18952 and EORTC 18991.* Eur J Cancer, 2012. **48**(2): p. 218-25.
74. Gogas, H., et al., *Biomarkers in melanoma.* Ann Oncol, 2009. **20 Suppl 6**: p. vi8-13.
75. McShane, L.M., et al., *REporting recommendations for tumor MARKer prognostic studies (REMARK).* Nat Clin Pract Urol, 2005. **2**(8): p. 416-22.
76. Gould Rothberg, B.E., M.B. Bracken, and D.L. Rimm, *Tissue biomarkers for prognosis in cutaneous melanoma: a systematic review and meta-analysis.* J Natl Cancer Inst, 2009. **101**(7): p. 452-74.
77. Excellence, N.I.f.H.a.C., *Melanoma: assessment and management.* NICE guidelines (NG14), 2015.
78. Newton-Bishop, J.A., et al., *Serum 25-hydroxyvitamin D3 levels are associated with breslow thickness at presentation and survival from melanoma.* J Clin Oncol, 2009. **27**(32): p. 5439-44.
79. Newton-Bishop, J.A., et al., *25-Hydroxyvitamin D2 /D3 levels and factors associated with systemic inflammation and melanoma survival in the Leeds Melanoma Cohort.* Int J Cancer, 2015. **136**(12): p. 2890-9.

80. Fang, S., et al., *Association of Vitamin D Levels With Outcome in Patients With Melanoma After Adjustment For C-Reactive Protein.* J Clin Oncol, 2016. **34**(15): p. 1741-7.
81. Luo, L., et al., *No prognostic value added by vitamin D pathway SNPs to current prognostic system for melanoma survival.* PLoS One, 2017. **12**(3): p. e0174234.
82. Saiag, P., et al., *Prognostic Value of 25-hydroxyvitamin D3 Levels at Diagnosis and During Follow-up in Melanoma Patients.* J Natl Cancer Inst, 2015. **107**(12): p. djv264.
83. Sullivan, R., *The challenge of developing useful blood-based biomarkers in melanoma.* Br J Dermatol, 2013. **168**(1): p. 3.
84. Verykiou, S., R. Ellis, and P. Lovat, *Established and Emerging Biomarkers in Cutaneous Malignant Melanoma.* Healthcare, 2014. **2**(1): p. 60.
85. Cirenajwis, H., et al., *Molecular stratification of metastatic melanoma using gene expression profiling: Prediction of survival outcome and benefit from molecular targeted therapy.* Oncotarget, 2015. **6**(14): p. 12297-309.
86. Jewell, R., et al., *The clinicopathological and gene expression patterns associated with ulceration of primary melanoma.* Pigment Cell Melanoma Res, 2015. **28**(1): p. 94-104.
87. Nsengimana, J., et al., *Independent replication of a melanoma subtype gene signature and evaluation of its prognostic value and biological correlates in a population cohort.* Oncotarget, 2015. **6**(13): p. 11683-93.
88. Gerami, P., et al., *Gene expression profiling for molecular staging of cutaneous melanoma in patients undergoing sentinel lymph node biopsy.* J Am Acad Dermatol, 2015. **72**(5): p. 780-5 e3.
89. Gerami, P., et al., *Development of a prognostic genetic signature to predict the metastatic risk associated with cutaneous melanoma.* Clin Cancer Res, 2015. **21**(1): p. 175-83.
90. Navneet, D., et al., *Gene expression profile signature (DecisionDx-Melanoma) to predict visceral metastatic risk in patients with stage I and stage II cutaneous melanoma.* Journal of Clinical Oncology, 2012. **30**(15_suppl): p. 8543-8543.
91. Lazova, R., V. Klump, and J. Pawelek, *Autophagy in cutaneous malignant melanoma.* J Cutan Pathol, 2010. **37**(2): p. 256-68.

92. Lazova, R., et al., *Punctate LC3B expression is a common feature of solid tumors and associated with proliferation, metastasis, and poor outcome.* Clin Cancer Res, 2012. **18**(2): p. 370-9.
93. Soengas, M.S. and S.W. Lowe, *Apoptosis and melanoma chemoresistance.* Oncogene, 2003. **22**(20): p. 3138-51.
94. Ellis, R.A., et al., *Prognostic impact of p62 expression in cutaneous malignant melanoma.* J Invest Dermatol, 2014. **134**(5): p. 1476-8.
95. Armstrong, J.L., et al., *Exploiting cannabinoid-induced cytotoxic autophagy to drive melanoma cell death.* J Invest Dermatol, 2015. **135**(6): p. 1629-37.
96. Chapman, P.B., et al., *Improved survival with vemurafenib in melanoma with BRAF V600E mutation.* N Engl J Med, 2011. **364**(26): p. 2507-16.
97. McArthur, G.A., et al., *Safety and efficacy of vemurafenib in BRAF(V600E) and BRAF(V600K) mutation-positive melanoma (BRIM-3): extended follow-up of a phase 3, randomised, open-label study.* Lancet Oncol, 2014. **15**(3): p. 323-32.
98. Hauschild, A., et al., *Dabrafenib in BRAF-mutated metastatic melanoma: a multicentre, open-label, phase 3 randomised controlled trial.* Lancet, 2012. **380**(9839): p. 358-65.
99. Long, G.V., et al., *Dabrafenib in patients with Val600Glu or Val600Lys BRAF-mutant melanoma metastatic to the brain (BREAK-MB): a multicentre, open-label, phase 2 trial.* Lancet Oncol, 2012. **13**(11): p. 1087-95.
100. Chan, M.M., et al., *The nature and management of metastatic melanoma after progression on BRAF inhibitors: effects of extended BRAF inhibition.* Cancer, 2014. **120**(20): p. 3142-53.
101. Sosman, J.A., et al., *Survival in BRAF V600-mutant advanced melanoma treated with vemurafenib.* N Engl J Med, 2012. **366**(8): p. 707-14.
102. Long, G.V., et al., *Dabrafenib and trametinib versus dabrafenib and placebo for Val600 BRAF-mutant melanoma: a multicentre, double-blind, phase 3 randomised controlled trial.* Lancet, 2015. **386**(9992): p. 444-51.
103. Larkin, J., et al., *Combined vemurafenib and cobimetinib in BRAF-mutated melanoma.* N Engl J Med, 2014. **371**(20): p. 1867-76.

104. Liu, M., et al., *Efficacy and safety of BRAF inhibition alone versus combined BRAF and MEK inhibition in melanoma: a meta-analysis of randomized controlled trials.* Oncotarget, 2017. **8**(19): p. 32258-32269.
105. Ascierto, P.A., et al., *Cobimetinib combined with vemurafenib in advanced BRAF(V600)-mutant melanoma (coBRIM): updated efficacy results from a randomised, double-blind, phase 3 trial.* Lancet Oncol, 2016. **17**(9): p. 1248-60.
106. Menzies, A.M. and G.V. Long, *Systemic treatment for BRAF-mutant melanoma: where do we go next?* Lancet Oncol, 2014. **15**(9): p. e371-81.
107. Wong, D.J. and A. Ribas, *Targeted Therapy for Melanoma.* Cancer Treat Res, 2016. **167**: p. 251-62.
108. Hodi, F.S., et al., *Improved survival with ipilimumab in patients with metastatic melanoma.* N Engl J Med, 2010. **363**(8): p. 711-23.
109. Robert, C., et al., *Ipilimumab plus dacarbazine for previously untreated metastatic melanoma.* N Engl J Med, 2011. **364**(26): p. 2517-26.
110. Robert, C., et al., *Anti-programmed-death-receptor-1 treatment with pembrolizumab in ipilimumab-refractory advanced melanoma: a randomised dose-comparison cohort of a phase 1 trial.* Lancet, 2014. **384**(9948): p. 1109-17.
111. Robert, C., et al., *Nivolumab in previously untreated melanoma without BRAF mutation.* N Engl J Med, 2015. **372**(4): p. 320-30.
112. Hu-Lieskovan, S., et al., *Combining targeted therapy with immunotherapy in BRAF-mutant melanoma: promise and challenges.* J Clin Oncol, 2014. **32**(21): p. 2248-54.
113. Hamanaka, R.B. and N.S. Chandel, *Mitochondrial metabolism as a regulator of keratinocyte differentiation.* Cell Logist, 2013. **3**(1): p. e25456.
114. Hamanaka, R.B., et al., *Mitochondrial reactive oxygen species promote epidermal differentiation and hair follicle development.* Sci Signal, 2013. **6**(261): p. ra8.
115. Fimia, G.M., et al., *Unleashing the Ambra1-Beclin 1 complex from dynein chains: Ulk1 sets Ambra1 free to induce autophagy.* Autophagy, 2011. **7**(1): p. 115-7.

116. Vazquez, P., et al., *Atg5 and Ambra1 differentially modulate neurogenesis in neural stem cells.* Autophagy, 2012. **8**(2): p. 187-99.
117. Cianfanelli, V., et al., *AMBRA1 links autophagy to cell proliferation and tumorigenesis by promoting c-Myc dephosphorylation and degradation.* Nat Cell Biol, 2015. **17**(5): p. 706.
118. Tang, D.Y., R.A. Ellis, and P.E. Lovat, *Prognostic Impact of Autophagy Biomarkers for Cutaneous Melanoma.* Front Oncol, 2016. **6**: p. 236.
119. Annes, J.P., J.S. Munger, and D.B. Rifkin, *Making sense of latent TGFbeta activation.* J Cell Sci, 2003. **116**(Pt 2): p. 217-24.
120. Papageorgis, P., *TGFbeta Signaling in Tumor Initiation, Epithelial-to-Mesenchymal Transition, and Metastasis.* J Oncol, 2015. **2015**: p. 587193.
121. Bierie, B. and H.L. Moses, *Tumour microenvironment: TGFbeta: the molecular Jekyll and Hyde of cancer.* Nat Rev Cancer, 2006. **6**(7): p. 506-20.
122. Huse, M., et al., *The TGF beta receptor activation process: an inhibitor- to substrate-binding switch.* Mol Cell, 2001. **8**(3): p. 671-82.
123. Massague, J., J. Seoane, and D. Wotton, *Smad transcription factors.* Genes Dev, 2005. **19**(23): p. 2783-810.
124. Nakao, A., et al., *Identification of Smad7, a TGFbeta-inducible antagonist of TGF-beta signalling.* Nature, 1997. **389**(6651): p. 631-5.
125. Hayashi, H., et al., *The MAD-related protein Smad7 associates with the TGFbeta receptor and functions as an antagonist of TGFbeta signaling.* Cell, 1997. **89**(7): p. 1165-73.
126. Kavsak, P., et al., *Smad7 binds to Smurf2 to form an E3 ubiquitin ligase that targets the TGF beta receptor for degradation.* Mol Cell, 2000. **6**(6): p. 1365-75.
127. Perrot, C.Y., D. Javelaud, and A. Mauviel, *Insights into the Transforming Growth Factor-beta Signaling Pathway in Cutaneous Melanoma.* Ann Dermatol, 2013. **25**(2): p. 135-44.
128. Derynck, R. and Y.E. Zhang, *Smad-dependent and Smad-independent pathways in TGF-beta family signalling.* Nature, 2003. **425**(6958): p. 577-84.
129. Goumans, M.J., et al., *Activin receptor-like kinase (ALK)1 is an antagonistic mediator of lateral TGFbeta/ALK5 signaling.* Mol Cell, 2003. **12**(4): p. 817-28.

130. Chen, Y.G. and J. Massague, *Smad1 recognition and activation by the ALK1 group of transforming growth factor-beta family receptors.* J Biol Chem, 1999. **274**(6): p. 3672-7.
131. Roelen, B.A., M.A. van Rooijen, and C.L. Mummery, *Expression of ALK-1, a type 1 serine/threonine kinase receptor, coincides with sites of vasculogenesis and angiogenesis in early mouse development.* Dev Dyn, 1997. **209**(4): p. 418-30.
132. Lebrin, F., et al., *TGF-beta receptor function in the endothelium.* Cardiovasc Res, 2005. **65**(3): p. 599-608.
133. Roberts, A.B. and L.M. Wakefield, *The two faces of transforming growth factor beta in carcinogenesis.* Proc Natl Acad Sci U S A, 2003. **100**(15): p. 8621-3.
134. Rodeck, U., T. Nishiyama, and A. Mauviel, *Independent regulation of growth and SMAD-mediated transcription by transforming growth factor beta in human melanoma cells.* Cancer Res, 1999. **59**(3): p. 547-50.
135. Lo, R.S. and O.N. Witte, *Transforming growth factor-beta activation promotes genetic context-dependent invasion of immortalized melanocytes.* Cancer Res, 2008. **68**(11): p. 4248-57.
136. Janji, B., et al., *Autocrine TGF-beta-regulated expression of adhesion receptors and integrin-linked kinase in HT-144 melanoma cells correlates with their metastatic phenotype.* Int J Cancer, 1999. **83**(2): p. 255-62.
137. De Craene, B. and G. Berx, *Regulatory networks defining EMT during cancer initiation and progression.* Nat Rev Cancer, 2013. **13**(2): p. 97-110.
138. Payne, A.S. and L.A. Cornelius, *The role of chemokines in melanoma tumor growth and metastasis.* J Invest Dermatol, 2002. **118**(6): p. 915-22.
139. Liu, G., et al., *Selective induction of interleukin-8 expression in metastatic melanoma cells by transforming growth factor-beta 1.* Cytokine, 2005. **31**(3): p. 241-9.
140. Javelaud, D., et al., *Stable overexpression of Smad7 in human melanoma cells inhibits their tumorigenicity in vitro and in vivo.* Oncogene, 2005. **24**(51): p. 7624-9.
141. Mnich, C.D., et al., *Reduced pSmad2 immunodetection correlates with increased primary melanoma thickness.* Melanoma Res, 2007. **17**(2): p. 131-6.

142. Lasfar, A. and K.A. Cohen-Solal, *Resistance to transforming growth factor beta-mediated tumor suppression in melanoma: are multiple mechanisms in place?* Carcinogenesis, 2010. **31**(10): p. 1710-7.
143. Javelaud, D., V.I. Alexaki, and A. Mauviel, *Transforming growth factor-beta in cutaneous melanoma.* Pigment Cell Melanoma Res, 2008. **21**(2): p. 123-32.
144. Krasagakis, K., et al., *Elevated plasma levels of transforming growth factor (TGF)-beta1 and TGF-beta2 in patients with disseminated malignant melanoma.* Br J Cancer, 1998. **77**(9): p. 1492-4.
145. Schmid, P., P. Itin, and T. Rufli, *In situ analysis of transforming growth factor-beta s (TGF-beta 1, TGF-beta 2, TGF-beta 3), and TGF-beta type II receptor expression in malignant melanoma.* Carcinogenesis, 1995. **16**(7): p. 1499-503.
146. Van Belle, P., et al., *Melanoma-associated expression of transforming growth factor-beta isoforms.* Am J Pathol, 1996. **148**(6): p. 1887-94.
147. Moretti, S., et al., *In situ expression of transforming growth factor beta is associated with melanoma progression and correlates with Ki67, HLA-DR and beta 3 integrin expression.* Melanoma Res, 1997. **7**(4): p. 313-21.
148. Reed, J.A., et al., *Expression of transforming growth factor-beta 2 in malignant melanoma correlates with the depth of tumor invasion. Implications for tumor progression.* Am J Pathol, 1994. **145**(1): p. 97-104.
149. Pinner, S., et al., *Intravital imaging reveals transient changes in pigment production and Brn2 expression during metastatic melanoma dissemination.* Cancer Res, 2009. **69**(20): p. 7969-77.
150. Perrot, C.Y., D. Javelaud, and A. Mauviel, *Overlapping activities of TGF-beta and Hedgehog signaling in cancer: therapeutic targets for cancer treatment.* Pharmacol Ther, 2013. **137**(2): p. 183-99.
151. Morris, J.C., et al., *Phase I study of GC1008 (fresolimumab): a human anti-transforming growth factor-beta (TGFbeta) monoclonal antibody in patients with advanced malignant melanoma or renal cell carcinoma.* PLoS One, 2014. **9**(3): p. e90353.
152. Lacouture, M.E., et al., *Cutaneous keratoacanthomas/squamous cell carcinomas associated with neutralization of transforming growth factor beta by*

the monoclonal antibody fresolimumab (GC1008). Cancer Immunol Immunother, 2015. **64**(4): p. 437-46.

153. Giaccone, G., et al., *A phase III study of belagenpumatucel-L, an allogeneic tumour cell vaccine, as maintenance therapy for non-small cell lung cancer.* Eur J Cancer, 2015. **51**(16): p. 2321-9.
154. Helmut, O., et al., *Final results of a phase I/II study in patients with pancreatic cancer, malignant melanoma, and colorectal carcinoma with trabedersen.* Journal of Clinical Oncology, 2012. **30**(15_suppl): p. 4034-4034.
155. Hau, P., et al., *Inhibition of TGF-beta2 with AP 12009 in recurrent malignant gliomas: from preclinical to phase I/II studies.* Oligonucleotides, 2007. **17**(2): p. 201-12.
156. Bogdahn, U., et al., *Targeted therapy for high-grade glioma with the TGF-beta2 inhibitor trabedersen: results of a randomized and controlled phase IIb study.* Neuro Oncol, 2011. **13**(1): p. 132-42.
157. Akhurst, R.J. and A. Hata, *Targeting the TGFbeta signalling pathway in disease.* Nat Rev Drug Discov, 2012. **11**(10): p. 790-811.
158. Senzer, N., et al., *Phase I Trial of "bi-shRNAifurin/GMCSF DNA/Autologous Tumor Cell" Vaccine (FANG) in Advanced Cancer.* Mol Ther, 2012. **20**(3): p. 679-686.
159. Connolly, E.C., J. Freimuth, and R.J. Akhurst, *Complexities of TGF-beta targeted cancer therapy.* Int J Biol Sci, 2012. **8**(7): p. 964-78.
160. Sandrine, J.F., et al., *A phase 2 study of galunisertib, a novel transforming growth factor-beta (TGF-β) receptor I kinase inhibitor, in patients with advanced hepatocellular carcinoma (HCC) and low serum alpha fetoprotein (AFP).* Journal of Clinical Oncology, 2016. **34**(15_suppl): p. 4070-4070.
161. Neuzillet, C., et al., *Targeting the TGFbeta pathway for cancer therapy.* Pharmacol Ther, 2015. **147**: p. 22-31.
162. Cunha, S.I. and K. Pietras, *ALK1 as an emerging target for antiangiogenic therapy of cancer.* Blood, 2011. **117**(26): p. 6999-7006.
163. Gupta, S., et al., *Activin receptor inhibitors--dalantercept.* Curr Oncol Rep, 2015. **17**(4): p. 14.

164. Jimeno, A., et al., *A phase 2 study of dalantercept, an activin receptor-like kinase-1 ligand trap, in patients with recurrent or metastatic squamous cell carcinoma of the head and neck.* Cancer, 2016. **122**(23): p. 3641-3649.
165. Wang, X., et al., *Inhibition of ALK1 signaling with dalantercept combined with VEGFR TKI leads to tumor stasis in renal cell carcinoma.* Oncotarget, 2016. **7**(27): p. 41857-41869.
166. Goff, L.W., et al., *A Phase I Study of the Anti-Activin Receptor-Like Kinase 1 (ALK-1) Monoclonal Antibody PF-03446962 in Patients with Advanced Solid Tumors.* Clin Cancer Res, 2016. **22**(9): p. 2146-54.
167. Simonelli, M., et al., *Phase I study of PF-03446962, a fully human monoclonal antibody against activin receptor-like kinase-1, in patients with hepatocellular carcinoma.* Ann Oncol, 2016. **27**(9): p. 1782-7.
168. Armstrong, J.L., et al., *Oncogenic B-RAF signaling in melanoma impairs the therapeutic advantage of autophagy inhibition.* Clin Cancer Res, 2011. **17**(8): p. 2216-26.
169. Gupta, K., et al., *A novel technique for culture of human dermal microvascular endothelial cells under either serum-free or serum-supplemented conditions: isolation by panning and stimulation with vascular endothelial growth factor.* Exp Cell Res, 1997. **230**(2): p. 244-51.
170. Corazzari, M., et al., *Targeting homeostatic mechanisms of endoplasmic reticulum stress to increase susceptibility of cancer cells to fenretinide-induced apoptosis: the role of stress proteins ERdj5 and ERp57.* Br J Cancer, 2007. **96**(7): p. 1062-71.
171. Altman, D.G. and J.M. Bland, *Diagnostic tests 2: Predictive values.* BMJ, 1994. **309**(6947): p. 102.
172. Altman, D.G. and J.M. Bland, *Diagnostic tests. 1: Sensitivity and specificity.* BMJ, 1994. **308**(6943): p. 1552.
173. Cecconi, F., et al., *A novel role for autophagy in neurodevelopment.* Autophagy, 2007. **3**(5): p. 506-8.
174. Aymard, E., et al., *Autophagy in human keratinocytes: an early step of the differentiation?* Exp Dermatol, 2011. **20**(3): p. 263-8.

175. Filipowska-Gronska, A., et al., *The frequency of polymorphic variants of filaggrin gene and clinical atopic dermatitis.* Postepy Dermatol Alergol, 2016. **33**(1): p. 37-41.
176. Amin, M.B., et al., *The Eighth Edition AJCC Cancer Staging Manual: Continuing to build a bridge from a population-based to a more "personalized" approach to cancer staging.* CA Cancer J Clin, 2017. **67**(2): p. 93-99.
177. Francken, A.B., E. Bastiaannet, and H.J. Hoekstra, *Follow-up in patients with localised primary cutaneous melanoma.* Lancet Oncol, 2005. **6**(8): p. 608-21.
178. Watts, C.G., et al., *Clinical practice guidelines for identification, screening and follow-up of individuals at high risk of primary cutaneous melanoma: a systematic review.* Br J Dermatol, 2015. **172**(1): p. 33-47.
179. Damude, S., et al., *The MELFO-Study: Prospective, Randomized, Clinical Trial for the Evaluation of a Stage-adjusted Reduced Follow-up Schedule in Cutaneous Melanoma Patients-Results after 1 Year.* Ann Surg Oncol, 2016. **23**(9): p. 2762-71.
180. Carillo, M.C., L. Alvarez Mde, and A.D. Quiroga, *Interferon alfa-2b triggers transforming growth factor-beta-induced apoptosis on preneoplasticliver.* Ann Hepatol, 2006. **5**(4): p. 244-50.
181. Zbytek, B., et al., *Current concepts of metastasis in melanoma.* Expert Rev Dermatol, 2008. **3**(5): p. 569-585.
182. Inagaki, Y., et al., *Interferon alfa down-regulates collagen gene transcription and suppresses experimental hepatic fibrosis in mice.* Hepatology, 2003. **38**(4): p. 890-9.
183. Maleszewska, M., et al., *IL-1beta and TGFbeta2 synergistically induce endothelial to mesenchymal transition in an NFkappaB-dependent manner.* Immunobiology, 2013. **218**(4): p. 443-54.
184. Nie, L., et al., *Endothelial-mesenchymal transition in normal human esophageal endothelial cells cocultured with esophageal adenocarcinoma cells: role of IL-1beta and TGF-beta2.* Am J Physiol Cell Physiol, 2014. **307**(9): p. C859-77.
185. Haroon, M. and O. Fitzgerald, *Vitamin D and its emerging role in immunopathology.* Clin Rheumatol, 2012. **31**(2): p. 199-202.

186. Cutolo, M., *Further emergent evidence for the vitamin D endocrine system involvement in autoimmune rheumatic disease risk and prognosis.* Ann Rheum Dis, 2013. **72**(4): p. 473-5.
187. Messa, P., C. Alfieri, and M.P. Rastaldi, *Recent insights into vitamin D and its receptor.* J Nephrol, 2011. **24 Suppl 18**: p. S30-7.
188. Yee, Y.K., et al., *Vitamin D receptor modulators for inflammation and cancer.* Mini Rev Med Chem, 2005. **5**(8): p. 761-78.
189. Zerr, P., et al., *Vitamin D receptor regulates TGF-beta signalling in systemic sclerosis.* Ann Rheum Dis, 2015. **74**(3): p. e20.
190. Hollis, B.W., *Assessment of vitamin D nutritional and hormonal status: what to measure and how to do it.* Calcif Tissue Int, 1996. **58**(1): p. 4-5.
191. Aschenbrenner, J.K., et al., *1,25-(OH(2))D(3) alters the transforming growth factor beta signaling pathway in renal tissue.* J Surg Res, 2001. **100**(2): p. 171-5.
192. Irani, M., et al., *Vitamin D Supplementation Decreases TGF-beta1 Bioavailability in PCOS: A Randomized Placebo-Controlled Trial.* J Clin Endocrinol Metab, 2015. **100**(11): p. 4307-14.
193. Fischer, K.D. and D.K. Agrawal, *Vitamin D regulating TGF-beta induced epithelial-mesenchymal transition.* Respir Res, 2014. **15**: p. 146.
194. Bikle, D.D., et al., *Development and progression of alopecia in the vitamin D receptor null mouse.* J Cell Physiol, 2006. **207**(2): p. 340-53.
195. Xie, Z., et al., *Lack of the vitamin D receptor is associated with reduced epidermal differentiation and hair follicle growth.* J Invest Dermatol, 2002. **118**(1): p. 11-6.
196. Mahabeleshwar, G.H. and T.V. Byzova, *Angiogenesis in melanoma.* Semin Oncol, 2007. **34**(6): p. 555-65.
197. Valastyan, S. and R.A. Weinberg, *Tumor metastasis: molecular insights and evolving paradigms.* Cell, 2011. **147**(2): p. 275-92.
198. Oh, S.P., et al., *Activin receptor-like kinase 1 modulates transforming growth factor-beta 1 signaling in the regulation of angiogenesis.* Proc Natl Acad Sci U S A, 2000. **97**(6): p. 2626-31.

199. Goumans, M.J., et al., *Balancing the activation state of the endothelium via two distinct TGF-beta type I receptors.* EMBO J, 2002. **21**(7): p. 1743-53.
200. Ota, T., et al., *Targets of transcriptional regulation by two distinct type I receptors for transforming growth factor-beta in human umbilical vein endothelial cells.* J Cell Physiol, 2002. **193**(3): p. 299-318.
201. Schmierer, B. and C.S. Hill, *TGFbeta-SMAD signal transduction: molecular specificity and functional flexibility.* Nat Rev Mol Cell Biol, 2007. **8**(12): p. 970-82.
202. Nagaraj, N.S. and P.K. Datta, *Targeting the transforming growth factor-beta signaling pathway in human cancer.* Expert Opinion on Investigational Drugs, 2010. **19**(1): p. 77-91.
203. Niessen, K., et al., *ALK1 signaling regulates early postnatal lymphatic vessel development.* Blood, 2010. **115**(8): p. 1654-61.
204. Mitchell, D., et al., *ALK1-Fc inhibits multiple mediators of angiogenesis and suppresses tumor growth.* Mol Cancer Ther, 2010. **9**(2): p. 379-88.
205. Cunha, S.I., et al., *Genetic and pharmacological targeting of activin receptor-like kinase 1 impairs tumor growth and angiogenesis.* J Exp Med, 2010. **207**(1): p. 85-100.
206. Hu-Lowe, D.D., et al., *Targeting activin receptor-like kinase 1 inhibits angiogenesis and tumorigenesis through a mechanism of action complementary to anti-VEGF therapies.* Cancer Res, 2011. **71**(4): p. 1362-73.
207. Vallejo-Torres, L., et al., *Measuring current and future cost of skin cancer in England.* J Public Health (Oxf), 2014. **36**(1): p. 140-8.
208. Duffy, M.J. and J. Crown, *Companion biomarkers: paving the pathway to personalized treatment for cancer.* Clin Chem, 2013. **59**(10): p. 1447-56.
209. Atkins, M.B., et al., *High-dose recombinant interleukin 2 therapy for patients with metastatic melanoma: analysis of 270 patients treated between 1985 and 1993.* J Clin Oncol, 1999. **17**(7): p. 2105-16.
210. Tsao, H., M.B. Atkins, and A.J. Sober, *Management of cutaneous melanoma.* N Engl J Med, 2004. **351**(10): p. 998-1012.

211. Khleif, S.N., et al., *AACR-FDA-NCI Cancer Biomarkers Collaborative consensus report: advancing the use of biomarkers in cancer drug development.* Clin Cancer Res, 2010. **16**(13): p. 3299-318.
212. Shaw, A.T., et al., *Effect of crizotinib on overall survival in patients with advanced non-small-cell lung cancer harbouring ALK gene rearrangement: a retrospective analysis.* Lancet Oncol, 2011. **12**(11): p. 1004-12.
213. Shaw, A.T., B. Solomon, and M.M. Kenudson, *Crizotinib and testing for ALK.* J Natl Compr Canc Netw, 2011. **9**(12): p. 1335-41.
214. Field, S., et al., *Do vitamin A serum levels moderate outcome or the protective effect of vitamin D on outcome from malignant melanoma?* Clin Nutr, 2013. **32**(6): p. 1012-6.
215. Roberts, A.B. and M.B. Sporn, *Mechanistic interrelationships between two superfamilies: the steroid/retinoid receptors and transforming growth factor-beta.* Cancer Surv, 1992. **14**: p. 205-20.
216. Glick, A.B., et al., *Complex regulation of TGF beta expression by retinoic acid in the vitamin A-deficient rat.* Development, 1991. **111**(4): p. 1081-6.
217. Pendaries, V., et al., *Retinoic acid receptors interfere with the TGF-beta/Smad signaling pathway in a ligand-specific manner.* Oncogene, 2003. **22**(50): p. 8212-20.
218. O'Shea, S.J., J.R. Davies, and J.A. Newton-Bishop, *Vitamin D, vitamin A, the primary melanoma transcriptome and survival.* Br J Dermatol, 2016. **175 Suppl 2**: p. 30-34.
219. Amer, M. and R. Qayyum, *Relation between serum 25-hydroxyvitamin D and C-reactive protein in asymptomatic adults (from the continuous National Health and Nutrition Examination Survey 2001 to 2006).* Am J Cardiol, 2012. **109**(2): p. 226-30.
220. McGee, D.W., et al., *Transforming growth factor-beta enhances interleukin-6 secretion by intestinal epithelial cells.* Immunology, 1992. **77**(1): p. 7-12.
221. Elias, J.A., V. Lentz, and P.J. Cummings, *Transforming growth factor-beta regulation of IL-6 production by unstimulated and IL-1-stimulated human fibroblasts.* J Immunol, 1991. **146**(10): p. 3437-43.

222. Kumar, N.M., et al., *Induction of interleukin-1 and interleukin-8 mRNAs and proteins by TGF beta 1 in rat lung alveolar epithelial cells.* J Cell Physiol, 1996. **169**(1): p. 186-99.
223. Lu, S. and Z. Dong, *Characterization of TGF-beta-regulated interleukin-8 expression in human prostate cancer cells.* Prostate, 2006. **66**(9): p. 996-1004.
224. Rohde, C.M., et al., *Vitamin A antagonizes the action of vitamin D in rats.* J Nutr, 1999. **129**(12): p. 2246-50.
225. Wadhwa, B., et al., *Vitamin D and skin diseases: A review.* Indian J Dermatol Venereol Leprol, 2015. **81**(4): p. 344-55.
226. Meng, X.M., D.J. Nikolic-Paterson, and H.Y. Lan, *TGF-beta: the master regulator of fibrosis.* Nat Rev Nephrol, 2016. **12**(6): p. 325-38.
227. Xu, F., et al., *TGF-beta/SMAD Pathway and Its Regulation in Hepatic Fibrosis.* J Histochem Cytochem, 2016. **64**(3): p. 157-67.
228. Fernandez, I.E. and O. Eickelberg, *The impact of TGF-beta on lung fibrosis: from targeting to biomarkers.* Proc Am Thorac Soc, 2012. **9**(3): p. 111-6.

Appendices

Appendix 1

The REMARK guidelines (McShane et al., 2005)

REporting recommendations for tumour MARKer prognostic studies (REMARK) guidelines [75]

Introduction

1. State the marker examined, the study objectives, and any prespecified hypotheses.

Materials and Methods

Patients

2. Describe the characteristics (e.g. disease stage or comorbidities) of the study patients, including their source and inclusion and exclusion criteria.
3. Describe treatments received and how chosen (e.g. randomised or rule-based).

Specimen characteristics

4. Describe type of biological material used (including control samples), and methods of preservation and storage.

Assay methods

5. Specify the assay method used and provide (or reference) a detailed protocol, including specific reagents or kits used, quality control procedures, reproducibility assessments, quantitation methods, and scoring and reporting protocols. Specify whether and how assays were performed blinded to the study end point.

Study design

6. State the method of case selection, including whether prospective or retrospective and whether stratification or matching (e.g. by stage of disease or age) was employed. Specify the time period from which cases were taken, the end of the follow-up period, and the median follow-up time.

7. Precisely define all clinical end points examined.
8. List all candidate variables initially examined or considered for inclusion in models.
9. Give rationale for sample size; if the study was designed to detect a specified effect size, give the target power and effect size.

Statistical analysis methods

10. Specify all statistical methods, including details of any variable selection procedures and other model-building issues, how model assumptions were verified, and how missing data were handled.
11. Clarify how marker values were handled in the analyses; if relevant, describe methods used for cutpoint determination.

Results

Data

12. Describe the flow of patients through the study, including the number of patients included in each stage of the analysis (a diagram may be helpful) and reasons for dropout. Specifically, both overall and for each subgroup extensively examined report the numbers of patients and the number of events.
13. Report distributions of basic demographic characteristics (at least age and sex), standard (disease-specific) prognostic variables, and tumour marker, including numbers of missing values.

Analysis and presentation

14. Show the relation of the marker to standard prognostic variables.
15. Present univariate analyses showing the relation between the marker and outcome, with the estimated effect (e.g. hazard ratio and survival probability). Preferably provide similar analyses for all other variables being analysed. For the effect of a tumour marker on a time-to-event outcome, a Kaplan–Meier plot is recommended.

16. For key multivariable analyses, report estimated effects (e.g. hazard ratio) with confidence intervals for the marker and, at least for the final model, all other variables in the model.
17. Among reported results, provide estimated effects with confidence intervals from an analysis in which the marker and standard prognostic variables are included, regardless of their significance.
18. If done, report results of further investigations, such as checking assumptions, sensitivity analyses, internal validation.

Discussion

19. Interpret the results in the context of the pre-specified hypotheses and other relevant studies; include a discussion of limitations of the study.
20. Discuss implications for future research and clinical value.

Published manuscripts, abstracts & submissions arising from this work

List of published manuscripts

Tang DYL, Ellis RA and Lovat PE.

Prognostic Impact of Autophagy Biomarkers for Cutaneous Melanoma.

Frontiers Oncology 2016; 6:236.

Muthiah S, **Tang D**, Nasr B and Verykiou S.

A new era in holistic care-bridging the gap between dermatologists and oncologists for the treatment of malignant melanoma.

British Journal of Dermatology Editorial 2017; (in press).

List of published abstracts

Tang DYL, Greenwood A, Murray A, Carling E, Horswell S, Lovat PE and Ellis RA.

Epidermal AMBRA1 and Loricrin as novel prognostic biomarkers for melanoma.

British Journal of Dermatology 2016; 174(5): e43.

Tang DYL, Greenwood A, Murray A, Carling E, Horswell S, Lovat P and Ellis R.

Combined loss of epidermal AMBRA1 and Loricrin identifies high risk AJCC Stage I melanomas.

Pigment Cell and Melanoma Research 2017; 30: 76–156.

Tang D, Murray A, Giglio P, Gagliardi M, Corazzari M, Ellis R and Lovat P.

Contribution of melanoma TGF-β2 secretion to the loss of endothelial integrity and tumour metastasis.

British Journal of Dermatology 2017; (*in press).*

Tang D, Nasr B, Horswell S, McConnell A, Labus M, Lovat P and Ellis R (2017).

Validation of AMLo as a novel prognostic biomarker for AJCC Stage I melanoma.

British Journal of Dermatology 2017; (in press).